

REVISED FOR TMDL SUBMISSION

**MODELING FRAMEWORK FOR SIMULATING HYDRODYNAMICS AND
WATER QUALITY IN THE TRIADELPHIA AND ROCKY GORGE
RESERVOIRS, PATUXENT RIVER BASIN, MARYLAND**

Prepared by:

Interstate Commission on the Potomac River Basin

51 Monroe Street
Suite PE-08
Rockville, MD 20850

Prepared for:

Maryland Department of the Environment

1800 Washington Boulevard, Suite 540
Baltimore, MD 21230

ICPRB Report 08-2

September 2007

ACKNOWLEDGEMENTS

The project could not be completed without the guidance and direction of Mr. Tim Rule, the project officer at the Maryland Department of the Environment, and Mr. Nauth Panday. The contribution of Mr. Sajan Pokharel, who collaborated with us on the technical work while he was at MDE, was essential to our efforts. We would also like to acknowledge the invaluable support provided by Mr. Tom Thornton of MDE.

We gratefully acknowledge the cooperation of the Washington Suburban Sanitary Commission (WSSC). In particular we would like to thank Mr. Mohammed Habibian for providing many helpful suggestions and comments on the project and Mr. Tobias Kagan for responding so quickly to our many requests for data and other information, without which this project would not have been possible. We would also like to thank the following staff at WSSC who shared their time and expertise with us: Karen Wright, Todd Supple, Jay Price, Terry Valentine, and Jamette Garnet.

We would also like to express our appreciation for the following researchers who shared their data and their experience working in the Patuxent River watershed: Thomas Jordan of Smithsonian Environmental Research Center; Richard Ortt and Darlene Wells of the Maryland Geological Survey; and Sean Smith of the Maryland Department of Natural Resources. We would especially like to thank Mr. Tom Jones of Versar, Inc., for updating and organizing the monitoring data collected by Versar to make it easier to use in the TMDL.

We also would like to thank the members of the Patuxent Reservoirs Technical Advisory Committee for providing an audience for us to present the project at critical stages in its development.

As explained in the Introduction, the project documented in this report is built upon previous work performed by Tetra-Tech, Inc, under the direction of Mr. Andrew Parker. We are grateful to Tetra-Tech for making their work available to us. It goes without saying that the responsibility for the analysis, modeling, and documentation in this report rests with the staff of the Interstate Commission on the Potomac River Basin (ICPRB) alone.

This report has been prepared by the staff of the Interstate Commission on the Potomac River Basin. Support was provided by the Maryland Department of the Environment. The opinions expressed are those of the authors and should not be construed as representing the opinions or policies of the United States or any of its agencies, the several states, or the Commissioners of the Interstate Commission on the Potomac River Basin.

TABLE OF CONTENTS

ACKNOWLEDGEMENTS ii

LIST OF FIGURES vi

LIST OF TABLES ix

LIST OF ABBREVIATIONS xi

E.0 EXECUTIVE SUMMARY xiii

 E.1 Revised Patuxent Reservoirs Watershed Model xiii

 E.2 W2 Models of Triadelphia and Rocky Gorge Reservoirs xvi

 E.3 Hypolimnetic Hypoxia and the All-Forest Scenario xviii

1.0 INTRODUCTION..... 1

2.0 DESCRIPTION OF THE TRIADELPHIA AND ROCKY GORGE WATERSHEDS 3

 2.1 General Features of Triadelphia and Rocky Gorge Reservoirs 3

 2.2 Climate..... 5

 2.3 Geology and Soils..... 5

 2.4 Land Use..... 6

3.0 OVERVIEW OF THE PATUXENT RESERVOIRS WATERSHED HSPF MODEL 9

 3.1 Introduction 9

 3.2. Overview of the Hydrologic Simulation Program Fortran (HSPF)..... 9

 3.3. Model Assumptions 10

 3.4 Watershed Segmentation 10

 3.5 Land Use..... 12

 3.6 Nonpoint Sources 13

 3.7 Point Sources 14

 3.8 Meteorological Data 15

 3.9 Model Calibration Data 15

 3.9.1 USGS Flow Daily Flow Data..... 15

 3.9.2 Water Quality Monitoring Data 18

4.0 PATUXENT RESERVOIRS WATERSHED MODEL CALIBRATION..... 20

 4.1 Hydrology Calibration 20

 4.2 Temperature Calibration..... 24

 4.3. Implementation of Sediment and Nutrient Dynamics In The Patuxent Watershed HSPF Model 26

 4.4 Sediment and Nutrient Target Loads 28

 4.4.1. Sediment EOF Targets 29

 4.4.2 Target Total Phosphorus EOS Loads 30

 4.4.3 Target Nitrogen EOS Loads 32

 4.4.4 Determination of Target Total Sediment and Phosphorus Loads Using ESTIMATOR..... 32

 4.5 Sediment and Nutrient Calibration 38

 4.5.1 Sediment Calibration..... 38

 4.5.2 Phosphorus Calibration 39

 4.5.3 Ammonia and Nitrate Calibration 40

 4.6 Phosphorus and Sediment Loads to the Patuxent River Reservoirs 40

4.6.1 Comparison of HSPF Sediment and Phosphorus Loads with Load Estimates From Other Sources	42
5.0 WATER QUALITY CHARACTERIZATION OF TRIADELPHIA AND ROCKY GORGE RESERVOIRS.....	45
5.1 Water Quality Monitoring Programs	45
5.2 Temperature Stratification	47
5.4 Phosphorus.....	51
5.5 Nitrogen	52
5.6 Nutrient Limitation	53
5.7 Algae and Chlorophyll <i>a</i>	54
5.8 Sedimentation	55
5.9 Water Quality Impairments	55
6.0 STRUCTURE AND CALIBRATION OF THE CE-QUAL-W2 MODELS	57
6.1 Overview of the CE-QUAL-W2 Model	57
6.2 Implementation of the CE-QUAL-W2 Model For Triadelphia and Rocky Gorge Reservoirs	60
6.2.1. Segmentation and Model Cell Properties.....	61
6.2.2. Inflows, Meteorological Data and Boundary Conditions.....	62
6.2.3. Configuration of Water Quality Constituents	62
6.3. Water Balance Calibration.....	64
6.4 Temperature Calibration.....	67
6.5 Phosphorus Calibration.....	68
6.6 Chlorophyll <i>a</i> Calibration	77
6.7 Dissolved Oxygen Calibration.....	83
6.7.1 Bottom DO Calibration	83
6.7.2 Surface DO Calibration.....	84
6.8 Nitrogen Calibration	90
6.8.1 Ammonia.....	90
6.8.2 Nitrate.....	92
6.8.3 Total Nitrogen	93
7.0 LOAD REDUCTION SCENARIOS AND SENSITIVITY ANALYSIS	100
7.1. Scenario Descriptions	100
7.1.1. TMDL Scenario.....	100
7.1.2. All Forest Scenario.....	100
7.1.3. Comparison of Scenario Loading Rates.....	101
7.2. Criteria Tests.....	102
7.2.1. Chlorophyll Tests.....	102
7.2.2. Dissolved Oxygen Tests.....	102
7.2.3. Determination of the Position of the Surface Layer.....	103
7.3. Response of Chlorophyll Concentrations to Reductions in Phosphorus Loads ...	106
7.4. The Response of DO Concentrations to Load Reductions	108
7.4.1. The Response of Simulated Bottom DO Concentrations to Load Reductions	108
7.4.2. The Response of Simulated Surface DO Concentrations to Load Reductions	110
8.0 SUMMARY AND RECOMMENDATIONS.....	113

8.1 Summary.....	113
8.2 Recommendations	113
8.2.1 Nitrogen.....	113
8.2.2 Additional Chlorophyll <i>a</i> and Algae Monitoring.....	114
8.2.3 Improvements in Watershed Monitoring	115
REFERENCES.....	116

LIST OF FIGURES

Figure E.1: Percent Contribution of Sources to Total Phosphorus Loads to Triadelphia Reservoir xiv

Figure E.2: Percent Contribution of Sources to Total Phosphorus Loads to Rocky Gorge Reservoir xv

Figure E.3: Percent Contribution of Sources to Sediment Loads to Triadelphia Reservoir xv

Figure E.4 Maximum Observed and Simulated Chla Concentrations By Season, Triadelphia Reservoir xvii

Figure E.5 Maximum Observed and Simulated Chla Concentrations By Season, Rocky Gorge Reservoir xvii

Figure E.6: Observed and Simulated Average Bottom DO Concentrations, Station TR1, All-Forest Scenario, Triadelphia Reservoir xix

Figure E.7: Observed and Simulated Average Bottom DO Concentrations, Station RG1, All-Forest Scenario, Rocky Gorge Reservoir xix

Figure E.8: Percent of Sampling Dates on which DO < 2.0 mg/l as a function of proportion of All-Forest Scenario xx

Figure 2.1-1. Location of Triadelphia and Rocky Gorge Reservoirs 4

Figure 2.4-1 Land Use in the Patuxent Reservoirs Watershed 7

Figure 2.4-2: Proportion of Land Use in the Triadelphia Reservoir Watershed..... 8

Figure 2.4-3: Proportion of Land Use in the Rocky Gorge Reservoir Watershed..... 8

Figure 3.4-1: HSPF Model Segmentation..... 11

Figure 3.9-1: Location of USGS Gages and Water Quality Monitoring Stations 17

Figure 4.6-1: Percent Contribution of Sources to Total Phosphorus Loads to Triadelphia Reservoir 41

Figure 4.6-2: Percent Contribution of Sources to Total Phosphorus Loads to Rocky Gorge Reservoir 41

Figure 4.6-3: Percent Contribution of Sources to Sediment Loads to Triadelphia Reservoir 42

Figure 5.1-1: Sampling Locations in Triadelphia Reservoir 46

Figure 5.1-2: Sampling Locations in Rocky Gorge Reservoir 47

Figure 5.2-1: Isothermal Contours, Triadelphia Reservoir just above Brighton Dam, 1998-2003..... 48

Figure 5.3-1: DO Contour, Triadelphia Reservoir just above Brighton Dam, 1998-2003 50

Figure 5.3-2: Surface Water Elevations in Triadelphia Reservoir, 1998-2003 50

Figure 6.1-1. The Basic Equations of CE-QUAL-W2..... 58

Figure 6.3-1 Observed and Simulated Water Surface Elevation, Triadelphia Reservoir . 66

Figure 6.3-2 Observed and Simulated Water Surface Elevation, Rocky Gorge Reservoir 66

Figure 6.5-1. Cumulative Distribution of Observed and Simulated Average TP Concentrations, Surface Layer, Triadelphia Reservoir 73

Figure 6.5-2. Cumulative Distribution of Observed and Simulated Average TP Concentrations, Bottom Layer, Triadelphia Reservoir 73

Figure 6.5-3. Cumulative Distribution of Observed and Simulated Average TP Concentrations, Surface Layer, Rocky Gorge Reservoir 74

Figure 6.5-4. Cumulative Distribution of Observed and Simulated Average TP Concentrations, Bottom Layer, Rocky Gorge Reservoir 74

Figure 6.5-5. Cumulative Distribution of Observed and Simulated Average PO4 Concentrations, Surface Layer, Triadelphia Reservoir 75

Figure 6.5-6. Cumulative Distribution of Observed and Simulated Average PO4 Concentrations, Bottom Layer, Triadelphia Reservoir 75

Figure 6.5-7. Cumulative Distribution of Observed and Simulated Average PO4 Concentrations, Surface Layer, Rocky Gorge Reservoir 76

Figure 6.5-8. Cumulative Distribution of Observed and Simulated Average PO4 Concentrations, Bottom Layer, Rocky Gorge Reservoir 76

Rocky Gorge Reservoir..... 79

Figure 6.6-1 Maximum Observed and Simulated Chla Concentrations By Season, Triadelphia Reservoir..... 80

Figure 6.6-2 Maximum Observed and Simulated Chla Concentrations By Season, Rocky Gorge Reservoir 80

6.6-3 Cumulative Distribution of Observed and Simulated Chla Concentrations, Triadelphia Reservoir..... 81

6.6-3 Cumulative Distribution of Observed and Simulated Chla Concentrations, Rocky Gorge Reservoir 81

Figure 6.6-5. Observed and Simulated Maximum Chla Concentrations By Sampling Date, Triadelphia Reservoir 82

Figure 6.6-6. Observed and Simulated Maximum Chla Concentrations By Sampling Date, Rocky Gorge Reservoir 82

Figure 6.7-1. Observed and Simulated Average Bottom DO Concentrations, TR1, Calibration Scenario, Triadelphia Reservoir..... 86

Figure 6.7-2. Observed and Simulated Average Bottom DO Concentrations, RG1, Calibration Scenario, Rocky Gorge Reservoir..... 86

Figure 6.7-3. Observed and Simulated Cumulative Distribution of Bottom DO Concentrations, Triadelphia Reservoir..... 87

Figure 6.7-4. Observed and Simulated Cumulative Distribution of Bottom DO Concentrations, Rocky Gorge Reservoir..... 87

Figure 6.7-5. Observed and Simulated Average Surface DO Concentrations, TR1, Calibration Scenario, Triadelphia Reservoir..... 88

Figure 6.7-6. Observed and Simulated Average Surface DO Concentrations, RG1, Calibration Scenario, Rocky Gorge Reservoir..... 88

Figure 6.7-7. Observed and Simulated Cumulative Distribution of Surface DO Concentrations, Triadelphia Reservoir..... 89

Figure 6.7-8. Observed and Simulated Cumulative Distribution of Surface DO Concentrations, Rocky Gorge Reservoir..... 89

Figure 6.8-1. Cumulative Distribution of Observed and Simulated Average NH4 Concentrations, Surface Layer, Triadelphia Reservoir 94

Figure 6.8-2. Cumulative Distribution of Observed and Simulated Average NH4 Concentrations, Bottom Layer, Triadelphia Reservoir 94

Figure 6.8-3. Cumulative Distribution of Observed and Simulated Average NH₄ Concentrations, Surface Layer, Rocky Gorge Reservoir 95

Figure 6.8-4. Cumulative Distribution of Observed and Simulated Average NH₄ Concentrations, Bottom Layer, Rocky Gorge Reservoir 95

Figure 6.8-5. Cumulative Distribution of Observed and Simulated Average NO₃ Concentrations, Surface Layer, Triadelphia Reservoir 96

Figure 6.8-6. Cumulative Distribution of Observed and Simulated Average NO₃ Concentrations, Bottom Layer, Triadelphia Reservoir 96

Figure 6.8-7. Cumulative Distribution of Observed and Simulated Average NO₃ Concentrations, Surface Layer, Rocky Gorge Reservoir 97

Figure 6.8-8. Cumulative Distribution of Observed and Simulated Average NO₃ Concentrations, Bottom Layer, Rocky Gorge Reservoir 97

Figure 6.8-9. Cumulative Distribution of Observed and Simulated Average TN Concentrations, Surface Layer, Triadelphia Reservoir 98

Figure 6.8-10. Cumulative Distribution of Observed and Simulated Average TN Concentrations, Bottom Layer, Triadelphia Reservoir 98

Figure 6.8-11. Cumulative Distribution of Observed and Simulated Average TN Concentrations, Surface Layer, Rocky Gorge Reservoir 99

Figure 6.8-12. Cumulative Distribution of Observed and Simulated Average TN Concentrations, Bottom Layer, Rocky Gorge Reservoir 99

Figure 7.2-1. Position of the Interface between Epilimnion and Metalimnion, Triadelphia Reservoir 105

Figure 7.2-2. Position of the Interface Between Epilimnion and Metalimnion, Rocky Gorge Reservoir 105

Figure 7.3-1. Observed and Simulated Maximum Chlorophyll Concentrations by Date, Triadelphia Reservoir 107

Figure 7.3-2. Observed and Simulated Maximum Chlorophyll Concentrations by Date, Rocky Gorge Reservoir 107

Figure 7.4-1 Average Bottom DO, Observed Data and All Scenarios, TR2, Triadelphia Reservoir 109

Figure 7.4-2 Average Bottom DO, Observed Data and All Scenarios, RG2, Rocky Gorge Reservoir 109

Figure 7.4-3. Percent of Sampling Dates on which DO < 2 mg/l at Sampling Locations as a function of Load Reductions from All-Forest Scenario 110

Figure 7.4-4 Surface DO, Observed Data and All Scenarios, TR1, Triadelphia Reservoir 112

Figure 7.4-5 Surface DO, Observed Data and All Scenarios, RG1, Rocky Gorge Reservoir 112

Figure 8.1-1 Observed DO Profile (mg/l) in Triadelphia Reservoir, TR1, May 8, 2001 115

LIST OF TABLES

Table 2.1-1. Current Physical Characteristics of Triadelphia and Rocky Gorge Reservoirs..... 3

Table 2.2-1. Summary Statistics Meteorological Data Clarksville, 1971 – 2000..... 5

Table 3.5-1 Reclassification of Tetra Tech (2000) Land Use..... 12

Table 3.5-2: HSPF Model Land Use By Segment..... 13

Table 3.6-1: Average Annual Septic System Load By Segment..... 14

Table 3.7-1. Annual Municipal Wastewater Treatment Plant Loads 1998-2003 15

Table 3.9-1: USGS Gages in the Patuxent River Watershed..... 16

Table 3.9-2: Characterization of Patuxent Reservoir Watershed Monitoring Programs .. 18

Table 3.9-3: Constituents Analyzed By Program 19

Table 4.0-1 Average Annual Flow, Patuxent River near Unity..... 20

Table 4.1-1 Key Hydrology Calibration Parameters 22

Table 4.1-2 Ratio of Cropland Parameters to Those for Other Land Uses..... 22

Table 4.1-3 Monthly Hydrology Parameters 22

Table 4.1-4. Revisions to the CBP Howard County Precipitation Time Series 23

Table 4.1-5. Revisions to the CBP Montgomery County Precipitation Time Series 23

Table 4.1-6 Hydrology Calibration Parameter Values 24

Table 4.1-7 Hydrology Calibration Results 24

Table 4.2-1. Temperature Calibration Parameters..... 25

Table 4.2-2. Temperature Calibration Parameter Results..... 25

Table 4.3-1. Description of HSPF Subroutines 26

Table 4.3-2 HSPF Subroutines Used in the HSPF Model by Land Use and Constituent. 27

Table 4.4-1 Target Loads For Agricultural Land Uses..... 29

Table 4.4-2. Average EMCs Derived From Maryland NPDES Stormwater Permits (Bahr, 1997)..... 30

Table 4.4-3 Sediment Delivery Ratios..... 30

Table 4.4-4: Source of TP Calibration Targets by Land Use and Flow Path 31

Table 4.4-5 Idealized Baseflow TP Concentrations (mg/l) 31

Table 4.4-6. Coefficients of Regression Equation and Regression Statistics, Sediment.. 35

Table 4.4-7. Coefficients of Regression Equation and Regression Statistics, Total Phosphorus 35

Table 4.4-8 Comparison of Sediment and TP Load Estimates in Patuxent River Watersheds 36

Table 4.4-9. Coefficients of Regression Equation and Regression Statistics, Ammonia Nitrogen..... 36

Table 4.4-10. Coefficients of Regression Equation and Regression Statistics, Nitrate Nitrogen..... 37

Table 4.4-11. Coefficients of Regression Equation and Regression Statistics, Total Nitrogen..... 37

Table 4.5-1. Summary Statistics Comparing Observed and Simulated Concentrations... 39

Table 4.6-1 Comparisons of Sediment and Total Phosphorus Load Estimates By Study 44

Table 5.1-1: Characterization of Reservoir Monitoring Programs 45

Table 5.4-1: Summary Statistics: TP Concentrations (mg/L) in Triadelphia Reservoir, 1998-2003.....	51
Table 5.4-2: Summary Statistics: TP Concentrations (mg/L) in Rocky Gorge Reservoir, 1998-2003.....	51
Table 5.6-1. Summary Statistic for N:P Ratio, Patuxent Reservoirs, 1998-2003.....	53
Table 5.7-1. Maximum Observed Chla Concentration, 1998-2003 Triadelphia Reservoir	54
Table 5.7-2. Maximum Observed Chla Concentration, 1998-2003 Rocky Gorge Reservoir	54
Table 5.8-1: Sedimentation Rates in Triadelphia Reservoir	55
Table 6.2-1 Assignments of HSPF Segments to W2 Segments, Triadelphia Reservoir...	61
Table 6.2-2 Assignments of HSPF Segments to W2 Segments, Rocky Gorge Reservoir	61
Table 6.2.3-1. Water Quality State Variables in CE-QUAL-W2 and their Realization in the Patuxent Reservoir Models	64
Table 6.4-1. Parameters Used in W2 Temperature Calibration.....	67
Table 6.4-2. Temperature Calibration Parameter Values, Triadelphia Reservoir	68
Table 6.4-3. Temperature Calibration Parameter Values, Rocky Gorge Reservoir	68
Table 6.5-1 Decay Rates and Settling Rates for Organic Matter.....	71
Table 6.5-4 Summary Statistics for Simulated and Observed Surface Layer PO4 (mg/l)	72
Table 6.6-1. Algae Species Parameterizations By Season.....	78
Table 6.6-2 Algal Growth Rates and Temperature Parameters	79
Table 6.7-1 Bottom DO Calibration Parameter Values	83
Table 6.8-1 Key Nitrogen Calibration Parameters	90
Table 6.8-3 Summary Statistics for Bottom Observed and Simulated NH4	91
Table 6.8-4 Summary Statistics for Surface Observed and Simulated NO3	92
Table 6.8-5 Summary Statistics for Bottom Observed and Simulated NO3	92
Table 6.8-6 Summary Statistics for Surface Observed and Simulated TN.....	93
Table 6.8-7 Summary Statistics for Bottom Observed and Simulated TN.....	93
Table 7.1-1. Scenario Annual Phosphorus Load (lbs/yr) By Species and Forest Scenario Percent of Calibration Load	101
Table 7.2-1 Monthly Average Daily Temperature Gradient (°C/m) Determining Relative Position of Epilimnion and Metalimnion in Triadelphia Reservoir	104
Table 7.2-2 Monthly Average Daily Temperature Gradient (°C/m) Determining Relative Position of Epilimnion and Metalimnion in Rocky Gorge Reservoir	104
Table 7.3-1. Scenario Summary Statistics for the Simulated Average Surface Concentrations (mg/l) of Total Phosphorus at Sampling Locations in Triadelphia and Rocky Gorge Reservoirs	106

LIST OF ABBREVIATIONS

BMP	Best Management Practice
BOD	Biochemical Oxygen Demand
CBOD	Carbonaceous Biochemical Oxygen Demand
CBP	Chesapeake Bay Program
CE-QUAL-W2	U.S. Army Corps of Engineers Water Quality and Hydrodynamic Model, Version 3
cfs	Cubic feet per second
Chla	Active Chlorophyll <i>a</i>
COMAR	Code of Maryland Regulations
CWA	Clean Water Act
CWAP	Clean Water Action Plan
DIP	Dissolved Inorganic Phosphorus
DNR	Maryland Department of Natural Resources
DO	Dissolved Oxygen
EMC	Event Mean Concentration
EPA	Environmental Protection Agency
FEMA	Federal Emergency Management Agency
HSPF	Hydrological Simulation Program Fortran
ICPRB	Interstate Commission on the Potomac River Basin
LA	Load Allocation
lbs/yr	Pounds per Year
MD	Maryland
MDA	Maryland Department of Agriculture
MDE	Maryland Department of the Environment
MDP	Maryland Department of Planning
MGS	Maryland Geological Survey
mg/l	Milligrams per Liter
MGD	Million Gallons per Day
MNCP&PC	Maryland National Capital Parks and Planning Commission
MOS	Margin of Safety

REVISED FOR TMDL SUBMISSION

MS4	Municipal Separate Storm Sewer System
NBOD	Nitrogenous Biochemical Oxygen Demand
NH4	Ammonia-Nitrogen
NMP	Nutrient Management Plan
NO23	Nitrite-Nitrate-Nitrogen
NO3	Nitrate-Nitrogen
NOAA	National Oceanic and Atmospheric Administration
NPDES	National Pollutant Discharge Elimination System
NPS	Nonpoint Source
POM	Particulate Organic Matter
PO4	Phosphate
SCWQP	Soil Conservation and Water Quality Plan
SERC	Smithsonian Environmental Research Center
SOD	Sediment Oxygen Demand
TAC	Patuxent Reservoirs Technical Advisory Committee
TKN	Total Kjeldahl Nitrogen
TMDL	Total Maximum Daily Load
TN	Total Nitrogen
TOP	Total Organic Phosphorus
TP	Total Phosphorus
TSI	Trophic State Index
TSS	Total Suspended Solids
USGS	United State Geological Survey
W2	CE-QUAL-W2
WLA	Wasteload Allocation
WQIA	Water Quality Improvement Act
WQLS	Water Quality Limited Segment
WSSC	Washington Suburban Sanitary Commission
WWTP	Waste Water Treatment Plant
µg/l	Micrograms per Liter

E.0 EXECUTIVE SUMMARY

This report documents the development of a modeling framework for determining Total Maximum Daily Loads (TMDLs) in Triadelphia and Rocky Gorge Reservoirs for nutrients, and, in the case of Triadelphia Reservoir, sediment. The modeling framework builds upon a set of computer simulation models previously developed by Tetra Tech for the Washington Suburban Sanitary Commission (WSSC), including (1) an HSPF (Hydrological Simulation Program–Fortran) model of the Patuxent River Watershed above Duckett Dam, which forms Rocky Gorge Reservoir, and (2) CE-QUAL-W2 models of each reservoir, simulating the hydrodynamics, eutrophication, and dissolved oxygen dynamics in the reservoirs. The HSPF model provides the input flows and loads for the W2 models of the reservoirs.

Tetra Tech developed these models to use for water quality planning; they do not have all the features necessary for TMDL development. The modeling framework for TMDLs for these reservoirs must (1) provide a budget for phosphorus, which will be shown in Chapter 5 to be the limiting nutrient in the reservoirs, and keep a mass balance of phosphorus; (2) determine the link between phosphorus loadings and eutrophication in the reservoirs, as expressed by chlorophyll *a* (Chla) concentrations; and (3) determine the link between the deposition of organic material and sediment oxygen demand (SOD) in the reservoirs.

E.1 Revised Patuxent Reservoirs Watershed Model

One of the goals in revising the HSPF model of the reservoir watersheds is to make the HSPF models more compatible with the Chesapeake Bay Program (CBP) Watershed Models, used for developing the Tributary Strategies for reducing sediment and nutrient loads to Chesapeake Bay, and with other TMDL models used in Maryland.

Compatibility with nutrient load estimates used in Maryland's Tributary Strategies is desirable because it provides stakeholders a consistent baseline for environmental planning and management. Originally, it was hoped that the Patuxent Reservoirs Watershed Model (PRWM) could adopt the same edge-of-field (EOF) and edge-of-stream (EOS) nutrient loading targets that will be used in the CBP Phase 5 Watershed Model, but the development of the Phase 5 model has fallen behind schedule. The following features of the CBP Watershed Models were incorporated into the Patuxent Reservoirs Watershed Model:

- Phase 4.3 Water Model land use categories were used in the PRWM and HSPF's AGCHEM modules were implemented to simulated phosphorus export from cropland and nitrogen export from all pervious land;
- Target EOF erosion rates from the Phase 5 model were used as EOF targets in the PRWM;
- Provisional EOS TP load targets from the Phase 5 model were used to determine EOS total phosphorus (TP) loads from cropland and pasture in the PRWM; and

- Simulated EOS ammonia and nitrate loads from the Phase 4.3 2000 Progress Scenario were used to set EOS targets for nitrogen species.

The second goal in revising the HSPF models is to incorporate all recently available water quality monitoring data, including the systematic storm and baseflow sampling performed by Versar, Inc. in Cattail Creek and Hawlings River, 1998-2001, on behalf of WSSC. The USGS software, ESTIMATOR, was used to calculate target sediment and total phosphorus loads for Cattail Creek, the Patuxent River near Unity, and Hawlings River. These target loads were used to calibrate the PRWM over the watershed model simulation period 1997-2003.

Figures E.1 and E.2 show the percentage of average annual TP loads by source in Triadelphia Reservoir and Rocky Gorge Reservoir, respectively. The average annual loads over the reservoir model simulation period, 1998-2003, are 65,953 lbs/yr and 46,935 lbs/yr in Triadelphia and Rocky Gorge Reservoirs, respectively. Figure E.3 shows the percentage of the average annual sediment load (32,141 tons/yr) by source in Triadelphia Reservoir.

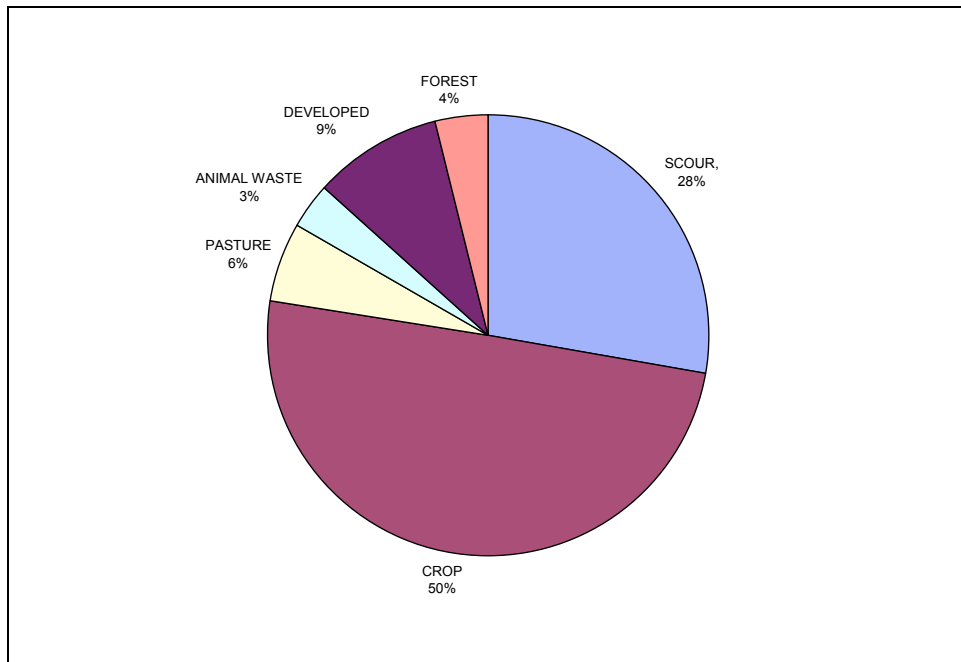


Figure E.1: Percent Contribution of Sources to Total Phosphorus Loads to Triadelphia Reservoir

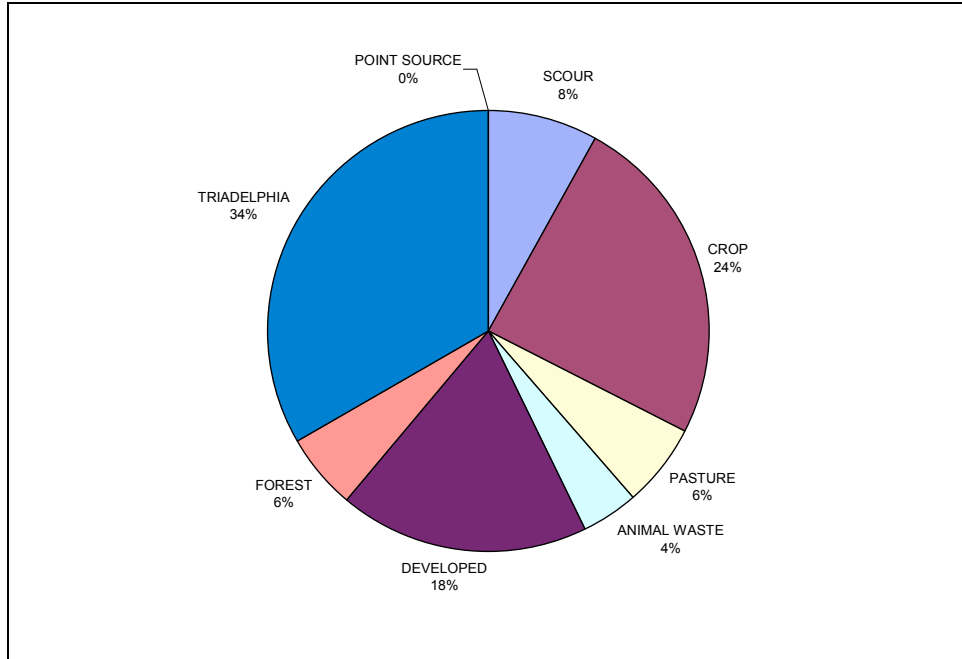


Figure E.2: Percent Contribution of Sources to Total Phosphorus Loads to Rocky Gorge Reservoir

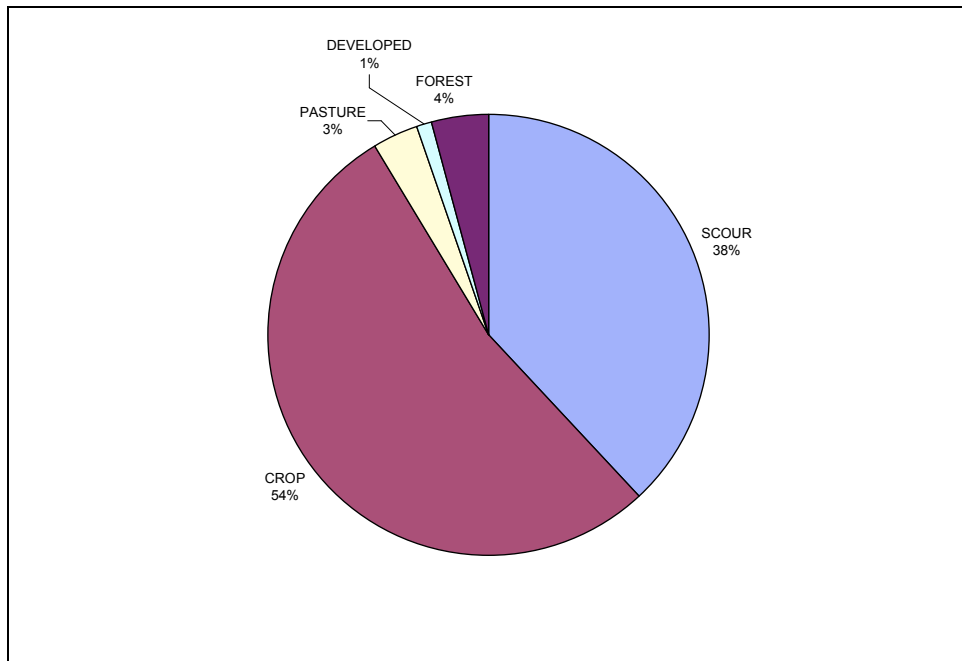


Figure E.3: Percent Contribution of Sources to Sediment Loads to Triadelphia Reservoir

E.2 W2 Models of Triadelphia and Rocky Gorge Reservoirs

Phosphorus is the limiting nutrient in both Triadelphia and Rocky Gorge Reservoirs. The overall objective of the nutrient TMDLs is to reduce phosphorus loads to the levels that are expected to result in attainment of water quality standards. Maryland's General Water Quality Criteria prohibit pollution of waters of the State by any material in amounts sufficient to create a nuisance or interfere directly or indirectly with designated uses (COMAR 26.08.02.03B(2)). In the case of excess eutrophication, this is interpreted to mean that (1) a ninetieth-percentile instantaneous Chla concentration is not to exceed 30 µg/l and (2) a 30-day moving average Chla concentration is not to exceed 10 µg/l. A concentration of 10 µg/l corresponds to a score of approximately 53 on the Carlson Trophic State Index (TSI). This is the approximate boundary between mesotrophic and eutrophic conditions, which is an appropriate trophic state at which to manage these reservoirs. Mean Chla concentrations exceeding 10 µg/l are associated with peaks exceeding 30 µg/l, which in turn are associated with a shift to blue-green assemblages, which present taste, odor and treatment problems (Walker 1984).

The W2 models of Triadelphia and Rocky Gorge Reservoirs were calibrated for the simulation period 1998-2003, when Chla data were available in the reservoirs. The goal of the Chla calibration is, for each season in which the observed Chla concentration is greater than 10 µg/l, that the maximum simulated Chla concentration, at the dates and locations monitored, should be equal to or greater than the maximum observed concentration in that season. In other words, the maximum observed concentration from all the observations taken in a reservoir in a season is compared to the maximum simulated concentration from the corresponding sampling locations and dates in a given season. This is a very conservative calibration strategy, which ensures that the cumulative distribution of simulated concentrations dominates the observed concentrations. Figure E.4 compares the monthly maximum observed and simulated concentrations at sampling dates and locations by season in Triadelphia Reservoir. Figure E.5 shows the maximum concentrations by season in Rocky Gorge Reservoir. As the figures show, the Chla calibration generally met its objective.

TMDL Scenarios were run for each reservoir using the calibrated models to determine the levels of phosphorus loads compatible with meeting the TMDL endpoints described above. Triadelphia Reservoir required a 58% reduction in phosphorus loads to meet water quality standards, while Rocky Gorge Reservoir required a 48% reduction in phosphorus loads.

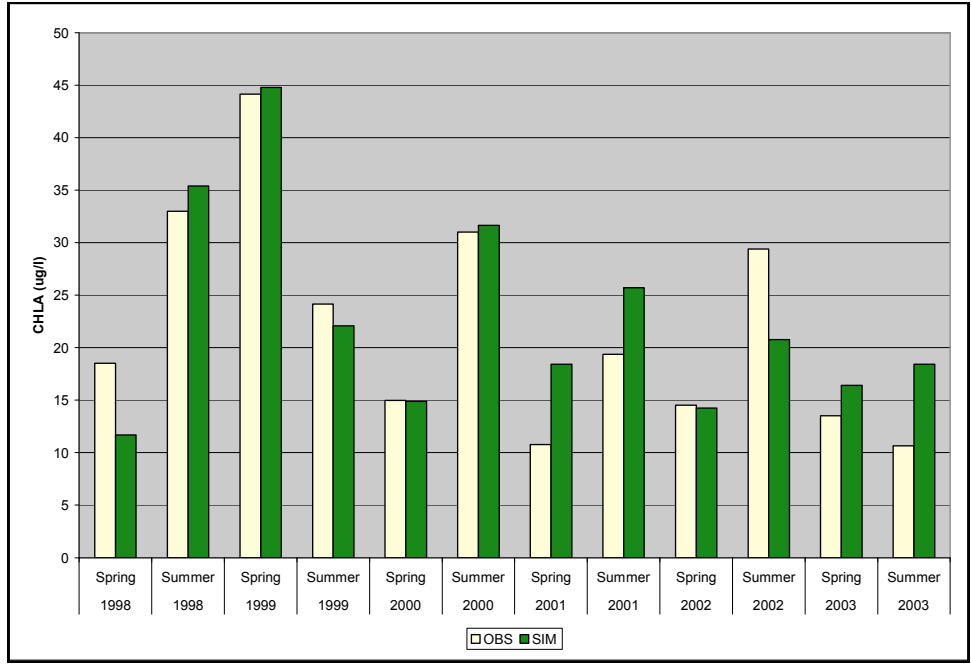


Figure E.4 Maximum Observed and Simulated Chla Concentrations By Season, Triadelphia Reservoir

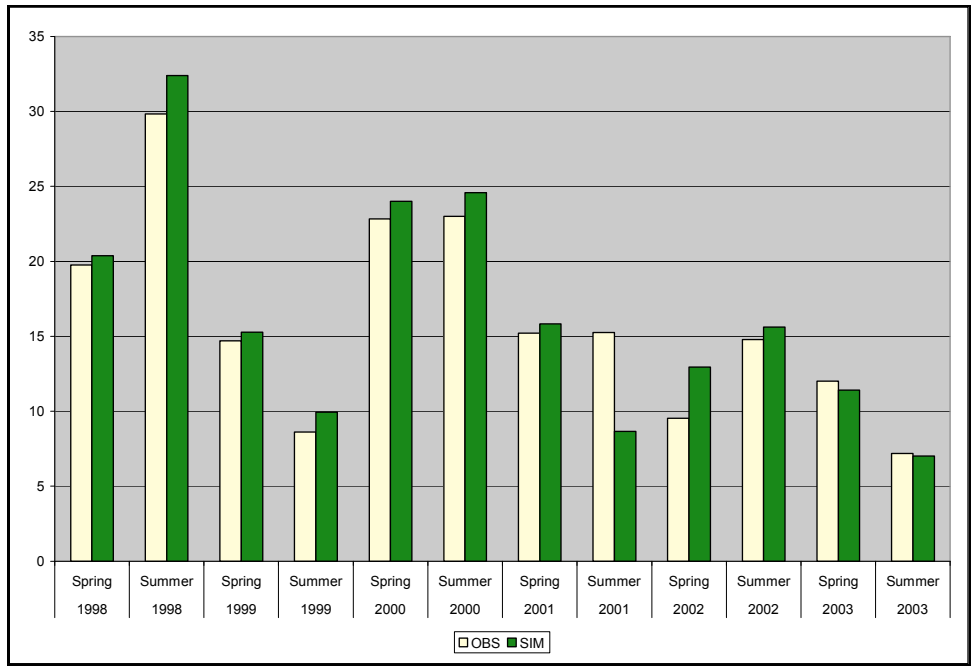


Figure E.5 Maximum Observed and Simulated Chla Concentrations By Season, Rocky Gorge Reservoir

E.3 Hypolimnetic Hypoxia and the All-Forest Scenario

Like many lakes and reservoirs, Triadelphia Reservoir and Rocky Gorge Reservoir are stratified by temperature-induced density differences from the spring through later summer and sometimes early fall, and **this** stratification can induce low dissolved oxygen (DO) concentrations in the hypolimnion or bottom layer of the reservoirs. The hypoxia is caused by the fact that decaying organic material in the sediments and water column consumes oxygen, while stratification dampens the mixing of DO from surface reaeration.

The water quality standards applicable to Triadelphia and Rocky Gorge Reservoirs require DO concentrations of not less 5.0 mg/l at any time (COMAR 26.08.02.03-3E(2)) unless natural conditions result in lower levels of DO (COMAR 26.08.02.03A(2)). New standards for tidal waters of the Chesapeake Bay and its tributaries take into account stratification and its impact on deeper waters. MDE recognizes that stratified reservoirs and impoundments present circumstances similar to stratified tidal waters, and is applying an interim interpretation of the existing standard to allow for the impact of stratification on DO concentrations. This interpretation recognizes that, given the morphology of the reservoir or impoundment, the resulting degree of stratification, and the naturally occurring sources of organic material in the watershed, hypoxia in the hypolimnion is a natural consequence.

An All-Forest Scenario simulates the response of the reservoirs to the phosphorus, sediment, nitrogen, and BOD loading rates that would occur if all of the land in the reservoirs' watersheds were forested. The All-Forest Scenario is used to determine to what extent hypoxic conditions in the hypolimnion are a function of external loading rates or reservoir morphology. The All-Forest Scenario constitutes an estimate of hypolimnetic DO concentrations under natural conditions. Flows and temperature were taken from the Calibration Scenario, while constituent loads were taken from the HSPF model simulation whereby all land in the watershed was forested. If hypoxia occurs even under all-forested loading rates, then reservoir stratification is the primary cause of hypoxia and it can be concluded that the reservoir meets the water quality standards for DO as described above.

Average annual TP loads in the All-Forest Scenario are 18% of the load in the Calibration Scenario in Triadelphia Reservoir, and 15% of the load in the Calibration Scenario in Rocky Gorge Reservoir. The reduction in average annual loads of particulate organic matter (POM), the precursor to sediment oxygen demand, is not as large. Average annual POM loads in the All-Forest Scenario are 29% of the load in Calibration Scenario in Triadelphia and 31% of the load in Calibration Scenario in Rocky Gorge. The POM load decrease is less in the Rocky Gorge watershed because of the high percentage of forested and developed land.

Figures E.6 and E.7 show the average bottom DO concentrations sampling locations just upstream of the dams in the reservoirs under the All-Forest Scenario. Minimum

concentrations at the sampling locations are also shown. Average DO in the bottom layers of both reservoirs improves considerably under the All-Forest Scenario. The minimum DO concentration, however, frequently drops below 5.0 mg/l. Even under the All-Forest Scenario, the hypolimnion remains hypoxic in many (but not all) years of the simulation. The hypoxia tends to be worse in the lower stations of the reservoirs where the depths are greatest.

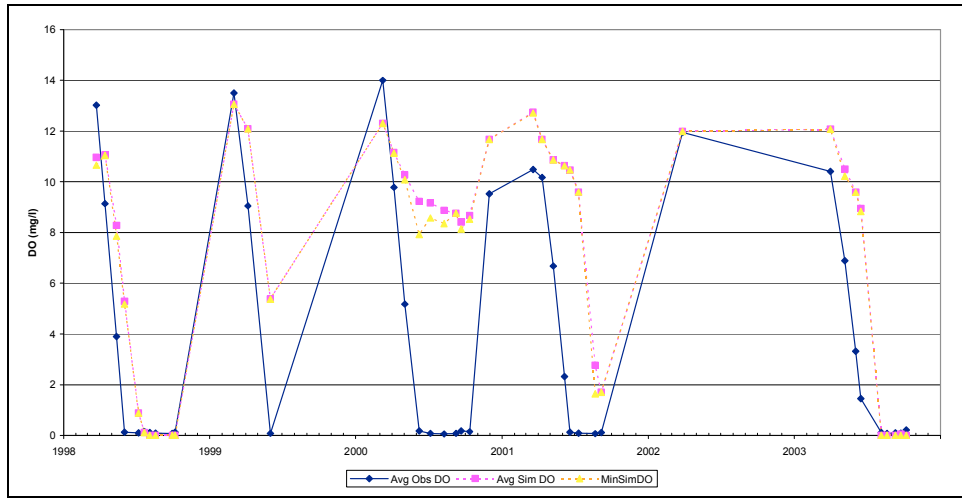


Figure E.6: Observed and Simulated Average Bottom DO Concentrations, Station TR1, All-Forest Scenario, Triadelphia Reservoir

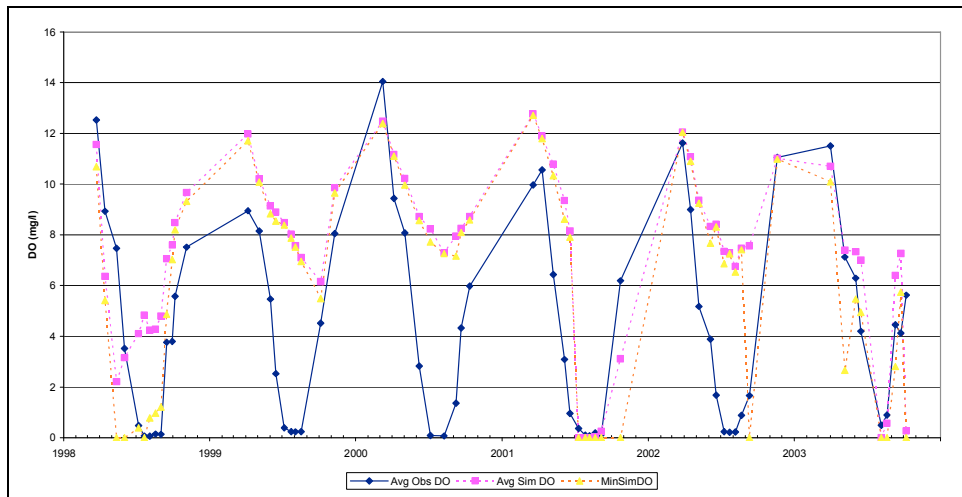


Figure E.7: Observed and Simulated Average Bottom DO Concentrations, Station RG1, All-Forest Scenario, Rocky Gorge Reservoir

A sensitivity analysis was performed to better determine how phosphorus and organic matter loading rates impact hypoxia in the hypolimnion. POM and TP loading rates were reduced to 50%, 20% and 10% of the loads of the All-Forest Scenario, and the percent of sampling dates where DO < 2.0 mg/l at the sampling locations was calculated. Figure E.8 shows the results. Significant hypoxia persists even when loads are reduced to only 10% of the All-Forest Scenario in Rocky Gorge Reservoir. Although hypoxia disappears in Triadelphia Reservoir when loading rates are 10% of the All-Forest Scenario, 5% of sampling dates under those loading conditions still have DO concentrations less than 5 mg/l in the hypolimnion. The sensitivity analysis shows that low DO in the bottom layers of the reservoirs is relatively insensitive to the particular assumptions used to determine organic matter loads in the models, and demonstrates that hypolimnetic hypoxia is primarily driven by stratification and reservoir morphology, rather than by external loads. The All-Forest Scenario demonstrates that current loads, and loads simulated under the TMDL Scenario, do not result in hypoxia that significantly exceeds that associated with natural conditions in the watershed. Low DO concentrations in the bottom layers of the reservoirs are therefore a naturally occurring condition, as described by the interim interpretation of Maryland’s water quality standards. The TMDL Scenario thus meets water quality standards for DO under the interim interpretation.

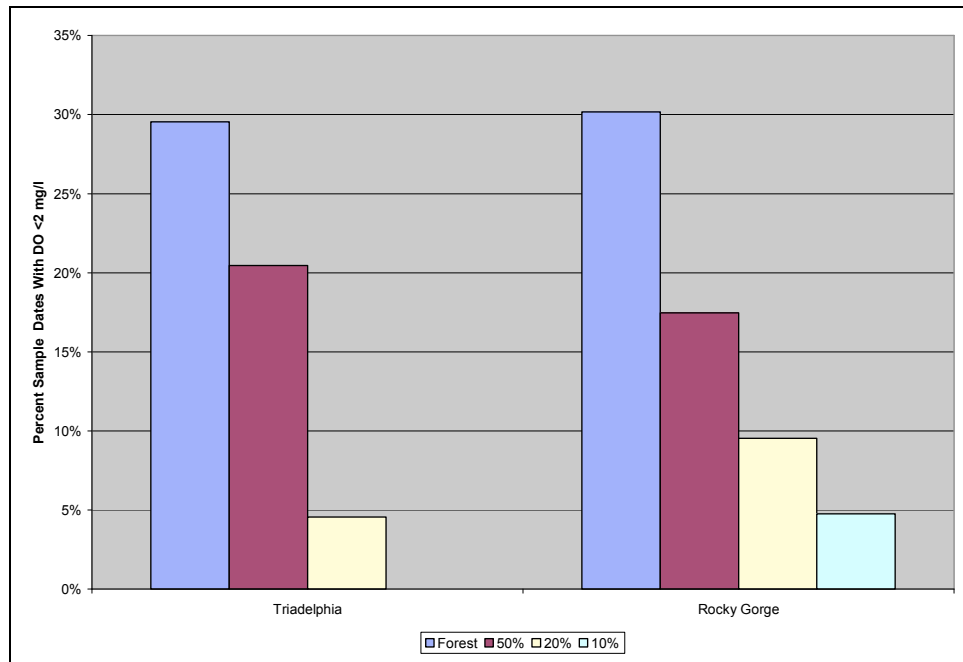


Figure E.8: Percent of Sampling Dates on which DO < 2.0 mg/l as a function of proportion of All-Forest Scenario

1.0 INTRODUCTION

Triadelphia Reservoir (also known as Brighton Dam) and Rocky Gorge Reservoir are two public water supply reservoirs operated by the Washington Suburban Sanitary Commission (WSSC) in the Patuxent River Watershed. Together with their intake on the Potomac River, the reservoirs form the core of the WSSC's water supply system, which provides water to about a half-million people in Montgomery and Prince George's Counties.

Triadelphia Reservoir and Rocky Gorge Dam have been designated as Use IV-P and Use I-P waterbodies, respectively, in the Code of Maryland Regulations (COMAR 26.08.02.08M(6) and COMAR 26.08.02.08M(1)). The Maryland Department of the Environment (MDE) placed both reservoirs on Maryland's 1998 303(d) List of impaired waters due to signs of eutrophication, expressed as high chlorophyll *a* (Chla) levels. Eutrophication is the over-enrichment of aquatic systems by excessive inputs of nutrients, especially nitrogen and/or phosphorus. The nutrients act as a fertilizer leading to the excessive growth of aquatic plants, which eventually die and decompose, leading to bacterial consumption of dissolved oxygen (DO). Triadelphia Reservoir is also listed as impaired because of sediment (1998).

Waters placed on the 303(d) List are not meeting water quality standards and are not expected to do so by the implementation of technology-based controls on permitted point sources. Under these conditions, the Clean Water Act specifies that a Total Maximum Daily Load (TMDL) must be determined. A TMDL is the maximum amount of a pollutant a waterbody can receive and still meet water quality standards. The water quality goal of the nutrient TMDLs is to reduce high chlorophyll *a* (Chla) concentrations that reflect excessive algal blooms, and to maintain dissolved oxygen (DO) at a level supportive of the designated uses for Triadelphia and Rocky Gorge Reservoirs. The water quality goal of the sediment TMDL for Triadelphia Reservoir is to increase the useful life of the reservoir for water supply by preserving storage capacity.

This report documents the development of a modeling framework for determining TMDLs in Triadelphia and Rocky Gorge Reservoirs for nutrients, and, in the case of Triadelphia Reservoir, sediment. The modeling framework builds upon a set of computer simulation models previously developed by Tetra Tech for WSSC, including (1) an HSPF (Hydrological Simulation Program–Fortran) model of the Patuxent River Watershed above Duckett Dam, which forms Rocky Gorge Reservoir, and (2) CE-QUAL-W2 models of each reservoir, simulating the hydrodynamics, eutrophication, and dissolved oxygen dynamics in the reservoirs. The HSPF model provides the input flows and loads for the W2 models of the reservoirs.

Tetra Tech (2000, 2002) developed these models to use for water quality planning; they do not have all the features necessary for TMDL development. The modeling framework for TMDLs for these reservoirs must (1) provide a budget for phosphorus, which will be shown in Chapter 5 to be the limiting nutrient in the reservoirs, and keep a mass balance

of phosphorus; (2) determine the link between phosphorus loadings and eutrophication in the reservoirs, as expressed by Chla concentrations; and (3) determine the link between the deposition of organic material and sediment oxygen demand in the reservoirs. The goal of the project described in this report is to bring this set of models up to code, so to speak, for their use in TMDL development. The following changes were made to the modeling framework to make its elements appropriate for TMDLs:

- The W2 models were set up to simulate the period 1998-2003, when chlorophyll *a* monitoring data were available in the reservoirs. The availability of this data is a necessary condition for calibrating the relation between nutrient loads, on the one hand, and eutrophication and algal growth, on the other, which is the most important function of the W2 models in TMDL development.
- The W2 code was altered so that a full mass balance of phosphorus, the limiting nutrient in the reservoirs, could be kept in the W2 simulations.
- The W2 code was altered so that internal and external organic material could be tracked separately and so that sediment oxygen demand was a function of the deposition of organic material from external and internal sources.
- The simulation of sediment, phosphorus, and nitrogen loads were reconfigured in the HSPF model to make the watershed simulation more compatible with the HSPF simulations used in the Chesapeake Bay Program's (CBP) Watershed Model and in other TMDLs in Maryland. It was originally intended for the revised watershed model to be fully compatible with the CBP Phase 5 Watershed Model, which will provide the load estimates for Maryland's Tributary Strategies for reducing nutrient and sediment loads to the bay and perhaps will also be used to develop nutrient TMDLs for Maryland's eight-digit scale watersheds. Unfortunately, the Phase 5 Model is behind schedule in development, so elements of the earlier Phase 4 Model had to be used to guide the revision of the watershed model for nutrient TMDLs for the Patuxent Reservoirs.
- The change in simulation period allowed additional monitoring data collected in the watershed 1999-2001 to be incorporated into the calibration of the watershed model.

These key features of the project will be discussed in more detail below. Chapter 2 provides a brief overview of the characteristics of the reservoirs and their watersheds. Chapters 3 and 4 discuss in detail the configuration and calibration of the HSPF model of the reservoir watersheds. Chapter 5 analyzes the water quality data collected in the reservoirs and explains the application of Maryland's water quality standards to the reservoirs. Chapter 6 discusses the configuration of W2 models of each reservoir, the alterations in the W2 model that were necessary to make it suitable for use in nutrient TMDLs, and calibration of the hydrodynamics, DO dynamics, and eutrophication kinetics in the reservoir models. Chapter 7 discusses model sensitivity to external loads and other aspects of the modeling framework that allow the framework to be used to determine nutrient and sediment TMDLs for the Patuxent reservoirs.

2.0 DESCRIPTION OF THE TRIADELPHIA AND ROCKY GORGE WATERSHEDS

2.1 General Features of Triadelphia and Rocky Gorge Reservoirs

Both Triadelphia Reservoir and Rocky Gorge Reservoir (also referred to as the Patuxent Reservoirs) lie in the Patuxent River watershed. Figure 2.1-1 shows the location of the reservoirs. The Patuxent River drains into Chesapeake Bay between Washington, DC and Annapolis, MD. The portion of the watershed draining to the reservoirs lies primarily in Howard and Montgomery Counties, but also includes a small portion of Prince George’s County. Both reservoirs are part of the Washington Suburban Sanitary Commission’s (WSSC) water supply system for Montgomery and Prince George’s Counties. Water supply intakes in Rocky Gorge Reservoir feed WSSC’s Patuxent River Filtration Plant near Burtonsville, MD. Triadelphia Reservoir, which is upstream of Rocky Gorge Reservoir, is used as a secondary reservoir to maintain capacity in Rocky Gorge Reservoir. Several relevant statistics for Triadelphia Reservoir and Rocky Gorge Reservoir are provided below in Table 2.1-1.

Table 2.1-1. Current Physical Characteristics of Triadelphia and Rocky Gorge Reservoirs

Characteristic	Triadelphia	Rocky Gorge
Location:	Howard County, MD Montgomery County, MD Lat. 39° 11’ 36” N Long. 77° 00’ 18” W	Howard County, MD Montgomery County, MD Prince George’s County MD Lat. 39° 07’ 00” N Long. 76° 52’ 36” W
Surface Area:	800 acres (34,848,000 ft ²)	773 acres (33,672,000 ft ²)
Normal Reservoir Depth:	52.0 feet	74.0 feet
Purpose:	Water Supply Recreation	Water Supply Recreation
Basin Code:	02-13-11-08	02-13-11-07
Volume:	19,000 acre-feet	17,000 acre-feet
Drainage Area to Reservoir:	77.3 mi ² (49,500 acres)	132 mi ² (84,480 acres)
Average Discharge ¹ :	82.4 ft ³ s ⁻¹	85.9 ft ³ s ⁻¹

Source: Inventory of Maryland Dams and Hydropower Resources (Weisberg et al. 1985).

¹ Water Resources Data Maryland and Delaware Water Year 2000 (USGS 2000).

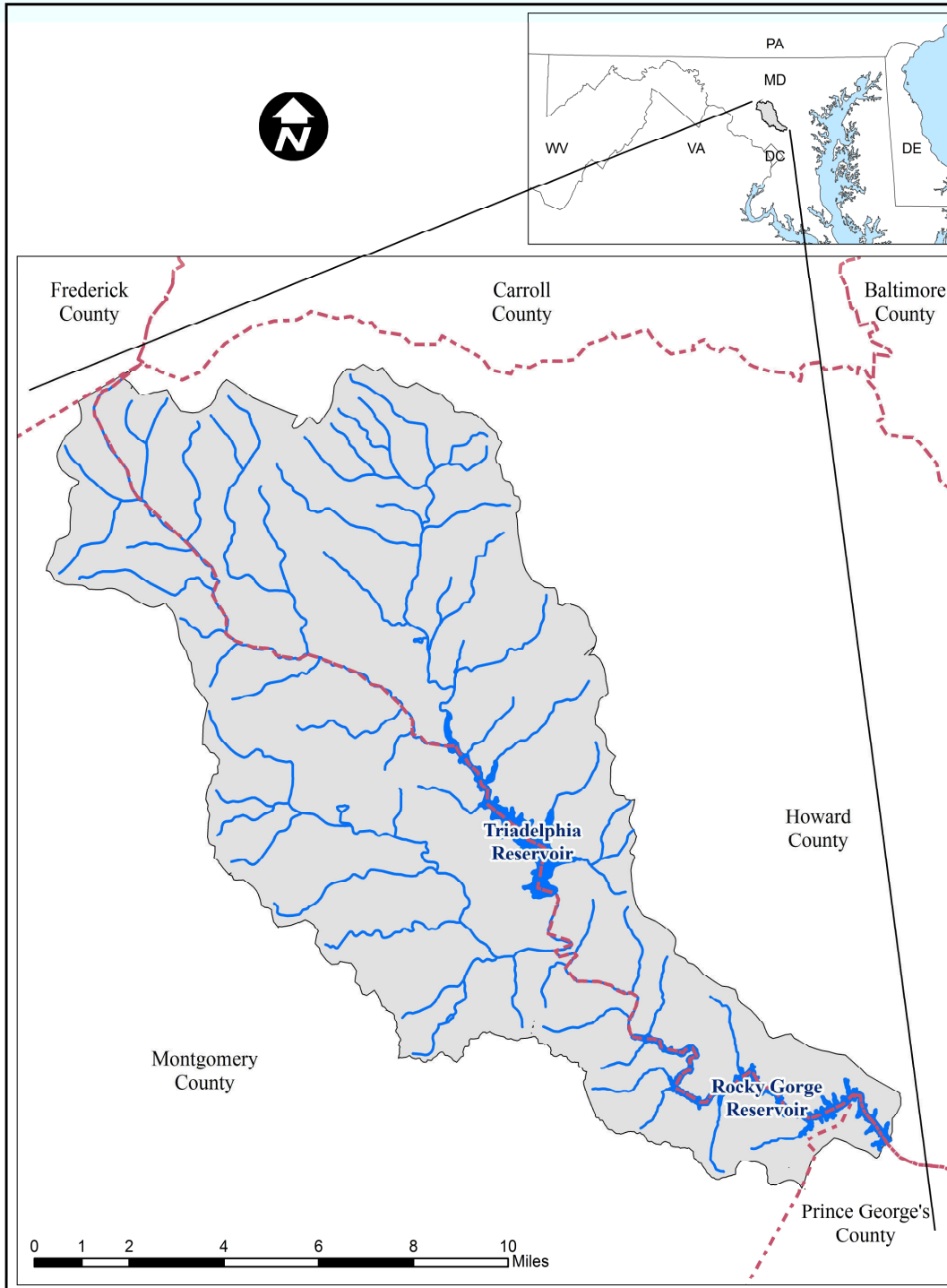


Figure 2.1-1. Location of Triadelphia and Rocky Gorge Reservoirs

Table 2.2-1. Summary Statistics Meteorological Data Clarksville, 1971 – 2000

Month	Normal Maximum Temperature (°F)	Normal Minimum Temperature (°F)	Normal Temperature (°F)	Normal Monthly Precipitation (in.)
January	40.7	22.0	31.4	3.42
February	45.0	23.5	34.3	2.97
March	54.5	31.1	42.8	4.15
April	65.6	39.1	52.4	3.51
May	75.1	49.3	62.2	4.71
June	83.1	58.2	70.7	3.84
July	87.1	63.1	75.1	4.03
August	85.3	61.2	73.3	3.90
September	79.1	54.2	66.7	4.17
October	67.7	41.7	54.7	3.49
November	56.0	33.5	44.8	3.56
December	45.4	26.2	35.8	3.52
Annual	65.4	41.9	53.7	45.27

Reference: Maryland State Climatologist Office (2007)

2.2 Climate

The climate of the region is humid, continental, with four distinct seasons modified by close proximity to the Chesapeake Bay. Table 2.2.-1 gives the mean, minimum, and maximum monthly temperatures and average monthly precipitation at Clarksville, in the northwest portion of the watershed. The prevailing direction of storm tracks is from the west-northwest from November through April with the prevailing direction shifting from the south in the month of May through September. The fall, winter and early spring storms tend to be of longer duration and lesser intensity than the summer storms. During the summer, convection storms often occur during the late afternoon and early evening producing scattered high-intensity storm cells that may produce significant amounts of rain in a short time span. Based on National Weather Service (NWS) data, thunderstorms occur approximately 30 days per year, with the majority occurring from May through August (Tetra Tech 1997).

2.3 Geology and Soils

The watersheds of Triadelphia and Rocky Gorge Reservoirs lie in the Piedmont physiographic province. The surficial geology is characterized by metamorphic rock of Late Precambrian age. The headwaters of the Patuxent River lie in the schists and meta-sedimentary rock of the Marburg formation. Almost all of the rest of the watershed lies

in the Wissahickon Formation of gniesses and schists. Upper Pelitic schist is the dominant bedrock of the headwaters of Cattail Creek and Hawlings River. Gneiss of the Sykesville Formation underlies the Patuxent River and Cattail Creek drainage to Triadelphia Reservoir, as well as Hawlings River. Lower Pelitic schist is the primary underlying bedrock of the direct drainage to Rocky Gorge and Triadelphia Reservoirs.

The soils found in the reservoir watersheds are primarily deep and well-drained to excessively drained (Mathews and Hershberger 1968; Brown and Dyer 1995). The dominant soil associations in the Rocky Gorge Reservoir watershed are the Glenelg-Manor-Chester and the Glenelg-Gaila-Occoquan associations. The Glenelg-Chester-Manor association forms the dominant soils of Cattail Creek and areas northwest of Triadelphia Reservoir, while the Mt. Airy-Glenelg-Chester association is dominant in the Patuxent River watershed draining into Triadelphia Reservoir. Mt. Airy soils belong to hydrologic group "A," while the rest of the dominant soils belong to group "B."

2.4 Land Use

Figure 2.4-1 shows the land use in the Triadelphia and Rocky Gorge watersheds. The land use is based on 1997 Maryland Department of Planning Land Use/Land Cover data. Triadelphia Reservoir watershed covers approximately 50,000 acres or 77 square miles. About half of the watershed is in crops or pasture, 32% in forest, and 15% in residential, commercial, or industrial land uses, as shown in Figure 2.4-2. The Rocky Gorge Reservoir watershed, excluding the drainage to Triadelphia Reservoir, covers approximately 34,000 acres or 53 square miles. Approximately 28% of the watershed is developed and 39% is forest, with the remainder in crops or pasture, as shown in Figure 2.4-3.

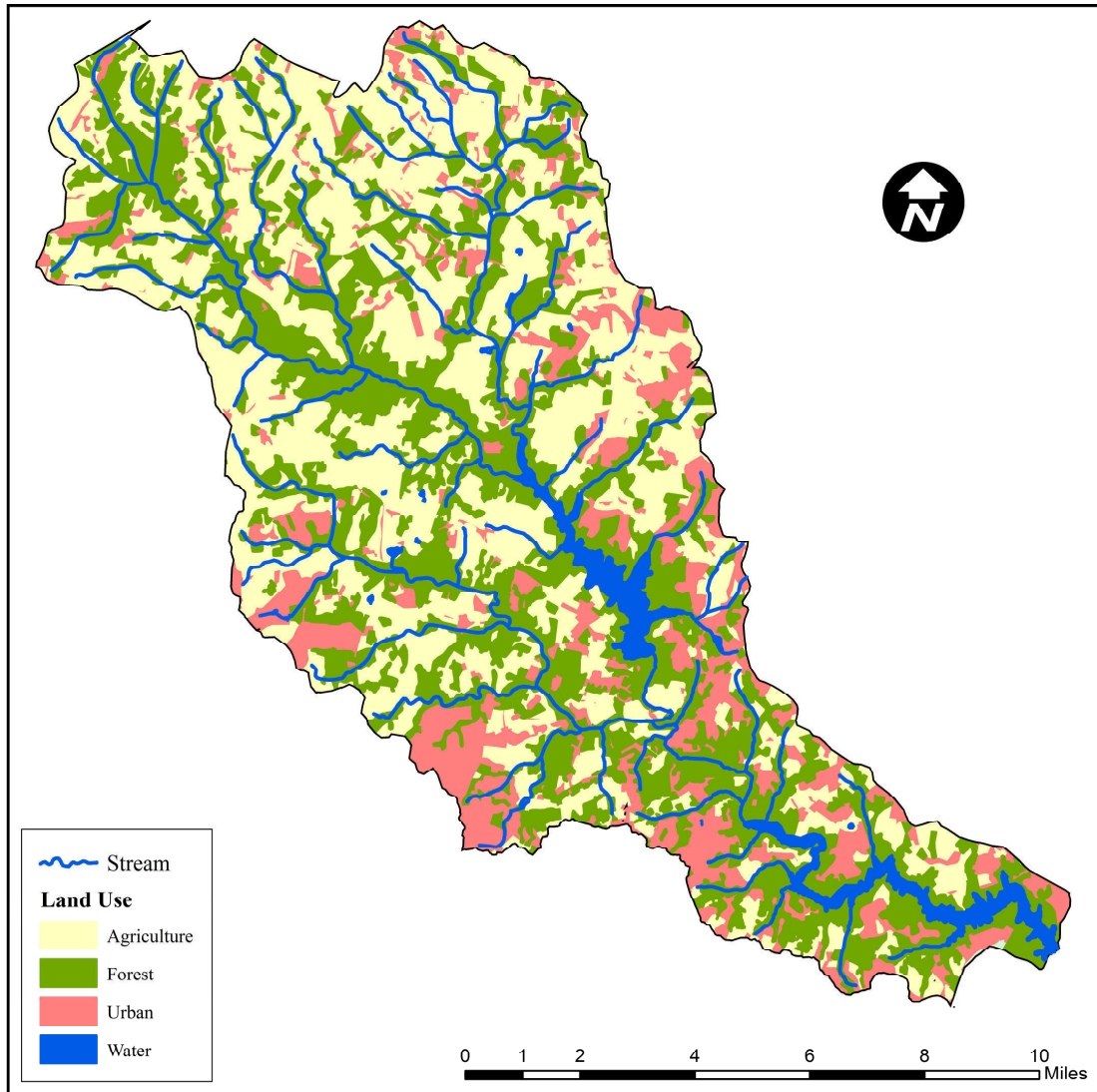


Figure 2.4-1 Land Use in the Patuxent Reservoirs Watershed

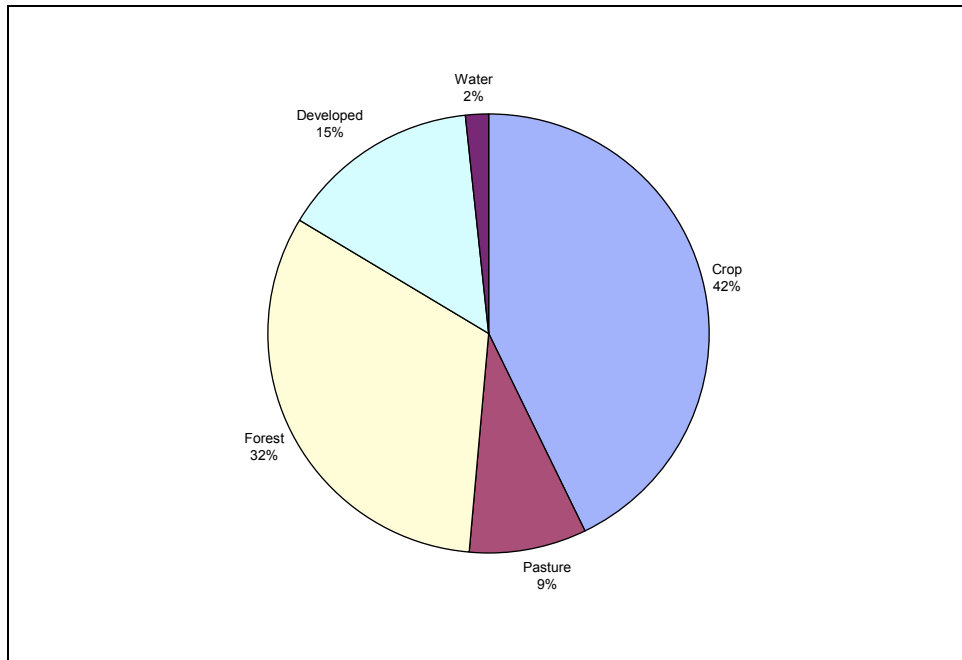


Figure 2.4-2: Proportion of Land Use in the Triadelphia Reservoir Watershed

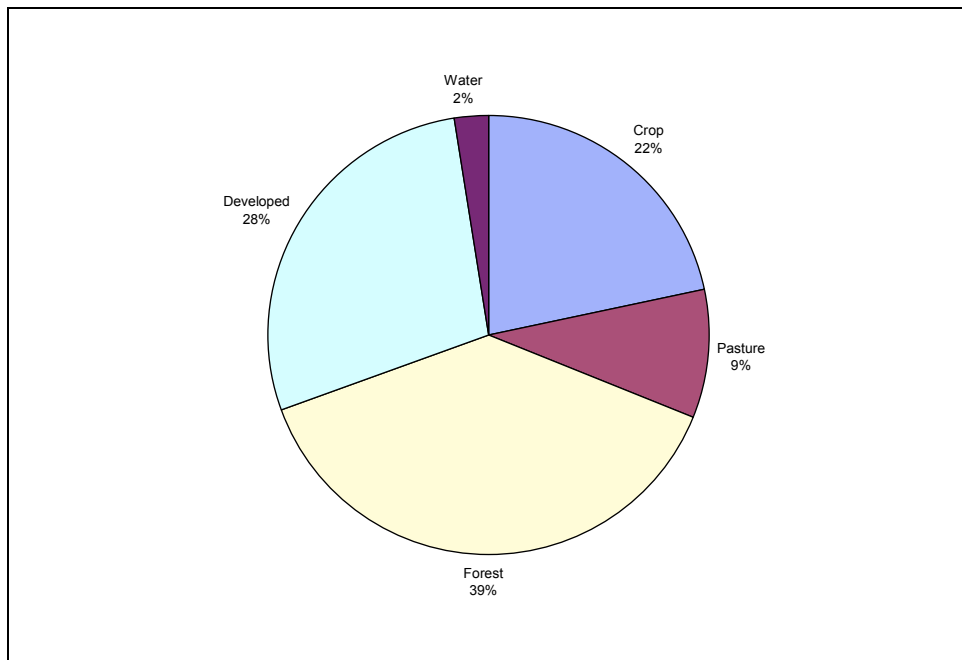


Figure 2.4-3: Proportion of Land Use in the Rocky Gorge Reservoir Watershed

3.0 OVERVIEW OF THE PATUXENT RESERVOIRS WATERSHED HSPF MODEL

3.1 Introduction

The modeling framework of the Patuxent Reservoirs watershed was developed primarily to provide loading estimates to the reservoir models for TMDL development, and secondarily to provide a tool to managers and planners to estimate the effects of various growth scenarios on nutrient loads. The framework consists of an HSPF (Hydrological Simulation Program—Fortran) watershed model to generate nutrient loads from the watershed subbasins, and a pair of two-dimensional CE-QUAL-W2 models to simulate hydrodynamics and water quality in Triadelphia and Rocky Gorge Reservoirs. The watershed model will be described in this and the following chapter. Subsequent chapters will describe the development and calibration of the reservoir models.

3.2. Overview of the Hydrologic Simulation Program Fortran (HSPF)

The HSPF Model simulates the fate and transport of pollutants over the entire hydrological cycle. Two distinct sets of processes are represented in HSPF: (1) processes that determine the fate and transport of pollutants at the surface or in the subsurface of a watershed, and (2) in-stream processes. The former will be referred to as land or watershed processes, the latter as in-stream or river reach processes.

Constituents can be represented at various levels of detail and simulated both on land and for in-stream environments. These choices are made in part by specifying the modules that are used, and thus the choices establish the model structure used for any one problem. In addition to the choice of modules, other types of information must be supplied for the HSPF calculations, including model parameters and time-series of input data. Time-series of input data include meteorological data, point sources, reservoir information, and other types of continuous data as needed for model development.

A watershed is subdivided into model segments, which are defined as areas with similar hydrologic characteristics. Within a model segment, multiple land use types can be simulated, each using different modules and different model parameters. There are two general types of land uses represented in the model: pervious land, which uses the PERLND module, and impervious land, which uses the IMPLND module. More specific land uses, like forest, crop, or developed land, can be implemented using these two general types. In terms of simulation, all land processes are computed for a spatial unit of one acre. The number or acres of each land use in a given model segment is multiplied by the values (fluxes, concentrations, and other processes) computed for the corresponding acre. Although the model simulation is performed on a temporal basis, land use information does not change with time.

Within HSPF, the RCHRES module sections are used to simulate hydraulics of river reaches and the sediment transport, water temperature, and water quality processes that result in the delivery of flow and pollutant loading to a bay, reservoir, ocean or any other body of water. Flow through a reach is assumed to be unidirectional. In the solution technique of normal advection, it is assumed that simulated constituents are uniformly dispersed throughout the waters of the RCHRES; constituents move at the same horizontal velocity as the water, and the inflow and outflow of materials are based on a mass balance. HSPF primarily uses the “level pool” method of routing flow through a reach. Outflow from a free-flowing reach is a single-valued function of reach volume, specified by the user in an F-Table, although within a time step, the HSPF model uses a convex routing method to move mass flow and mass within the reach. Outflow may leave the reach through as many as five possible exits, which can represent water withdrawals or other diversions.

Bicknell et al. (1996) discuss the HSPF model in more detail.

3.3. Model Assumptions

The simulation of the Patuxent Reservoirs watershed used the following assumptions: (1) variability in patterns of precipitation were estimated from existing National Oceanic and Atmospheric Administration (NOAA) meteorological stations; (2) hydrologic response of land areas was estimated for a simplified set of land uses in the basin; and (3) agricultural information was estimated from the Maryland Department of Planning (MDP) land use data and the 1997 Agricultural Census Data.

3.4 Watershed Segmentation

The HSPF model for the Patuxent Reservoirs watershed developed by Tetra Tech (2000) was the starting point for the development of segmentation for the current model. The segmentation of the Tetra Tech model was simplified by combining the multiple segments representing the watersheds for Cattail Creek, Hawlings River, the Patuxent River above Unity, and the Patuxent between Triadelphia and Rocky Gorge Reservoirs, into a single segment for each of the four watersheds. Segment 10, which represents Cattail Creek, terminates at the point of inflow to the reservoir. The segments representing smaller tributaries to the reservoirs and direct drainage were adopted unchanged from the Tetra Tech model. Figure 3.4-1 shows the new model segmentation.

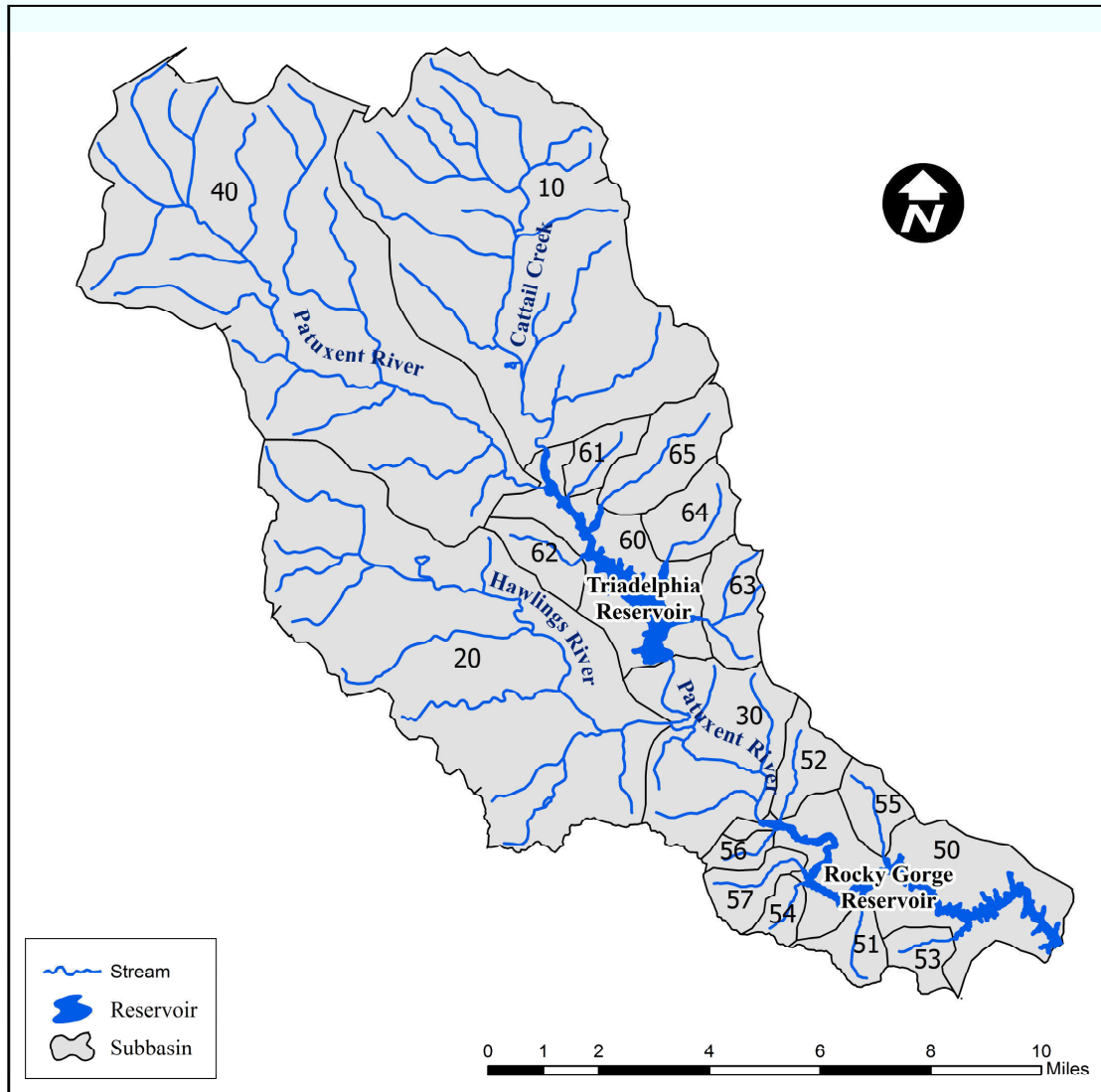


Figure 3.4-1: HSPF Model Segmentation

3.5 Land Use

The Tetra Tech HSPF model (2000) again provided the starting point for developing the land use for the current Patuxent Reservoirs Watershed Model. Table 3.5-1 shows Tetra Tech’s land use categories and the percent impervious land under each category. Land use acreages in the Tetra Tech model are based on the 1997 Maryland Department of Planning (MDP) land use.

Table 3.5-1 Reclassification of Tetra Tech (2000) Land Use

Tetra Tech Land Use	Percent Impervious	HSPF Model Land Use
Forest	0%	Forest
Agricultural Pasture	0%	Pasture
Agricultural Crop	0%	Hi-Till Crop Lo-Till Crop Hay
Low Density Residential	11%	Developed (Pervious) Impervious
Medium/High Density Residential	30%	
Commercial/Institutional/Industrial	80%	

The Chesapeake Bay Program Phase 4.3 Watershed Model land use categories were used in the Patuxent Reservoirs Watershed HSPF Model. Table 3.5-1 shows the Phase 4.3 land use categories. The Tetra Tech land use categories were converted to Phase 4.3 land use categories in the following steps:

1. The amounts of pervious and impervious land in the Tetra Tech residential, commercial, institutional, and industrial categories were calculated and aggregated into the Phase 4.3 categories for impervious and developed pervious land.
2. The Tetra Tech cropland was divided into conventional (high-till) crop, conservation (low-till) crop, and hay according to the proportion of these land uses in Segment 330 in the Phase 4.3 2000 Progress Scenario (Segment 330 represents the Patuxent watershed upstream of Duckett Dam); and
3. Phase 4.3 manure acres, which represent runoff from confined animal operations, were divided among model segments in proportion to the amount of pasture in each segment.

Table 3.5-2 shows the acreage of model land use by segment.

Table 3.5-2: HSPF Model Land Use By Segment

Segment	Developed	Forest	Hay	HT Crop	Impervious	LT Crop	Manure	Pasture
10	2,724	4,387	2,064	1,634	571	4,903	2	1,756
20	3,186	5,778	1,357	1,074	1,367	3,222	2	1,701
30	1,492	2,317	79	62	190	187	1	535
40	1,223	8,439	2,390	1,892	231	5,677	2	1,683
50	1,252	2,764	174	137	291	412	1	399
51	179	373	21	17	68	51	0	107
52	252	443	53	42	77	126	0	74
53	109	314	28	22	47	65	0	89
54	109	258	0	0	16	0	0	114
55	281	314	50	39	40	118	0	30
56	223	126	0	0	28	0	0	37
57	333	336	4	4	51	11	0	137
60	541	1,867	110	87	68	261	1	373
61	127	111	120	95	24	286	0	7
62	85	221	145	115	11	345	0	55
63	628	233	58	46	99	137	0	185
64	425	347	65	51	84	154	0	188
65	417	635	176	140	63	419	0	96

3.6 Nonpoint Sources

Nutrient loading rates were taken directly from the CBP Phase 4.3 Watershed Model 2000 Progress Scenario. Palace et al. (1998) documents how manure application rates to agricultural land and fertilizer application rates to both agricultural land and developed land were calculated in the Phase 4.3 Model. Wang et al. (1997) documents how atmospheric nitrogen loads were calculated in the Phase 4.3 Model.

According to the Phase 4.3 Model, only nitrate is discharged to receiving waters from on-site wastewater systems. Overall septic nitrate loads were taken from the Phase 4.3 Model 2000 Progress Scenario, and apportioned to model segments in proportion to the amount of pervious developed land in the segment. Table 3.6-1 shows the average annual septic load by segment.

Table 3.6-1: Average Annual Septic System Load By Segment

Segment	Septic Nitrate Load (lbs/yr)
10	11,228
20	13,135
30	6,151
40	5,040
50	5,159
51	739
52	1,037
53	447
54	450
55	1,157
56	920
57	1,371
60	2,231
61	524
62	352
63	2,590
64	1,753
65	1,718
Triadelphia	25,435
Rocky Gorge	30,565
Total	56,000

3.7 Point Sources

The development of nutrient TMDLs for Triadelphia and Rocky Gorge Reservoirs was based on computer simulation modeling of water quality conditions from 1998 to 2003. During that time, there was only one permitted facility discharging nutrients in the Triadelphia and Rocky Gorge watersheds, the Federal Management Agency Region 2 Wastewater Treatment Plant (WWTP) (MD0025666), which discharges into the Haulings River. Table 3.7-1 shows the annual phosphorus loads from this facility during the simulation period, 1998-2004.

Table 3.7-1. Annual Municipal Wastewater Treatment Plant Loads 1998-2003

Year	Federal Emergency Management Agency (MD0025666)			
	Flow (MGD)	PO4 ¹ (lbs/yr)	TOP ² (lbs/yr)	TP ³ (lbs/yr)
1998	0.001	2.92	0.37	3.29
1999	0	1.46	0.37	1.83
2000	0	0.37	0.37	0.73
2001	0	0.37	0.37	0.73
2002	0.001	2.19	0.37	2.56
2003	0.007	21.54	4.02	25.55
Average	0.0015	4.81	0.97	5.78

¹Phosphate

²Total Organic Phosphorus

³Total Phosphorus

There are no industrial sources permitted for discharging nutrients or sediments in the watershed of either reservoir.

3.8 Meteorological Data

The HSPF model needs hourly precipitation, potential evapotranspiration, wind speed, air temperature, dewpoint temperature, and cloud cover as meteorological inputs. After examining the performance of the model with different meteorological data sets, it appeared that the meteorological data from the CBP Phase 5 Watershed Model would yield the best hydrological calibration. The Phase 5 precipitation and temperature data are based on a regional regression of available data against latitude, longitude, and elevation. EPA (2008) explains the methodology in detail. The data have been prepared by county. Howard County meteorological data were used for all watersheds except Segment 20, Hawlings River, where the Montgomery County data set was used.

Potential evapotranspiration in the Phase 5 Model is calculated using the Hamon method from the Phase 5 temperature time series. Other time series in the CBP meteorological data set were taken from hourly observations at Dulles Airport in Herndon, VA. Additional documentation of the development of meteorological time series for the Phase 5 Model can be found in EPA (2008).

3.9 Model Calibration Data

3.9.1 USGS Flow Daily Flow Data

There were four active USGS gages in the Patuxent watershed upstream of Duckett Dam. Table 3.9-1 gives the name, gage number, drainage area, and modeling segment for each gage. Figure 3.9-1 shows their location. One of the gages is at the outflow of Brighton Dam and was not used to calibrate the HSPF model, but did provide flows to Segment 30, the mainstem of the Patuxent River below the dam. The other three gages were used to calibrate the HSPF model. The gage on Cattail Creek is not at the outlet of Segment 10, but during calibration the land use acreage was adjusted to match the location of the gage.

Table 3.9-1: USGS Gages in the Patuxent River Watershed

Gage ID	Name	Drainage Area (mi²)	Period of Record	Segment
01591000	Patuxent River near Unity	34.8	1944-	40
01591400	Cattail Creek near Glenwood	22.9	1978-	10
01591610	Patuxent River Below Brighton Dam	78.6	1980-	Inputs to 30
01591700	Hawlings River near Sandy Spring	27.0	1978-	20
01592500	Patuxent River near Laurel	132	1944-	Output to Rocky Gorge W2 Model

In addition to the four gages above the Rocky Gorge Reservoir, a fifth gage (01592500), at the outlet of Duckett Dam, was used to help calibrate the water balance in the CE-QUAL-W2 model of Rocky Gorge. See Section 6.3 for additional details.

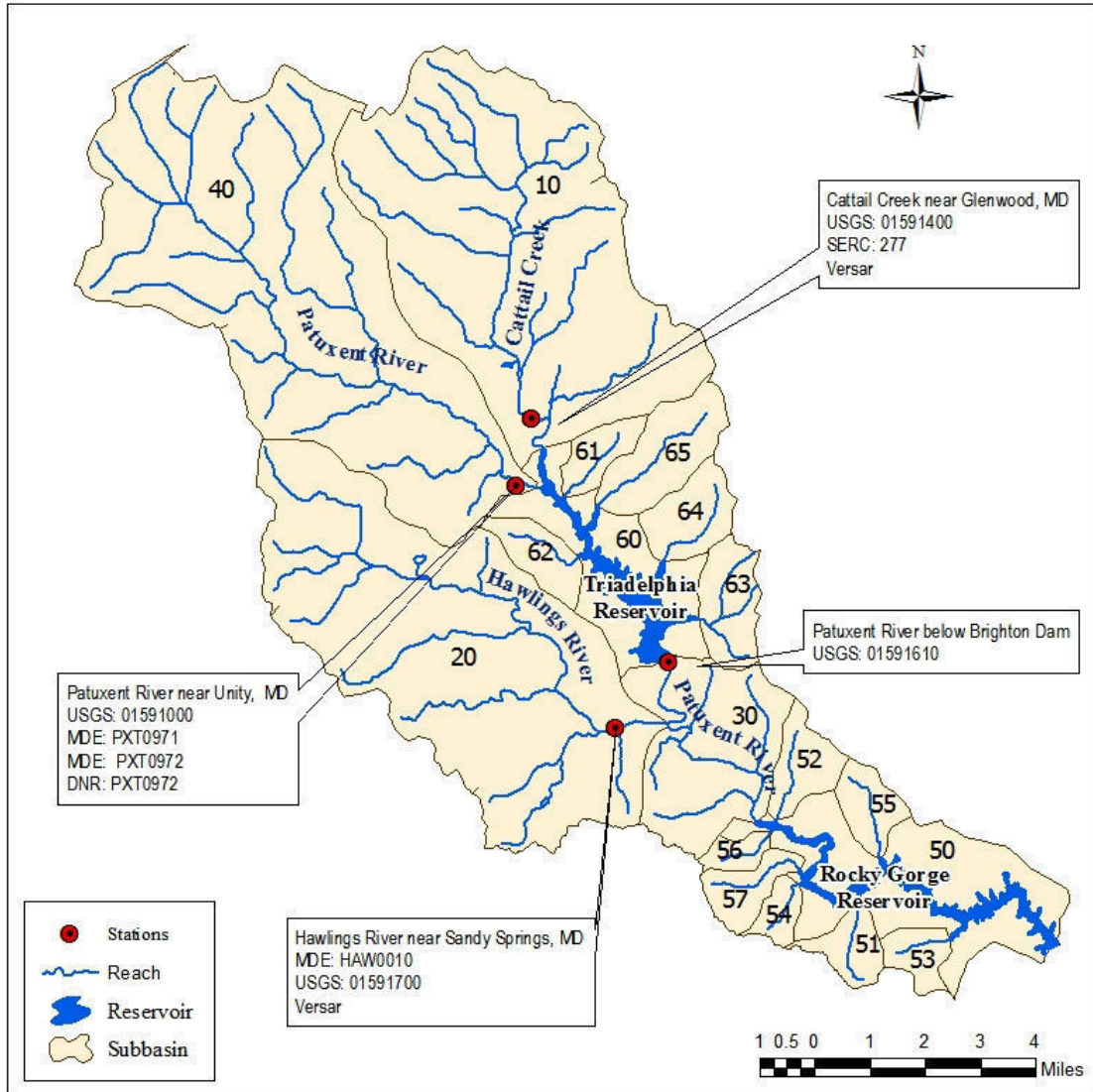


Figure 3.9-1: Location of USGS Gages and Water Quality Monitoring Stations

3.9.2 Water Quality Monitoring Data

The Patuxent Reservoir watersheds cannot be characterized as poor in monitoring data. During the watershed simulation period, 1997-2003, five different water quality monitoring programs operated: (1) Smithsonian Environmental Research Center (SERC), (2) USGS, (3) DNR, (4) MDE, and (5) Versar, Inc., operating on behalf of WSSC. Table 3.9-2 characterizes the monitoring programs. Figure 3.9-1 shows the location of the major water quality monitoring locations. The SERC monitoring program collected data at smaller watersheds not shown in Figure 3.9-1; otherwise, the sampling locations are at the USGS gages in the watershed.

Table 3.9-2: Characterization of Patuxent Reservoir Watershed Monitoring Programs

Program	Sampling Period	Approx. No. of Samples per Location	Description
SERC	8/97-8/99	105	Weekly flow-weighted composites
DNR	1/98* - present	82	Monthly ambient sampling
MDE	10/99-9/00	16	Monthly ambient sampling
USGS	9/85-9/01	531	Instantaneous storm and grab samples
Versar	10/98-9/01	122	Baseflow grab samples Three flow-weighted composite storm samples representing rising limb, falling limb, and peak flow

* Some overlap with USGS

Characterization of concentrations and loads of TSS and TP require monitoring during both low-flow and stormflow periods. USGS performs both baseflow and stormflow monitoring at their gage on the Patuxent River near Unity. Versar collects both baseflow and stormflow samples at Cattail Creek and Hawlings River. SERC also monitored Cattail Creek, in addition to several small subwatersheds in Cattail Creek and the Patuxent River above Triadelphia Reservoir.

Each of these programs has its eccentricities. USGS seems to have monitored storms only during odd-numbered water years, thus missing the wetter years like 1996 and 1998. SERC collected weekly flow-weighted samples, which in theory provide accurate weekly load estimates but are difficult to compare to model output. The monitoring data Versar collected were originally reported with incorrect sampling dates and detection limits, which made the data unusable. (It should be noted that Versar worked with two different laboratories and was not responsible for the original data transmission.) For this project, Thomas Jones of Versar corrected reported sampling dates and detection limits for their monitoring results, which enabled the data to be incorporated into the calibration of the watershed model. Versar also collected flow and temperature samples at 15-minute intervals on Hawlings River and Cattail Creek.

Table 3.9-3 shows the relevant constituents reported by each sampling program. Not all of the information reported could be used to help calibrate the model. In the baseflow samples collected by Versar, the majority of the samples analyzed for ammonia, phosphate, and BOD were below the high detection limits used in the analysis. Tetra Tech (2000) argued that the preservation methods used by SERC rendered their analysis of nutrient species suspect. Putting these caveats aside, while there are very few models that couldn't be improved with additional monitoring data, there is a sufficient amount of water quality monitoring data during the period 1997-2003 under variety hydrological conditions to calibrate the Patuxent Reservoir Watershed Model.

Table 3.9-3: Constituents Analyzed By Program

Parameter	USGS	DNR	MDE	VERSAR	SERC
5-day Total BOD	X	X	X		
Active Chlorophyll <i>a</i>	X	X	X		
Dissolved Inorganic Nitrogen			X		
Dissolved Oxygen	X	X	X		
Dissolved Organic Nitrogen			X		
Dissolved Organic Phosphorus			X		
Dissolved Ammonia Nitrogen	X		X	X	X
Total Ammonia Nitrogen		X			
Dissolved Nitrite-Nitrate Nitrogen	X			X	
Total Nitrite-Nitrate Nitrogen	X	X			
Dissolved Nitrite Nitrogen	X		X	X	
Total Nitrite Nitrogen		X			
Dissolved Nitrate Nitrogen			X	X	X
Total Nitrate Nitrogen		X			
Particulate Inorganic Phosphorus			X		
Particulate Nitrogen	X		X		
Dissolved Phosphate Phosphorus	X		X	X	
Total Phosphate Phosphorus		X	X		X
Particulate Phosphorus	X		X		
Total Chlorophyll <i>a</i>			X		
Dissolved Nitrogen	X	X	X		
Dissolved Phosphorus	X	X	X	X	
Total Inorganic Phosphorus			X		
Total Kjeldahl Nitrogen (TKN)	X	X	X	X	
Total Nitrogen	X	X	X	X	X
Total Organic Nitrogen			X		X
Total Organic Phosphorus			X		X
Total Phosphorus	X	X	X	X	X
Total Suspended Solids	X	X	X	X	X

4.0 PATUXENT RESERVOIRS WATERSHED MODEL CALIBRATION

The simulation period of the Patuxent Reservoirs Watershed Model (PRWM) is 1997-2003. This period captures both the simulation period of the W2 models, 1998-2003, and the period within which SERC performed its watershed monitoring, as described in Section 3.9.

Table 4.0-1 shows the average annual flow and the ranking of the years according to the period of record at the USGS gage 01591000, the Patuxent River near Unity. The average annual flow over the 62-year period of record is 39 cfs. The average annual flows for the HSPF model simulation period, 1997-2003, and the W2 models simulation period, 1998-2003, are both 40 cfs, close to the long-term average. The simulation period contains a variety of hydrological conditions. Both the wettest year, 2003, and the driest year, 2002, are in the simulation period. 1999 was also a very dry year. 1997, 2000, and 2001 can be considered average years, within the first and third quartiles of annual flow for the period of record. 1998, an average year overall, had an extremely wet winter and spring followed by an extremely dry summer and fall.

Table 4.0-1 Average Annual Flow, Patuxent River near Unity

Year	Rank	Average Annual Flow (cfs)
1997	37	34
1998	21	43
1999	56	23
2000	38	33
2001	46	28
2002	62	17
2003	1	92
Average Annual Flow (cfs) 1944-2006		39
Average Annual Flow (cfs) 1997-2003		40
Average Annual Flow (cfs) 1998-2003		40

4.1 Hydrology Calibration

The hydrology calibrations were performed using version 5 of PEST, the model-independent parameter estimation software developed by J. Doherty (Doherty 2001). PEST determines the values of parameters that optimize a user-specified objective function. In these simulations, the objective function was the sum of the squares of the differences between daily observed and simulated flows. This is equivalent to maximizing the coefficient of determination (R^2) between observed and simulated flows.

Table 4.1-1 gives the key parameters adjusted in hydrology calibration. Each land use represented in HSPF has its own set of hydrology parameters. Comparing observed to simulated flows can help determine the best values of infiltration rates and baseflow

recession coefficient, but cannot, by itself, help distinguish the infiltration rates for different land uses, like forest, pasture, or cropland. In the development of the Chesapeake Bay Program Phase 5 Watershed Model, a set of rules relating the values of calibration parameters on different land uses was determined by best professional judgment. These rules were adopted for the calibration of the PRWM. The rules can be formulated in terms of the values of parameters for cropland. Table 4.1-2 gives the ratio of cropland parameters to other land uses. The seasonal distribution of monthly UZSN values, shown in Table 4.1-3, was also adopted from the Phase 5 Model. The calibration of the PRWM differed from the Phase 5 Model primarily in two respects. First, the ratio between UZSN and LZSN was allowed to vary; in the Phase 5 Model it had a fixed value for each land use. The rules specifying the variability of the ratio with land use, however, were adopted from the Phase 5 Model. These are given in Table 4.1-3. Second, the LZETP was also treated as a calibration parameter, varying monthly. Table 4.1-3 shows the monthly values of the LZETP as a function of the base rate for pasture and urban land.

Several storms were undersimulated in the initial phases of the calibration. An analysis of precipitation inputs from the CBP Watershed Model showed that in many cases CBP precipitation time series appeared to underestimate the magnitude of the storms. In these cases, daily precipitation collected at Brighton Dam or Duckett Dam were substituted for the original daily totals in CBP time series on an hourly basis, in proportion to the hourly precipitation in the CBP time series. Table 4.1-4 shows the substitutions made for the Howard County time series and Table 4.1-5 shows the substitutions made in the Montgomery County time series.

Table 4.1-6 gives the final hydrology simulation parameters used in the simulation. Table 4.1-7 shows the coefficient of determination for monthly flows, the overall bias, and stormflow and low flow volumes, as represented by the sum of flows greater than 90th percentile and less than the 50th percentile flows. Figures A.1 through A.4, A.5 through A.8, and A.9 through A.12 in Appendix A show, for Cattail Creek, the Patuxent River near Unity, and Hawlings River, respectively, (1) time series of simulated and observed daily flows, (2) scatter plots of daily flows, (3) scatter plots of monthly flows, and (4) comparative empirical cumulative distribution of flows over the simulation period.

The hydrology calibration shows reasonable agreement between daily average observed and simulated flows, especially given the extreme hydrological conditions during the simulation period. The agreement between observed and simulated flows on a monthly timescale is very good. All of the measures of simulated flow volume are within 10% of their observed counterparts except for low flows in Hawlings River.

Table 4.1-1 Key Hydrology Calibration Parameters

Parameter	Description
LAND_EVAP	PET adjustment (similar to pan evaporation coefficient)
INFILT	Base infiltration rate
LZSN	Lower zone soil moisture storage index
UZSN	Upper zone soil moisture storage index
AGWR	Baseflow recession coefficient
INTFW	Ratio of interflow to surface runoff
IRC	Interflow recession coefficient
LZETP	Evapotranspiration from lower zone storage
RETSC	Impervious surface retention storage

Table 4.1-2 Ratio of Cropland Parameters to Those for Other Land Uses

Land use	INFILT	LZSN	AGWR	INTFW	IRC	Max LZETP
Forest	1.6	1.0	1.0	1.25	1.0	1.1
Grasses	1.0	1.0	1.0	1.0	1.0	1.0
Pervious Urban	0.8	1.0	1.0	1.0	1.0	1.0

Table 4.1-3 Monthly Hydrology Parameters

Month	Fraction Max Crop UZSN	Fraction Max Crop LZETP	Grassland Base and Winter LZETP	Forest Base and Winter LZETP
Jan	0.6	0.1	0.1	0.1
Feb	0.6	0.1	0.1	0.1
Mar	0.6	0.1	0.1	0.1
Apr	0.6	0.1	Base	0.1
May	0.6	0.1	Base	Base
Jun	0.7	0.5*Base	Base	Base
Jul	0.95	0.67*Base	Base	Base
Aug	1.0	Base	Base	Base
Sep	1.0	Base	Base	Base
Oct	0.8	0.67*Base	Base	Base
Nov	0.7	0.5*Base	Base	0.1
Dec	0.65	0.1	0.1	0.1

Table 4.1-4. Revisions to the CBP Howard County Precipitation Time Series

Date	Howard CBP	Revised	Source
6/7/2003	1.09	1.91	Triadelphia
6/19/2003	0.30	1.36	Triadelphia
6/20/2003	0.58	0.72	Triadelphia
6/21/2003	0.22	0.39	Triadelphia
8/11/2003	0.69	1.17	Triadelphia
9/4/2003	0.36	0.60	Triadelphia
9/15/2003	0.18	0.44	Triadelphia
9/18/2003	1.61	2.60	Triadelphia

Table 4.1-5. Revisions to the CBP Montgomery County Precipitation Time Series

Date	Montgomery CBP	Revised	Source
6/23/1998	0.64	1.19	Triadelphia
6/22/2001	0.22	0.64	Rocky Gorge
6/23/2001	1.05	2.35	Rocky Gorge
3/6/2003	0.32	0.60	Rocky Gorge
6/13/2003	0.25	0.47	Triadelphia
9/18/2003	1.01	2.18	Rocky Gorge

Table 4.1-6 Hydrology Calibration Parameter Values

Parameter	10 Cattail Creek	40 Patuxent River near Unity	20 Hawlings River
LAND_EVAP	0.99	0.99	0.94
CCFACT	0.521	0.457	0.743
INFILT	0.066	0.070	0.036
LZSN	10.7	12.00	13.2
UZSN	3.00	3.36	3.67
AGWR	0.9678	0.938	0.954
INTFW	5.00	3.77	2.20
IRC	0.013	0.034	0.084
LZETP	0.99	0.99	0.98
RETSC	0.011	0.027	0.02

Table 4.1-7 Hydrology Calibration Results

Statistic	10 Cattail Creek	40 Patuxent River near Unity	20 Hawling River
Water Balance	102%	100%	103%
Flows < 50 th Percentile	100%	98%	134%
Flows > 90 th Percentile	98%	100%	90%
Daily R ²	0.67	0.70	0.71
Monthly R ²	0.83	0.83	0.82

4.2 Temperature Calibration

Inflow temperatures are an important factor in determining temperature dynamics and the dynamics of stratification in reservoirs. PEST was again used to help calibrate the simulation of water temperatures in river reaches. Because temperature can vary considerably during the day, the objective function used in the calibration was the sum of the differences between observed and simulated hourly temperatures. Table 4.2-1 shows the parameters varied during the calibration and the final calibration parameters for each reach with temperature monitoring data on it. Table 4.2-2 shows the coefficient of determination between observed and simulated hourly temperature at the calibration points.

Table 4.2-1. Temperature Calibration Parameters

Parameter	Description
CFSAEX	Solar radiation correction factor; fraction of exposed reach surface.
KATRAD	Longwave radiation coefficient.
KCOND	Conduction convection heat transport coefficient.
KEVAP	Evaporation coefficient.

Table 4.2-2. Temperature Calibration Parameter Results

Parameter	Segment		
	10	40	20
CFSAEX	0.0017	0.556	0.0075
KATRAD	19.0	19.8	18.9
KCOND	20.0	20.0	20.0
KEVAP	4.31	10.0	5.64
R2	0.85	0.89	0.85

4.3. Implementation of Sediment and Nutrient Dynamics In The Patuxent Watershed HSPF Model

HSPF is a modular simulation program. The user can choose how to simulate constituents by turning modules on or off. Table 4.3-1 lists the relevant modules available in HSPF.

In simulating nutrients, the primary choice is between using the PQUAL module or the AGCHEM modules, NITR and PHOS. The PQUAL module simulates user-specified constituents. The concentration of the constituent in eroded sediment, interflow, and baseflow is fixed by the user. The concentration of the constituent in runoff is determined by a simple build-up, wash-off model, which can also take into account the decay of the constituent on the land surface. In the AGCHEM modules, on the other hand, the nitrogen and phosphorus species are defined in the model. The AGCHEM modules keep a mass balance of nitrogen and phosphorus. Inputs, losses, and the transformation of one species to another are all explicitly simulated.

Table 4.3-1. Description of HSPF Subroutines

Subroutine	Description
MSTLAY	Solute transport (pervious land)
PQUAL	Build-up, wash-off, decay of constituent on surface; Fixed monthly concentrations in subsurface. For PERLND (pervious land)
IQUAL	Build-up, wash-off, decay of constituent on surface. For IMPLND (impervious land)
NITR	Full mass balance: nitrification, mineralization, vegetation uptake and cycling.
PHOS	Full mass balance: sorption, mineralization, vegetation uptake and cycling.
SEDMNT	Detachment, washoff, and storage of sediment. For PERLND (pervious land).
SOLIDS	Accumulation and washoff of solids. For IMPLND (impervious land).
NUTRX	Transformation of inorganic nitrogen and phosphorus by nitrification, denitrification, sorption, deposition, and scour.
OXRX	Oxygen dynamics: reoxygenation, BOD decay.
PLANK	Phytoplankton dynamics and organic nutrient cycling.
SEDTRN	Deposition, scour and transport of sediment.

Following the CBP Phase 4.3 Watershed Model and previous MDE HSPF models, the AGCHEM module NITR was used to simulate nitrogen species on all pervious land uses. PHOS, on the other hand, was used to simulate phosphorus species on crops and hay; PQUAL was used to simulate phosphorus on forest, pasture, and pervious developed land. As will be explained in Section 4.4, PQUAL was also used to simulate baseflow TP loads for all land uses. IQUAL, the impervious equivalent to PQUAL, is the only choice for simulating nutrients on impervious surfaces. Full nutrient cycling of inorganic and organic nutrient species, including plankton dynamics, was simulated in river

reaches. Table 4.3-2 summarizes the constituents simulated and the modules used to simulate them.

Table 4.3-2 HSPF Subroutines Used in the HSPF Model by Land Use and Constituent

Land Use	Ammonia	Nitrate	Organic N	Total P	BOD	DO	Chla	Sediment
Cropland	NITR	NITR	NITR	PHOS	PQUAL			SEDMNT
Pasture	NITR	NITR	NITR	PQUAL	PQUAL			SEDMNT
Forest	NITR	NITR	NITR	PQUAL	PQUAL			SEDMNT
Pervious Urban	PQUAL IQUAL	PQUAL IQUAL	PQUAL IQUAL	PQUAL IQUAL	PQUAL IQUAL			SEDMNT SOLIDS
Impervious Urban	PQUAL IQUAL	PQUAL IQUAL	PQUAL IQUAL	PQUAL IQUAL	PQUAL IQUAL			SEDMNT SOLIDS
River Reach	NUTRX	NUTRX	PLANK	NUTRX PLANK	OXRX	OXRX	PLANK	SEDTRN

Model parameters affect the speciation of nutrients lost from pervious land. Nutrient speciation, however, has added complications for the following three reasons:

1. The reservoir TMDLs will be expressed in terms of total phosphorus. It is therefore important to preserve a mass balance of total phosphorus throughout the simulation.
2. There is a mismatch between the nutrient species simulated in NITR and PHOS modules for pervious land and the nitrogen and phosphorus species simulated in river reaches. NITR simulates labile organic nitrogen; PHOS simulates organic phosphorus in total and only as attached to sediment; NUTRX does not explicitly simulate labile organic nitrogen or phosphorus, although they are implicitly simulated as part of the BOD state variable.
3. THE CE-QUAL-W2 does not simulate organic nitrogen or organic phosphorus as separate state variables; it simulates organic matter in various forms (labile, refractory, particulate, and dissolved) with fixed stoichiometry of nitrogen and phosphorus, and BOD, also with fixed stoichiometry of nitrogen and phosphorus.

Because of these constraints, the inputs of organic matter to the reservoir were set in the following way:

1. All organic matter inputs were calculated on the basis of organic phosphorus.
2. Organic phosphorus from the land simulation was divided between BOD and organic refractory phosphorus (ORP) in the river reaches. BOD was used to represent dissolved organic matter and ORP was used to represent particulate organic matter.

3. The oxygen content of BOD was determined by comparison with limited in-stream monitoring data; the oxygen content of ORP was determined by the reservoir DO calibration.
4. Organic nitrogen, although simulated, was not used to calculate input loads to the reservoir models.
5. The nitrogen content of the simulated organic matter entering the reservoir was determined by setting the stoichiometry of the reservoir organic matter.

The matching of HSPF nutrient species outputs to QUAL-W2 inputs is described in more detail in Chapter 6.

4.4 Sediment and Nutrient Target Loads

The purpose of the Patuxent Reservoirs Watershed HSPF Model is, first, to determine the sediment and nutrient loads to Triadelphia and Rocky Gorge Reservoirs, and second, to determine the sources of the loads to the reservoirs, primarily in terms of land use. To facilitate these goals, the PRWM was calibrated primarily to target loads. The following three types of target loads can be distinguished:

1. Edge-of-Field (EOF) Loads: These loads represent the amount of constituent lost from a field per unit time. It is primarily used to characterize sediment loads, since sediment losses can be measured from a field and losses from a field can be estimated using accepted techniques like the Universal Soil Loss Equation (USLE) or its descendent, the revised Universal Soil Loss Equation (RUSLE).
2. Edge-of-Stream (EOS) Loads: The EOS load is the load delivered to the represented river or stream from the land segments. Not all of the EOF sediment load is delivered to the stream or river. Some of it is stored on fields down slope, at the foot of hillsides, or in smaller rivers or streams that are not represented in the model. For constituents like nitrogen or phosphorus, most empirical loading estimates are derived from studies of small homogeneous watersheds and therefore represent EOS loads at that scale.
3. Total Loads: The total load is the load determined at the watershed outlet.

The total load is the sum of the EOS loads plus or minus gains or losses from in-stream processes or other erosion processes not accounted for in EOF loads, such as gully erosion. EOS loads can be represented as a fraction of the EOF loads. For sediment, the ratio of the sediment load at a watershed outlet to the EOF load generated in the watershed is the sediment delivery ratio. The EOS sediment load can therefore be represented as the product of the EOF load and the sediment delivery ratio.

In addition to the target loads mentioned above, target concentrations were used to calibrate baseflow phosphorus concentrations.

4.4.1. Sediment EOF Targets

One of the main goals in revising the HSPF model is to calibrate the model so that the EOF loads for sediment and the EOS loads for nutrients are in greater agreement with the load estimates used in the Chesapeake Bay Program. CBP load estimates by land use are key ingredients in Maryland’s tributary strategies to reduce nutrients and sediment loads to the Bay. MDE has used CBP target loads from the Phase 5 Watershed Model to develop sediment TMDLs for non-urban watersheds. MDE is also hoping to use the Phase 5 Model as a basis for developing nutrient TMDLs.

The Phase 5 Model, like its predecessors, sets target agricultural sediment EOF loads based on the National Resource Inventory (NRI) survey of erosion rates on crop and pasture. The survey gives average annual erosion rates by county. The Phase 5 targets for Howard County were used in the PRWM, because the Patuxent watershed occupies a larger percentage of Howard County than Montgomery County, and the Howard County rates are more likely to be typical of erosion rates in the watershed. Table 4.4-1 shows the target loads by land use for agricultural land. The target EOF annual average erosion rate for forest was derived from NRI estimates of watershed erosion rates used in Phase 2 of the CBP Watershed Model, which have continued to be used, at smaller scales, in the Phase 5 CBP Watershed Model. For forests, the average of the Howard and Montgomery County rates was used, because, unlike the agricultural rates for the two counties, the forest erosion rates were significantly different.

Calibration targets for developed land were derived from average event mean concentrations reported for monitoring performed as part of the Phase I MS4 permits for Maryland counties. Table 4.4-2 gives the average EMCs for modeled constituents, including sediment. The EMCs were used to derive calibration target annual average loads by multiplying the EMC by the average annual runoff, as simulated in the model. Pervious and impervious land had the same calibration targets.

EOS loads for these land uses were determined by applying a sediment delivery ratio based on watershed size, using the following formula:

$$\text{Sediment Delivery Ratio} = 0.417762 * (\text{Watershed Area})^{-0.134958} - 0.127097$$

(SCS,1983)

Table 4.4-3 gives the sediment delivery ratio for each segment. The relevant area was taken to be either the calibration point for the segment or the reservoirs themselves.

Table 4.4-1 Target Loads For Agricultural Land Uses

Land Use	Sediment EOF (tons/year)	TP EOS (lbs/yr)	NH4 EOS (lbs/yr)	NO3 EOS (lbs/yr)
Hi-Till Crop	7.89	1.98	1.6	14.8
Low-Till Crop	4.73	1.24	1.0	16.9
Hay	1.69	0.732	0.2	5.0
Pasture	1.28	0.565	0.9	5.0

Table 4.4-2. Average EMCs Derived From Maryland NPDES Stormwater Permits (Bahr, 1997)

Constituent	Average Event Mean Concentration (mg/l)
Total Suspended Solids	66.6
Total Phosphorus	0.33
Nitrate	0.85
TKN	1.94
BOD	14.44

Table 4.4-3 Sediment Delivery Ratios

Segment	Area (mi ²)	Sediment Delivery Ratio
10	28.19	0.14
20	27.64	0.14
30	7.60	0.19
40	33.65	0.13
50	8.48	0.19
51	1.27	0.28
52	1.67	0.26
53	1.05	0.29
54	0.78	0.31
55	1.36	0.27
56	0.65	0.32
57	1.37	0.27
60	5.17	0.21
61	1.20	0.28
62	1.53	0.27
63	2.16	0.25
64	2.05	0.25
65	3.04	0.23

4.4.2 Target Total Phosphorus EOS Loads

Target TP EOS loads were established based on land use and transport path—sediment, runoff, interflow and baseflow. Table 4.4-4 gives a summary of the target load by land use and transport path.

Table 4.4-4: Source of TP Calibration Targets by Land Use and Flow Path

Land Use	Surface	Interflow	Baseflow
Hi-Till Crop Lo-Till Crop Hay	Calibrated to CPB Phase 5 EOF Targets for Howard Co.		Idealized seasonal concentrated weighted by contribution to surface/interflow TP loads
Pasture	Soil P concentration McElroy et al. (1976) ¹	Calibrated so overall load matches EOF Targets for Howard Co.	
Forest	Soil P concentration McElroy et al. (1976) ¹	Omernik (1977) ²	
Developed (pervious)	Soil P concentration McElroy et al.	Average MD MS4 Concentration	
Impervious	Average MD MS4 Concentration	Not Applicable	Not Applicable

¹ McElroy et al. 1976. Loading Functions for Assessment of Water Pollution From Nonpoint Sources. EPA-600/2-76-151.

² Omernik, 1977. Nonpoint Source—Stream Nutrient Level Relationships: A Nationwide Study. EPA-600/3-77-105.

The specification of targets by transport path was necessary because it is not easy to calibrate the baseflow component of the AGCHEM module for phosphate. Very little of baseflow phosphate in the Phase 4.3 Model is derived from agricultural land. The National Eutrophication Study (Omernik 1977) strongly suggests that baseflow TP loads should increase with increasing percent of a watershed in agricultural use. Because a significant portion of the simulation period contains extremely dry conditions, it was decided to use PQUAL’s capacity to set monthly concentrations of a constituent in baseflow to simulate TP loads in baseflow. Idealized baseflow TP concentrations were determined for each watershed based on an analysis of monitoring data. Table 4.4-5 shows the idealized concentrations. These concentrations were then entered into PQUAL module in proportion to the stormflow TP load targets discussed below, so that each land use contributed to baseflow loads in proportion to its contribution to total loads.

Total phosphorus stormflow (runoff and interflow) EOS target loads for agricultural land were taken from the Phase 5 Watershed Model targets for Howard County. These targets are based on the anticipated nutrient loading rates and previous experience calibrating earlier versions of the CBP Watershed Model. Table 4.4-1 shows the target loads by land use. Although the Phase 5 Model is still under development, target TP EOS loads are not likely to change (G. Shenk 2007).

Table 4.4-5 Idealized Baseflow TP Concentrations (mg/l)

Months	Patuxent River near Unity	All other watersheds
November – April	0.01	0.02
May, October	0.02	0.035
June – September	0.03	0.05

Target EOS loads for total phosphorus for developed land were derived from average event mean concentrations of TP reported for monitoring performed as part of the Phase I MS4 permits for Maryland counties. Table 4.4-2 gives the average EMCs for modeled constituents, including TP. The EMCs were used to derive calibration target annual average loads by multiplying the EMC by the average annual runoff, as simulated in the model. Pervious and impervious land had the same calibration targets.

Stormflow TP load targets for forested watersheds were determined essentially as a loading function based on eroded sediment. The phosphorus load for forest is a product of eroded sediment, an enrichment factor of 2.0, and a soil phosphorus concentration. The minimum value soil phosphorus concentrations for the Maryland Piedmont region, 430 mg P/kg, as reported in McElroy et al. (1976), was used in the model. A similar approach was used for stormwater loads from pasture, except that the median concentration, 650 mg P/kg, not the minimum value, was used for the soil phosphorus concentration from pasture. Interflow concentrations of TP from forests were set at the average observed streamflow concentration in the Eastern U. S. as reported by Omernik (1977). Interflow concentrations for pasture were calibrated so that stormflow loads approximated the Phase 5 pasture load targets.

4.4.3 Target Nitrogen EOS Loads

Unlike phosphorus, the Phase 5 Model calibration targets for nitrogen had not been finalized at the time the Patuxent Watershed HSPF Model was calibrated. EOF targets for ammonia-N and nitrate-N for agricultural and developed pervious land were taken from the CBP Phase 4.3 Model's 2000 Progress Scenario. Table 4.4-1 shows the EOS nitrogen targets. No targets were used for organic nitrogen, because organic nitrogen loads to the reservoirs are dependent on organic phosphorus loads, as explained in Section 4.3.

Targets for impervious land were again based on the statewide average EMC from MD MS4 permits. Target concentrations were available for TKN and nitrate. Table 4.4-2 gives the average EMCs for TKN and Nitrate. Ammonia-N was taken to be 10% of the TKN value.

The original Phase 4.3 parameterization of forest land was carried over into the Patuxent HSPF Model, and changes in nitrogen export were assumed to be a function of changes in atmospheric deposition and hydrologic conditions.

4.4.4 Determination of Target Total Sediment and Phosphorus Loads Using ESTIMATOR

Phosphorus is the limiting nutrient in both reservoirs, and their nutrient TMDLs will be expressed in total phosphorus. Storm-driven sediment loads will transport much of the phosphorus loads to the reservoirs; Triadelphia Reservoir also has a sediment impairment

that will be addressed by a sediment TMDL. It is important, therefore, that the Patuxent Reservoirs Watershed Model represent storm loads of phosphorus and sediment accurately.

It is difficult to determine, however, the nutrient and sediment loads in storms, unless continuous monitoring is performed, because storm concentrations of nutrients and sediments are highly variable. It is generally agreed that concentrations of sediment and total phosphorus increase with flow. Concentrations vary, however, both between storms and within storms. Statistical inference is therefore necessary to determine storm loads from monitoring data.

The USGS has developed the software program, ESTIMATOR, for that purpose. ESTIMATOR calculates daily, monthly, or annual constituent loads based on observed daily average flows and grab-sample monitoring data. ESTIMATOR has been used to calculate nutrient and sediment loads for the RIM (River Input Monitoring) program for the Chesapeake Bay Program, as well as to estimate sediment and nutrient trends in the region. Cohn et al. (1989) and Cohn et al. (1992) give the theory behind ESTIMATOR. Langland et al. (2001, 2005) demonstrate the application of ESTIMATOR in the Chesapeake Bay Watershed.

ESTIMATOR contains three elements. The heart of ESTIMATOR is a multiple regression equation that relates the log of constituent concentrations to flow, time and season. The equation for C, the constituent concentration in mg/l, takes the following form:

$$\ln[C] = \beta_0 + \beta_1 \ln[Q] + \beta_2 \ln[Q]^2 + \beta_3 T + \beta_4 T^2 + \beta_5 \sin[2\pi T] + \beta_6 \cos[2\pi T] + \varepsilon$$

where Q is flow (cfs) and T is time (yrs).

The flow and time variables are centered so that terms are orthogonal. Regression relation is essentially a multivariate rating curve, which takes into account temporal trends and seasonal trends as well as trends in flow.

The second element is the use of a minimum variance unbiased (MVUE) procedure to obtain estimates of concentrations and loads from the log of constituent concentrations determined from the regression. Cohn et al. (1989) describe the motivations for using the MVUE procedure, as opposed to simpler methods.

The transformed constituent concentrations are combined with daily flows to estimate daily, monthly, and annual loads. Standard errors, confidence intervals, and standard errors of prediction can also be calculated.

In order for ESTIMATOR to provide good estimates of nutrient and sediment loads, monitoring data must be available over the range of flows for which loads are to be calculated. In particular, there must be monitoring data taken during storm events. As noted in Section 3.9, both the USGS and Versar have performed storm sample

monitoring in the Patuxent River watershed. Three monitoring locations are on reaches represented in the model: Cattail Creek, Hawlings River and the Patuxent River near Unity. ESTIMATOR was used to calculate the total load of suspended sediment and total phosphorus at these locations.

Because the time span of available data for Cattail Creek and Hawlings River was only three years, the time terms were not used in the regression equation for the loads for these watersheds. Two statistical models were used to represent the Patuxent River near Unity, (1) a regression equation with time terms that used all available data starting in 1985 and (2) a regression equation without time terms that used only the data starting in 1997. Tables 4.4-6 and 4.4-7 show the estimated coefficients, statistics, and average annual loads for the ESTIMATOR models of sediment and TP, respectively.

As the tables show, the two models for the Patuxent River give dramatically different results. The loads calculated using only the most recent data are considerably larger than the loads that use all the available data from 1985. The models using all the data tend to predict that constituent concentrations level off at high flows, as shown by the smaller or negative coefficients for the log flow squared. Almost all the difference in the two estimates occurs in their predictions for 2003, a very wet year.

Table 4.4-8 shows the average annual EOS sediment and TP loads, ESTIMATOR loads, and the difference between them, which must be accounted for by instream processes like streambank erosion. It also shows the yield of sediment or phosphorus by acre. The results for both types of ESTIMATOR models are shown in the table. Apart from land use, there is no reason to suspect that the Patuxent River watershed is radically different from the watersheds of either Cattail Creek or Hawlings River. They are similar in soils, topography, and geology, and it should be expected that sediment yields should be similar. The average annual sediment yield from the ESTIMATOR model using all available data is closer to that of the other watersheds, so that was used as a total sediment load target for the Patuxent River. For TP, on the other hand, the yield from the ESTIMATOR model using all the data is considerably smaller than that of the other two watersheds. Even the load from the second ESTIMATOR model is slightly smaller than the average annual EOS load for the Patuxent watershed. It is unlikely, however, that the Patuxent River is losing phosphorus instream while the Cattail Creek and Hawlings River are gaining it, especially since the river is gaining sediment from streambank erosion. For these reasons, the target total TP load for the Patuxent River near Unity was set at the EOS load plus 10% of the EOS load for the instream contribution. This target load is consistent with the assumptions used in the rest of the HSPF model and well within the confidence interval for the TP loads from the second ESTIMATOR model.

Tables 4.4-9, 4.4-10, and 4.4-11 show the results for ESTIMATOR models of ammonia-N, nitrate-N, and TN, respectively, in Cattail Creek, Hawlings River, and Patuxent River. Generally, the regression equations for nitrogen fit the data poorly and explained little of the variability in nitrogen concentrations. The ESTIMATOR models for the Patuxent River are marginally better than the other watersheds but still have significantly non-normal residuals. Perhaps surprisingly, the two types of ESTIMATOR models used for

the Patuxent River show much better agreement for nitrogen species than they did for sediment or phosphorus, but this is mainly because the constant term primarily determines the load estimate. The average annual loads determined by ESTIMATOR were not used as calibration targets for nitrogen in the Patuxent River Watershed Model.

Table 4.4-6. Coefficients of Regression Equation and Regression Statistics, Sediment

Coefficient or Statistic	Cattail	Hawlings	Patuxent (All Data)	Patuxent (‘97-‘01 Data)
Constant	2.8005	2.8065	3.2642	2.3416
Log Flow	1.0349	.9379	1.0946	1.4121
Log Flow ²	0.1246	.1384	-.0347	.2194
Time (years)			-.0358	
Time ²			.0054	
Sin (2 π *Time)	0.1607	.1299	.1137	-.7530
Cos(2 π *Time)	-1.04	-.9640	.1243	-.7516
Standard Error of Regression	1.34	1.32739	1.56123	1.15911
Number of Observations	144	144	414	87
Coefficient of Determination	44.4	42.0	43.5	64.0
Serial Correlation Coefficient	.3508	.35975	.41012	.33074
Probability Plot Correlation Coefficient	.99294	.99214	.99347	.99242
Average Annual Load (tons)	9,148	12,682	10,872	45,017

Table 4.4-7. Coefficients of Regression Equation and Regression Statistics, Total Phosphorus

Coefficient or Statistic	Cattail	Hawlings	Patuxent (All Data)	Patuxent (‘97-‘01 Data)
Constant	-2.7369	-2.9072	-2.8313	-3.6712
Log Flow	.7209	.5290	.8008	.7275
Log Flow ²	.1420	.1455	.0485	.1623
Time (years)			-.1053	
Time ²			.0091	
Sin (2 π *Time)			-.5001	-.6519
Cos(2 π *Time)			.0647	-.4644
Standard Error of Regression	.9831	.9400	.94154	.90835
Number of Observations	160	128	532	90
Coefficient of Determination	36.8	30.6	51.6	42.7
Serial Correlation Coefficient	.40381	.23978	.29199	.08611
Probability Plot Correlation Coefficient	.98606	.98830	.99431	.98667
Average Annual Load (lbs)	22,642	19,531	9,858	15,572

Table 4.4-8 Comparison of Sediment and TP Load Estimates in Patuxent River Watersheds

	Cattail Creek	Hawlings River	Patuxent River (All Data)	Patuxent River (1997-2001)
Area (acres)	14,872	17,688	21,536	21,536
Sediment (tons/year)				
EOS	5,286	4,986	6,923	6,923
ESTIMATOR	9,148	12,682	10,872	45,017
In-stream	3,862	7,696	3,949	38,094
Yield (tons/ac.)	0.62	0.72	0.50	2.09
Total Phosphorus (lbs/year)				
EOS	13,075	14,233	16,627	16,627
ESTIMATOR	22,642	19,521	9,858	15,572
In-stream	9,567	5,298	-6,769	-1,055
Yield (lbs/ac.)	1.52	1.10	0.46	0.72

Table 4.4-9. Coefficients of Regression Equation and Regression Statistics, Ammonia Nitrogen

Coefficient or Statistic	Cattail	Hawlings	Patuxent (All Data)	Patuxent ('97-'01 Data)
Constant	-3.1225	-3.2403	-3.9571	-4.3815
Log Flow	0.1682	0.1534	0.2952	0.2265
Log Flow ²	0.0457	-0.0429	0.0374	0.0667
Time (years)			-0.0445	
Time ²			0.0017	
Sin (2 π *Time)	0.0586	0.1302	0.1191	0.1572
Cos(2 π *Time)	-0.4718	-0.4828	-0.4189	-0.4349
Standard Error of Regression	1.06389	1.08991	0.92728	1.06798
Number of Observations	141	142	470	81
Coefficient of Determination	10.8	10.1	19.2	12.6
Serial Correlation Coefficient	0.27687	0.30961	0.33215	0.21657
Probability Plot Correlation Coefficient	0.95432	0.93002		0.98645
Average Annual Load (tons)	4,425	4,248	1,969	2,220

Table 4.4-10. Coefficients of Regression Equation and Regression Statistics, Nitrate Nitrogen

Coefficient or Statistic	Cattail	Hawlings	Patuxent (All Data)	Patuxent (‘97-‘01 Data)
Constant	0.6052	0.2377	0.8569	0.9492
Log Flow	-0.1857	0.0871	-0.0725	-0.0750
Log Flow ²	-0.0165	-0.1168	-0.0864	-0.1657
Time (years)			0.0022	
Time ²			-0.0011	
Sin (2 π *Time)	0.4965	0.4809	-0.0048	0.0815
Cos(2 π *Time)	-0.2122	-0.2987	-0.0106	0.0187
Standard Error of Regression	1.62125	1.33678	0.36970	0.24694
Number of Observations	142	143	507	91
Coefficient of Determination	6.3	12.7	25.3	73.5
Serial Correlation Coefficient	0.41063	0.40909	0.20500	0.33446
Probability Plot Correlation Coefficient	0.90681	0.93081	0.82093	0.99438
Average Annual Load (tons)	325,268	184,506	164,861	165,178

Table 4.4-11. Coefficients of Regression Equation and Regression Statistics, Total Nitrogen

Coefficient or Statistic	Cattail	Hawlings	Patuxent (All Data)	Patuxent (‘97-‘01 Data)
Constant	1.0512	0.6130	1.0494	1.0156
Log Flow	-0.0709	0.1558	0.0357	-0.0286
Log Flow ²	-0.0098	-0.0096	-0.0415	-0.0515
Time (years)			-0.0089	
Time ²			0.0007	
Sin (2 π *Time)	0.1826	0.2577	-0.0475	0.1806
Cos(2 π *Time)	-0.1961	-0.0343	-0.0873	-0.1256
Standard Error of Regression	1.06980	0.63171	0.30210	0.09474
Number of Observations	143	143	426	82
Coefficient of Determination	3.5	15.4	11.4	66.9
Serial Correlation Coefficient	0.45755	0.50556	0.34728	-0.04824
Probability Plot Correlation Coefficient	0.93118	0.95839	0.92338	0.80115
Average Annual Load (tons)	236,366	315,917	204,998	202,057

4.5 Sediment and Nutrient Calibration

The calibration of the simulation of sediments and nutrients was a two-stage process. First the land modules in the HSPF model were calibrated to their EOS targets. Tables A.1–A.4 in Appendix A show the average annual EOS loads by land use and segment for sediment, TP, ammonia, and nitrate, respectively. Generally, the EOS loads were successfully calibrated to their targets. In the case of TP loads from forest and pasture, which were determined by TP content of the eroded sediment, overall EOS loads were allowed to surpass their target values for segments directly draining into the reservoirs if the surface TP load was greater than the target EOS load. The smaller drainage area for the direct drainage segments implies a larger sediment delivery ratio and greater sediment yield, which also implies a greater yield for sediment-transported phosphorus.

For sediment and total phosphorus, the second stage of the calibration involved adjusting instream erosion rates and the phosphorus concentrations associated with them so that average annual sediment and phosphorus loads matched target loads. For ammonia and nitrate, the only instream calibration performed was adjusting the nitrification rate. Results of the instream calibration of total loads are given below.

4.5.1 Sediment Calibration

Figure A.13 compares the time series of monthly sediment loads determined with ESTIMATOR and the HSPF model for Cattail Creek. Figure A.14 shows a scatter plot of the same data. Figure A.15 shows a scatter plot comparing annual sediment loads from ESTIMATOR and the HSPF model. Figures A.16–A.18, and A.19–A.21 show the same plots for the Patuxent River near Unity and for Hawlings River, respectively.

As the time series show, sediment loads are dominated by the wet year 2003 and the first half of 1998. There is good agreement between ESTIMATOR and the HSPF model on an annual basis. There is some discrepancy in the timing of monthly loads, but the HSPF model captures a significant portion of the variability in monthly loads determined by ESTIMATOR for Cattail Creek and the Patuxent River.

Table 4.5-1 gives summary statistics comparing observed and simulated concentrations of sediment for Cattail Creek, the Patuxent River near Unity, and Hawlings River. Statistics for the HSPF model are based on all simulated output, not just on those dates when there are observations. Because no observations were made during 2003, it should be expected that distribution of simulated sediment concentrations dominate observed values; nevertheless, as the coefficients of determination show, the HSPF model captures some of the variability in the observed data.

Table 4.5-1. Summary Statistics Comparing Observed and Simulated Concentrations

SEG	STAT	Ammonia		NO3		Total Phosphorus		Sediment	
		OBS	MODEL	OBS	MODEL	OBS	MODEL	OBS	MODEL
10	MEAN	0.162	0.083	5.206	2.301	0.155	0.166	59.681	75.162
	STDEV	0.180	0.140	13.384	0.937	0.213	0.385	120.811	163.699
	MIN	0.000	0.000	0.020	1.008	0.010	0.006	1.000	0.001
	1STQ	0.100	0.013	1.553	1.793	0.051	0.020	5.000	0.053
	MED	0.100	0.025	3.268	2.107	0.098	0.034	13.000	2.792
	3RDQ	0.200	0.097	3.955	2.562	0.178	0.214	47.000	107.120
	MAX	1.000	2.242	92.165	12.949	1.625	12.434	584.000	3822.354
	COUNT	109	2556	109	2556	109	2556	109	2556
	R ²	0.12		0.28		0.17		0.23	
20	MEAN	0.155	0.107	2.650	1.791	0.133	0.123	62.351	86.951
	STDEV	0.186	0.096	6.719	0.877	0.163	0.202	126.290	164.131
	MIN	0.003	0.003	0.023	0.389	0.010	0.010	1.000	0.000
	1STQ	0.076	0.070	0.889	1.272	0.050	0.020	5.000	0.320
	MED	0.100	0.091	1.508	1.569	0.088	0.041	15.000	8.236
	3RDQ	0.133	0.118	1.909	2.089	0.150	0.147	57.750	107.199
	MAX	1.000	3.274	57.760	9.513	1.087	2.702	932.000	2661.553
	COUNT	107	2556	107	2556	107	2556	107	2556
	R ²	0.22		0.58		0.30		0.13	
40	MEAN	0.036	0.047	2.297	1.975	0.038	0.071	24.712	34.403
	STDEV	0.056	0.112	0.667	0.929	0.049	0.351	63.261	141.945
	MIN	0.001	0.000	0.109	0.491	0.003	0.005	0.300	0.000
	1STQ	0.010	0.004	1.932	1.488	0.016	0.017	3.000	0.014
	MED	0.017	0.011	2.356	1.786	0.023	0.024	5.225	0.373
	3RDQ	0.034	0.038	2.777	2.164	0.040	0.037	13.000	6.750
	MAX	0.380	2.231	3.608	9.768	0.351	14.778	400.500	3462.957
	COUNT	84	2556	162	2556	162	2556	164	2556
	R ²	0.02		0.04		0.18		0.40	

4.5.2 Phosphorus Calibration

Figure A.22 compares the time series of monthly phosphorus loads determined with ESTIMATOR and the HSPF model for Cattail Creek. Figure A.23 shows a scatter plot of the same data. Figure A.24 shows a scatter plot comparing annual TP loads from ESTIMATOR and the HSPF model. Figures A.25–A.27, and A.28–A.30 show the same plots for the Patuxent River near Unity and for Hawlings River, respectively. The version of the ESTIMATOR model with data restricted to the calibration period was used in the Patuxent River plots.

Just as in the case of sediment, phosphorus loads are dominated by the wet year 2003 and the first half of 1998. There is good agreement between ESTIMATOR and the HSPF model on an annual basis. There is some discrepancy in the timing of monthly loads but the HSPF model captures a significant portion of the variability in monthly loads determined by ESTIMATOR.

Table 4.5-1 gives summary statistics comparing observed and simulated concentrations of TP. As the coefficients of determination show, the HSPF model captures some of the variability in the observed data.

4.5.3 Ammonia and Nitrate Calibration

Options for calibrating nitrogen loads were limited. As explained earlier, because the state variables in the W2 models are organic material, organic nitrogen loads were tied to organic phosphorus, in order to keep a mass balance of phosphorus. The only instream calibration performed was the adjustment of nitrification so that simulated ammonia concentrations better match observed data. Even accounting for some large observed concentrations, Table 4.5-1 suggests that nitrate is undersimulated in Cattail Creek and the Patuxent River near Unity. The undersimulation of nitrate could only be addressed by increasing EOS loads, since the only instream process that could produce more nitrate, the conversion of organic nitrogen to ammonia and nitrate, was not available because of the constraint on organic nitrogen introduced by the W2 model. Because of the limited role nitrogen plays in the nutrient TMDLs, it was decided not to increase the EOS load of nitrate to try to match observed concentrations. As long as the simulated nitrate and ammonia loads are large enough that phosphorus remains the limiting nutrient, the simulation of algal growth in the W2 models is unaffected by the nitrogen load.

4.6 Phosphorus and Sediment Loads to the Patuxent River Reservoirs

Table A.5 in Appendix A shows the average annual total phosphorus load to Triadelphia Reservoir by source and segment for the period 1998-2003, the simulation period of the Triadelphia Reservoir W2 model. Table A.6 shows the total phosphorus load to Rocky Gorge Reservoir by source and segment, 1998-2003. Table A.7 shows the total sediment load to Triadelphia Reservoir by source and segment for the period 1998-2003.

Figures 4.6-1, 4.6-2, and 4.6-3 show the percent of the load by source for phosphorus loads to Triadelphia Reservoir, phosphorus loads to Rocky Gorge Reservoir, and sediment loads to Triadelphia Reservoir, respectively. Cropland is the dominant source of phosphorus in Triadelphia Reservoir watershed, followed by streambank erosion and gully erosion. Crops account for 50% of the load and off-field erosion accounts for 28% of the load. Not surprisingly, the crops and off-field erosion are the largest sources of sediment as well, accounting for 54% and 38% of the sediment load to Triadelphia Reservoir, respectively. The largest source of phosphorus to Rocky Gorge Reservoir is Triadelphia Reservoir, with 34% of the total load, followed by crops (24%) and

developed land (18%). The Triadelphia phosphorus load is taken from the output to the Triadelphia W2 model.

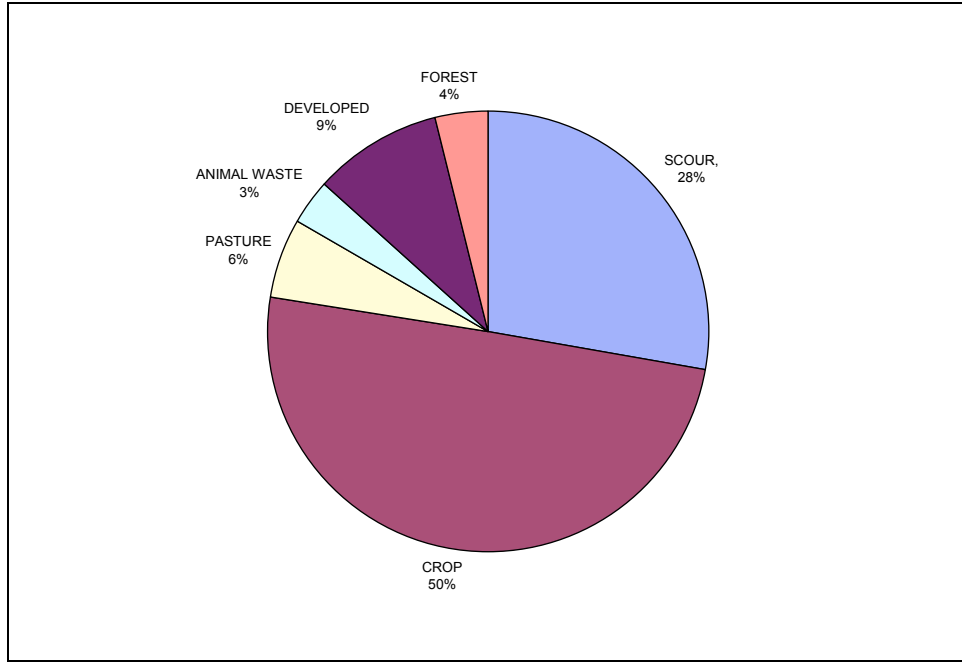


Figure 4.6-1: Percent Contribution of Sources to Total Phosphorus Loads to Triadelphia Reservoir

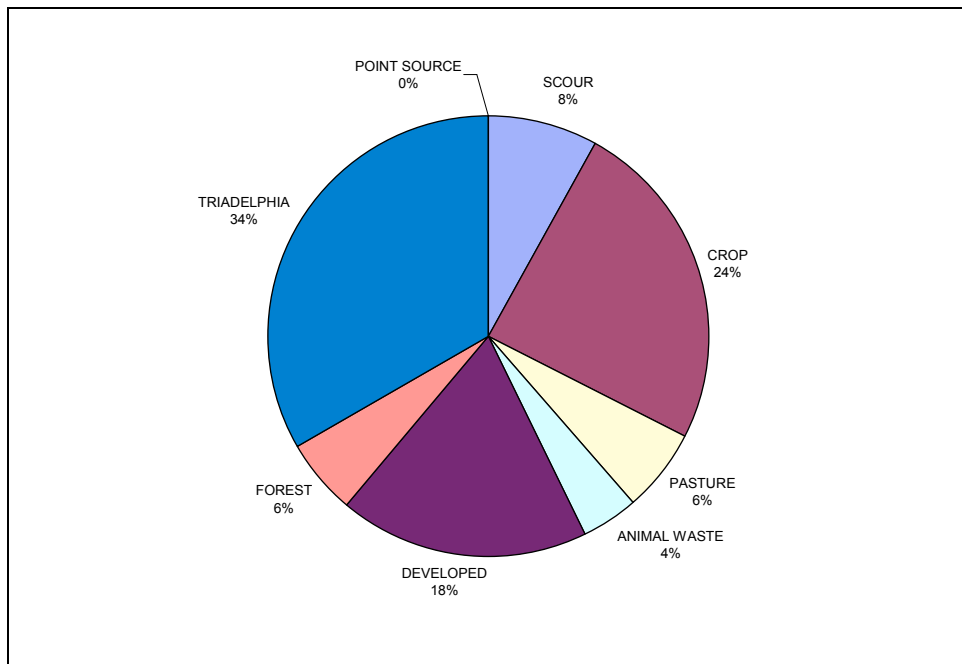


Figure 4.6-2: Percent Contribution of Sources to Total Phosphorus Loads to Rocky Gorge Reservoir

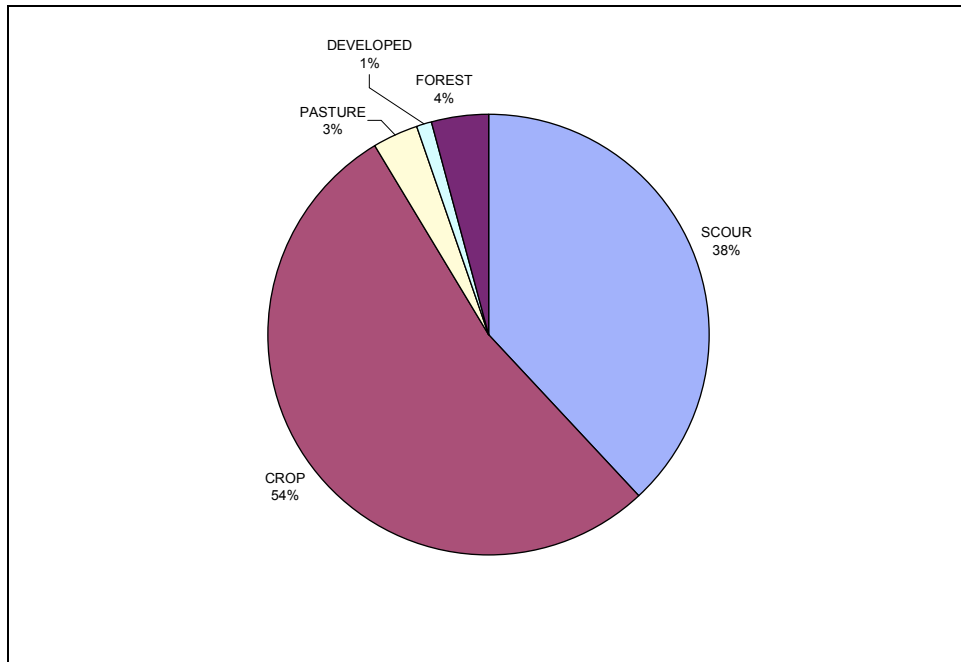


Figure 4.6-3: Percent Contribution of Sources to Sediment Loads to Triadelphia Reservoir

4.6.1 Comparison of HSPF Sediment and Phosphorus Loads with Load Estimates From Other Sources

Table 4.6-1 compares the simulated sediment and total phosphorus loads from the HSPF model with loads for comparable periods as estimated by SERC, Versar, Tetra Tech, and the CBP Phase 4.3 Progress Scenario.

The CBP estimate is for the average annual load over a ten-year period using the hydrology from 1985-1994. The average annual TP EOS load for the entire watershed above Duckett Dam is about two-thirds the load of the HSPF model. This is not surprising, since the crop target loading rates in the CBP Phase 5 Watershed Model, which were adopted for the Patuxent HSPF Model, are higher than the Phase 4.3 Model, and the forest target loading rate developed for the Patuxent HSPF Model is also higher than the Phase 4.3 loading rate.

The SERC loads are derived from weekly flow-weighted concentrations and weekly flows. The TP loads for Cattail Creek from the HSPF Model are within 10% of the load over the entire period monitored by SERC. Sediment loads from the HSPF Model are about 25% higher than the SERC loads over the same period. The differences between the SERC estimates and the HSPF Model are likely to be due in part to the fact that the HSPF Model's simulated flows do not perfectly match the observed flows used to calculate the SERC loads.

The Versar load estimates were determined by estimating event mean concentrations for baseflow and stormflow by year. Observed flows were separated into baseflow and stormflow, and the loads were estimated as the product of the observed storm or baseflow and appropriate event mean concentrations. The HSPF model shows considerable agreement with the load estimates for Cattail Creek from Versar, when taken in total over the period 1998-2001 in which Versar estimated loads. For Hawlings River, HSPF estimates of TP loads are almost twice as high as the Versar estimate; sediment loads are almost three times as high. The difference is due primarily to the load estimation methodology: ESTIMATOR, and the HSPF Model calibrated against it, assumes that concentration of constituents varies with flow, whereas the Versar estimates assume an average concentration by year.

Tetra Tech's load estimates are based on the original HSPF model used in their study of the Patuxent reservoirs. The HSPF model was calibrated to observed concentrations, primarily the SERC monitoring data. Generally, Tetra Tech's estimates of TP loads are significantly higher for calendar year 1997 and somewhat higher for 1998. Tetra Tech's estimates of sediment loads are higher for 1997 but lower for 1998. The difference between 1997 and 1998 loads are smaller for Tetra Tech's estimates than for the current HSPF model. It is not possible to analyze the possible source for the differences in load estimates, because Tetra Tech's estimates depend on the details of their HSPF calibration.

There are many different approaches to estimating loads based on flows and observed data. Each has its own strengths and weaknesses. When a statistically significant relation between flows and concentrations can be identified, as was the case here for sediment and phosphorus, the rating curve methodology, as used in ESTIMATOR, can make the best use of available data, and permits sound inferences beyond the time within which the data was collected.

Table 4.6-1 Comparisons of Sediment and Total Phosphorus Load Estimates By Study

Program	Watershed	Date	Sediment (Tons/yr)	TP (Lbs/yr)	Patuxent HSPF	
					Sediment (Tons/yr)	TP (Lbs/yr)
SERC	Cattail Creek	8/97-12/97	679	2,441	150	936
SERC	Cattail Creek	1998	8,900	29,732	12,478	34,846
SERC	Cattail Creek	1/99-8/99	688	3,247	388	2,696
Versar	Cattail Creek	WY 1999	2,865	9,900	912	5,356
Versar	Cattail Creek	WY 2000	1,972	10,700	3,177	14,756
Versar	Cattail Creek	WY 2001	1,471	12,400	2,921	12,336
Versar	Hawlings River	WY 1999	680	11,100	6,409	11,909
Versar	Hawlings River	WY 2000	4,288	6,200	6,059	13,891
Versar	Hawlings River	WY 2001	1,644	7,500	9,823	18,109
Tetra Tech	Patuxent River	1997	9,493	37,918	2,743	2,960
Tetra Tech	Patuxent River	1998	11,383	44,275	13,619	21,297
Tetra Tech	Cattail Creek*	1997	7,575	37,634	5,999	17,630
Tetra Tech	Cattail Creek*	1998	8,812	46,482	16,104	44,973
Tetra Tech	Hawlings River	1997	8,374	25,812	5,661	8,176
Tetra Tech	Hawlings River	1998	9,851	28,254	15,636	23,069
CBP	Total EOS Segment 330 Phase 4.3 Progress Scenario			50,020		75,215

* Includes watershed area below USGS gage.

5.0 WATER QUALITY CHARACTERIZATION OF TRIADELPHIA AND ROCKY GORGE RESERVOIRS

5.1 Water Quality Monitoring Programs

Both WSSC and MDE performed water quality monitoring in the reservoirs during the period 1998-2003. Table 5.1-1 summarizes the characteristics of the monitoring programs.

WSSC maintains a regular water quality monitoring program. Each reservoir is sampled at three locations. Figure 5.1-1 shows the locations monitored by WSSC in Triadelphia Reservoir and Figure 5.1-2 shows the locations in Rocky Gorge Reservoir. Sampling is performed monthly from March or April through October or November, and sometimes biweekly in the summer months. At each location, temperature and dissolved oxygen (DO) are measured at each meter of depth, and water quality samples are collected at the surface, bottom, and middle of the reservoir. If the reservoir is stratified, the middle sample is collected in the metalimnion; otherwise, it is collected at the midpoint of reservoir depth. Water quality samples are analyzed for ammonia, nitrite, nitrate, total Kjeldahl nitrogen, phosphate, total phosphorus, total organic carbon, chlorophyll *a*, iron, manganese, turbidity, and alkalinity. Secchi depth measurements are made at each sampling location.

MDE performed a special water quality monitoring study in support of TMDL development in 2000. Four locations were sampled in each reservoir, shown in Figures 5.1-1 and 5.1-2. Six samples were taken at approximately monthly intervals between March and September. Approximately five measurements of temperature and DO were taken at different depths at each monitoring location per sampling date. Water quality samples were taken from the surface and bottom at the location just upstream of the dam; otherwise samples were taken only at the surface at a depth of 0.5 m. MDE's samples are analyzed for the same constituents as WSSC's, but in addition, samples are analyzed for dissolved and particulate nitrogen, phosphorus, and organic carbon species, BOD5, and TSS.

Table 5.1-1: Characterization of Reservoir Monitoring Programs

Characteristic	WSSC	MDE
Collection Period	3/98-11/04	3/00-9/00
Number of locations per reservoir	3	4
Temperature and DO measurements	One per meter starting from surface	Approximately 5 from surface to bottom
Water quality samples per location	Surface, middle, and bottom	Surface only, except surface and bottom just above dams
Key water quality constituents	NH3, NO23, PO4, TKN, TP, TOC, Chla, Turbidity, Secchi depth	NH3, NO2, NO3, TKN, DON, PON, TN, PO4, POP, DOP, PIP, TP, CBOD, DOC, POC, TOC, Chla, TSS, Turbidity, Secchi depth

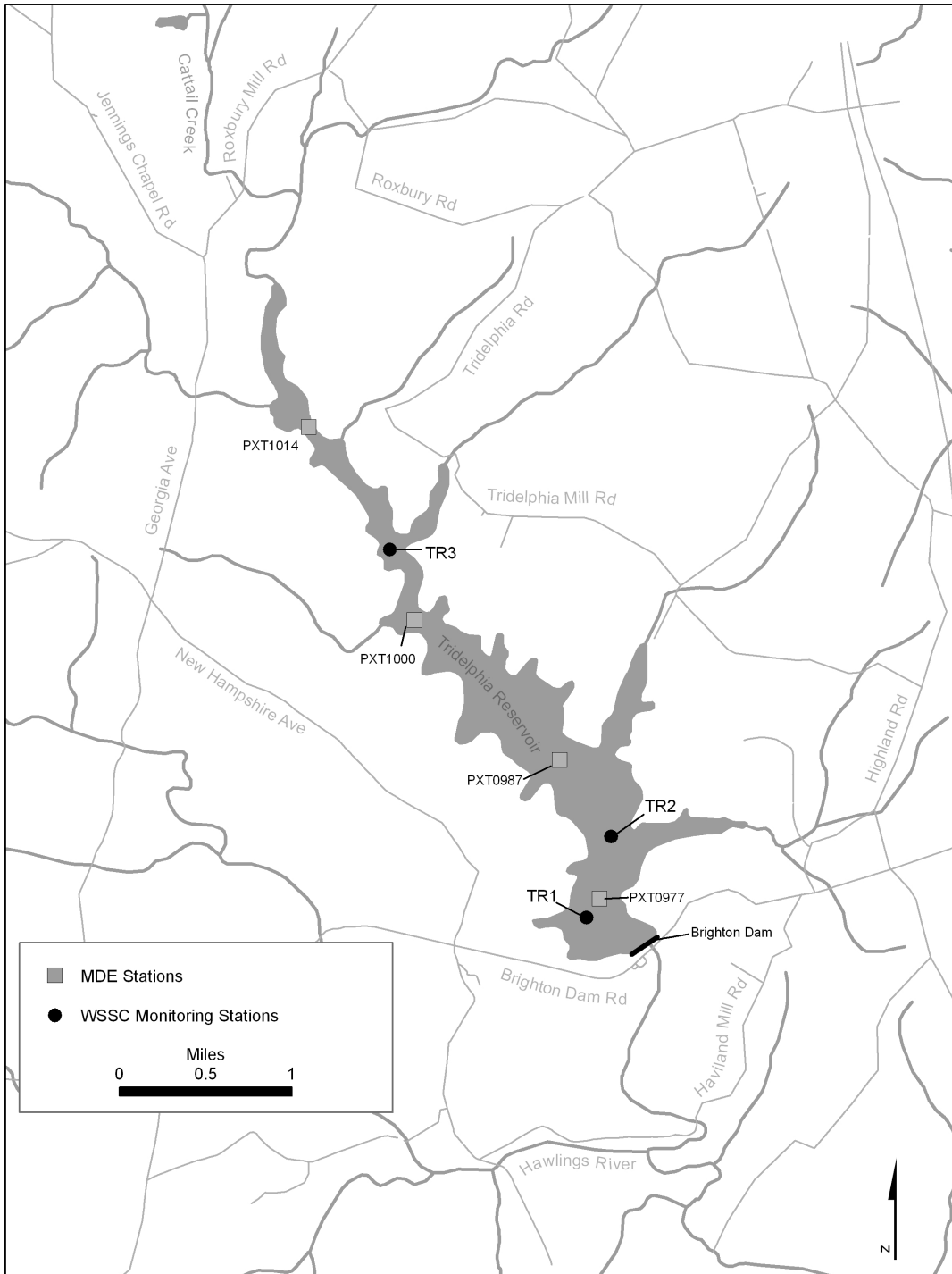


Figure 5.1-1: Sampling Locations in Triadelphia Reservoir

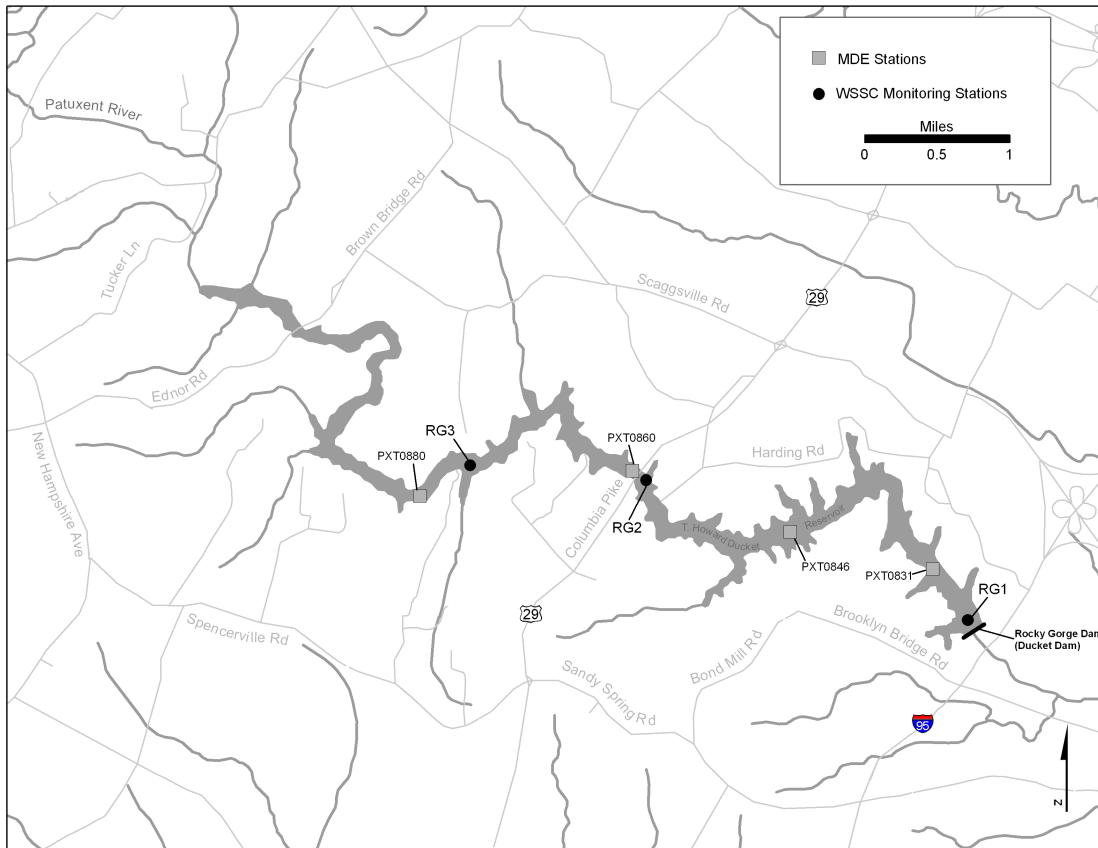


Figure 5.1-2: Sampling Locations in Rocky Gorge Reservoir

5.2 Temperature Stratification

Triadelphia and Rocky Gorge Reservoirs both regularly exhibit temperature stratification starting in late spring and lasting to early fall. Under stratified conditions during the summer and early fall, bottom waters in both reservoirs can become hypoxic, because stable density differences inhibit the turbulent mixing that transports oxygen from the surface. Under such conditions, the reservoirs can be divided vertically into a well-mixed surface layer, or epilimnion; a relatively homogeneous bottom layer or hypolimnion; and a transitional zone between them, the metalimnion, characterized by a sharp density gradient.

Contour plots of isotherms effectively illustrate seasonal position of the well-mixed surface layer or epilimnion. Figure 5.2-1 presents a contour plot of isothermals for TR1 in Triadelphia Reservoir. In the winter, isothermal lines are vertical, showing that the reservoir has fairly uniform temperature. In spring, isothermal lines begin to tilt away from the vertical, until by summer at depths greater than about four meters they are

nearly parallel to each other horizontally. At the surface, isothermal lines run vertically to a depth of about four meters; this defines the epilimnion.

Figures B.1–B.5 in Appendix B present contour plots for each WSSC monitoring location for the period 1998-2003. The thermal profile at RG1, the station just above the dam and water intakes in Rocky Gorge Reservoir, shows less stratification here than other locations. It may be impacted not only by water withdrawals, but also by WSSC’s aeration of water adjacent to the intakes, which may cause mixing that dampens stratification.

Generally, in both reservoirs, the epilimnion is limited to a depth of no more than four meters in the summer. For the purposes of data analysis, the surface layer is considered to be four meters deep, with the understanding that in spring and fall the epilimnion can extend deeper than six to seven meters, and in the summer it is likely as shallow as one to two meters. For screening purposes, samples taken at depths of ten meters or greater are considered to be in the bottom layer or hypolimnion.

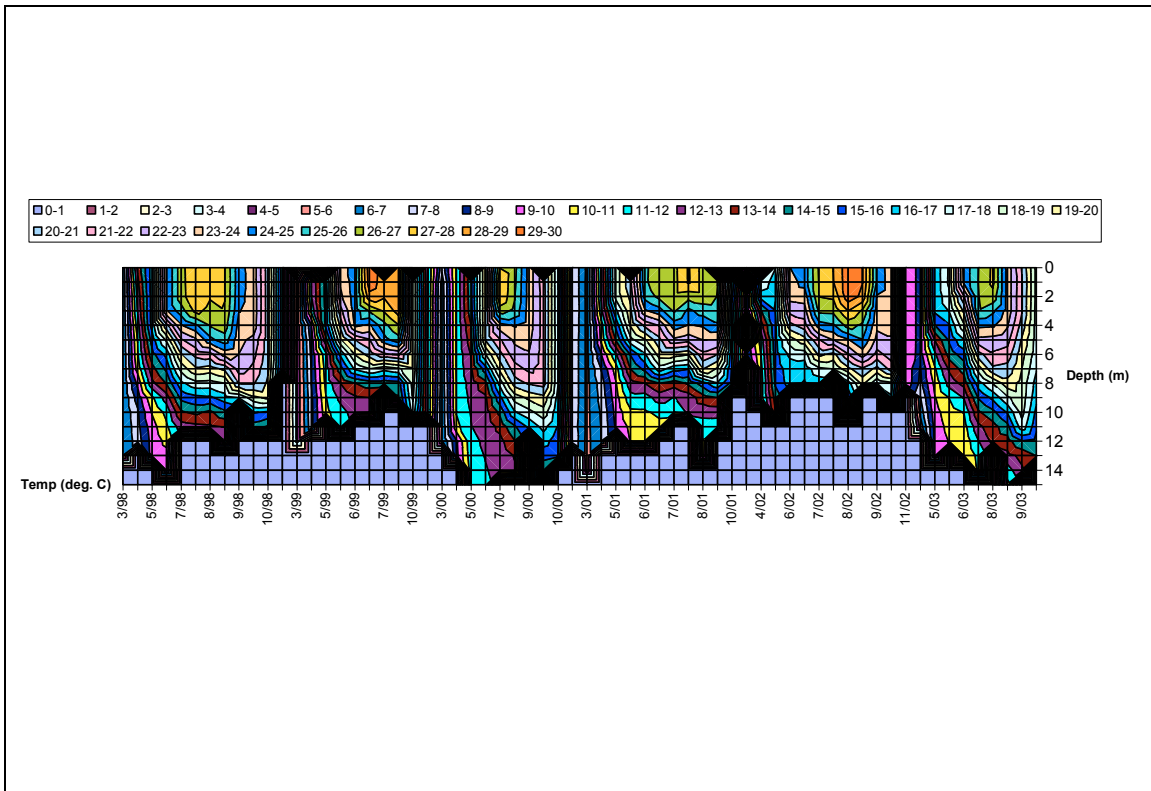


Figure 5.2-1: Isothermal Contours, Triadelphia Reservoir just above Brighton Dam, 1998-2003

5.3 Dissolved Oxygen

Figure 5.3-1 shows a contour plot of observed DO concentrations at TR1 in Triadelphia Reservoir, 1998-2003, corresponding to the temperature contour plot in Figure 5.2-1. There is a clear seasonal pattern to DO concentrations. In the early spring and late fall, DO concentrations are fairly uniform with depth. As temperature stratification sets in, DO concentrations in the surface layer remain relatively uniform, but the metalimnion shows a gradient in DO concentrations that grows stronger as the summer progresses. A region of hypoxia in the hypolimnion increases with thickness from late spring through summer.

Figures B.6 and B.7 in Appendix B show contour plots of DO concentrations at TR2 and TR3 in Triadelphia Reservoir, 1998-2003. Figures B.8–B.10 show contour plots of DO concentrations at RG1, RG2, and RG3 in Rocky Gorge Reservoir over the same period. Quite clearly, hypoxia occurs in the hypolimnion of both Triadelphia and Rocky Gorge Reservoirs with regularity.

Generally, DO concentrations remain above 5.0 mg/l in the surface layers of the reservoirs, but there are exceptions. There are two related causes of these low DO concentrations. The first is temperature stratification. As mentioned earlier, sometimes the epilimnion in the reservoirs is no more than one to two meters deep. DO is not transported below the well-mixed surface layer and DO concentrations decrease relative to the well-mixed layer. The second cause of low DO in surface layers is the entrainment of low DO waters into the epilimnion. Entrainment refers to the process by which turbulent layers spread into a non-turbulent region (Ford and Johnson 1986). The onset of cool weather causes the epilimnion to increase in depth by entraining water from the metalimnion. This water can be low in oxygen and reduce the DO concentration in the well-mixed layer. This can occur any time under stratified conditions when the surface mixed-layer deepens, often well before the fall overturn typical of many lakes and reservoirs (including Triadelphia and Rocky Gorge), when the surface and bottom layers displace one another.

Another factor that also can influence entrainment is drawdown. Withdrawals from a reservoir can induce currents that enhance mixing. Figure 5.3-2 shows the surface elevation of Triadelphia Reservoir from 1998 through 2003. In 1999 and 2002 (drought years), releases from Triadelphia to fill Rocky Gorge dropped the surface elevation by as much as 25 feet. These drawdowns are probably a contributing factor in mixing low DO concentrations into the surface levels of the reservoir.

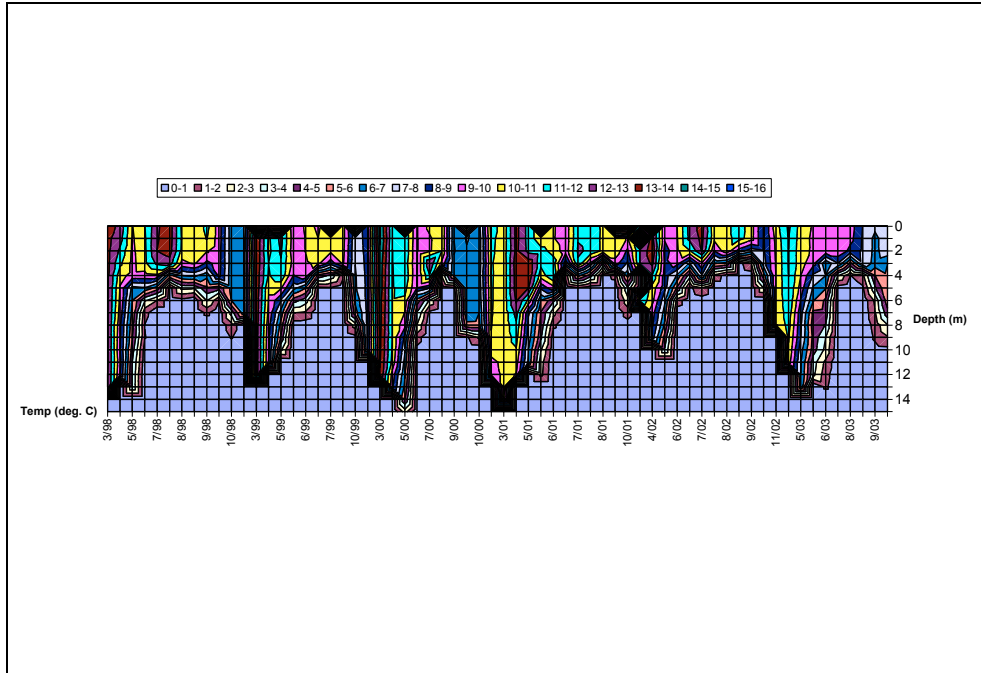


Figure 5.3-1: DO Contour, Triadelphia Reservoir just above Brighton Dam, 1998-2003

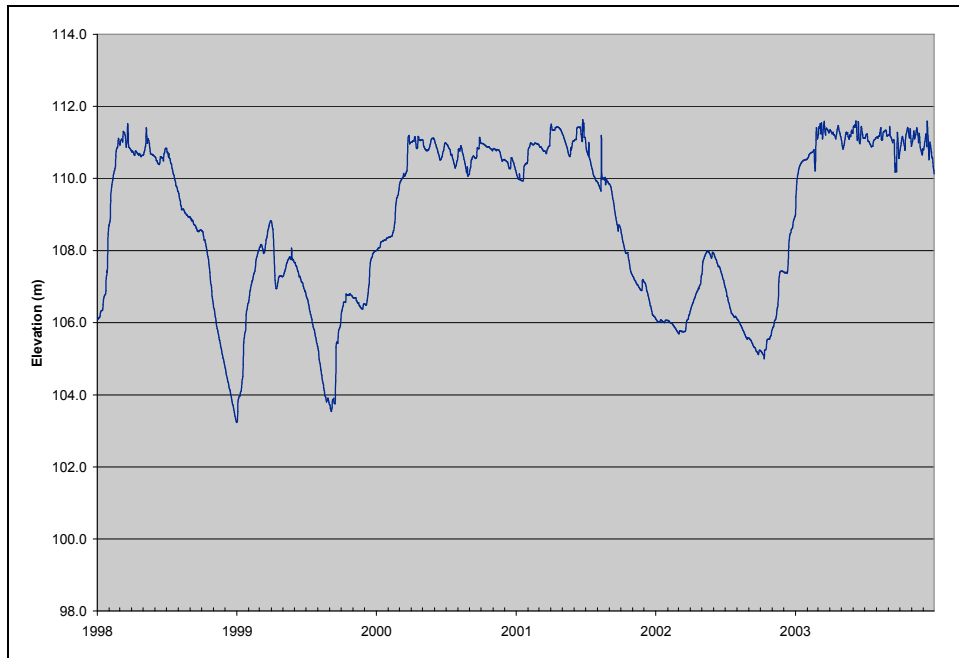


Figure 5.3-2: Surface Water Elevations in Triadelphia Reservoir, 1998-2003

5.4 Phosphorus

Figures B.11–B.13 in Appendix B show observed total phosphorus concentrations at each sampling depth at TR1, TR2, and TR3 in Triadelphia Reservoir. Figures B.14–B.16 in Appendix B show observed concentrations at RG1, RG2, and RG3 in Rocky Gorge Reservoir. Figures B17 and B18 show the concentrations observed at the MDE monitoring locations in Triadelphia and Rocky Gorge Reservoirs, respectively. Tables 5.4-1 and 5.4-2 give summary statistics for TP concentrations in Triadelphia and Rocky Gorge Reservoirs, respectively.

As Tables 5.4-1 and 5.4-2 show, median TP concentrations in the surfaces of the reservoirs is at or above 34 µg/l, which is the boundary between eutrophic and mesotrophic conditions according to the Carlson Trophic Index, a widely used measure of eutrophic conditions (Carlson 1977). Tables 5.4-1 and 5.4-2 also show little evidence of a pronounced longitudinal gradient in phosphorus concentrations, which is frequently a feature of reservoirs.

Table 5.4-1: Summary Statistics: TP Concentrations (mg/L) in Triadelphia Reservoir, 1998-2003

Station	Depth	Mean	St.Dev.	Min	1 st Q	Median	3 rd Q	Max	Count
TR1	Surface	0.040	0.023	0.000	0.022	0.035	0.056	0.095	47
	Middle	0.047	0.039	0.011	0.019	0.036	0.062	0.204	28
	Bottom	0.067	0.052	0.013	0.035	0.057	0.080	0.295	46
TR2	Surface	0.044	0.028	0.002	0.024	0.038	0.058	0.155	47
	Middle	0.045	0.036	0.000	0.019	0.034	0.064	0.174	28
	Bottom	0.065	0.043	0.004	0.030	0.053	0.085	0.211	46
TR3	Surface	0.063	0.048	0.000	0.029	0.051	0.086	0.205	47
	Middle	0.068	0.056	0.018	0.030	0.047	0.096	0.244	27
	Bottom	0.093	0.058	0.012	0.056	0.077	0.110	0.297	45

Table 5.4-2: Summary Statistics: TP Concentrations (mg/L) in Rocky Gorge Reservoir, 1998-2003

Station	Depth	Mean	St.Dev.	Min	1 st Q	Median	3 rd Q	Max	Count
RG1	Surface	0.044	0.042	0.012	0.023	0.037	0.048	0.280	44
	Middle	0.037	0.025	0.010	0.018	0.024	0.049	0.102	27
	Bottom	0.055	0.034	0.014	0.027	0.048	0.071	0.142	43
RG2	Surface	0.046	0.041	0.009	0.024	0.034	0.048	0.225	44
	Middle	0.039	0.030	0.006	0.020	0.026	0.056	0.128	27
	Bottom	0.063	0.040	0.012	0.033	0.053	0.085	0.214	43
RG3	Surface	0.044	0.035	0.005	0.024	0.033	0.053	0.219	44
	Middle	0.043	0.037	0.011	0.026	0.032	0.048	0.203	27
	Bottom	0.077	0.094	0.011	0.033	0.051	0.081	0.568	43

Figures B.19–B.21 in Appendix B show observed phosphate-P concentrations at each sampling depth at TR1, TR2, and TR3 in Triadelphia Reservoir. Figures B.22–B.24 in Appendix B show observed concentrations at RG1, RG2, and RG3 in Rocky Gorge Reservoir. Figures B.25 and B.26 show the concentrations observed at the MDE monitoring locations in Triadelphia and Rocky Gorge Reservoirs, respectively.

In Triadelphia Reservoir, the median value of the percent phosphate in total phosphorus in observed samples is 13%. In Rocky Gorge Reservoir, the median percent of phosphate in samples was about 15%. Bottom samples tended to have a slightly lower fraction of phosphate.

Bottom concentrations of total phosphorus and phosphate in both reservoirs tend to be larger than concentrations at other depths. This is more likely due to the accumulation of solid-phase phosphorus and resuspension during storm events, rather than the release of phosphate under anoxic conditions. As a comparison of the corresponding figures shows, large increases in bottom total phosphorus concentrations are not matched by increases in phosphate concentrations of the same magnitude.

5.5 Nitrogen

Figures B.27–B.29 in Appendix B show observed ammonia-N concentrations at each sampling depth at TR1, TR2, and TR3 in Triadelphia Reservoir. Figures B.30–B.32 in Appendix B show observed concentrations at RG1, RG2, and RG3 in Rocky Gorge Reservoir. Figures B.33 and B.34 show the concentrations observed at the MDE monitoring locations in Triadelphia and Rocky Gorge Reservoirs, respectively.

The Figures B.27, B.28, B.30, and, to a lesser extent, B.31, which represent the deeper portions of the reservoirs, all show that in both reservoirs there are regular significant increases in ammonia in the summer months due to diagenesis in the sediments. The same phenomenon occurs in the shallower, upstream stations, TR3 and RG3, shown in Figures B.29 and B.32, but perhaps not as regularly. The release of ammonia from the sediments contributes to oxygen demand. Although observed ammonia concentrations range as high as 2.7 mg/l, Maryland's ammonia water quality criteria (COMAR 26.08.02.03-2H(1)) were not exceeded.

Figures B.35–B.37 in Appendix B show observed nitrate-N concentrations at each sampling depth at TR1, TR2, and TR3 in Triadelphia Reservoir. Figures B.38–B.40 in Appendix B show observed concentrations at RG1, RG2, and RG3 in Rocky Gorge Reservoir. Figures B.41 and B.42 show the concentrations observed at the MDE monitoring locations in Triadelphia and Rocky Gorge Reservoirs, respectively.

Nitrate concentrations in the reservoirs show a strong seasonal pattern, decreasing significantly at all depths during the summer months. In the surface layers, the seasonal

decrease in both ammonia and nitrate is most likely due to the uptake of nitrogen by algae. In the bottom layers, after anoxia is established, nitrate is the preferred electron acceptor in metabolic processes, and significant denitrification takes place in the sediments and the water column. Nitrate concentrations can reach very low levels in the bottom layer, suggesting that sometimes iron oxides, which help bind phosphorus to the sediments, may be reduced by biologically-mediated reactions, and that at least some limited phosphorus release from the sediments does take place.

Figures B.43–B.45 in Appendix B show observed TN concentrations at each sampling depth at TR1, TR2, and TR3 in Triadelphia Reservoir. Figures B.46–B.48 in Appendix B show observed concentrations at RG1, RG2, and RG3 in Rocky Gorge Reservoir. Figures B.49 and B.50 show the concentrations observed at the MDE monitoring locations in Triadelphia and Rocky Gorge Reservoirs, respectively.

As the figures show, TN concentrations follow the pattern of nitrate concentrations. This is not surprising, since the median value of the percent of TN that is nitrate is 69% for observations from Triadelphia Reservoir and 68% from Rocky Gorge Reservoir, and varies little with depth.

5.6 Nutrient Limitation

Nitrogen and phosphorus are essential nutrients for algae growth. If one nutrient is available in great abundance relative to the other, then the nutrient that is less available limits the amount of plant matter that can be produced; this is known as the “limiting nutrient.” The amount of the abundant nutrient does not matter because both nutrients are needed for algae growth. In general, a Nitrogen:Phosphorus (N:P) ratio in the range of 5:1 to 10:1 by mass is associated with plant growth being limited by neither phosphorus nor nitrogen. If the N:P ratio is greater than 10:1, phosphorus tends to be limiting; if the N:P ratio is less than 5:1, nitrogen tends to be limiting (Chiandani et al. 1974).

Table 5.6-1 gives summary statistics for the N:P ratio observed in samples collected at the WSSC monitoring stations. Fewer than 2% of the samples had N:P ratios less than 10:1, strongly indicating that both reservoirs are phosphorus limited.

Table 5.6-1. Summary Statistic for N:P Ratio, Patuxent Reservoirs, 1998-2003

Statistic	Triadelphia	Rocky Gorge
Mean	64	52
Std. Dev.	59	38
Min	8	7
1stQ	29	26
Median	51	43
3rdQ	77	67
Max	508	312
Percent <10	2%	2%
Count	133	128

5.7 Algae and Chlorophyll *a*

Figures B.51 and B.52 in Appendix B show the time series of Chla concentrations in the WSSC sampling locations in Triadelphia and Rocky Gorge Reservoirs, 1998-2003.

Figures B.53 and B.54 show observed Chla concentrations at MDE's sampling locations in 2000. Tables 5.7-1 and 5.7-2 show maximum Chla concentrations by month and year, 1998-2003, for Triadelphia and Rocky Gorge Reservoirs, respectively.

As these tables indicate, Chla concentrations above 10 µg/l occur frequently. 44% of samples taken at WSSC's monitoring locations in Triadelphia Reservoir and 23% of the samples taken in Rocky Gorge Reservoir had concentrations above 10 µg/l. Concentrations above 30 µg/l are infrequent but not unusual in Triadelphia Reservoir. In Triadelphia Reservoir, three samples collected by WSSC over the period 1998–2003 and two samples collected by MDE in 2002 had concentrations above 30 µg/l. None of samples collected by WSSC in Rocky Gorge Reservoir, 1998 through 2003, or by MDE in 2000, had concentrations over 30 µg/l. Generally, Triadelphia Reservoir has higher Chla concentrations than Rocky Gorge Reservoir, though in any given month, Rocky Gorge Reservoir can have higher concentrations. In both reservoirs, higher concentrations tend to occur in early spring (March or April) or late summer (August or September), though a concentration just under 30 µg/l was observed in Rocky Gorge Reservoir in October, 1998.

Table 5.7-1. Maximum Observed Chla Concentration, 1998-2003 Triadelphia Reservoir

Year	Mar	Apr	May	Jun	Jul	Aug	Sep	Oct	Nov
1998	19	3	2	1	9	21	33	10	12
1999	44	9	18	17	23	24		9	13
2000	17	18	11	9	16	32	20	7	4
2001	3	11	7	11	12	19			
2002		11	15	8	29	26	19		15
2003		14	5	4	18	11	8	7	

Table 5.7-2. Maximum Observed Chla Concentration, 1998-2003 Rocky Gorge Reservoir

Year	Mar	Apr	May	Jun	Jul	Aug	Sep	Oct	Nov
1998	20	4	2	1	2	12	9	30	12
1999		14	15	5	6	6		9	6
2000	16	23	9	8	13	21	14	6	
2001	3	15	4	8	15	13			
2002		8	10	4	12	15	7		4
2003		12	8	7	16	7	6	4	

5.8 Sedimentation

Resource Management Concepts (2002) analyzed the changes in bathymetry and loss of volume in Triadelphia Reservoir due to sedimentation. They calculated the original volume capacity of the reservoir when it was constructed in 1942 and compared it to the capacity reported by Ocean Surveys (1997) based on their 1995 bathymetry survey. Table 5.8-1 summarizes the capacity losses for Triadelphia Reservoir.

The annual percent capacity loss (volumetric reduction) rate in Triadelphia Reservoir, 0.18%, compares favorably with the national averages. The mean average capacity loss rate for comparably sized reservoirs is 0.43%; the median is 0.27% (Ortt et al. 2000).

Table 5.8-1: Sedimentation Rates in Triadelphia Reservoir

Original (1942) Surface Area (acres)	882
Original (1942) Capacity (acre-ft.)	21,903
Capacity (1995) Bathymetric Survey (acre-ft)	19,785
Capacity Lost Since Construction (acre-ft)	2,118
Average Annual Capacity Loss (acre-ft/yr)	40
Annual Average Capacity Lost (%)	0.18%

Source: Resource Management Concepts (2002).

5.9 Water Quality Impairments

The Maryland Water Quality Standards Stream Segment Designation for Triadelphia Reservoir is Use IV-P: Recreational Trout Waters and Public Water Supply (COMAR 26.08.02.08M(6)). Rocky Gorge Reservoir is designated Use I-P: Water Contact Recreation, Fishing and Protection of Aquatic Life and Wildlife, and Public Water Supply (COMAR 26.08.02.08M(1)). Designated Uses present in the Triadelphia and Rocky Gorge Reservoirs are: 1) capable of holding and supporting adult trout for put-and-take fishing and 2) public water supply.

Maryland's General Water Quality Criteria prohibit pollution of waters of the State by any material in amounts sufficient to create a nuisance or interfere directly or indirectly with designated uses (COMAR 26.08.02.03B(2)). Excessive eutrophication, indicated by elevated levels of Chla, can produce nuisance levels of algae and interfere with designated uses such as fishing and swimming. The excess algal blooms eventually die off and decompose, consuming oxygen. Excessive eutrophication in Triadelphia and Rocky Gorge Reservoirs is ultimately caused by nutrient overenrichment. An analysis of the available water quality data presented in Section 5.6 has demonstrated that phosphorus is the limiting nutrient. In conjunction with excessive nutrients, Triadelphia Reservoir has experienced excessive sediment loads, resulting in a shortened projected lifespan of the reservoir.

Use I-P and Use IV-P waters are subject to DO criteria of not less 5.0 mg/l at any time (COMAR 26.08.02.03-3E(2)) unless natural conditions result in lower levels of DO (COMAR 26.08.02.03A(2)). New standards for tidal waters of the Chesapeake Bay and its tributaries take into account stratification and its impact on deeper waters. MDE recognizes that stratified reservoirs and impoundments (there are no natural lakes in Maryland) present circumstances similar to stratified tidal waters, and is applying an interim interpretation of the existing standard to allow for the impact of stratification on DO concentrations. This interpretation recognizes that, given the morphology of the reservoir or impoundment, the resulting degree of stratification, and the naturally occurring sources of organic material in the watershed, hypoxia in the hypolimnion is a natural consequence. The interim interpretation of the non-tidal DO standard, as applied to reservoirs, is as follows:

- A minimum DO concentration of 5.0 mg/l will be maintained throughout the water column during periods of complete and stable mixing;
- A minimum DO concentration of 5.0 mg/l will be maintained in the mixed surface layer at all times, including during stratified conditions, except during periods of overturn or other naturally-occurring disruptions of stratification; and
- Hypolimnetic hypoxia will be addressed on a case-by-case basis, taking into account morphology, degree of stratification, sources of diagenic organic material in reservoir sediments, and other such factors.

The analysis of water quality data in Section 5.2 has shown that all observed DO concentrations below 5.0 mg/l in the surface layers of Triadelphia and Rocky Gorge Reservoirs are associated with stratification or the mixing of stratified waters into the surface layers during periods of reservoir overturn or drawdown. On the other hand, seasonal hypoxia occurs regularly in both reservoirs in the hypolimnion.

6.0 STRUCTURE AND CALIBRATION OF THE CE-QUAL-W2 MODELS

This chapter describes the CE-QUAL-W2 models in general and the modifications made to the W2 models in this project to facilitate their use in TMDL development. It further describes the implementation of the W2 models in Triadelphia and Rocky Gorge Reservoirs, and the calibration of the models representing the reservoirs.

6.1 Overview of the CE-QUAL-W2 Model

CE-QUAL-W2 is a laterally-averaged, two-dimensional computer simulation model capable, in its most recent formulations, of representing the hydrodynamics and water quality of rivers, lakes, and estuaries. It is particularly suited for representing temperature stratification that occurs in reservoirs like Triadelphia and Rocky Gorge.

The original version of CE-QUAL-W2 was the LARM (Laterally Averaged Reservoir Model) by Edinger and Buchak (1975). US Army Engineer Waterways Experiment Station (WES) added a water quality component to make CE-QUAL-W2 version 1. Version 2 (Cole and Buchak 1995) added many computational improvements and permitted the simulation of reservoirs with multiple branches. Version 3 (Cole and Wells 2003) expanded the hydrodynamic simulation capacities of the model so that rivers and estuaries could also be simulated.

Waterbodies represented in CE-QUAL-W2 are divided longitudinally into segments and vertically into layers. A model cell is defined by the intersection of layers and segments. The bottom cell in a segment is fixed by the waterbody's bathymetry. The number of cells in a segment varies with the position of the free surface of the waterbody. Every time step CE-QUAL-W2 simulates the location of the free surface in each segment.

Cole and Buchak (1995) provide a clear exposition of the CE-QUAL-W2 model structure as it is implemented for simulating reservoirs. Figure 6.1-1 gives six basic equations that constitute the W2 model. There are six unknowns associated with these six equations: (1) the free surface, η ; (2) the pressure, P ; (3) the horizontal velocity, U ; (4) the vertical velocity, W ; (5) the constituent concentration, ϕ ; and (6) the density, ρ . Substituting the horizontal momentum equation (A-1), the pressure equation (A-4), and the equation of state (A-6) into the free surface equation and integrating in the vertical direction, an equation for the free surface can be determined which is a function of waterbody geometry and the hydrodynamic variables from the previous time step:

Figure 6.1-1. The Basic Equations of CE-QUAL-W2
(Cole and Buchak 1995)

Horizontal Momentum

$$\frac{\partial UB}{\partial t} + \frac{\partial UUB}{\partial x} + \frac{\partial WUB}{\partial z} = - \frac{1}{\rho} \frac{\partial BP}{\partial x} + \frac{\partial \left(BA_x \frac{\partial U}{\partial x} \right)}{\partial x} + \frac{\partial B\tau_x}{\partial z} \quad (A-1)$$

where

- U = longitudinal, laterally averaged velocity, $m \text{ sec}^{-1}$
- B = waterbody width, m
- t = time, sec
- x = longitudinal Cartesian coordinate: x is along the lake centerline at the water surface, positive to the right
- z = vertical Cartesian coordinate: z is positive downward
- W = vertical, laterally averaged velocity, $m \text{ sec}^{-1}$
- ρ = density, $kg \text{ m}^{-3}$
- P = pressure, $N \text{ m}^{-2}$
- A_x = longitudinal momentum dispersion coefficient, $m^2 \text{ sec}^{-1}$
- τ_x = shear stress per unit mass resulting from the vertical gradient of the horizontal velocity, U, $m^2 \text{ sec}^{-2}$

Constituent Transport

$$\frac{\partial B\Phi}{\partial t} + \frac{\partial UB\Phi}{\partial x} + \frac{\partial WB\Phi}{\partial z} - \frac{\partial \left(BD_x \frac{\partial \Phi}{\partial x} \right)}{\partial x} - \frac{\partial \left(BD_z \frac{\partial \Phi}{\partial z} \right)}{\partial z} = q_\Phi B + S_\Phi B \quad (A-2)$$

where

- Φ = laterally averaged constituent concentration, $g \text{ m}^{-3}$
- D_x = longitudinal temperature and constituent dispersion coefficient, $m^2 \text{ sec}^{-1}$
- D_z = vertical temperature and constituent dispersion coefficient, $m^2 \text{ sec}^{-1}$
- q_Φ = lateral inflow or outflow mass flow rate of constituent per unit volume, $g \text{ m}^{-3} \text{ sec}^{-1}$
- S_Φ = kinetics source/sink term for constituent concentrations, $g \text{ m}^{-3} \text{ sec}^{-1}$

Free Water Surface Elevation

$$\frac{\partial B_{\eta} \eta}{\partial t} = \frac{\partial}{\partial x} \int_{\eta}^h UB \, dz - \int_{\eta}^h qB \, dz \quad (A-3)$$

Where

- B_{η} = time and spatially varying surface width, m
- η = free water surface location, m
- h = total depth, m
- q = lateral boundary inflow or outflow, $m^3 \, sec^{-1}$

Hydrostatic Pressure

$$\frac{\partial P}{\partial z} = \rho g \quad (A-4)$$

Where

- g = acceleration due to gravity, $m \, sec^{-2}$

Continuity

$$\frac{\partial UB}{\partial x} + \frac{\partial WB}{\partial z} = qB \quad (A-5)$$

Equation of State

$$\rho = f(T_w, \Phi_{TDS}, \Phi_{ss}) \quad (A-6)$$

Where

$f(T, \Phi_{TDS}, \Phi_{ss})$ = density function dependent upon temperature, total dissolved solids or salinity, and suspended solids

$$\begin{aligned}
 \frac{\partial \bar{B}\eta}{\partial t} - g \Delta t \frac{\partial}{\partial x} \left(\frac{\partial \eta}{\partial x} \int_{\eta}^h B \, dz \right) &= \frac{\partial}{\partial x} \int_{\eta}^h UB \, dz - \frac{g\Delta t}{\rho_{\eta}} \frac{\partial}{\partial x} \int_{\eta}^h \left[B \int_{\eta}^z \frac{\partial \rho}{\partial x} \, dz \right] dz \\
 &+ \frac{\partial}{\partial x} \left[B_h \tau_h - B_{\eta} \tau_{\eta} - \int_{\eta}^h \tau_x \frac{\partial B}{\partial z} \, dz \right] \Delta t \\
 &+ \frac{\partial}{\partial x} \left[\int_{\eta}^h F_x \, dz \right] \Delta t - \int_{\eta}^h qB \, dz
 \end{aligned}
 \tag{A-7}$$

(Cole and Burchak 1995)

Each time step, the following computations are performed:

1. Equation A-7 is solved implicitly for the free surface elevation, η ;
2. Horizontal velocities are calculated from wind shear, bottom shear, and the baroclinic and barotropic pressure gradients;
3. Vertical velocities are determined from the free surface elevations, horizontal velocities, and the continuity equation; and
4. Constituent concentrations are calculated using equation A-2.

More details of the CE-QUAL-W2 model structure can be found in Cole and Buchak (1995) and Cole and Wells (2003).

Model parameters specify, among other things, the kinetic rates which control how constituents are transformed among themselves. These transformations are counted among the sources and sinks of constituents in Equation A-2. In addition to model parameters, W2 requires (1) the specification of a time series of inflow volumes, temperatures, and constituent concentrations; (2) meteorological inputs such as wind speed, air temperature, dew point, and cloud cover; and (3) boundary conditions such as outflows or water surface elevations.

6.2 Implementation of the CE-QUAL-W2 Model For Triadelphia and Rocky Gorge Reservoirs

The original W2 models of Triadelphia and Rocky Gorge Reservoirs used Version 2 of the CE-QUAL-W2 model. Two years were simulated, 1997 and 1998. The current reservoir models use version 3.2 of CE-QUAL-W2. The simulation period was expanded to 1998-2003 to coincide with the period within which Chla data were available to calibrate the models. Each year was simulated separately, but the simulations were restarted using the RESTART files produced from the previous year's simulation.

6.2.1. Segmentation and Model Cell Properties

The model segmentation for Triadelphia and Rocky Gorge Reservoirs was adopted from the original Tetra Tech models. Figures 6.2.1-1 and 6.2.1-2 show the longitudinal segmentation of Triadelphia and Rocky Gorge Reservoirs, respectively. Two changes were made to the original segmentation: (1) an additional layer was added to the segmentation of Rocky Gorge Reservoir, and (2) the tributary branches in Triadelphia Reservoir—Segments 26 through 29, 31 through 34, and 36 through 39—were incorporated into Segments 10, 19, and 21, respectively. Both reservoirs are modeled as a single main branch. Tables C.1 and C.2 show the number of cells and layer depths of the segments of Triadelphia and Rocky Gorge Reservoirs, respectively. Each layer is one meter thick.

The linkages between reservoir segments and tributary inflows were also adopted from the original model. Tables 6.2.1-1 and 6.2.1-2 show the connection between HSPF model segments and reservoir model segments for Triadelphia and Rocky Gorge Reservoirs, respectively. Because distributed inflows were used to adjust the water balance, the inflows and loads from direct drainage Segments 500 and 600 were apportioned to the tributary segments. Tables 6.2.1-1 and 6.2.1-2 show the proportion of each direct drainage segment applied to the tributary segments. The HSPF model's SCHEMATIC section was used to route direct drainage flows to the tributaries.

Table 6.2-1 Assignments of HSPF Segments to W2 Segments, Triadelphia Reservoir

HSPF Segment	W2 Segment	Fraction of Segment 60 Inputs
10	2	0.00
40	5	0.00
61	7	0.14
62	12	0.20
63	21	0.15
64	19	0.18
65	10	0.33

Table 6.2-2 Assignments of HSPF Segments to W2 Segments, Rocky Gorge Reservoir

HSPF Segment	W2 Segment	Fraction of Segment 50 Inputs
30	2	0.00
51	14	0.16
52	2	0.20
53	21	0.13
54	11	0.10
55	16	0.17
56	2	0.08
57	10	0.17

6.2.2. Inflows, Meteorological Data and Boundary Conditions

The CE-QUAL-W2 Model requires time series of inflows, inflow temperature, and inflow constituent concentrations. These were all taken from the output of the Patuxent Watershed HSPF Model, according to the linkage between HSPF and W2 model segments described in Tables 6.2.1-1 and 6.2.1-2. Hourly time series were used to represent inflows and temperature and constituent concentrations.

The W2 model requires time series of air temperature, dewpoint temperature, cloud cover, wind speed and wind direction. All meteorological data was taken from BWI Airport. Hourly time series were used to input meteorological data. Direct precipitation to the reservoir was not simulated.

Boundary conditions for the CE-QUAL-W2 can be specified as either the elevation or flows across the model boundaries in the most upstream and downstream segments. The upstream boundary conditions were specified by the inflows from the HSPF model. Downstream boundary conditions were specified by reservoir outflows. The time series of reservoir outflows was determined in the water balance calibration described in Section 6.3. The elevation of the outflow was determined in the temperature calibration described in Section 6.4. No outlet structures except the spillway in Rocky Gorge Reservoir were explicitly modeled.

6.2.3. Configuration of Water Quality Constituents

Table 6.2.3-1 shows the state variables that represent water quality constituents in Version 3.2 of the CE-QUAL-W2 model. The model can represent any number of user-specified inorganic solids, CBOD species, or algal species.

Total phosphorus is the regulated constituent for the nutrient TMDLs in Triadelphia and Rocky Gorge Reservoirs. It is critical, therefore, that the modeling framework maintain a mass balance of total phosphorus throughout the simulation. Dissolved inorganic phosphorus (DIP) is the only phosphorus species directly represented as a state variable in the W2 model. Phosphorus attached to sediment can be modeled by specifying the concentration of phosphorus on attached sediment. Organic phosphorus is modeled by specifying the stoichiometric ratio between phosphorus and organic matter or oxygen demand (in the case of CBOD species).

It is not possible to maintain a mass balance of total phosphorus by fixing a ratio to a state variable unless the quantity of the state variable is determined by its phosphorus content. This is exactly how the mass balance of phosphorus was implemented in the reservoir models. Specifically, the state variables in the W2 models were configured as follows:

The inorganic phosphorus attached to silt and clay was modeled as distinct inorganic solids. Sorption between sediment and the water column was not simulated in the model.

Three CBOD variables were used to represent allochthonous organic matter inputs to the reservoirs: (1) labile dissolved CBOD, (2) labile particulate CBOD, and (3) refractory particulate CBOD. The concentrations of these CBOD inputs were calculated based on the concentration of organic phosphorus determined by the HSPF model, using the stoichiometric ratio between phosphorus and oxygen demand in the reservoir models. The fraction of total CBOD in each species was calibrated based on reservoir response. The organic matter state variables were reserved to represent the recycling of nutrients within the reservoir between algal biomass and reservoir nutrient pools. No organic matter, as represented by these variables, was input into the reservoirs. They were used only to track nutrients released from algal decomposition.

To use the W2 model in this configuration, several minor changes had to be made to the W2 code. Inorganic solids contribute to light extinction. The inorganic solids representing solid-phase phosphorus do not contribute to light extinction over and above the sediment to which they are attached. The W2 code was changed so that they don't contribute to light extinction.

The original CBOD variables in W2 do not contribute to light extinction, do not settle, and do not contribute to the organic matter in the sediment available for diagenesis. The W2 code was altered to represent BOD species which settled and which could contribute to both light extinction and sediment organic matter.

Table 6.2.3-1 summarizes the water quality state variables used in the CE-QUAL-W2 models of Triadelphia and Rocky Gorge Reservoirs. More of the details of the implementation of water quality simulation will be provided in sections on the calibration of constituents.

Table 6.2.3-1. Water Quality State Variables in CE-QUAL-W2 and their Realization in the Patuxent Reservoir Models

W2 State Variable	Patuxent State Variable	Description
DO	DO	Dissolved Oxygen
NH4	NH4	Ammonia Nitrogen
NO3	NO3	Nitrate Nitrogen
PO4	PO4	Dissolved Inorganic Phosphorus
LPOM	LPOM	Autochthonous Labile Particulate Organic Matter
RPOM	RPOM	Autochthonous Refractory Particulate Organic Matter
LDOM	LDOM	Autochthonous Labile Dissolved Organic Matter
RDOM	RDOM	Autochthonous Refractory Dissolved Organic Matter
CBOD	CBOD1	Allochthonous Labile Dissolved Organic Matter
	CBOD2	Allochthonous Labile Particulate Organic Matter
	CBOD3	Allochthonous Refractory Particulate Organic Matter
ISS (inorganic solids)	ISS1	Sand
	ISS2	Silt
	ISS3	Clay
	ISS4	Particulate Inorganic Phosphorus on Silt
	ISS5	Particulate Inorganic Phosphorus on Clay
AGL (algal biomass)	ALG1	Winter: diatoms
	ALG2	Spring: summer diatoms; green algae
	ALG3	Summer or fall: blue-green algae, diatoms

6.3. Water Balance Calibration

The objective of the water balance calibration is to calibrate the time series of inflows and outflows so that simulated water surface elevations match observed levels. WSSC provided bi-daily water elevation levels at the dams for both Triadelphia and Rocky Gorge Reservoirs. Some days had no observations. These were filled in by linear interpolation from days that had observations to make a complete time series of elevations for each reservoir.

Measured outflows were available from the USGS gages 01591610, below Brighton Dam, and 01592500, below Duckett Dam. WSSC also supplied information on water withdrawals from Rocky Gorge Reservoir. Water surface elevations were also used to

estimate the outflow over the spillways when observed elevations exceeded spillway crests. All this information was used to set the initial estimate of daily outflows. These outflows were used as the starting point for the calibration, but were not used to constrain the final calibrated time series of daily outflows.

CE-QUAL-W2 comes with a calibration utility, `waterbalance.exe`, which, when given the time series of observed water surface elevations, determines how much the inflows or outflows need to be adjusted in order to minimize the error in the simulated water surface elevations. The inflows to the W2 model can be adjusted by using distributed tributary files. The distributed tributary inflow file applies a time series of inflows across all segments, in proportion to their surface area. It is intended to be used in conjunction with the `waterbalance.exe` to adjust inflows to match observed surface elevations (Cole and Wells 2003).

The water balance was calibrated as follows. First, only the outflow time series were adjusted until the net adjustment in outflows, as determined by the water balance utility, were insignificant. At this point, if any adjustment needed to be made to the inflows, they usually occurred at particular points in time. Some of these were clearly storms that HSPF failed to simulate, because they were not present in the precipitation record. At this point, flows from the distributed tributaries were added to the simulation. The distributed tributary requires a time series of temperature inputs, which were taken from the main inflow to each reservoir. No constituent concentrations were associated with the distributed tributary inflows.

Figures 6.3-1 and 6.3-2 compare the simulated and observed water surface elevations at the dams for Triadelphia and Rocky Gorge Reservoirs, respectively. As the figures indicate, the error in simulated surface elevations is almost insignificant.

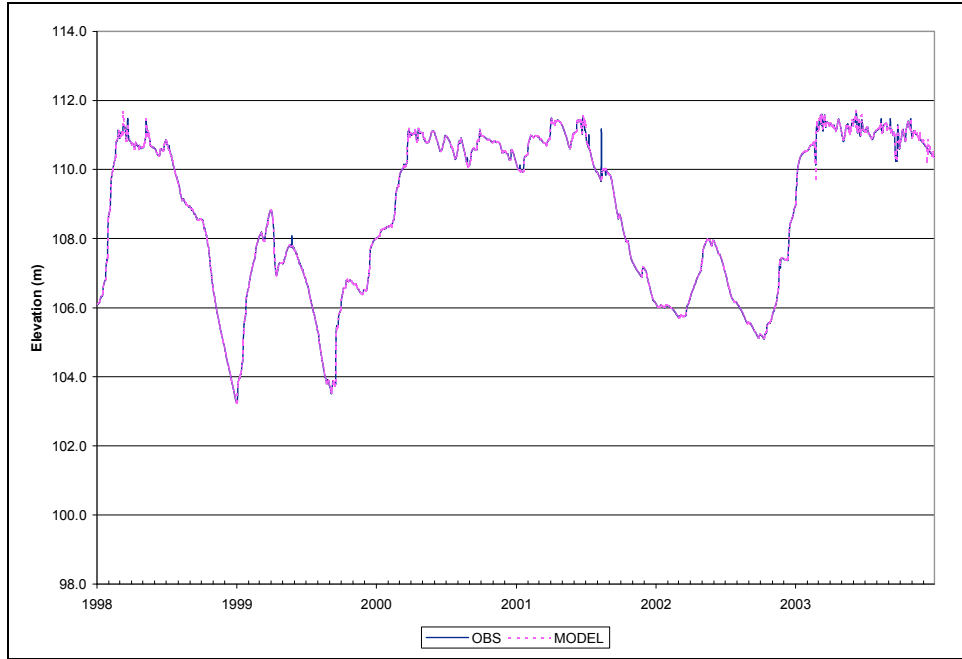


Figure 6.3-1 Observed and Simulated Water Surface Elevation, Triadelphia Reservoir

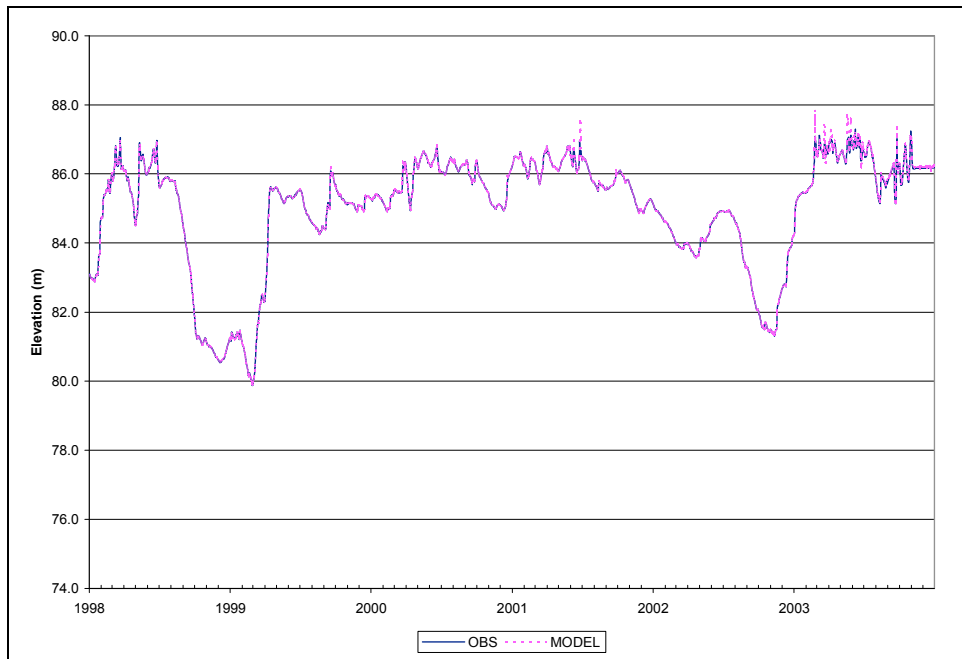


Figure 6.3-2 Observed and Simulated Water Surface Elevation, Rocky Gorge Reservoir

6.4 Temperature Calibration

The simulation of temperature is among the most important aspects of reservoir modeling. Water temperature is the cause of the density differences that constitute stratification in the reservoirs and inhibit turbulent mixing between layers. The inhibition of mixing of course leads to low dissolved oxygen concentration in the hypolimnion during stratified conditions. In addition, most of the kinetic processes, including algal growth rates, are temperature dependent, and thus an accurate representation of temperature facilitates simulating eutrophication dynamics.

Calibrating the temperature simulation of the W2 model primarily involves balancing the magnitude and timing of mixing forces—primarily wind but also inflow and outflows—with heat exchange and transport. The sensitivity of the temperature simulation to about a dozen variables was tested, but, in the end, four variables were identified as significantly impacting the calibration: BETA, the surface heat exchange coefficient; WSC, the wind sheltering coefficient; SHD, the shading coefficient; and ESTR, the elevation of the outflows from the reservoirs. These are summarized in Table 6.4-1.

Table 6.4-1. Parameters Used in W2 Temperature Calibration

Parameter	Description
BETA	Fraction of radiation absorbed at the water surface
ESTR	Elevation of outflow from reservoir
WSC	Fraction of input wind speed applied to water surface
SHD	Fraction of reservoir not in shade

The values of these parameters were calibrated as follows: Multiple parameter combinations were tested using the PEST utility, SENSAN, which automates the process of substituting parameter sets into model input files, performing multiple model runs, and recording the outcomes from the simulations. The outcomes measured were the root mean square error between observed and simulated temperatures and the mean absolute error of the same quantities. SENSAN also saved the output files so the simulations could be examined graphically. The first sets of parameters spanned the entire range of parameter values. Subsequent sets refined the results of previous sets. Hundreds, if not thousands, of parameter combinations were simulated for each simulation year.

Cole and Wells (2003) suggest that it should be possible to achieve a temperature simulation in which the absolute mean error is less than 1° C. This was the calibration target, subject to the following constraints. The surface heat absorption coefficient, BETA, is a model parameter and should not vary through the simulation. Therefore, BETA must be the same for each simulation year, but not necessarily the same for each reservoir. Similarly, the shading coefficient can vary spatially by segment but not over time. The same shading coefficient was therefore used for each simulation year. As a matter of fact, but not necessity, the same shading coefficient was used for each segment. The outflow elevation and the wind sheltering coefficient, which can vary in time, were

allowed to vary by simulation year. The final calibration parameter values were selected by first choosing values of the surface heat exchange coefficient and shading coefficient that had simulation runs with AME of less than 1° C, then by choosing the wind sheltering coefficient and outflow elevation in each simulation year that minimized the AME in that year. Parameter values determined in the reservoir simulations are given in Table 6.4-2 and 6.4-3 for Triadelphia and Rocky Gorge Reservoirs, respectively. The overall AME for Triadelphia Reservoir was 0.94 ° C and the overall AME for Rocky Gorge Reservoir was 0.87 ° C. It should be noted, however, that during the subsequent water quality calibration in Triadelphia, AME values increased slightly in a few years primarily because high solids concentrations inhibited light penetration and decreased heat transfer to lower layers.

Table 6.4-2. Temperature Calibration Parameter Values, Triadelphia Reservoir

Year	SHD	WSC	BETA	ESTR	AME
1998	1.0	0.85	0.55	95.0	0.93
1999	1.0	0.8	0.55	103.0	1.00
2000	1.0	0.9	0.55	95.0	0.82
2001	1.0	0.75	0.55	95.0	1.04
2002	1.0	0.75	0.55	95.0	0.87
2003	1.0	0.7	0.55	95.0	1.00

Table 6.4-3. Temperature Calibration Parameter Values, Rocky Gorge Reservoir

Year	SHD	WSC	BETA	ESTR	AME
1998	1.0	1.0	0.65	79.5	0.80
1999	1.0	1.0	0.65	60.0	0.74
2000	1.0	1.0	0.65	79.5	0.84
2001	1.0	0.8	0.65	79.5	0.84
2002	1.0	1.0	0.65	60.0	1.08
2003	1.0	1.0	0.65	79.5	0.93

6.5 Phosphorus Calibration

The goal of the phosphorus calibration was to reproduce the distribution of observed phosphate-P (PO4) and TP concentrations in the surface and bottom of the reservoirs. No attempt was made to calibrate either PO4 or TP to individual observed values.

For PO4, calibration was implemented (1) primarily by adjusting the PO4 fraction in input loads and (2) adjusting the decay and settling rates for BOD, algae, and autochthonous organic matter. Table 6.5-1 gives the decay and settling rates for allochthonous and autochthonous organic matter. TP concentrations were controlled primarily by adjusting the settling rates of inorganic phosphorus. Table 6.5-2 gives the inorganic phosphorus settling rates.

Tables 6.5-3 and 6.5-4 show summary statistics for surface and bottom TP concentrations. Figures 6.5.1 and 6.5.2 show the cumulative distribution of observed and simulated surface and bottom TP concentrations in Triadelphia Reservoir. Figures 6.5.3 and 6.5.4 show the distributions of surface and bottom TP in Rocky Gorge Reservoir. Generally, there is very good agreement in the distribution of observed and simulated TP concentrations. The highest percentile concentrations are overpredicted in the bottom of Triadelphia and underpredicted in Rocky Gorge, but the distributions generally agree below the 90th percentile values.

Dissolved ortho-phosphate, or dissolved inorganic phosphorus (DIP), is the form in which algae can uptake phosphorus. It is also referred to “bio-available phosphorus.” Tables 6.5-5 and 6.5-6 show summary statistics for surface and bottom PO₄ concentrations. Figures 6.5.5 and 6.5.6 show the cumulative distribution of observed and simulated surface and bottom PO₄ concentrations in Triadelphia Reservoir. Figures 6.5.7 and 6.5.8 show the distributions of surface and bottom PO₄ in Rocky Gorge Reservoir. The overall average concentrations of PO₄ for observed and simulated values agree except in the surface layer of Triadelphia Reservoir, where some of the highest reported observed values could be misreported. On the other hand, there is reasonable agreement in the distribution of observed and simulated PO₄ concentrations in the surface layer of Triadelphia reservoir; otherwise, the simulated concentrations tend to dominate observed values over the lower three quartiles of the distribution, and underpredict observed concentrations for the highest values, some of which are also suspect. It is fair to say, as the standard deviations show, that the models show considerably less variability than the observed data.

Figures C.7–C.18 in Appendix C give time series of observed and simulated PO₄ and TP in the surface and bottom layers of Triadelphia Reservoir. Figures C.43– C.54 show the same time series in Rocky Gorge Reservoir.

Bottom concentrations of total phosphorus and phosphate in both reservoirs tend to be larger than concentrations at other depths. This is more likely due to underflow, the accumulation of solid-phase phosphorus, and its resuspension during storm events, rather than the release of phosphate under anoxic conditions. Cornwell and Owens (2002) attempted to directly measure the release of phosphate from the sediments in Triadelphia Reservoir, as part of a broader study of exchange of nutrients and dissolved oxygen between the sediments and the water column. They made three attempts to measure phosphate flux rates by incubating sediment cores in the laboratory. In 1999, they were unable to measure phosphate releases from the sediments, either because fluxes were so low or because high water column phosphate concentrations rendered their methods insensitive. During a second attempt in August, 2000, low-to-modest fluxes of phosphate (5.6 -7.4 $\mu\text{mol}/\text{m}^2/\text{hr}$) were observed using longer incubation periods. A third set of cores, taken from July 2001, also yielded low-to-modest flux rates between 2 -11 $\mu\text{mol}/\text{m}^2/\text{hr}$. Cornwell and Owens (2002) concluded that under aerobic conditions phosphorus is tightly bound to the sediments and under aerobic conditions the release of phosphate is modest at best.

An analysis of available monitoring data for the period 1998 through 2003 also suggests that phosphate release from the sediment is not a significant source of phosphorus. Significant phosphate releases are expected to occur only under anoxic conditions, but an examination of the Figures B.19 through B.24 in Appendix B does not show the seasonal pattern in bottom phosphate concentrations apparent in ammonia concentrations, shown in Figures B.27 through B.32, or nitrate concentrations, shown in Figures B.35 through B.40. Moreover, for sediment release to be the source of the increase in bottom phosphate concentrations, it must be apparent that the increase is not due to an external influx of phosphorus. Generally speaking, increases in bottom phosphate are often accompanied by even greater increases in total phosphorus, which suggests that sediment release may not be the primary source of the increase in phosphate. As Figure B.19 shows, there is a significant increase in phosphate concentrations during the summer of 1998 in Triadelphia Reservoir. This year presents the best evidence for a phosphate release from sediments, but even in this case, the increase in bottom total phosphorus concentrations is 50% greater than the increase in phosphate concentrations, as shown in Figure B.11. Years such as 2001 which show an increasing trend in phosphate concentrations during hypoxia also show increases in phosphate at all depths and also increases in total phosphorus concentrations at all depths.

Table 6.5-1 Decay Rates and Settling Rates for Organic Matter

Constituent	Triadelphia Reservoir		Rocky Gorge Reservoir	
	Decay Rate (1/d)	Settling Rate (m/d)	Decay Rate (1/d)	Settling Rate (m/d)
CBOD1	0.1	0.0	0.125	0.0
CBOD2	0.001	0.2	0.06	0.5
CBOD3	0.001	5.0	0.001	5.0
Dissolved Organic Matter	0.06	0.0	0.06	0.0
Particulate Organic Matter	0.06	1.35	0.06	1.35

Table 6.5-2 Settling Rates for Inorganic Sediments and Adsorbed Particulate Phosphorus

Size Fraction	Triadelphia Reservoir Settling Rate (m/d)	Rocky Gorge Reservoir Settling Rate (m/d)
Sand	5.0	5.0
Silt	3.0	1.0
Clay	0.3	0.05

Table 6.5-3 Summary Statistics for Simulated and Observed Surface TP (mg/l)

Statistic: Surface TP	Triadelphia Reservoir		Rocky Gorge Reservoir	
	Observed	Simulated	Observed	Simulated
Min	0.0000	0.0133	0.0052	0.0152
1 st Q	0.0243	0.0230	0.0240	0.0243
Median	0.0414	0.0322	0.0344	0.0332
3 rd Q	0.0627	0.0580	0.0508	0.0479
Max	0.2049	0.2327	0.2796	0.1116
Mean	0.0492	0.0472	0.0449	0.0390
Std. Dev.	0.0365	0.0406	0.0395	0.0215
R ²	0.0157		0.0906	

Table 6.5-4 Summary Statistics for Simulated and Observed Bottom TP (mg/l)

Statistic: Bottom TP	Triadelphia Reservoir		Rocky Gorge Reservoir	
	Observed	Simulated	Observed	Simulated
Min	0.0035	0.0152	0.0108	0.0150
1 st Q	0.0397	0.0367	0.0322	0.0311
Median	0.0609	0.0600	0.0523	0.0498
3 rd Q	0.0959	0.1003	0.0814	0.0657
Max	0.2970	2.6715	0.5680	0.2828
Mean	0.0749	0.1569	0.0660	0.0588
Std. Dev.	0.0531	0.3665	0.0628	0.0426
R ²	0.0062		0.0041	

Table 6.5-4 Summary Statistics for Simulated and Observed Surface Layer PO4 (mg/l)

Statistic: Surface PO4	Triadelphia Reservoir		Rocky Gorge Reservoir	
	Observed	Simulated	Observed	Simulated
Min	0.001	0.001	0.000	0.002
1 st Q	0.003	0.003	0.002	0.006
Median	0.006	0.007	0.004	0.008
3 rd Q	0.011	0.012	0.007	0.010
Max	0.048	0.025	0.212	0.030
Mean	0.008	0.008	0.008	0.009
Std. Dev.	0.008	0.006	0.021	0.005
R ²	0.0087		0.0011	

Table 6.5-5 Summary Statistics for Simulated and Observed Bottom Layer PO4 (mg/l)

Statistic: Bottom PO4	Triadelphia Reservoir		Rocky Gorge Reservoir	
	Observed	Simulated	Observed	Simulated
Min	0.001	0.002	0.000	0.002
1 st Q	0.004	0.013	0.003	0.007
Median	0.006	0.014	0.005	0.010
3 rd Q	0.012	0.016	0.009	0.012
Max	0.880	0.020	0.096	0.032
Mean	0.023	0.014	0.008	0.010
Std. Dev.	0.101	0.004	0.012	0.005
R ²	0.0007		0.0059	

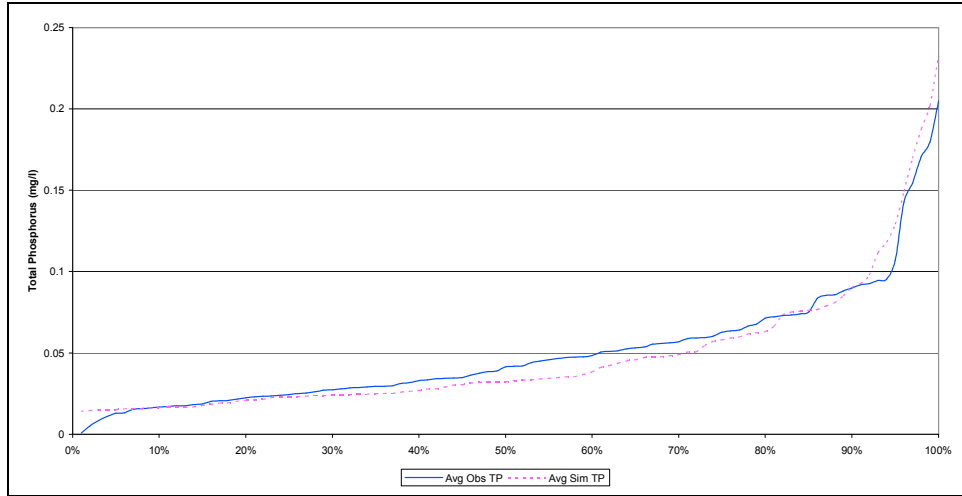


Figure 6.5-1. Cumulative Distribution of Observed and Simulated Average TP Concentrations, Surface Layer, Triadelphia Reservoir

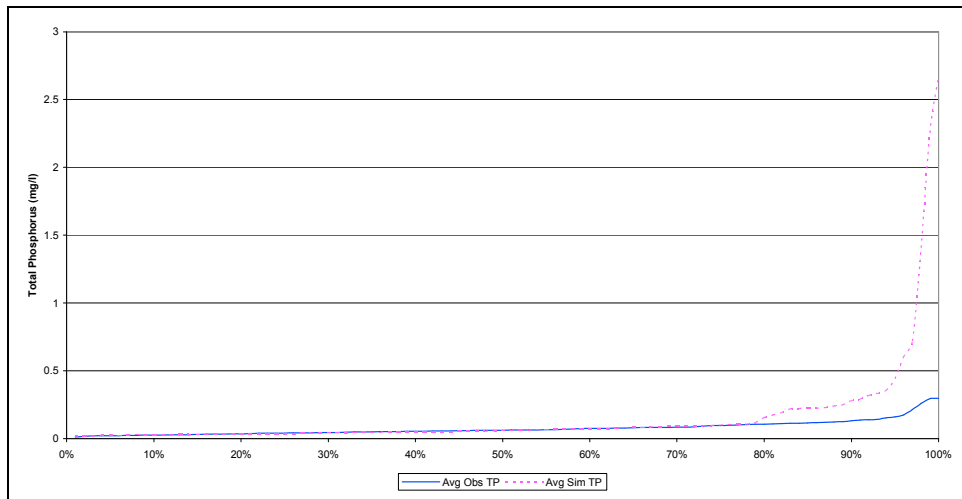


Figure 6.5-2. Cumulative Distribution of Observed and Simulated Average TP Concentrations, Bottom Layer, Triadelphia Reservoir

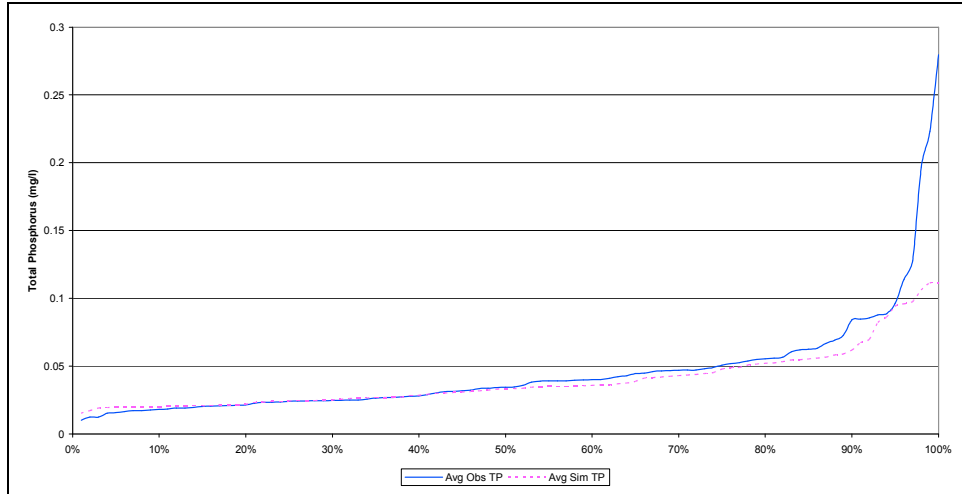


Figure 6.5-3. Cumulative Distribution of Observed and Simulated Average TP Concentrations, Surface Layer, Rocky Gorge Reservoir

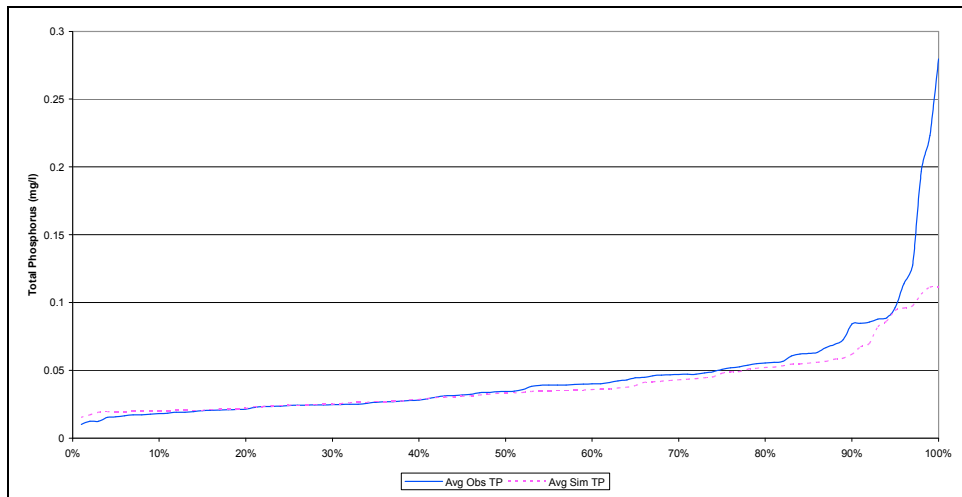


Figure 6.5-4. Cumulative Distribution of Observed and Simulated Average TP Concentrations, Bottom Layer, Rocky Gorge Reservoir

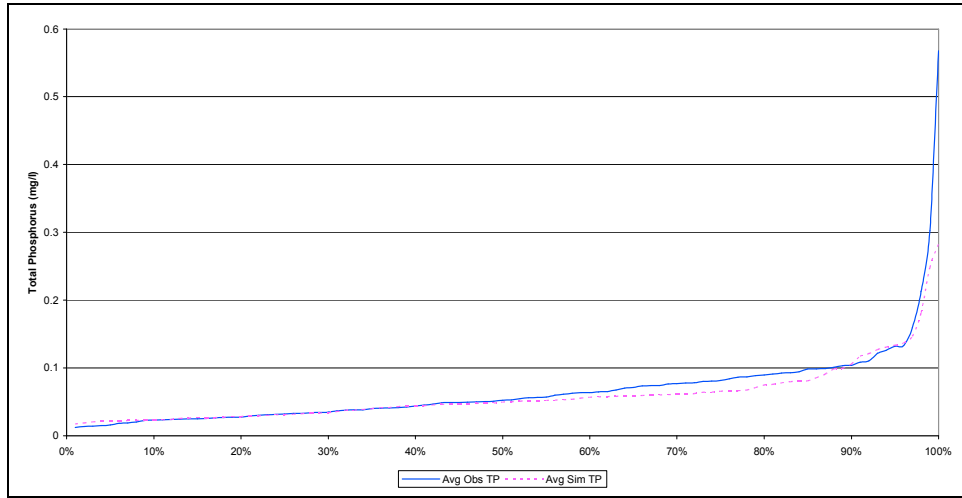


Figure 6.5-5. Cumulative Distribution of Observed and Simulated Average PO4 Concentrations, Surface Layer, Triadelphia Reservoir

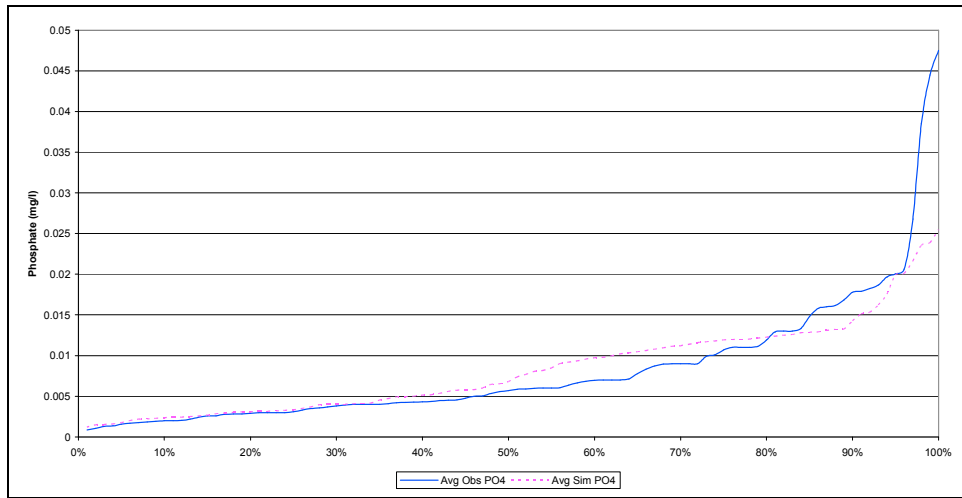


Figure 6.5-6. Cumulative Distribution of Observed and Simulated Average PO4 Concentrations, Bottom Layer, Triadelphia Reservoir

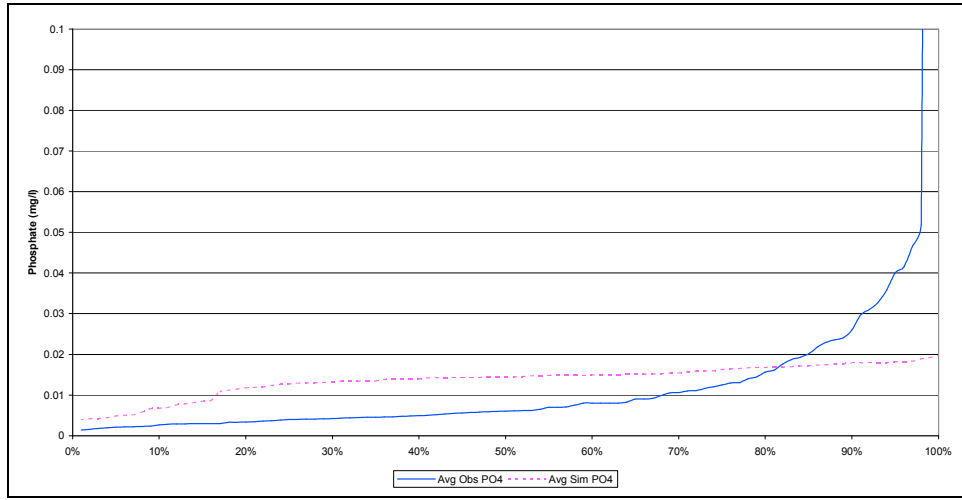


Figure 6.5-7. Cumulative Distribution of Observed and Simulated Average PO4 Concentrations, Surface Layer, Rocky Gorge Reservoir

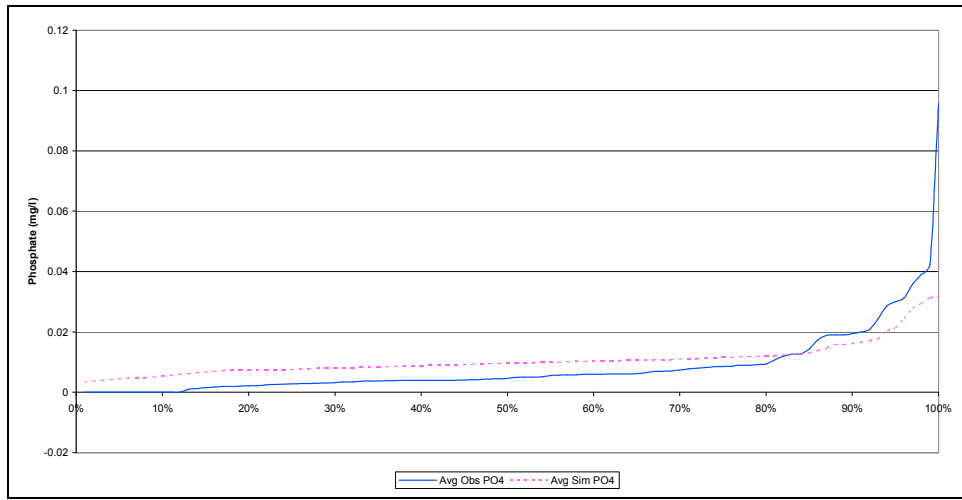


Figure 6.5-8. Cumulative Distribution of Observed and Simulated Average PO4 Concentrations, Bottom Layer, Rocky Gorge Reservoir

6.6 Chlorophyll *a* Calibration

The endpoint for the nutrient TMDLs for the reservoirs is based on chlorophyll *a* concentrations. The calibration of the simulation of Chla and the underlying algal biomass is therefore probably the most important aspect of the calibration.

The Chla calibration establishes the link between nutrient concentrations, on the one hand, and Chla concentrations, and associated biomass, on the other. In addition to the availability of nutrients, algal growth and Chla concentrations are dependent on temperature, algal taxonomy and competition, and predation by zooplankton.

The W2 model permits the simulation of multiple algal species. There was little data on algal taxa in the Patuxent Reservoirs. Taxonomic counts at the water intakes in Rocky Gorge Reservoirs generally were dominated by green algae and diatoms. More extensive taxa data from the Gunpowder Reservoirs, however, suggest that algal taxa in this region can vary widely from season to season and year to year (ICPRB 2006). The algae bloom that occurred in late summer and early fall in 1998 suggests the presence of blue-green algae. The subsequent winter bloom in late winter and early spring in 1999 in Triadelphia Reservoir may also suggest dominance of an algal species not normally present at that time.

For the Patuxent Reservoirs, six algal species were simulated in each reservoir. The six species are intended to cover a variety of potential algal taxa and also to represent the effects of predation and competition that cannot be simulated in the W2 model. Only three species at most were simulated in any given year: a winter species (December through February), a spring species (March through June), and a summer-fall species (July through November). Since there has been no Chla data collected during the winter, the winter species is to some extent a placeholder and could not be calibrated. In some years only two species were simulated, a winter species and a species dominant from spring to fall. Table 6.6-1 shows species simulated by season. Table 6.6-2 shows the growth rate parameters by species, and the temperature parameters by season.

The goal of the Chla calibration is, for each season in which the observed Chla concentration is greater than 10 ug/l, that the maximum simulated Chla concentration, at the dates and locations monitored, should be equal to or greater than maximum observed concentration in that season. In other words, the maximum observed concentration from all the observations taken in a reservoir in a season is compared to the maximum simulated concentration from the corresponding sampling location and dates in a given season. The calibration target is thus less restrictive than a strict pair-wise comparison of observed and simulated concentrations; the maximum simulated concentration can occur at any sample location at any sample date within a season. It is nevertheless a very conservative calibration strategy which ensures that the cumulative distribution of simulated concentrations dominates the observed concentrations.

Figure 6.6-1 compares the monthly maximum observed and simulated concentrations at sampling dates and locations by season in Triadelphia Reservoir. Figure 6.6-2 shows the maximum concentrations by season in Rocky Gorge Reservoir. The data includes the samples taken by MDE in 2000. As the figures show, the Chla calibration generally met its objective. Maximum simulated concentrations by season tend to be equal or greater than their observed counterparts, though there are a few exceptions. Figure 6.6-2 and 6.6-3 show the cumulative distribution of observed and simulated Chla concentrations in Triadelphia and Rocky Gorge Reservoirs, respectively. Both observed and simulated data are restricted to the dates and locations of WSSC’s monitoring program. As the figures show, the distribution of simulated Chla concentrations clearly dominates the observed concentrations for concentrations greater than 10 ug/l.

Figures 6.6-5 and 6.6-6 compare observed and simulated Chla concentrations by sampling date in Triadelphia Reservoir and Rocky Gorge Reservoir, respectively. As both figures show, although it wasn’t the primary objective of the calibration, simulated concentrations do follow the temporal trend in the observed data. Figures C.1–C.3 in Appendix C show time series of observed and simulated maximum Chla concentrations at TR1, TR2, and TR3 in Triadelphia Reservoir, respectively, and Figures C.37–C.39 show the corresponding plots for RG1, RG2, and RG3 in Rocky Gorge Reservoir.

Table 6.6-1. Algae Species Parameterizations By Season

Year	Season	Triadelphia Species	Rocky Gorge Species
1998	Winter	1	1
	Spring	2	2
	Summer	3	3
1999	Winter	1	1
	Spring	4	4
	Summer	5	4
2000	Winter	1	1
	Spring	2	5
	Summer	6	6
2001	Winter	1	1
	Spring	2	4
	Summer	5	4
2002	Winter	1	1
	Spring	2	4
	Summer	5	4
2003	Winter	1	1
	Spring	2	4
	Summer	5	4

Table 6.6-2 Algal Growth Rates and Temperature Parameters

Triadelphia Reservoir									
Season	Rate	Temp1	Temp2	Temp3	Temp4	Fraction1	Fraction2	Fraction3	Fraction4
1	1.0	-2	4	8	10	0.49	0.99	0.99	0.7
2	3.0	10	12	16	25	0.79	0.99	0.99	0.7
3	1.72	27	28	30	32	0.89	0.99	0.99	0.9
4	3.9	3	7.5	8	10	0.79	0.99	0.99	0.9
5	1.5	20	21	23	35	0.79	0.99	0.99	0.3
6	1.6	22	23	25	28	0.79	0.29	0.99	0.3
Rocky Gorge Reservoir									
Season	Rate	Temp1	Temp2	Temp3	Temp4	Fraction1	Fraction2	Fraction3	Fraction4
1	1.00	-2	4	8	10	0.79	0.99	0.99	0.7
2	6.2	10	12	16	20	0.79	0.99	0.99	0.7
3	2.5	20	21	23	25	0.79	0.49	0.99	0.5
4	3.0	10	12	20	28	0.79	0.99	0.99	0.6
5	7.5	5	10	12	14	0.79	0.99	0.99	0.5
6	2.1	25	26	27	30	0.79	0.79	0.99	0.3

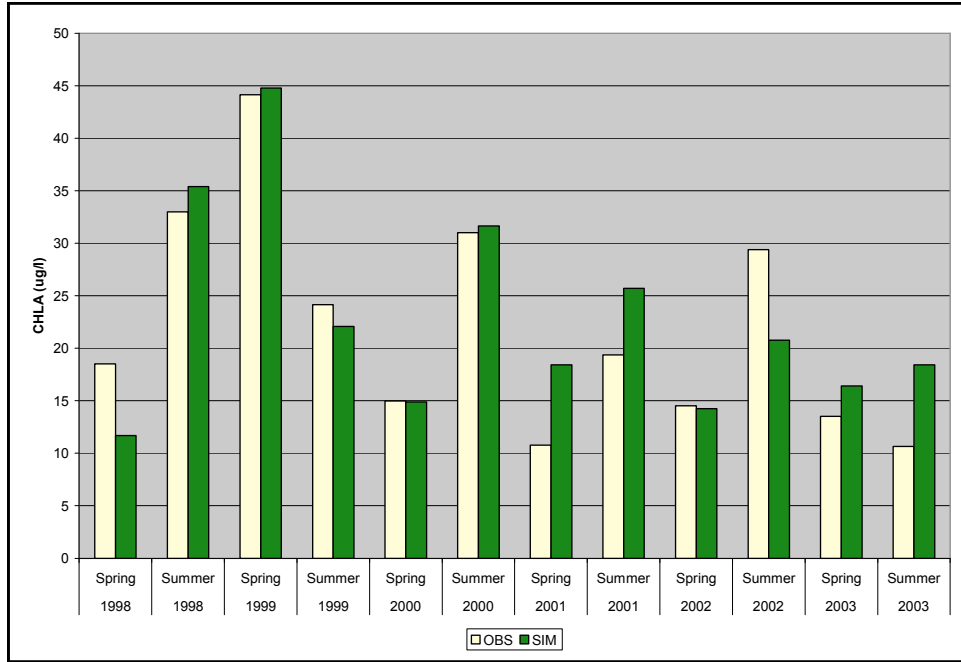


Figure 6.6-1 Maximum Observed and Simulated Chla Concentrations By Season, Triadelphia Reservoir

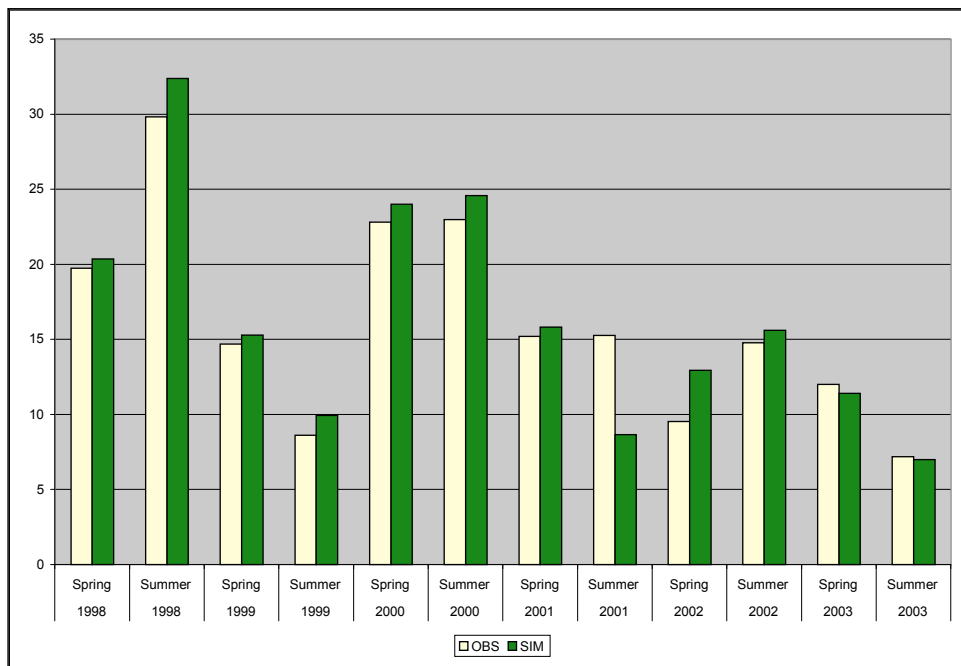
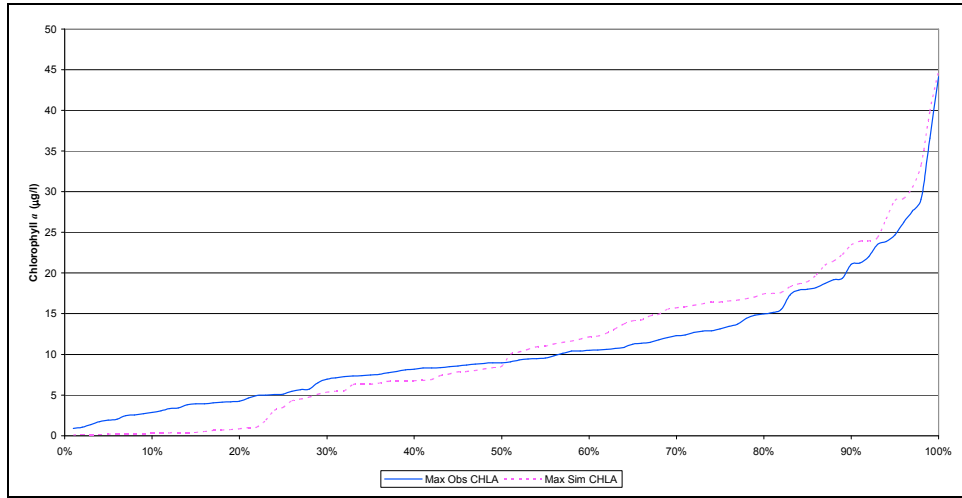
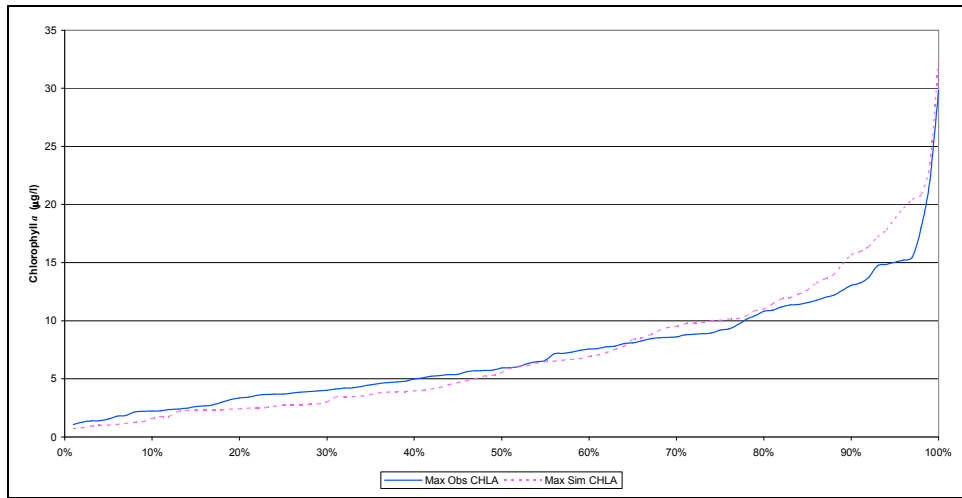


Figure 6.6-2 Maximum Observed and Simulated Chla Concentrations By Season, Rocky Gorge Reservoir



6.6-3 Cumulative Distribution of Observed and Simulated Chla Concentrations, Triadelphia Reservoir



6.6-3 Cumulative Distribution of Observed and Simulated Chla Concentrations, Rocky Gorge Reservoir

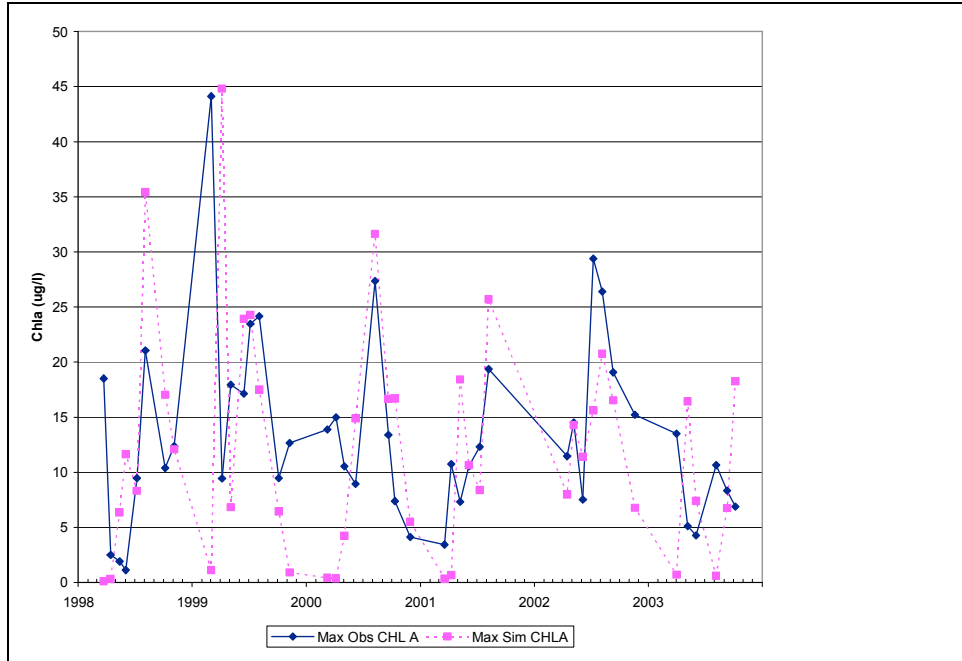


Figure 6.6-5. Observed and Simulated Maximum Chla Concentrations By Sampling Date, Triadelphia Reservoir

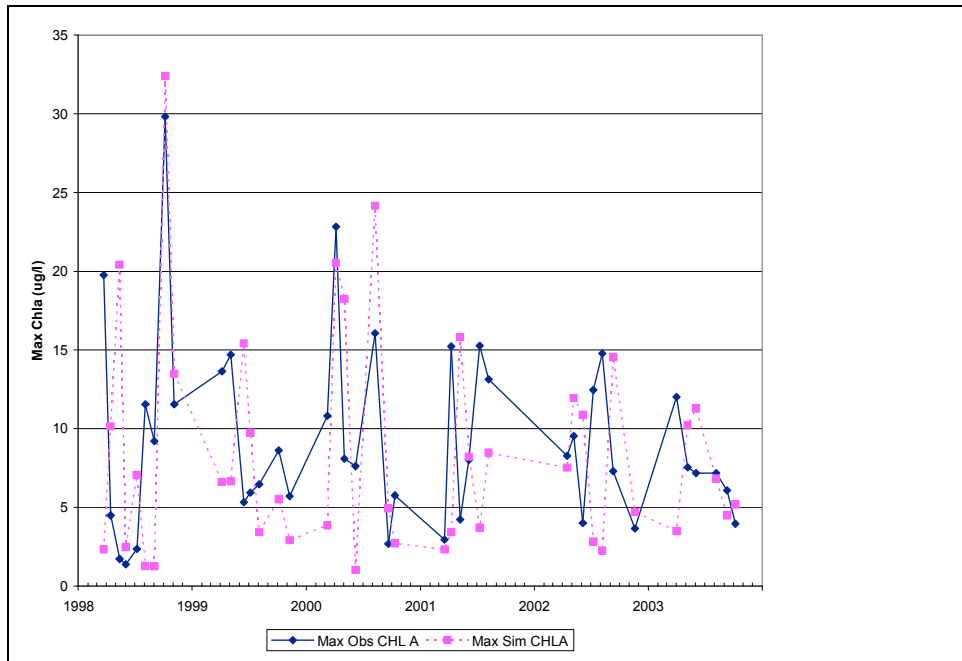


Figure 6.6-6. Observed and Simulated Maximum Chla Concentrations By Sampling Date, Rocky Gorge Reservoir

6.7 Dissolved Oxygen Calibration

After the calibration of the simulation of chlorophyll *a* and the corresponding algal biomass, the calibration of the simulation of dissolved oxygen is probably the most important task of the calibration. The W2 models must simulate the hypoxia observed in the hypolimnia of both Triadelphia and Rocky Gorge Reservoirs, as a function of allochthonous and autochthonous organic matter loading rates. The surface layer DO simulation must demonstrate that DO standards are met under the TMDL loading rates.

6.7.1 Bottom DO Calibration

Figure 6.7-1 shows the observed and simulated average bottom DO concentrations in Triadelphia Reservoir at TR1 just upstream of Brighton Dam. Figure 6.7-2 shows observed and simulated average bottom DO concentrations at RG1 upstream of Brighton Dam. The simulation very successfully captures the seasonal hypoxia in Triadelphia Reservoir. The simulation of seasonal hypoxia is somewhat less successfully captured in Rocky Gorge Reservoir. In two years, 2000 and 2002, simulated DO concentrations do not drop as far as observed values. The timing of the simulated DO concentrations Rocky Gorge Reservoir follows the observed data less well than in Triadelphia Reservoir.

Table 6.7-1 shows the key parameters that determine SOD in the calibration of bottom DO. One difficulty in the calibration of Rocky Gorge Reservoir is that temperature in the bottom layers varies more widely through the year and between years. It is therefore difficult to determine a single set of temperature profiles that fits all years. In contrast there is much less variation in temperature in the bottom layer of Rocky Gorge.

Table 6.7-2 shows summary statistics for observed and simulated DO in the bottom layers of the reservoirs. Figures 6.7-3 and 6.7-4 show the cumulative distribution of observed and simulated DO concentrations in the bottom layers of Triadelphia and Rocky Gorge Reservoirs, respectively. Figures C6 and C.42 in Appendix C show average observed and simulated DO concentrations in the bottom layers of the reservoirs at TR2 and RG2, respectively.

Table 6.7-1 Bottom DO Calibration Parameter Values

Parameter	Triadelphia	Rocky Gorge
Organic Sediment Decay Rate (day-1)	0.065	0.06
Sediment Decay Temperature Start °C (% decay rate)	8.5 (20%)	15 (80%)
Sediment Decay Temperature Max °C (%decay rate)	10 (99%)	20 (99%)

Table 6.7-2 Summary Statistics for Observed and Simulated Bottom DO

Statistic: Bottom DO	Triadelphia Reservoir		Rocky Gorge Reservoir	
	Observed	Simulated	Observed	Simulated
Min	0.0533	0.0000	0.0650	0.0000
1 st Q	0.0875	0.0000	0.9225	0.5868
Median	0.1467	0.0700	3.6133	3.0288
3 rd Q	6.7850	8.1000	7.4413	7.0050
Max	13.9950	12.9850	14.0442	12.3325
Mean	3.4050	3.5972	4.4165	4.1238
Std. Dev.	4.6686	4.8697	3.7605	3.8048
R ²	0.9061		0.5448	

6.7.2 Surface DO Calibration

Figure 6.7-5 shows the average observed and simulated surface DO concentrations in Triadelphia Reservoir at TR1 just upstream of Brighton Dam. Figure 6.7-2 shows average observed and simulated surface DO concentrations at RG1 upstream of Brighton Dam. Both simulations capture the seasonal trend in observed surface DO concentrations and their observed range. The simulation of surface DO concentrations in Rocky Gorge matches the observed data better than the simulation of Triadelphia, because the observed surface DO concentrations in Triadelphia exhibit significant intra-seasonal variability which the W2 model does not reproduce.

Table 6.7-3 shows the key parameters controlling re-aeration used in the W2 simulations. Table 6.7-4 shows summary statistics for observed and simulated DO in the surface layers of the reservoirs. Figures 6.7-7 and 6.7-8 show the cumulative distribution of observed and simulated DO concentrations in the surface layers of Triadelphia and Rocky Gorge Reservoirs, respectively. Figures C.4 and C.5 in Appendix C show average observed and simulated DO concentrations in the surface layers of Triadelphia Reservoir at TR2 and TR3, respectively. Figures C.40 and C.41 in Appendix C show average observed and simulated DO concentrations in the surface layers of Rocky Gorge Reservoir at RG2 and RG3, respectively.

Table 6.7-3. Surface DO Calibration Parameter Values

Parameter	Triadelphia	Rocky Gorge
Reaeration Coefficient-1	3.0	2.0
Reaeration Coefficient-2	0.10	0.10
Reaeration Coefficient-3	3.0	3.0

Table 6.7-4 Summary Statistics for Observed and Simulated Surface DO

Statistic: Surface DO	Triadelphia Reservoir		Rocky Gorge Reservoir	
	Observed	Simulated	Observed	Simulated
Min	5.5300	6.5600	3.3875	4.1500
1 st Q	8.6063	7.8300	6.8150	7.5209
Median	9.7988	8.4700	8.4073	7.9213
3 rd Q	11.1883	9.6867	9.9854	9.1250
Max	14.9400	13.0550	14.3150	12.3200
Mean	9.8821	8.9354	8.4678	8.4153
Std. Dev.	1.9540	1.4150	2.2044	1.5201
R ²	0.2284		0.4394	

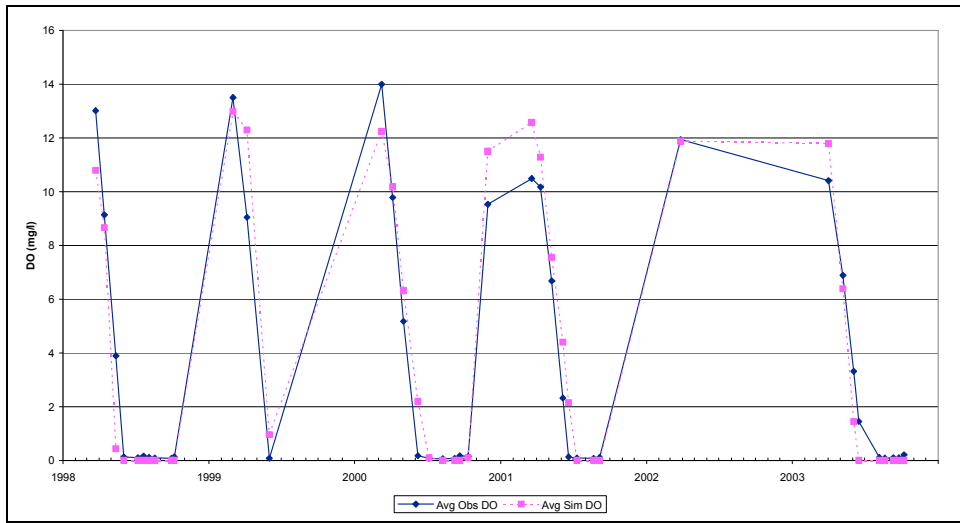


Figure 6.7-1. Observed and Simulated Average Bottom DO Concentrations, TR1, Calibration Scenario, Triadelphia Reservoir

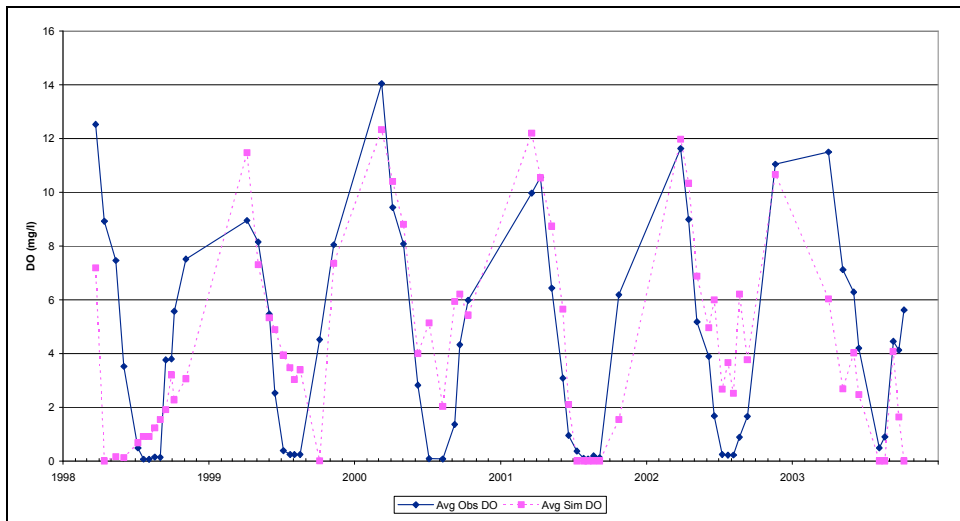


Figure 6.7-2. Observed and Simulated Average Bottom DO Concentrations, RG1, Calibration Scenario, Rocky Gorge Reservoir

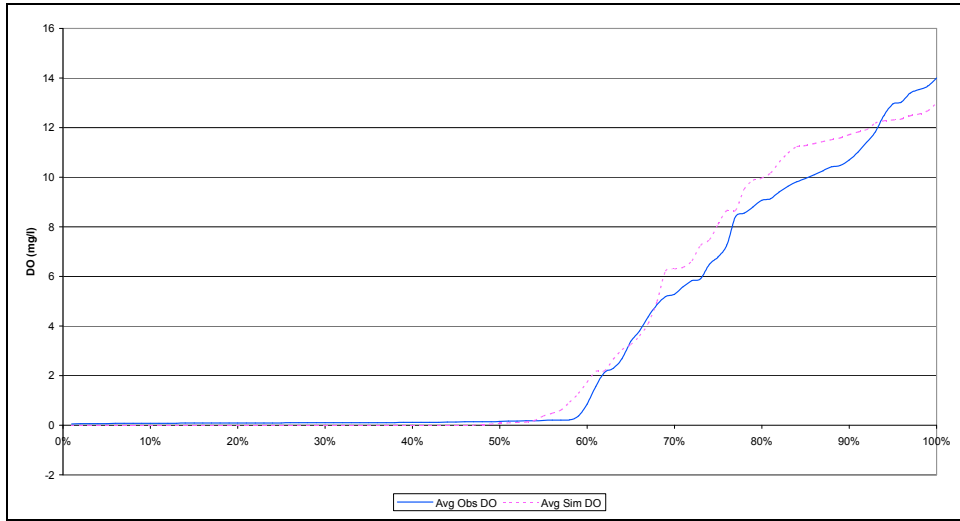


Figure 6.7-3. Observed and Simulated Cumulative Distribution of Bottom DO Concentrations, Triadelphia Reservoir

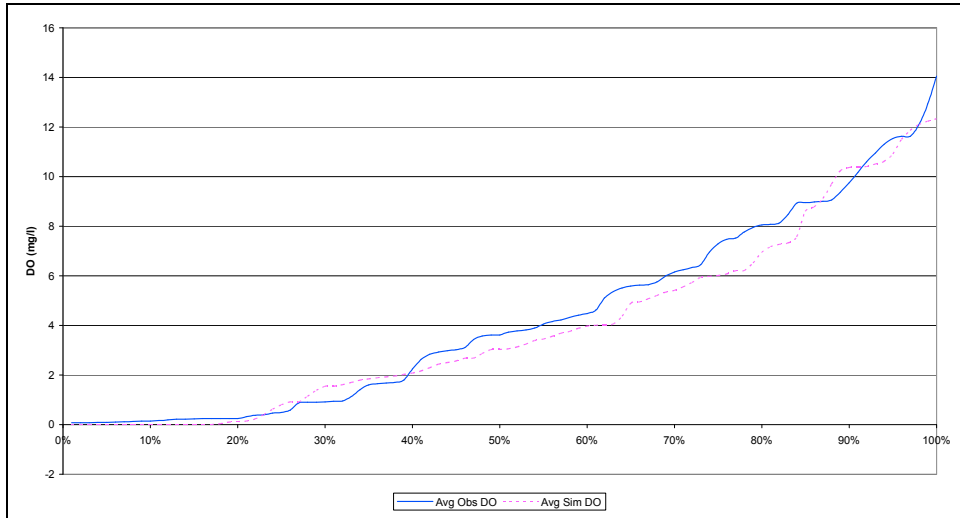


Figure 6.7-4. Observed and Simulated Cumulative Distribution of Bottom DO Concentrations, Rocky Gorge Reservoir

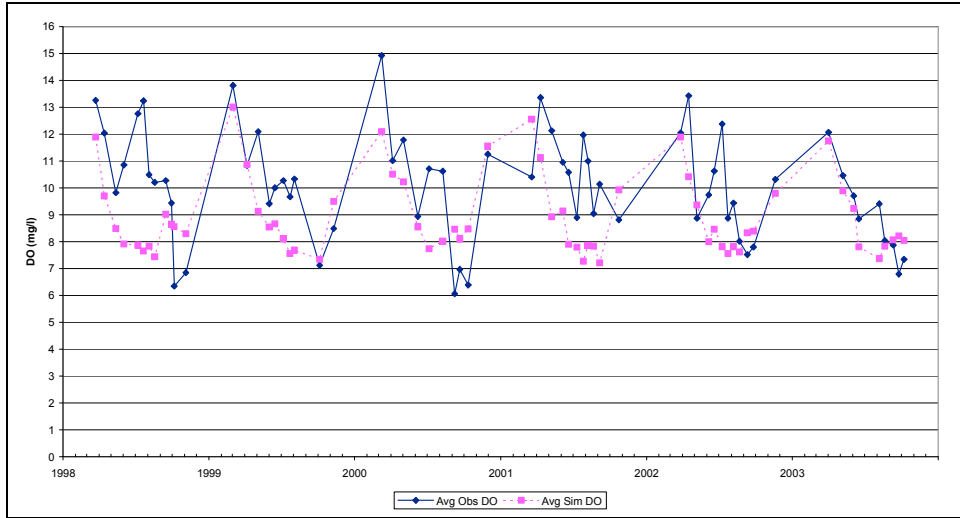


Figure 6.7-5. Observed and Simulated Average Surface DO Concentrations, TR1, Calibration Scenario, Triadelphia Reservoir

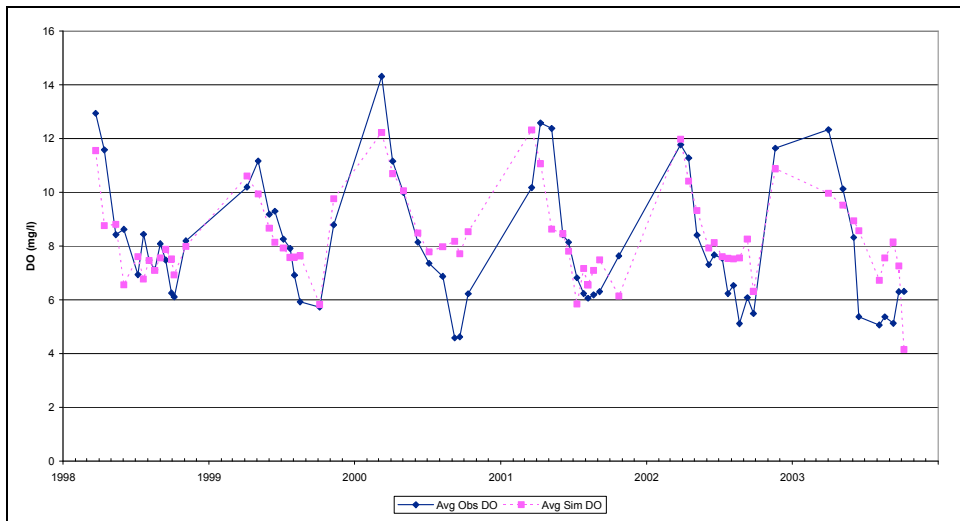


Figure 6.7-6. Observed and Simulated Average Surface DO Concentrations, RG1, Calibration Scenario, Rocky Gorge Reservoir

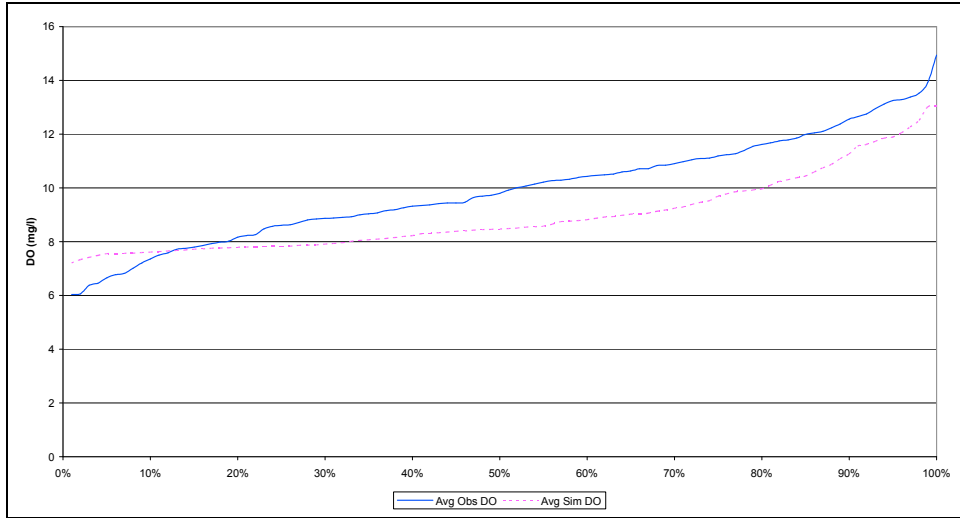


Figure 6.7-7. Observed and Simulated Cumulative Distribution of Surface DO Concentrations, Triadelphia Reservoir

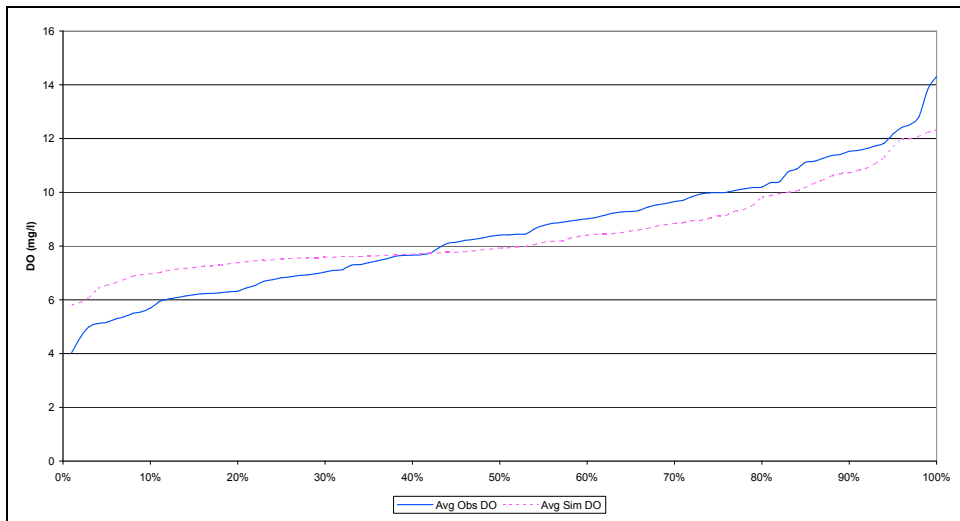


Figure 6.7-8. Observed and Simulated Cumulative Distribution of Surface DO Concentrations, Rocky Gorge Reservoir

6.8 Nitrogen Calibration

The goals of the nitrogen calibration were modest. As Section 5.8 shows, the reservoirs are phosphorus limited, and, consequently, the nutrient TMDL is expressed in terms of total phosphorus. Sections 4.3 and 6.2.3 describes how the fact that forms of organic material are the state variables in the W2 model force organic nitrogen to be determined as a fixed stoichiometric ratio of organic phosphorus, in order to maintain a mass balance of phosphorus. Section 4.5.3. explains how there is some evidence that nitrate is underpredicted in the HSPF model. Given these constraints, the primary goal of the nitrogen calibration of the W2 models was to do no harm, by avoiding inducing an artificial nitrogen limitation to algal growth were none exists. A more idealized goal is (1) to reproduce the distribution of observed ammonia-N (NH₄), nitrate-N (NO₃), and TN concentrations in the surface and bottom layers of the reservoirs, and (2) capture the seasonal trends in NH₄, NO₃, and TN demonstrated in Section 5.5.

The calibration was moderately successful at meeting these ideal goals. Since algal growth dynamics and the decay organic material were determined through the calibration of phosphorus and chlorophyll, only three processes could be parameterized to calibrate NH₄, NO₃, and TN: (1) the release of NH₄ from sediments through diagenesis, (2) nitrification or the conversion of NH₄ to NO₃, and (3) denitrification of NO₃ under anaerobic conditions in the sediment and water column. As a matter of fact, the release of NH₄ from the sediments is entirely determined by the SOD rate and the fixed nitrogen content of organic material, so really only nitrification and denitrification could be parameterized. Table 6.8-1 shows the key rate parameters for these processes. It should be noted that there are two denitrification pathways, one is based on water-column denitrification under anaerobic conditions, and the other represents the flux of nitrate into the sediments as a “settling” velocity.

Table 6.8-1 Key Nitrogen Calibration Parameters

Parameter	Triadelphia Reservoir	Rocky Gorge Reservoir
Nitrification Rate (1/d)	0.1	0.2
Denitrification Rate (1/d)	0.01	0.0
Denitrification Velocity (m/d)	0.1	0.1

6.8.1 Ammonia

Tables 6.8-2 and 6.8-3 show summary statistics comparing observed and simulated surface and bottom ammonia concentrations in Triadelphia and Rocky Gorge Reservoirs. Figures 6.8-1 through 6.8-4 show the cumulative distributions of observed and simulated NH₄ concentrations in the surface and bottom layers of Triadelphia and Rocky Gorge Reservoirs.

As shown in Section 5.5, there is a distinct seasonal pattern of NH₄ concentrations in the bottom layer of Triadelphia Reservoir due to the release of ammonia in diagenesis. The W2 model doesn't capture that pattern. The calibration of NH₄ in Triadelphia represents a compromise between matching the distribution of observed values and matching the average concentration overall. In Rocky Gorge, there is less of a distinct seasonal trend in NH₄ concentrations. And the simulation better matches the distribution of observed NH₄ concentrations.

Figures C.19–C.24 in Appendix C show time series of observed and simulated NH₄ concentrations in the surface and bottom layers of Triadelphia Reservoir at stations TR1, TR2, and TR3. Figures C.55–C.60 show the same time series for stations RG1, RG2, and RG3 in Rocky Gorge Reservoir.

Table 6.8-2 Summary Statistics for Surface Observed and Simulated NH₄

Statistic: Surface NH₄	Triadelphia Reservoir		Rocky Gorge Reservoir	
	Observed	Simulated	Observed	Simulated
Min	0.0000	0.0013	0.0000	0.0008
1 st Q	0.0000	0.0029	0.0000	0.0086
Median	0.0190	0.0337	0.0100	0.0242
3 rd Q	0.0727	0.1292	0.0586	0.0602
Max	2.4659	1.5700	1.1956	0.2091
Mean	0.1103	0.0752	0.0513	0.0418
Std. Dev.	0.3400	0.1478	0.1271	0.0462
R ²	0.1597		0.0027	

Table 6.8-3 Summary Statistics for Bottom Observed and Simulated NH₄

Statistic: Bottom NH₄	Triadelphia Reservoir		Rocky Gorge Reservoir	
	Observed	Simulated	Observed	Simulated
Min	0.0019	0.0146	0.0000	0.0122
1 st Q	0.0906	0.1897	0.0312	0.1190
Median	0.1904	0.2676	0.1399	0.1838
3 rd Q	0.5611	0.4285	0.2637	0.2935
Max	2.6510	0.6484	1.0014	0.6099
Mean	0.4413	0.2907	0.1758	0.2168
Std. Dev.	0.5860	0.1423	0.1811	0.1385
R ²	0.0004		0.0079	

6.8.2 Nitrate

Figures C.25–C.30 in Appendix C show time series of observed and simulated NO₃ concentrations in the surface and bottom layers of Triadelphia Reservoir at stations TR1, TR2, and TR3. Figures C.61–C.65 show the same time series for stations RG1, RG2, and RG3 in Rocky Gorge Reservoir. As the figures show, the W2 simulations in both reservoirs successfully reproduce the seasonal trends in NO₃ concentrations.

Tables 6.8-4 and 6.8-5 show summary statistics comparing observed and simulated surface and bottom nitrate concentrations in Triadelphia and Rocky Gorge Reservoirs. Figures 6.8-5–6.8-8 show the cumulative distributions of observed and simulated NO₃ concentrations in the surface and bottom layers of Triadelphia and Rocky Gorge Reservoirs. As the tables show, the coefficient of determination (R^2) shows that a significant portion of the variability in observed NO₃ concentrations are captured in the W2 models. This reflects the agreement in seasonal trend between the models and the observed data. As both the tables and figures show, there is good agreement between the observed and simulated distributions of NO₃ concentrations in Triadelphia Reservoir. Observed concentrations in Rocky Gorge Reservoir are under predicted by about 20%. This is most likely due to under predicting nitrate-loading rates.

Table 6.8-4 Summary Statistics for Surface Observed and Simulated NO₃

Statistic:	Triadelphia Reservoir		Rocky Gorge Reservoir	
	Observed	Simulated	Observed	Simulated
Surface NO ₃				
Min	0.0000	0.6500	0.2243	0.2900
1 st Q	0.9749	1.0550	0.7604	0.4600
Median	1.4405	1.5200	1.0929	0.6700
3 rd Q	1.9386	1.8500	1.4589	1.1400
Max	3.1093	3.9300	2.5423	1.7200
Mean	1.4182	1.5253	1.0953	0.7934
Std. Dev.	0.6777	0.6067	0.4530	0.3859
R^2	0.3687		0.5197	

Table 6.8-5 Summary Statistics for Bottom Observed and Simulated NO₃

Statistic:	Triadelphia Reservoir		Rocky Gorge Reservoir	
	Observed	Simulated	Observed	Simulated
Bottom NO ₃				
Min	0.0007	0.2000	0.0026	0.2000
1 st Q	0.9776	0.7400	0.6965	0.4775
Median	1.4662	1.1800	1.0594	0.7250
3 rd Q	1.9718	1.6600	1.3274	1.1375
Max	3.1315	3.0200	1.8360	1.7500
Mean	1.3901	1.2468	1.0245	0.8171
Std. Dev.	0.7603	0.6271	0.4348	0.3991
R^2	0.4329		0.4281	

6.8.3 Total Nitrogen

Tables 6.8-6 and 6.8-7 show summary statistics comparing observed and simulated surface and bottom TN concentrations in Triadelphia and Rocky Gorge Reservoirs. Figures 6.8-9–6.8-12 show the cumulative distributions of observed and simulated TN concentrations in the surface and bottom layers of Triadelphia and Rocky Gorge Reservoirs. TN is underpredicted in both reservoirs. Simulated TN concentrations are about 15–20 % less than observed concentrations in Triadelphia Reservoir and by 30–40% in Rocky Gorge Reservoir. Since simulated nitrate matched observed levels in Triadelphia Reservoir, the undersimulation of TN is due to an undersimulation of organic nitrogen. In Rocky Gorge, half the undersimulation is due to the undersimulation of nitrate.

Figures C.31–C.36 in Appendix C show time series of observed and simulated NO₃ concentrations in the surface and bottom layers of Triadelphia Reservoir at stations TR1, TR2, and TR3. Figures C.66–C.72 show the same time series for stations RG1, RG2, and RG3 in Rocky Gorge Reservoir.

Table 6.8-6 Summary Statistics for Surface Observed and Simulated TN

Statistic:	Triadelphia Reservoir		Rocky Gorge Reservoir	
	Observed	Simulated	Observed	Simulated
Surface TN				
Min	0.3484	0.8300	0.6930	0.3300
1 st Q	1.6315	1.2650	1.2109	0.5000
Median	2.0911	1.7000	1.5760	0.7700
3 rd Q	2.4614	2.0550	1.9176	1.2700
Max	3.5908	4.2400	2.9909	1.9600
Mean	2.0590	1.7224	1.5639	0.8970
Std. Dev.	0.5980	0.6121	0.4588	0.4270
R ²	0.2878		0.4881	

Table 6.8-7 Summary Statistics for Bottom Observed and Simulated TN

Statistic:	Triadelphia Reservoir		Rocky Gorge Reservoir	
	Observed	Simulated	Observed	Simulated
Bottom TN				
Min	1.0928	0.4500	0.7567	0.4000
1 st Q	1.8897	1.0800	1.3782	0.7325
Median	2.3564	1.6000	1.7260	1.1000
3 rd Q	2.5840	2.0950	1.9531	1.3900
Max	3.7070	8.4200	2.5626	2.7100
Mean	2.2682	1.7979	1.6543	1.1156
Std. Dev.	0.5497	1.2105	0.3947	0.4633
R ²	0.0387		0.3919	

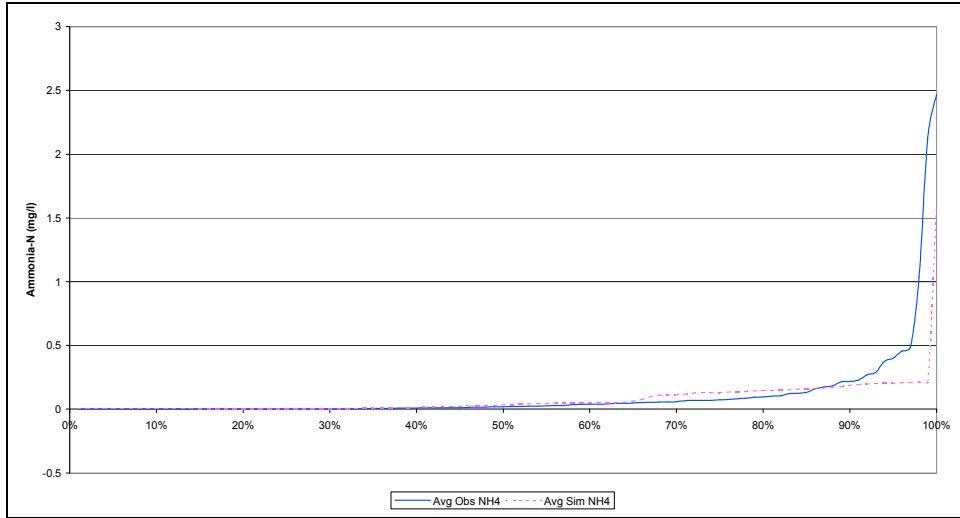


Figure 6.8-1. Cumulative Distribution of Observed and Simulated Average NH4 Concentrations, Surface Layer, Triadelphia Reservoir

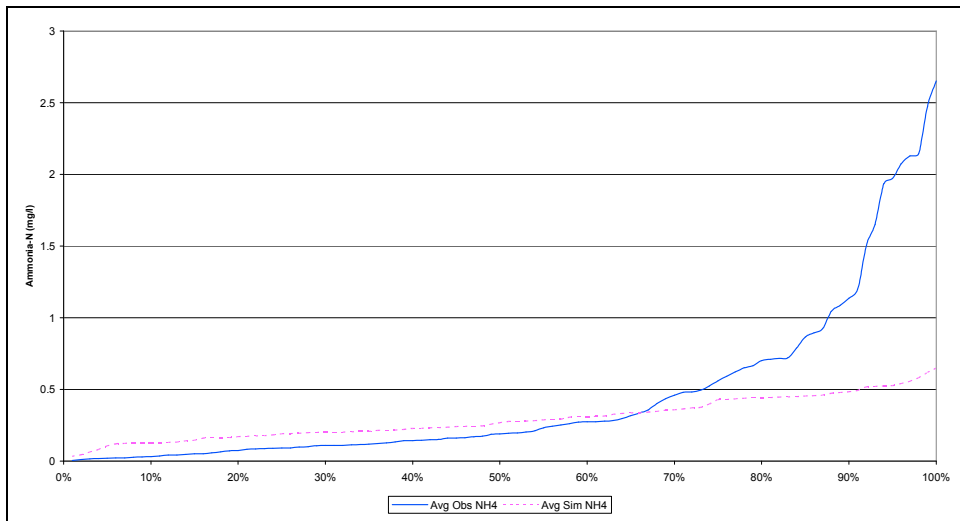


Figure 6.8-2. Cumulative Distribution of Observed and Simulated Average NH4 Concentrations, Bottom Layer, Triadelphia Reservoir

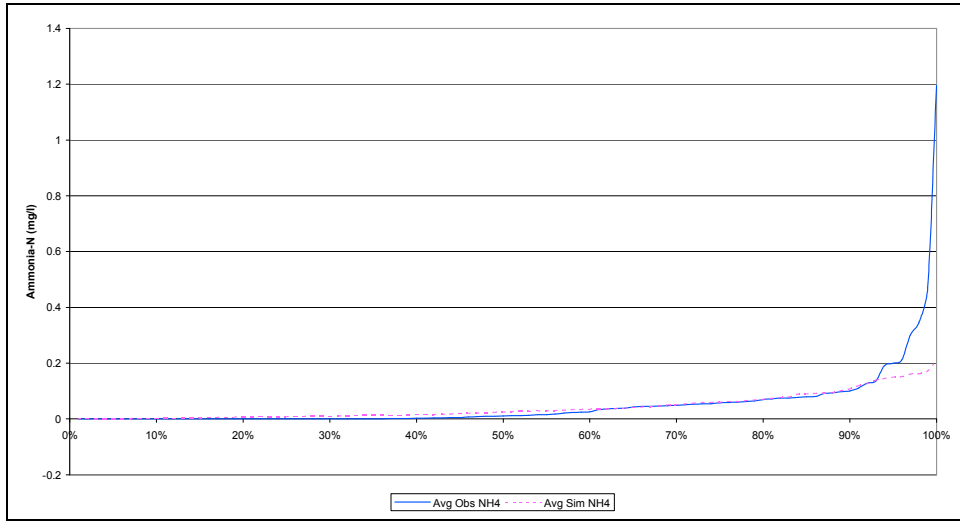


Figure 6.8-3. Cumulative Distribution of Observed and Simulated Average NH4 Concentrations, Surface Layer, Rocky Gorge Reservoir

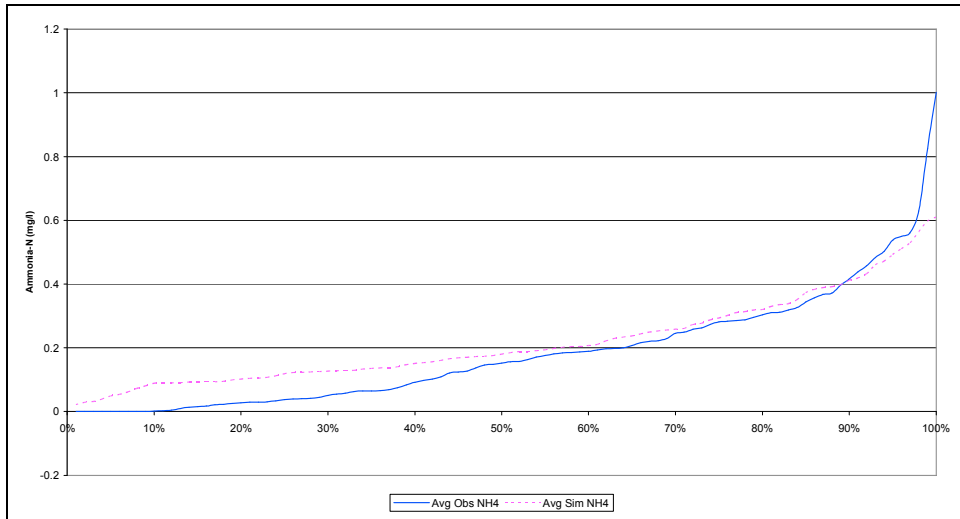


Figure 6.8-4. Cumulative Distribution of Observed and Simulated Average NH4 Concentrations, Bottom Layer, Rocky Gorge Reservoir

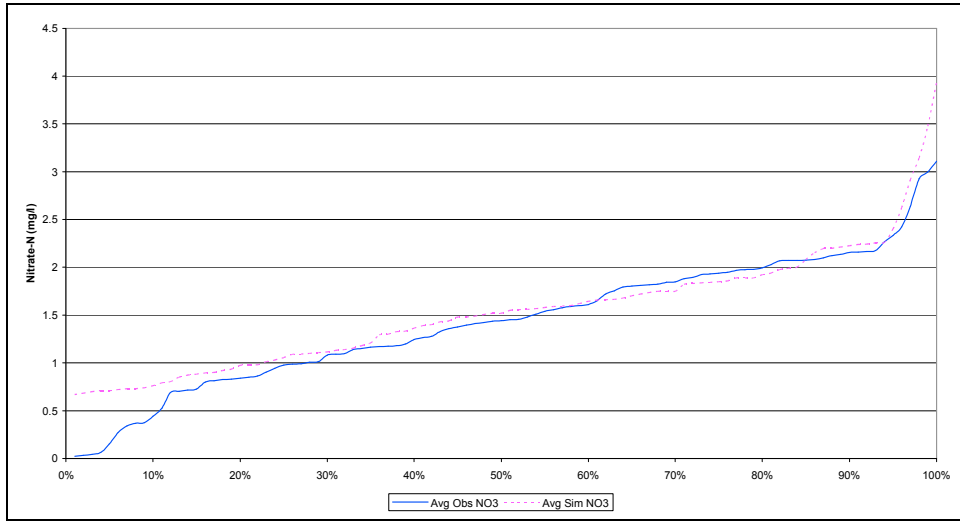


Figure 6.8-5. Cumulative Distribution of Observed and Simulated Average NO3 Concentrations, Surface Layer, Triadelphia Reservoir

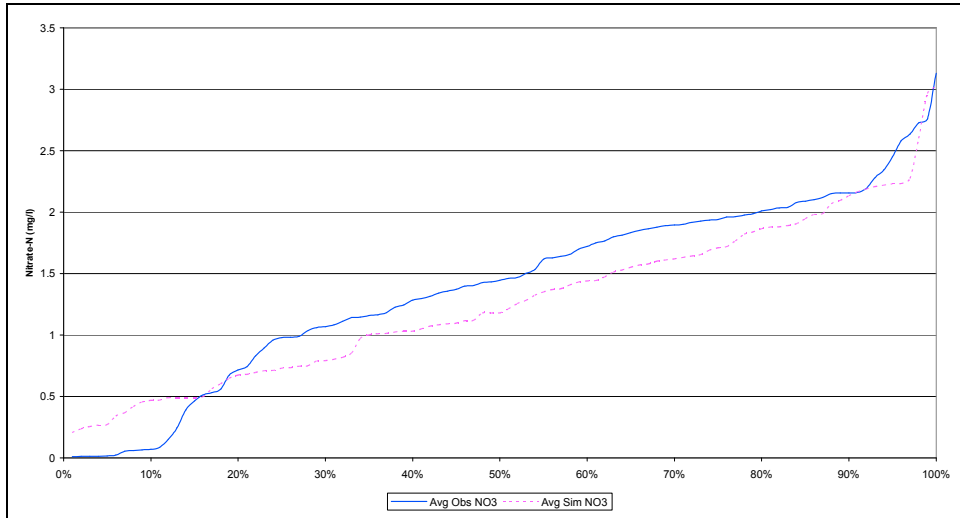


Figure 6.8-6. Cumulative Distribution of Observed and Simulated Average NO3 Concentrations, Bottom Layer, Triadelphia Reservoir

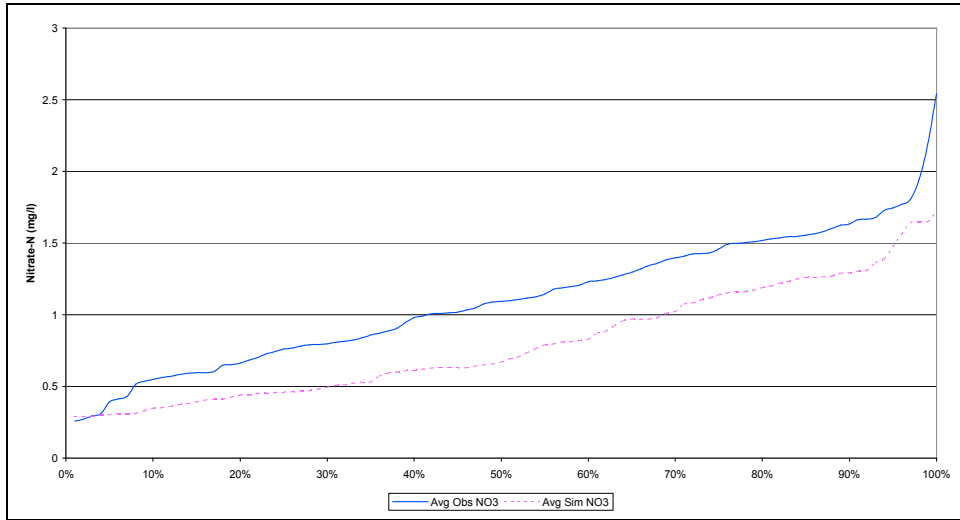


Figure 6.8-7. Cumulative Distribution of Observed and Simulated Average NO3 Concentrations, Surface Layer, Rocky Gorge Reservoir

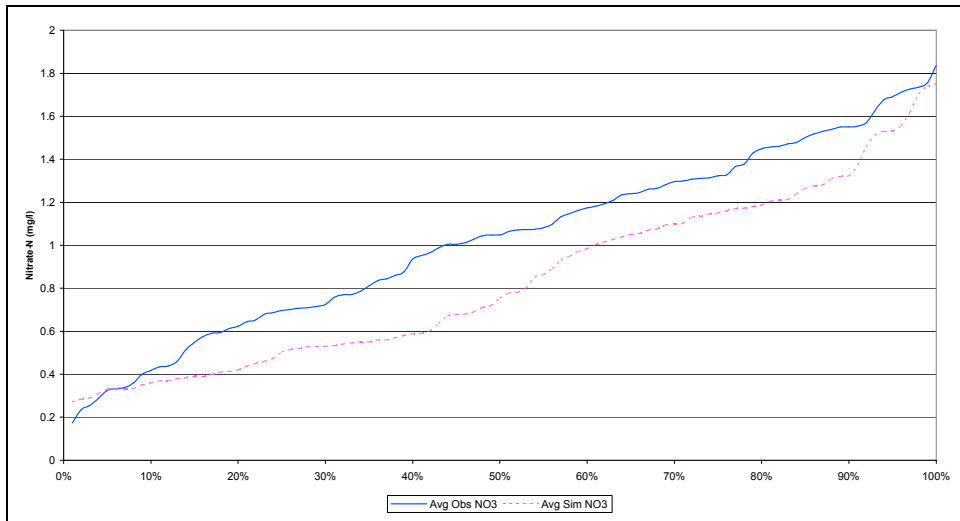


Figure 6.8-8. Cumulative Distribution of Observed and Simulated Average NO3 Concentrations, Bottom Layer, Rocky Gorge Reservoir

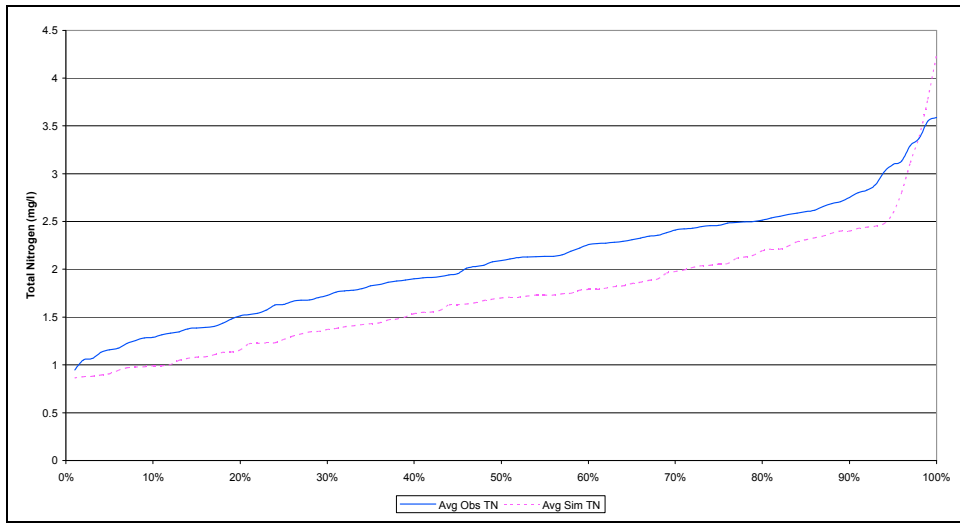


Figure 6.8-9. Cumulative Distribution of Observed and Simulated Average TN Concentrations, Surface Layer, Triadelphia Reservoir

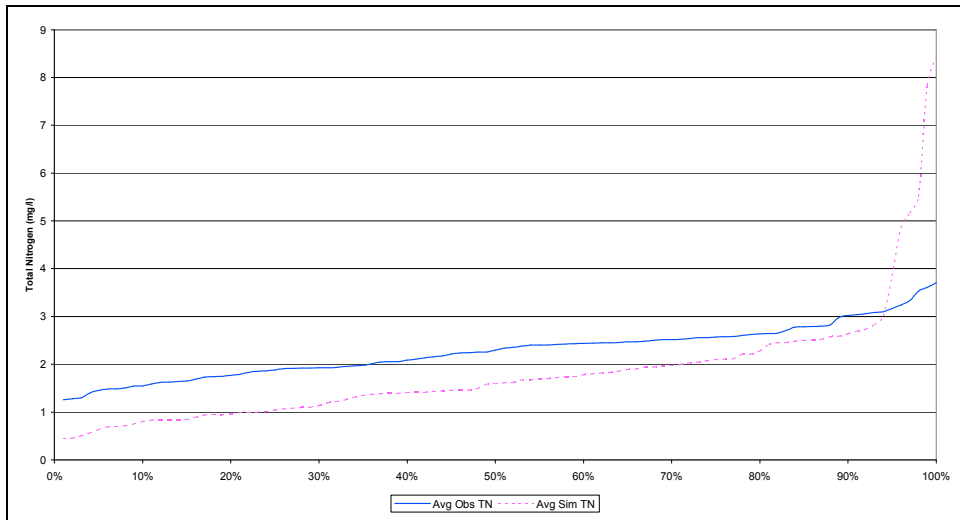


Figure 6.8-10. Cumulative Distribution of Observed and Simulated Average TN Concentrations, Bottom Layer, Triadelphia Reservoir

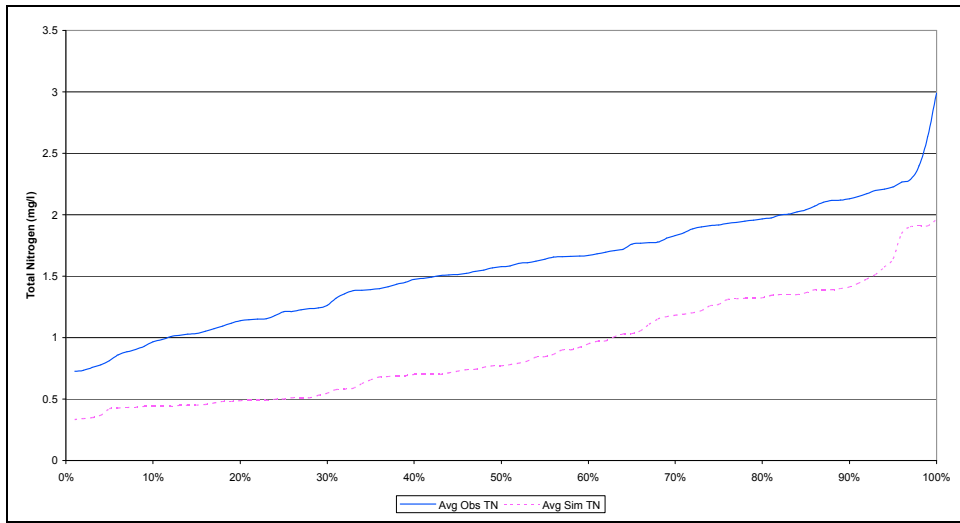


Figure 6.8-11. Cumulative Distribution of Observed and Simulated Average TN Concentrations, Surface Layer, Rocky Gorge Reservoir

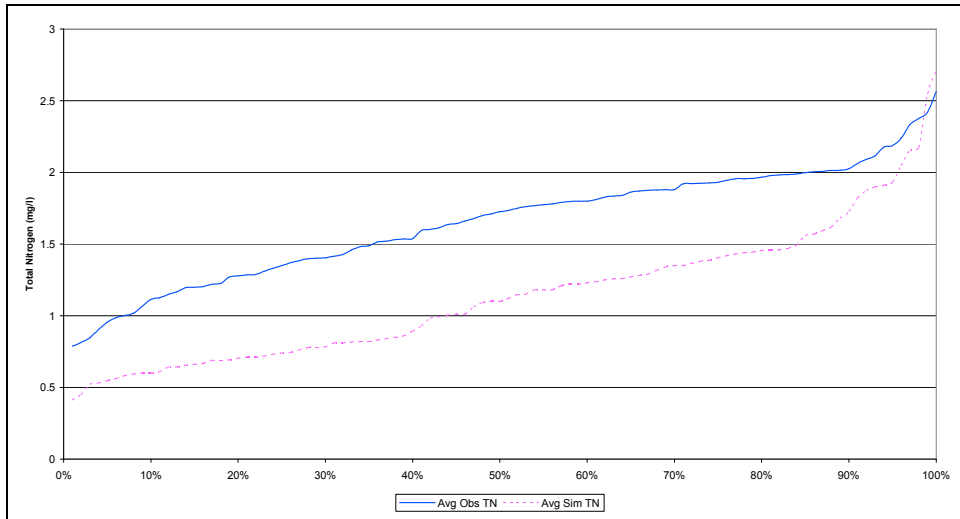


Figure 6.8-12. Cumulative Distribution of Observed and Simulated Average TN Concentrations, Bottom Layer, Rocky Gorge Reservoir

7.0 LOAD REDUCTION SCENARIOS AND SENSITIVITY ANALYSIS

The primary purpose of the Patuxent Reservoirs modeling framework, including the W2 models of Triadelphia and Rocky Gorge Reservoirs, is to determine the maximum total phosphorus loads which allow the reservoirs to meet the TMDL endpoints for chlorophyll and dissolved oxygen described in section 5.1.1.

Using the calibrated reservoir models, phosphorus loads were reduced until a simulated load reduction achieved the desired TMDL endpoints. It was determined that a total phosphorus load reduction of 58% in Triadelphia Reservoir and 48% in Rocky Gorge Reservoir met the TMDL endpoints for chlorophyll. These TMDL Scenarios also met the dissolved oxygen endpoints in the well-mixed surface layer under stratified conditions; deviations from the endpoints only occurred when oxygen-poorer layers from the metalimnion were mixed into the surface layer. Hypoxia still occurred in the bottom layers even under reduced loading rates.

The interim DO criteria for reservoirs recognize that hypolimnetic hypoxia may be a natural condition determined by reservoir morphology and stratification. A scenario was developed which represented the loads that would occur if the watersheds draining to Triadelphia and Rocky Gorge Reservoirs were entirely forested. The All-Forest Scenario was used to test whether hypoxia would occur in the hypolimnion even under natural conditions. The scenario confirmed that hypoxia would occur even under all-forested conditions and that therefore, Triadelphia and Rocky Gorge Reservoirs would meet the interim DO criteria under the TMDL Scenarios.

The actual TMDLs for Triadelphia and Rocky Gorge Reservoirs, specified according to the provisions of the Clean Water Act, are described in the TMDL documentation (MDE 2007). This chapter describes the TMDL Scenario and All-Forest Scenario in the context of model sensitivity analysis, after providing technical details on how the scenarios and other sensitivity analyses were implemented.

7.1. Scenario Descriptions

7.1.1. TMDL Scenario

The TMDL load reduction scenarios were taken equally across all species of phosphorus: dissolved phosphate, particulate organic and inorganic phosphorus, and the phosphorus in labile CBOD, dissolved labile organic matter.

7.1.2. All Forest Scenario

In the all-forest scenario, flows were taken from all land uses, but constituent EOS loads were determined as if all the land in each subwatershed was forested. The

parameterization of all in-stream processes, including scour and phosphorus sorption dynamics, were taken from the Calibration Scenario. If the reservoir watersheds were truly all-forested, inflows to the reservoirs would be different, but different inflows would demand different outflows, and setting the outflows would require determining how the reservoirs would be operated under all-forested conditions. The All-Forest Scenario constructed here represents a controlled simulation experiment, in which only one set of factors, the loads of dissolved and labile particulate organic phosphorus, are changed from the Calibration Scenario. Under this scenario, all other factors, including reservoir stratification, remain unchanged, and are therefore comparable to the Calibration Scenario.

Sensitivity runs on the All-Forest Scenario were conducted by making an across-the-board cut in labile particulate organic phosphorus, which is the W2 state variable that represents particulate labile particulate organic matter.

7.1.3. Comparison of Scenario Loading Rates

Table 7.1-1 compares the loading rates of phosphorus species for the Calibration, TMDL, and All-Forest Scenarios. The Forest Scenario phosphorus loads are less than half of the TMDL Scenario Loads, or in other words, the All-Forest Scenario represents more than twice as great a reduction as the TMDL Scenario. Since the TMDL Scenario is an across-the-board reduction in TP (58% in Triadelphia and 48% in Rocky Gorge) the relative fractions of each species in the TMDL Scenario is the same as the Calibration Scenario. The All-Forest Scenario has relatively less PIP and relatively more POP than the Calibration Scenario. PIP in Rocky Gorge Reservoir under the All-Forest Scenario is artificially underestimated, because there were computational difficulties that prevented routing the outflow of approximately 900 ton/year PIP though the HSPF model Segment 30.

Table 7.1-1. Scenario Annual Phosphorus Load (lbs/yr) By Species and Forest Scenario Percent of Calibration Load

Phosphorus Species	Triadelphia Reservoir				Rocky Gorge Reservoir			
	Calibration	TMDL (42%)	Forest	Percent of Calibration	Calibration	TMDL (52%)	Forest	Percent of Calibration
DOP	3,161	1,328	259	8%	1,659	862	292	18%
DIP	1,134	476	104	9%	1,009	525	148	15%
PIP	40,935	17,193	5,287	13%	29,784	15,487	944	3%
POP	20,721	8,703	5,126	25%	14,484	7,532	3,825	26%
TP	65,953	27,700	10,776	16%	46,935	24,406	5,208	11%

7.2. Criteria Tests

Up to this point much of the evaluation of model performance focused on comparing simulated concentrations with their observed counterparts. In evaluating whether a scenario meets water quality standards, simulated concentrations must be evaluated everywhere in the reservoir where relevant, not just at the sampling locations and sampling depths. At their maximum surface water elevations, Triadelphia Reservoir contains 281 cells and Rocky Gorge Reservoir contains 325 cells. Advances in computer speed and memory has fortunately made processing the sheer amount of output to be evaluated a minor challenge. The primary challenge is determining, when applying the interim dissolved oxygen criteria, whether under stratified conditions a cell is the mixed surface layer.

7.2.1. Chlorophyll Tests

Each cell in the first 15 layers (15-meter depth) was tested to determine whether (1) the instantaneous concentration of chlorophyll was above 30 $\mu\text{g/l}$ and (2) whether the 30-day moving average of the chlorophyll concentration was above 10 $\mu\text{g/l}$. Daily output was used to make the test. A cell's identity was fixed relative to the surface for the 30-day moving average. In other words, the average was made over the cell that was, for example six meters deep in segment four, even if a layer was added or subtracted during the 30-day period so that the cell's indices changed. Tracking cells relative to the surface better simulates how monitoring would actually be performed and can in many cases better track identity of the mass of material.

7.2.2. Dissolved Oxygen Tests

Determining whether the reservoirs meet the interim DO standards can be broken down into three steps. First, the DO concentrations in a cell must be checked to determine if the concentration is below 5.0 mg/l. If a cell's concentration is below 5.0 mg/l, it must be determined whether or not it is in the surface layer. If it fails either test and is in the surface layer it must be further determined whether or not it is impacted by the entrainment of low DO caused by the deepening of the surface layer or, as can also happen, the cell was itself previously below the well-mixed surface layer and has been recently mixed into the surface layer. Finally, it must be determined whether the low DO under stratified conditions is due primarily to constituent loads or is a naturally-occurring consequence of stratification and reservoir morphology.

The All-Forest Scenario and subsequent sensitivity analyses will demonstrate that hypoxia would occur even under the low constituent loading rates associated with an all-forested watershed. If the hypoxia in the reservoirs is a naturally-occurring condition, then the interim DO criteria would be violated if the all of the following conditions are met:

1. DO concentrations in a cell are below 5.0 mg/l;
2. The cell is in the well-mixed surface layer or the reservoirs are unstratified; and
3. The low DO concentration in the cell is not explainable as a result the entrainment of low DO layers in the metalimnion such as occurs during the fall overturn.

To determine the instantaneous DO concentrations in a cell, DO concentrations for potential surface layer cells were output every half of a day at 6AM and 6PM. Each concentration was checked to determine whether it was below 5.0 mg/l.

7.2.3. Determination of the Position of the Surface Layer

The key difficulty is determining whether a cell is in the well-mixed surface layer. There are no agreed-upon numerical criteria for defining the boundaries of epilimnion, metalimnion, and hypolimnion. A temperature gradient of 1 °C/m is often used as a rule-of-thumb to determine the location of the thermocline (Wetzel 2005), but others reject that criteria (Hutchinson 1967; Ford and Johnson 1986). A glance at Figure 5.2-1 or the temperature contours in Appendix B clearly shows that temperature stratification regularly takes place in both Triadelphia and Rocky Gorge Reservoirs; it is difficult to determine a simple numerical criterion that captures the evident stratification. The temptation to paraphrase what one Supreme Court justice said in another context is strong: “I can’t define stratification but I know it when I see it.”

The following more-sophisticated procedure was used to determine the location of the surface layer on a daily basis:

1. A preliminary criterion is chosen which represents the temperature gradient that marks the boundary between the epilimnion and metalimnion.
2. On each day the average temperature in a layer was calculated for all model segments more than 10 meters deep.
3. The temperature difference between layers was calculated, starting from the surface layer. Since each layer except the surface layer is one meter thick, the temperature difference is easily translated into a temperature gradient.
4. Starting from the surface, the temperature differences are compared to the predetermined criterion. The bottom of the surface layer is the place where the temperature difference or gradient is larger than the criterion.
5. The location of the surface layer is checked for continuity. The reservoirs should be stratified between May and September. If there are days during that time when there were no temperature differences between layers greater than the criterion, then a smaller temperature gradient criterion was chosen and steps 3 and 4 were repeated.
6. Step 5 was repeated until there was continuous stratification from May into September.

The initial criterion chosen was the rule-of-thumb of 1 °C/m. The final criterion used was 0.4 °C/m in Triadelphia Reservoir and 0.2 °C/m in Rocky Gorge Reservoir. In Rocky

Gorge Reservoir, the true depth of the surface layer is probably frequently less than the depth of the model surface layer, requiring a smaller temperature difference to define the surface layer. The average temperature difference defining the surface layer is much larger than the criteria, average about 0.8 °C/m. Table 7.2-1 and Table 7.2-2 show the monthly average of daily temperature difference used to determine the surface layer in Triadelphia and Rocky Gorge Reservoirs. The simulated overturn in Rocky Gorge also can begin as early as mid-August, which reduces the average temperature gradient for August and September.

Table 7.2-1 Monthly Average Daily Temperature Gradient (°C/m) Determining Relative Position of Epilimnion and Metalimnion in Triadelphia Reservoir

Year	May	June	July	August	September
1998	0.93	0.73	0.70	0.76	0.72
1999	0.77	0.69	0.83	0.81	0.52
2000	0.91	0.89	0.57	0.64	0.47
2001	0.89	0.67	0.78	0.80	1.02
2002	0.63	0.97	1.14	0.85	0.75
2003	0.75	0.91	0.73	0.86	0.71
Average	0.81	0.81	0.79	0.78	0.70

Table 7.2-2 Monthly Average Daily Temperature Gradient (°C/m) Determining Relative Position of Epilimnion and Metalimnion in Rocky Gorge Reservoir

Year	May	June	July	August	September
1998	0.86	0.74	0.48	0.61	0.61
1999	0.81	0.63	0.93	0.66	1.38
2000	0.93	0.87	0.55	0.57	0.37
2001	0.90	1.11	0.64	0.58	0.68
2002	0.80	0.90	0.85	0.74	1.26
2003	0.70	1.43	0.70	0.53	0.60
Average	0.83	0.95	0.69	0.62	0.82

As describe in Section 5.9, low DO concentrations caused by fluctuations in the position of the surface layer are an effect of stratification and are compatible with the interim interpretation of the DO standards for impoundments. To facilitate analyzing simulated low DO concentrations, the surface layer was smoothed by defining an envelop of the minimum surface layer so that low DO concentrations caused by fluctuations in the surface layer position could be more easily indentified. Figures 7.2-1 and 7.2-2 show the position of the interface between epilimnion and metalimnion in Triadelphia and Rocky Gorge Reservoirs, May through September, for the simulation period. As the figures show, there is considerable fluctuation in the position of the layer. Fluctuations as much as five meters can occur in summer months. Figures 7.2-1 and 7.2-2 also show the location of the smoothed surface layer used to facilitate the analysis of low DO concentrations.

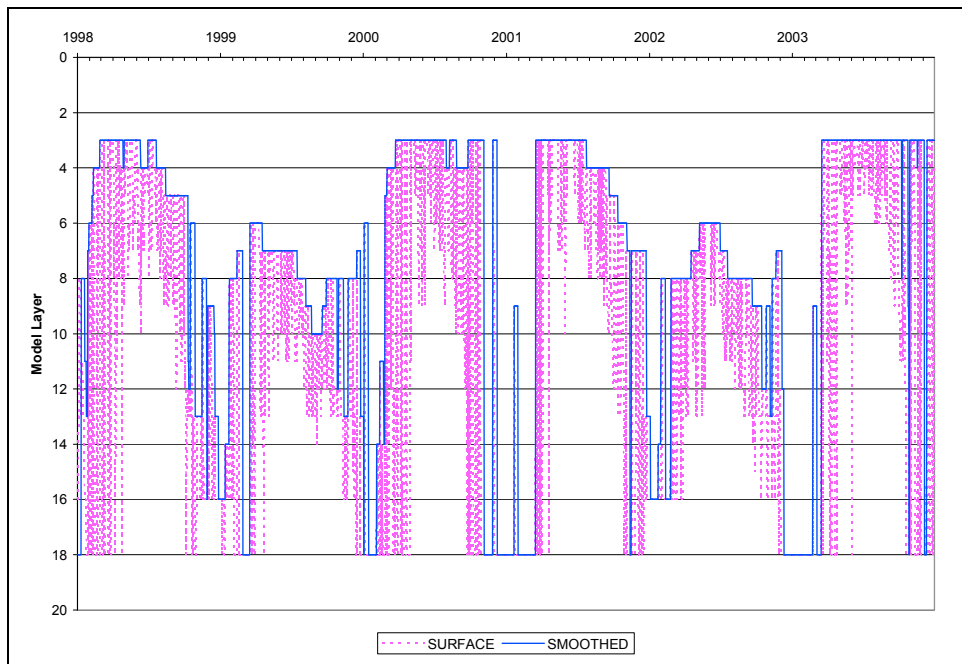


Figure 7.2-1. Position of the Interface between Epilimnion and Metalimnion, Triadelphia Reservoir

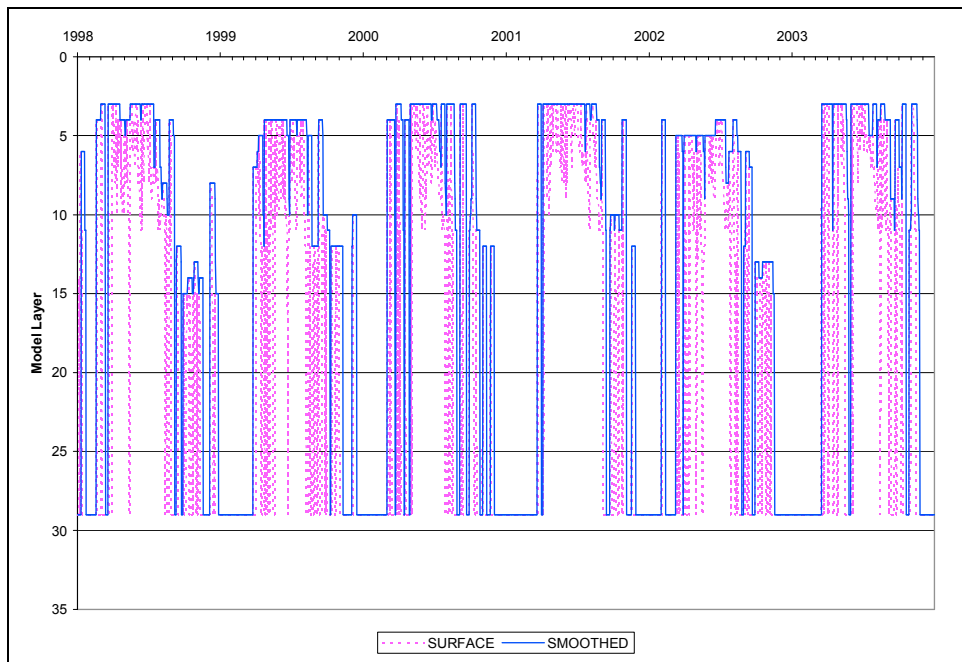


Figure 7.2-2. Position of the Interface Between Epilimnion and Metalimnion, Rocky Gorge Reservoir

7.3. Response of Chlorophyll Concentrations to Reductions in Phosphorus Loads

As input loads to the reservoirs decrease, TP concentrations in the reservoirs decrease. Table 7.3-1 gives summary statistics for average surface TP concentrations in the reservoirs under the Calibration, TMDL, and All-Forest Scenarios.

Table 7.3-1. Scenario Summary Statistics for the Simulated Average Surface Concentrations (mg/l) of Total Phosphorus at Sampling Locations in Triadelphia and Rocky Gorge Reservoirs

Statistic	Triadelphia Reservoir			Rocky Gorge Reservoir		
	Calibration	TMDL	Forest	Calibration	TMDL	Forest
Minimum	0.013	0.006	0.005	0.015	0.009	0.004
1stQ	0.023	0.010	0.006	0.024	0.013	0.005
Median	0.032	0.015	0.009	0.033	0.018	0.006
3rdQ	0.058	0.025	0.012	0.048	0.025	0.007
Maximum	0.233	0.098	0.036	0.112	0.058	0.021
Average	0.047	0.021	0.010	0.039	0.021	0.007

The reservoir models are responsive to reductions in chlorophyll loads. Figures 7.3-1 and 7.3-2 show the maximum chlorophyll concentrations by sampling date in Triadelphia Reservoir and Rocky Gorge Reservoir under the TMDL Scenario and All Forest Scenario and contrast them with the maximum observed concentrations and the maximum simulated concentrations under the Calibration Scenario. In Triadelphia Reservoir, Chla concentrations are at a minimum in the All Forest Scenario. The average maximum concentration on sampling dates for the TMDL Scenario is about 3 ug/l and in the Forest Scenario it is 0.2 ug/l, an order of magnitude less. In Rocky Gorge Reservoir, the average maximum Chla concentration in the TMDL Scenario on sampling dates is 2.6 ug/l compared to 1.5 ug/l in the All-Forest Scenario. Almost always, Chla concentrations in the All-Forest Scenario are about 40% less than the TMDL Scenario, although occasionally, such as March 1998, All-Forest concentrations can exceed those in the TMDL Scenario. The timing of forest loads can be different than loads from other sources, and a greater proportion of the forest load is exported in March 1998, causing an increase in Chla concentrations not found in the other scenarios.

Figures D.1–D.3 in Appendix D show the maximum Chla concentrations for all scenarios at TR1, TR2, and TR3, respectively, in the Triadelphia Reservoir, and Figures D.7–D.9 show the maximum Chla concentrations for all scenarios at RG1, RG2, and RG3, respectively, in the Rocky Gorge Reservoir

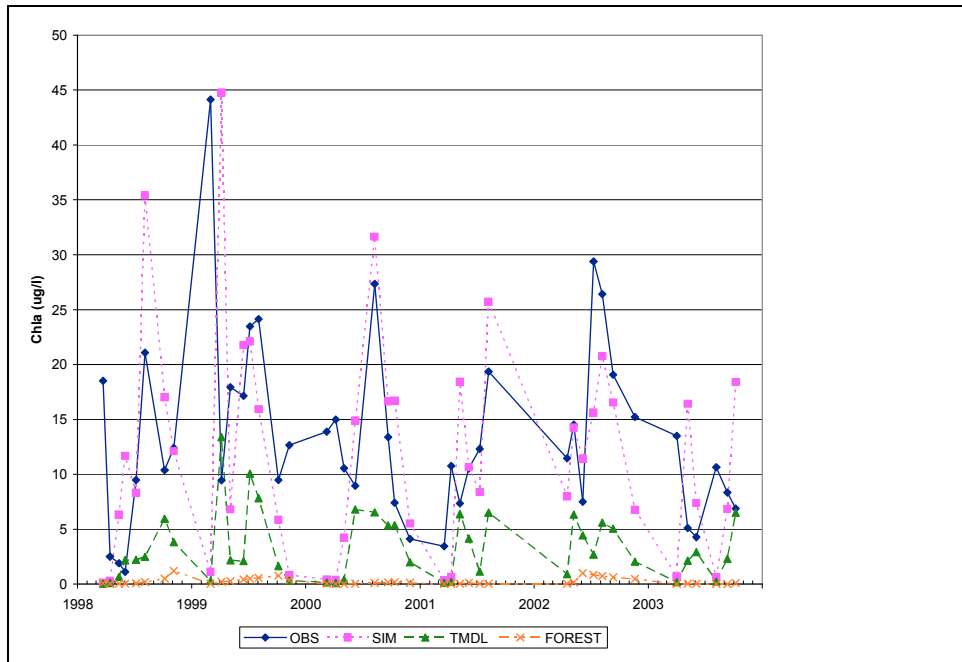


Figure 7.3-1. Observed and Simulated Maximum Chlorophyll Concentrations by Date, Triadelphia Reservoir

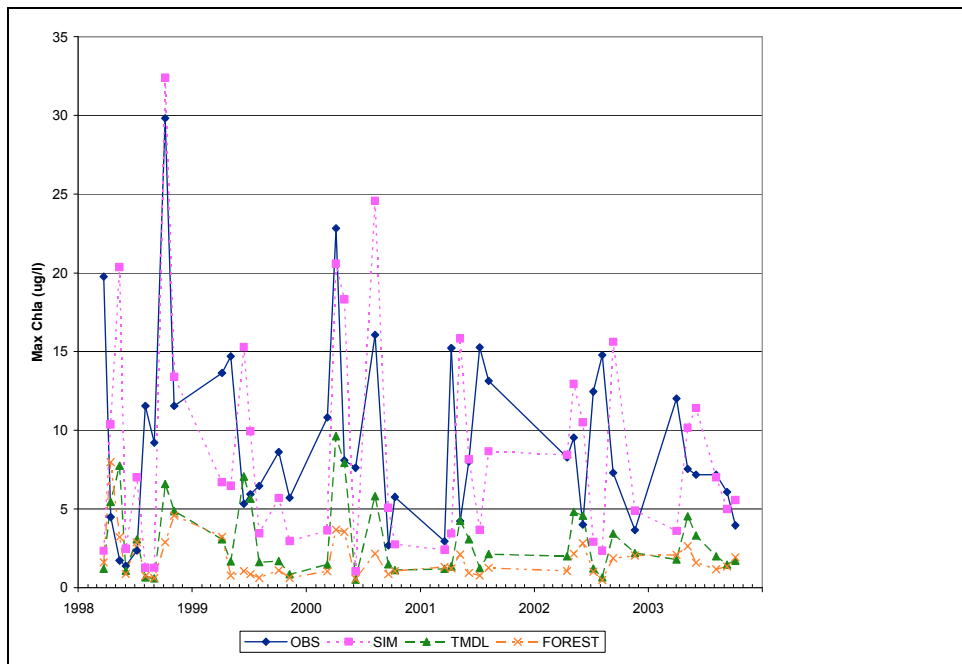


Figure 7.3-2. Observed and Simulated Maximum Chlorophyll Concentrations by Date, Rocky Gorge Reservoir

7.4. The Response of DO Concentrations to Load Reductions

Since the factors which determine DO concentrations in the surface layer and the bottom layer are different, and they are treated differently under the interim DO criteria, the simulated response of DO concentrations to load reductions will be discussed separately below.

7.4.1. The Response of Simulated Bottom DO Concentrations to Load Reductions

Figures 7.4-1 and 7.4-2 show the average bottom DO concentration for the Calibration Scenario, TMDL Scenario, and All-Forest Scenario, as well as the observed data, at TR1 in Triadelphia Reservoir and RG1 in Rocky Gorge Reservoir, respectively. Figures D.4–D.10 show the average bottom DO concentration at TR2 and RG2, respectively. The models respond to reductions in particulate organic phosphorus, but clearly do not meet the 5.0 mg/l DO criterion, even averaged over the bottom layers.

The All-Forest Scenario, as described in Section 7.1, was simulated to determine whether the source of the hypoxia in the hypolimnion is a natural consequence of stratification and would occur under the loading rates of an all-forested watershed. In both reservoirs, average bottom DO concentrations improve significantly under the All-Forest Scenario, but hypoxia persists in both reservoirs in the summer of some of the years simulated. A sensitivity analysis was performed to reinforce the conclusion that hypoxia in the hypolimnion of both Triadelphia and Rocky Gorge Reservoirs is a natural condition due to thermal stratification. Given the low concentration of algal biomass in the All-Forest Scenario, the allochthonous sources of sediment oxygen demand, as represented by labile particulate organic phosphorus, are the primary cause of hypoxia in the hypolimnia of the reservoirs. The forest TP loading rates were based on available data, but some uncertainty may linger over (1) the fraction of phosphorus that is labile or (2) the oxygen equivalence of the organic material associated with organic phosphorus. These were calibrated in general but not specifically for forest loads. The loading rate of labile particulate phosphorus was reduced to 50%, 20%, and 10% of its value in the All-Forest Scenario in both reservoirs. Figure 7.4-3 shows the results, summarized as the percent of sampling dates under each sensitivity scenario in which the minimum DO concentration was less than 2.0 mg/l. Significant hypoxia persists even when loads are reduced to only 10% of the All-Forest Scenario in Rocky Gorge Reservoir. Although hypoxia disappears in Triadelphia Reservoir when loading rates are 10% of the All-Forest Scenario, 5% of sampling dates under those loading conditions still have DO concentrations less than 5.0 mg/l in the hypolimnion. The sensitivity analysis shows that low DO in the bottom layers of the reservoirs is relatively insensitive to the particular assumptions used to determine organic matter loads in the models, and demonstrates that hypolimnetic hypoxia is primarily driven by stratification and reservoir morphology, rather than by external loads.

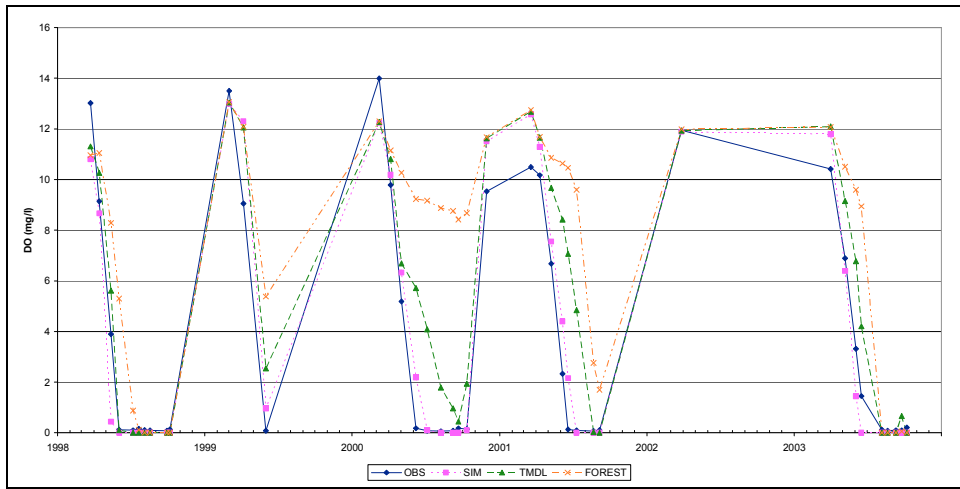


Figure 7.4-1 Average Bottom DO, Observed Data and All Scenarios, TR2, Triadelphia Reservoir

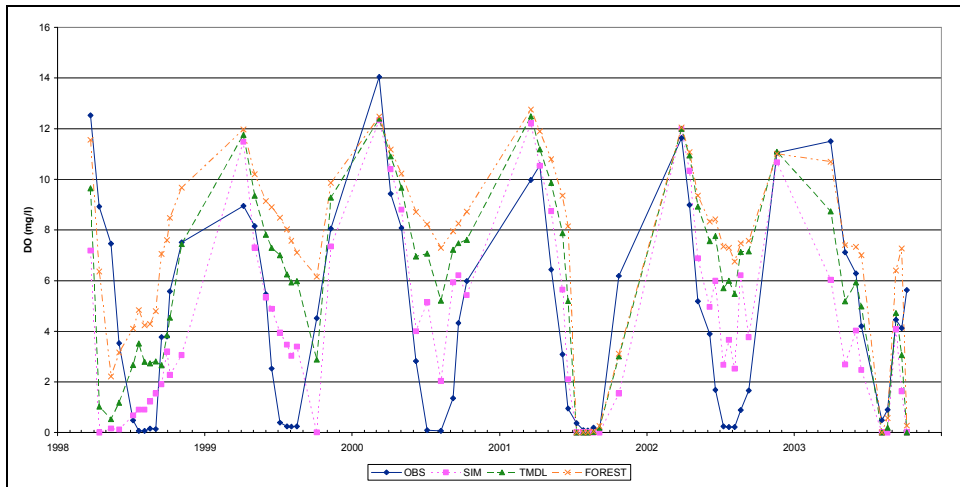


Figure 7.4-2 Average Bottom DO, Observed Data and All Scenarios, RG2, Rocky Gorge Reservoir

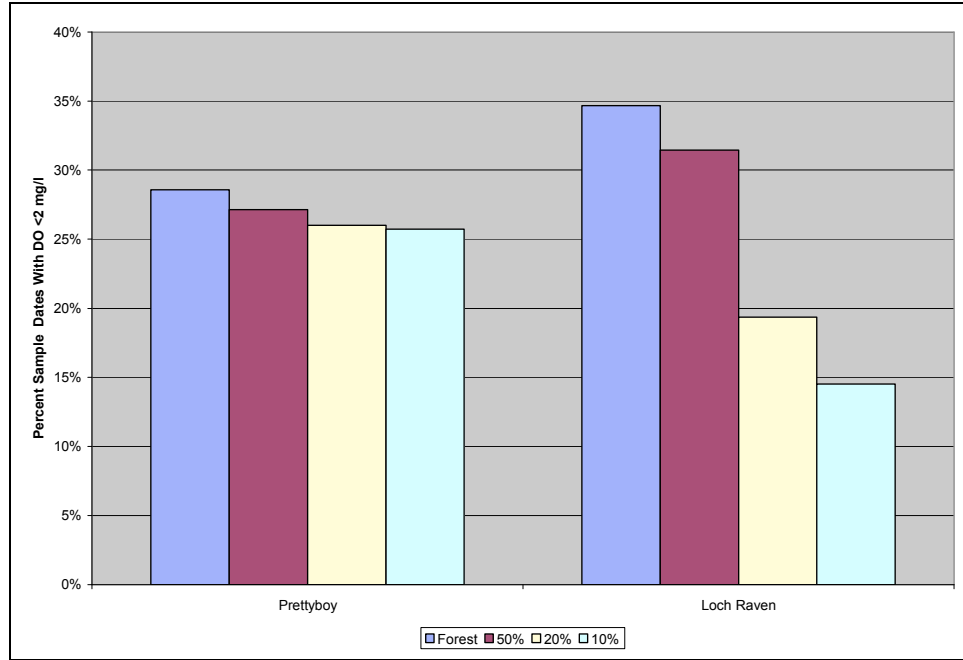


Figure 7.4-3. Percent of Sampling Dates on which DO < 2 mg/l at Sampling Locations as a function of Load Reductions from All-Forest Scenario

7.4.2. The Response of Simulated Surface DO Concentrations to Load Reductions

As discussed in Section 5.1.1, there is no evidence that DO concentrations fall below 5.0 mg/l in the surface layer except during periods of overturn or other fluctuations in the depth of the surface layer. Thus, there is no evidence that the instantaneous DO criterion of 5.0 mg/l is violated, provided that it can be shown that the low DO that occurs under stratification is a natural phenomenon.

Nonetheless, it is necessary to evaluate the simulation of DO in the TMDL Scenario to make sure that the scenario predicts that water quality standards for DO will be met under the TMDL loading rates. The screening procedures described in 7.2.2 were applied to the TMDL Scenario. No cells in the surface layers of Triadelphia Reservoir failed to meet DO standard under the screening procedure. In Rocky Gorge the screening procedure identified three potential cases where DO concentrations in the surface layers were below 5.0 mg/l, but on closer investigation none of the three cases represented a violation of the interim interpretation of the DO standard. In one case, on July 30, 1998, the surface layer as measured by temperature differenced deepened in the course of the day. In the second case, an established stratification overturned in the last week of May, 2003. In the last case, one cell in the Rocky Gorge Reservoir was flagged by the screening procedure on July 16, 2003, in Segment 27, but in this case the location of the surface layer in Segment

27 was above the average surface layer depth, as shown by the temperature differences with depth. (Segment 27 is just above the Duckett Dam and subject to water withdrawals that may alter the location of the surface layer.) Thus there were no cases of low DO in the surface layer of either reservoir except in cases of the entrainment of low DO during fluctuations of the position of the surface layer such as during the fall overturn, and therefore there were no violations of interim interpretation of the DO criteria as applied to Maryland's impoundments.

Figures 7.4-4 and 7.4-5 show the average surface DO concentration for the Calibration Scenario, TMDL Scenario and All-Forest Scenario, as well as the observed data, at TR1 in Triadelphia Reservoir and RG1 in Rocky Gorge Reservoir, respectively. Figures D.5 and D.6 show surface DO for all scenarios at TR2 and TR3 in Triadelphia Reservoir, respectively, while Figures D.11 and D.12 shows surface DO for RG2 and RG3 in Rocky Gorge Reservoir. As the figures show, surface DO concentrations show modest improvements with reductions in phosphorus and, consequently, organic matter loading rates. The improvements are modest because the surface oxygen deficit is modest; to reiterate, there is no evidence of low dissolved oxygen concentrations in the surface layer of the reservoirs that is not a result of stratification.

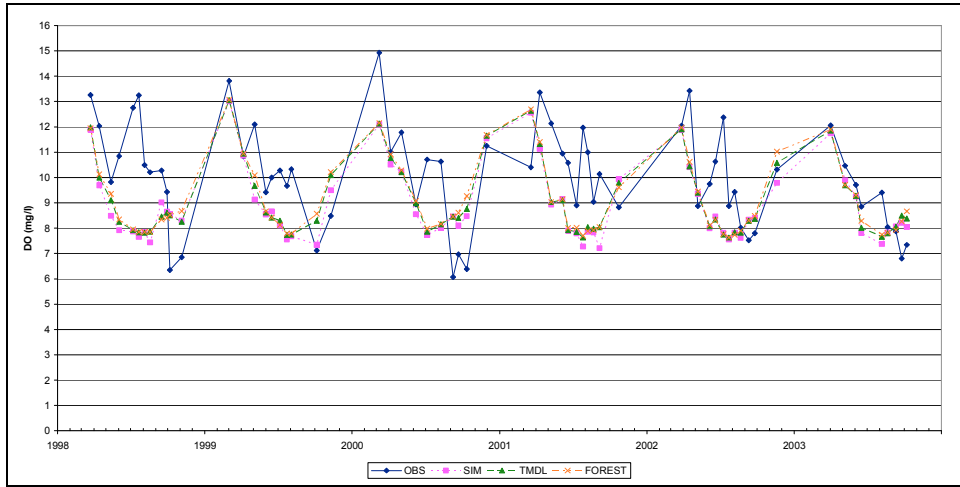


Figure 7.4-4 Surface DO, Observed Data and All Scenarios, TR1, Triadelphia Reservoir

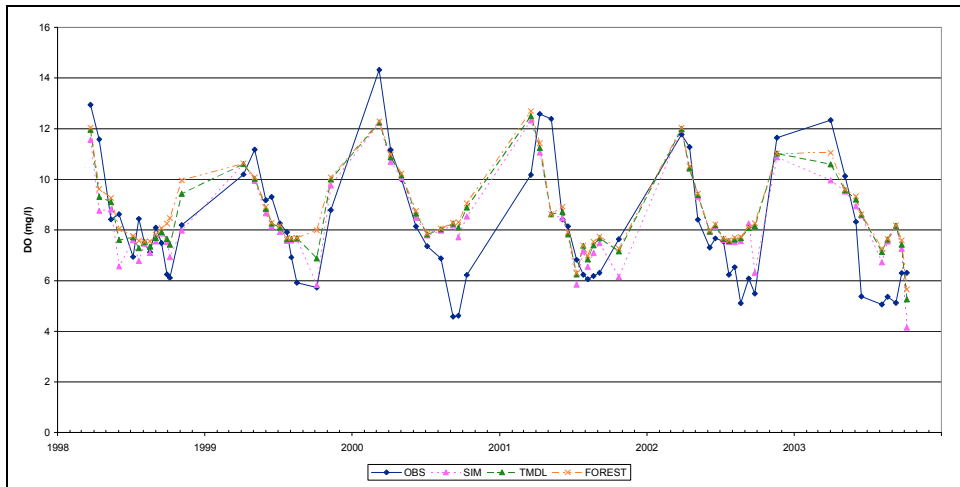


Figure 7.4-5 Surface DO, Observed Data and All Scenarios, RG1, Rocky Gorge Reservoir

8.0 SUMMARY AND RECOMMENDATIONS

8.1 Summary

The modeling framework outlined in this report meets all of the following major objectives set for its design:

1. The revised HSPF model of the Patuxent Reservoirs watershed has been calibrated to load estimates of sediment and total phosphorus that incorporate all the recent available monitoring data, including data collected by MDE, DNR, USGS, SERC, and Versar.
2. Simulated EOF sediment loads for non-developed land uses and EOS nutrient loads have been calibrated to agree with loading rates from CBP Watershed Models. The agreement between TMDL loading rates and Tributary Strategy loading rates from the CBP Watershed Models should facilitate water quality planning and management.
3. The W2 models of Triadelphia and Rocky Gorge Reservoirs have been calibrated conservatively against observed Chla concentrations. The models establish linkage between phosphorus loads, on the one hand, and Chla concentrations in terms of which the nutrient TMDL endpoints are expressed.
4. The W2 models also establish a linkage between observed hypoxia in the hypolimnion of the reservoirs and internal and external organic matter loading rates. The loading rates for external organic matter have been expressed in terms of organic phosphorus, thus linking nutrient loading rates with SOD and bottom DO concentrations in the reservoirs.
5. With respect to both simulated Chla concentrations and bottom DO, the W2 models have been shown to be sensitive to external phosphorus loading rates.
6. An All-Forest Scenario, which simulates the effect on the reservoirs of loading rates characteristic of an all-forested watershed, demonstrates that hypolimnetic hypoxia is primarily the result of stratification, not autochthonous or allochthonous organic matter loading rates.

8.2 Recommendations

8.2.1 Nitrogen

The modeling framework falls short of a secondary goal: estimating nitrogen loads to the reservoirs. Determining nitrogen loads was secondary because (1) water quality analysis shows that both reservoirs are phosphorus limited, and (2) because of the state variables in the W2 model, full mass balance could be kept only on one nutrient, in this case phosphorus. Nevertheless, it would have been desirable to have determined better estimates of nitrogen loading rates.

As described in Section 4.4, the ESTIMATOR software was unable to determine satisfactory regression equations relating ammonia, nitrate, or total nitrogen to variables representing flow or seasonality. Had time permitted, another load estimation method, such as the Autobeale implementation of the Beale Ratio Estimator (Richards 1999), could have been explored. With better total nitrogen load estimates, a better estimate of the appropriate N-to-P ratio in allochthonous organic matter could have been obtained that would enable the W2 model to keep a better long-term mass balance on nitrogen. (Given the limitations of the W2 model, it would still be impossible to keep a continuous mass balance on nitrogen, as is done for phosphorus.)

8.2.2 Additional Chlorophyll *a* and Algae Monitoring

The existing chlorophyll *a* monitoring data are more than adequate to develop the modeling framework for the nutrient TMDLs in Triadelphia Reservoir and Rocky Gorge Reservoir. There are three areas in which the existing monitoring program could be improved to help future modeling efforts.

First, data on algal species could be collected from a variety of locations in both reservoirs, not just at the intakes. It would be helpful to coordinate algal taxonomic data with chlorophyll *a* monitoring data, to see if higher concentrations are associated with specific species.

Second, it could be useful to conduct water quality sampling through the winter. Although observing high algal concentrations during the winter is unlikely, winter sampling might shed some light on the size and duration of spring algal blooms. The largest observed bloom during the simulation period, 44 ug/l, occurred in March, 1999, and March samples are frequently above 10 ug/l. It may help to know the state of the reservoirs just before these high concentrations. Measurements of phosphate and total phosphorus would also help to establish what the conditions in the reservoirs were prior to the high observed concentrations in March.

Third, more chlorophyll *a* samples could be taken at depths below the surface. Sampling in Prettyboy and Loch Raven Reservoirs in the City of Baltimore's reservoir system suggests that the maximum Chla concentrations may not occur at the surface, particularly during the summer, when it is possible that the algae become light inhibited. The DO concentration profiles from the Patuxent reservoirs also suggest that primary production could be taking place several meters below the surface. Figure 8-1.1 shows the DO profile for May 8, 2001 at TR1 in Triadelphia Reservoir. The increase in DO concentrations four meters below the surface could be the result of primary production by algae.

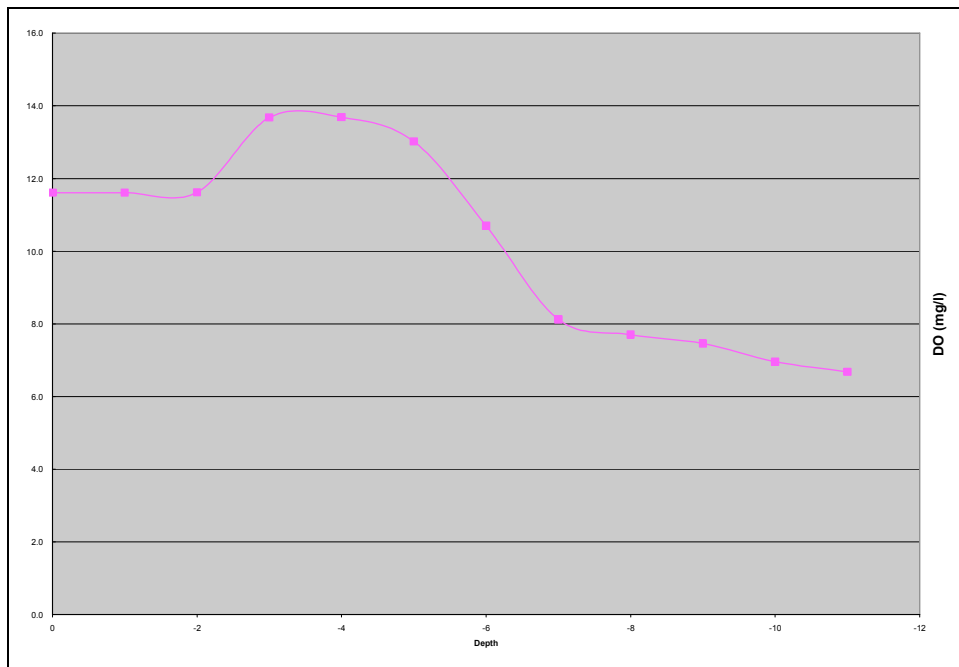


Figure 8.1-1 Observed DO Profile (mg/l) in Triadelphia Reservoir, TR1, May 8, 2001

8.2.3 Improvements in Watershed Monitoring

Generally speaking, the water quality monitoring program implemented by Versar provided a good picture of water quality in Cattail Creek and Hawlings River. Future water quality monitoring programs in the reservoirs' watersheds could use lower detection limits to get a more accurate representation of baseflow conditions. It would be better to sample Cattail Creek, Hawlings River, and the Patuxent River near Unity under the same protocols or at least to coordinate monitoring programs, so that water quality in these tributaries could be more easily compared. It may also be preferable to follow USGS storm sampling protocols to facilitate comparison between these tributaries and other rivers in the region.

None of these recommendations addresses issues that were essential to developing the models for the nutrient TMDLs in the reservoirs. They represent areas where the monitoring could be improved in the future. The water quality monitoring data that have been collected, in part, to support the development of nutrient TMDLs for the reservoirs, have provided a good foundation for developing the modeling framework described in this report.

REFERENCES

- Bahr, R.P. 1997. Maryland's National Pollutant Discharge Elimination System Municipal Stormwater Monitoring. Maryland Department of the Environment. Baltimore, MD.
- Beaulac, M.N., and K.H. Reckhow. 1982. An Examination of Land Use—Nutrient Export Relationships. *Water Resources Bulletin* 18, pp. 1013-1022.
- Bicknell, B. R., Donigian, A.S., and Jobes, T.H. 1996. "Modeling Nitrogen Cycling and Export in Forested Watersheds Using HSPF." U.S. EPA, Athens, GA.
- Brown, J. H. and S. T. Dyer. 1995. Soil Survey of Montgomery County, Maryland. Natural Resource Conservation Service. Washington, DC.
- Carlson, R. E. 1977. A Trophic State Index for Lakes. *Limnology and Oceanography* 22:361-369.
- Chiandani, G. and M. Vighi. 1974. The N:P Ratio and Tests with *Selenastrum* to Predict Eutrophication in Lakes. *Water Research*, Vol. 8, pp. 1063-1069.
- COMAR (Code of Maryland Regulations). 2006. 26.08.02.03; 26.08.02.08.
- Cole, T. M. and E. M. Buchak. 1995. CE-QUAL-W2: A Two-Dimensional Laterally Averaged, Hydrodynamic and Water Quality Model, Version 2.0. User Manual. Washington, DC. U.S. Army Corps of Engineers. Instruction Report EL-95-1.
- Cole, T. M. and S. A. Wells. 2003. CE-QUAL-W2: A Two-Dimensional Laterally Averaged, Hydrodynamic and Water Quality Model, Version 3.2. User Manual. Washington, DC. U.S. Army Corps of Engineers. Instruction Report EL-03-1.
- Cohn, T. A., L. L. Delong, E. J. Gilroy, R. M. Hirsch, and D. Wells. 1989. Estimating Constituent Loads. *Water Resources Research* 28, pp.937-942.
- Cohn, T. A., D. L. Caulder, E. J. Gilroy, L. D. Zynjuk, and R. M. Summers. 1992. The Validity of a Simple Log-linear Model for Estimating Fluvial Constituent Loads. *Water Resources Research* 28, pp. 2353-2364.
- Cornwell, J. and M. Owens. 2002. Triadelphia Sediment-Water Exchange Study. University of Maryland Center for Environmental Science. UMCES Report TS-364-02. Cambridge, MD.
- Doherty, J. 2001. PEST: Model independent parameter estimation - User's Manual. Watermark Numerical Computing.

Donigian, A.S., Imhoff, J.C., and Bicknell, B. R. 1983. "Modeling Water Quality and the Effects of Agricultural Best Management Practices in Four Mile Creek." U.S. EPA, Athens, GA.

EA Engineering, Science, and Technology. 1991. Water Quality Monitoring and Nutrient Loading Analysis of the Patuxent River Reservoirs Watershed. EA Mid-Atlantic Regional Operations. Sparks, MD.

Edinger, J. E. and E. M. Buchak. 1975. A Hydrodynamic, Two-Dimensional Reservoir Model: The Computational Basis. U.S. Army Engineer Division, Ohio River. Cincinnati, OH.

Ford, D. E. and L. S. Johnson. 1986. An Assessment of Reservoir Mixing Processes. U.S. Army Corps of Engineers Waterways Experimental Station. Vicksburg, MS. Technical Report E-86-7.

Hutchinson, G. E. 1967. A Treatise on Limnology. 3 volumes. John Wiley and Sons. New York.

ICPRB (Interstate Commission on the Potomac River Basin) and Maryland Department of the Environment. 2006. Modeling Framework for Simulating Hydrodynamics and Water Quality in the Prettyboy and Loch Raven Reservoirs. Rockville, MD.

Jones, T.S. 2002. Washington Suburban Sanitary Commission Patuxent Reservoirs Watershed Tributary Monitoring and Sediment Nutrient Flux Testing Program Third Annual Report. Versar, Inc. Columbia, MD.

Jordan, T.E., D.E. Weller, and D.L. Correll. 2003. Sources of Nutrient Inputs to the Patuxent River Estuary. *Estuaries* 26:226-243.

Langland, M.J., R. E. Edwards, L. A. Sprague, and S. E. Yochum. 2001. Summary of Trends and Status Analysis for Flow, Nutrients, and Sediments at Selected Nontidal Sites, Chesapeake Bay Basin, 1985-99: U.S. Geological Survey Open File Report 01-73.

Langland, M.J., S.W. Phillips, J.P. Raffensperger, and D.L. Moyer. 2005. Changes in streamflow and water quality in selected nontidal sites in the Chesapeake Bay Basin, 1985-2003. U.S. Geological Survey Scientific Investigations Report 2004-5259.

MDE (Maryland Department of the Environment). 2002. Total Maximum Loads of Phosphorus and Sediment For Lake Linganore, Frederick County, Maryland. Baltimore, MD.

MDE and DNR (Maryland Department of Natural Resources). 2004. 2004 List of Impaired Surface Waters [303(d) List] and Integrated Assessment of Water Quality in Maryland. Baltimore, MD.

REVISED FOR TMDL SUBMISSION

Maryland Department of Planning. 1997. Land Use Data.

Maryland State Climatologist Office. 2007. <http://www.atmos.umd.edu/~climate/>

Matthews, E. D. and M.F. Hershberger. 1968. Soil Survey of Howard County, Maryland. Soil Conservation Service. Washington, DC.

Ocean Surveys, Inc. 1997. Sedimentation Surveys. Phases I, II, and III.

Omernik, J.M. 1977. Nonpoint Source—Stream Nutrient Level Relationships: A Nationwide Study. U.S. Environmental Protection Agency. EPA-600/3-77-105.

Palace, M.W., J.E. Hannawald, L.C. Linker, G.W. Shenk, J.M. Storrick, M.L. Clipper. 1998. Chesapeake Bay Watershed Model Application and Calculation of Nutrient and Sediment Loadings, Appendix H: Tracking Best Management Practice Nutrient Reductions in the Chesapeake Bay Program. United States Environmental Protection Agency. Annapolis, MD.

Patuxent Reservoirs Technical Advisory Committee. 2005. Supplemental Documentation in Support of the Patuxent Reservoirs Technical Advisory Committee's Annual Report.

Patuxent Reservoirs Technical Advisory Committee. 2006. Supplemental Documentation in Support of the Patuxent Reservoirs Watershed Annual Report.

Resource Management Concepts. 2002. Draft Reservoir Data Analysis. Lexington Park, MD.

Richards, R.P. 1999. Estimation of Pollutant Loads in Rivers and Streams: A Guidance Document for NPS Programs. Prepared under Grant X998397-01-0. U.S. Environmental Protection Agency

Shenk, G. 2007. Personal communication.

Tetra Tech. 1997. Water Quality Management Plan for Loch Raven Watershed. Fairfax, VA.

Tetra Tech. 2000. Patuxent Reservoirs Watershed Model. Fairfax, VA.

Tetra Tech. 2002. Patuxent Reservoirs Eutrophication Model. Fairfax, VA.

U.S. Department of Commerce. 1997. Census of Agriculture. Volume 1. Geographic Area Series. Washington, DC.

U.S. EPA (United States Environmental Protection Agency). 2002. Establishing Total Maximum Daily Load (TMDL) Wasteload Allocations (WLAs) for Storm Water Sources

and NPDES Permit Requirements Based on Those WLAs. Washington, DC. November 2002.

———. 1991. Technical Support Document for Water Quality-based Toxics Control. Office of Water/OW Environment Protection (OW/OWEP) and Office of Water Regulations and Standards (OWRS), Washington, DC. April 23, 1991.

———. 1999. Protocol for Developing Nutrient TMDLs. EPA 841-B-99-007. Office of Water (4503F), United States Environmental Protection Agency, Washington DC.

———. 1997. Technical Guidance Manual for Developing Total Maximum Daily Loads, Book 2: Streams and Rivers, Part 1: Biochemical Oxygen Demand/ Dissolved Oxygen and Nutrients/ Eutrophication. Office of Water, Washington DC. March, 1997.

———. Chesapeake Bay Program Office. 1996. Chesapeake Bay Program: Watershed Model Application to Calculate Bay Nutrient Loadings: Final Findings and Recommendations, and Appendices.

———. Chesapeake Bay Program Office. 1998. Table H.2.2, Chesapeake Bay Watershed Model BMP Matrix with Associated Nutrient Reduction Efficiencies, provided by Bill Brown, CBPO, Oct. 1998.

———. 2007. CBP Watershed Model Scenario Output Database, Phase 4.3. Chesapeake Bay Program Office. Annapolis, MD.
<http://www.chesapeakebay.net/data/index.htm>

———. 2008. Chesapeake Bay Phase 5 Community Watershed Model. In preparation. EPA XXX-X-XX-008 Chesapeake Bay Program Office, Annapolis MD. January 2008. <http://www.chesapeakebay.net/model.htm>

Walker, W.W., Jr. 1984. Statistical Bases for Mean Chlorophyll a Criteria. *Lake and Reservoir Management: Proceedings of Fourth Annual Conference*. North American Lake Management Society, pp. 57 – 62.

Walker, William, Jr. 1988. Evaluating Watershed Monitoring Programs. Concord, MA.

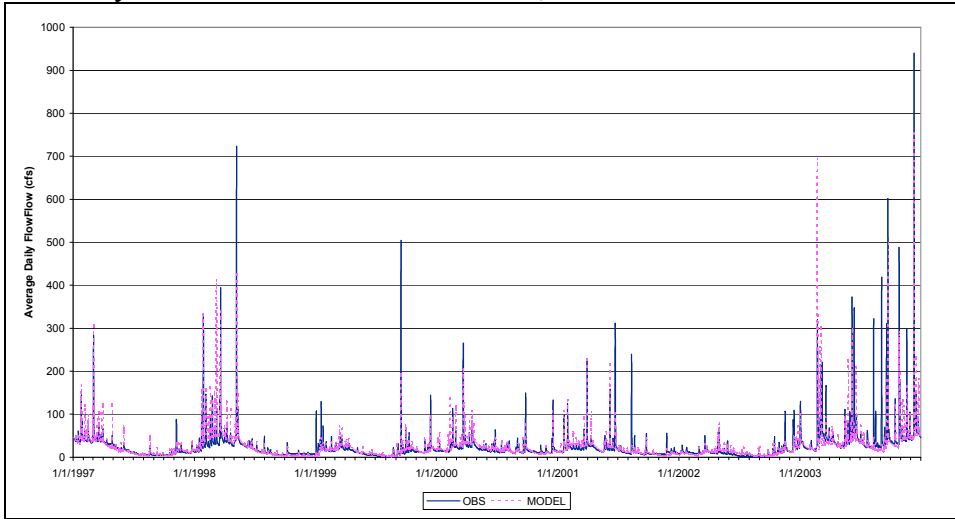
Walker, William, Jr. 1999. Simplified Procedures for Eutrophication Assessment and Prediction: User Manual. Instruction Report W-96-2. Waterways Experiment Station, U.S. Corps of Engineers. Washington, DC.

Wang, P., L.C. Linker, J.M. Storrick. 1997. Chesapeake Bay Watershed Model Application and Calculation of Nutrient and Sediment Loadings, Appendix D: Phase IV Chesapeake Bay Watershed Model Precipitation and Meteorological Data Development and Atmospheric Nutrient Deposition. United States Environmental Protection Agency. Annapolis, MD.

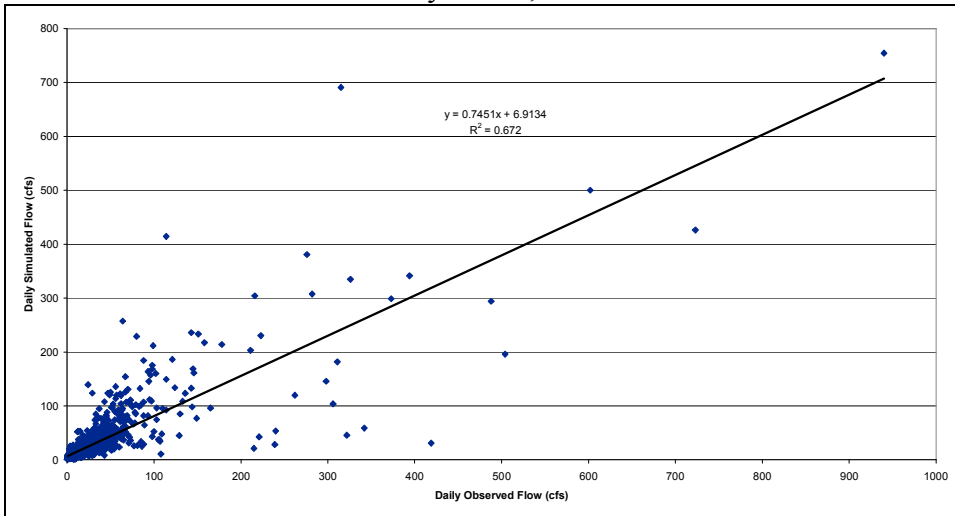
Weisberg, S. B., K. A. Rose, B. S. Clevenger, and J. O. Smith. 1985. Inventory of Maryland Dams and Assessment of Hydropower Resources. Martin Marietta Environmental Systems. Columbia, Maryland.

APPENDIX A

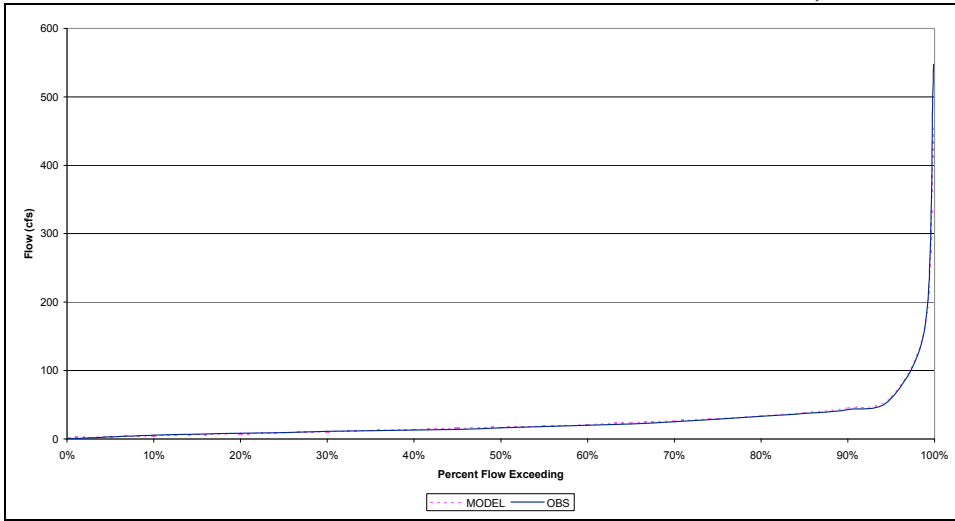
A.1 Daily Observed and Simulated Flows, Cattail Creek



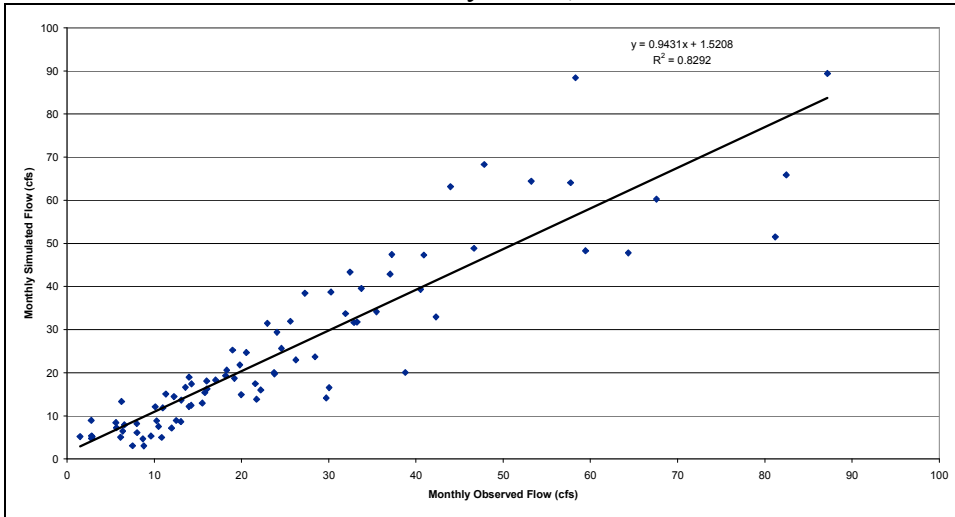
A.2 Observed vs. Simulated Daily Flows, Cattail Creek



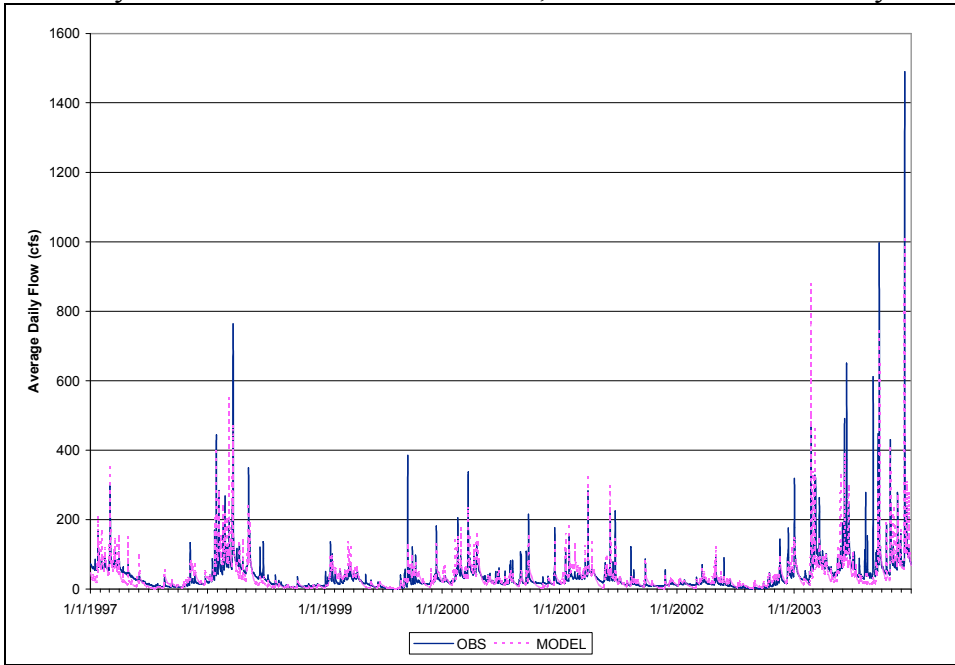
A.3 Cumulative Distribution of Observed and Simulated Flows, Cattail Creek



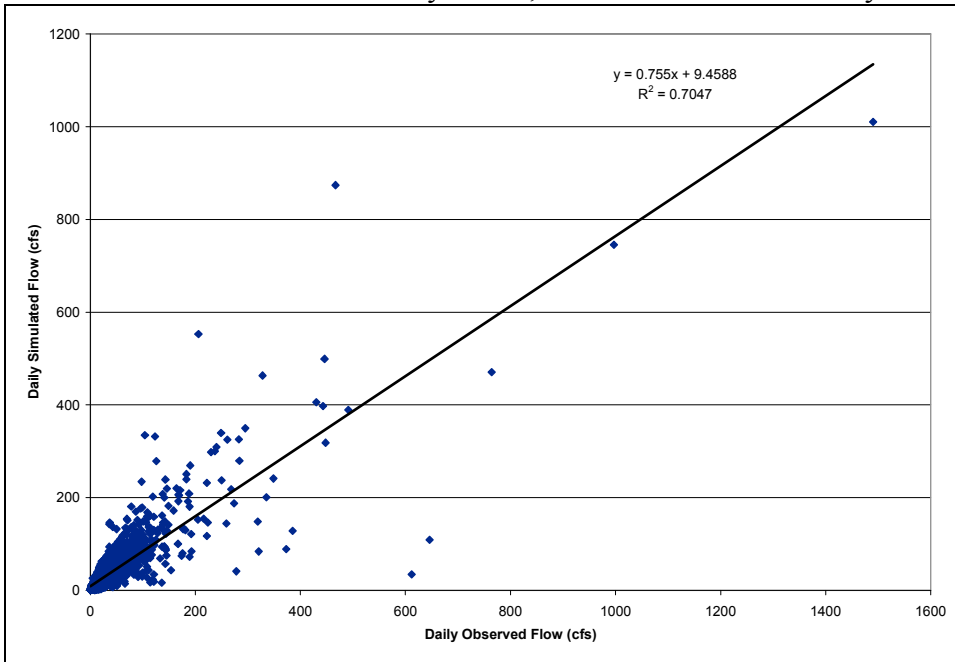
A.4 Observed vs. Simulated Monthly Flows, Cattail Creek



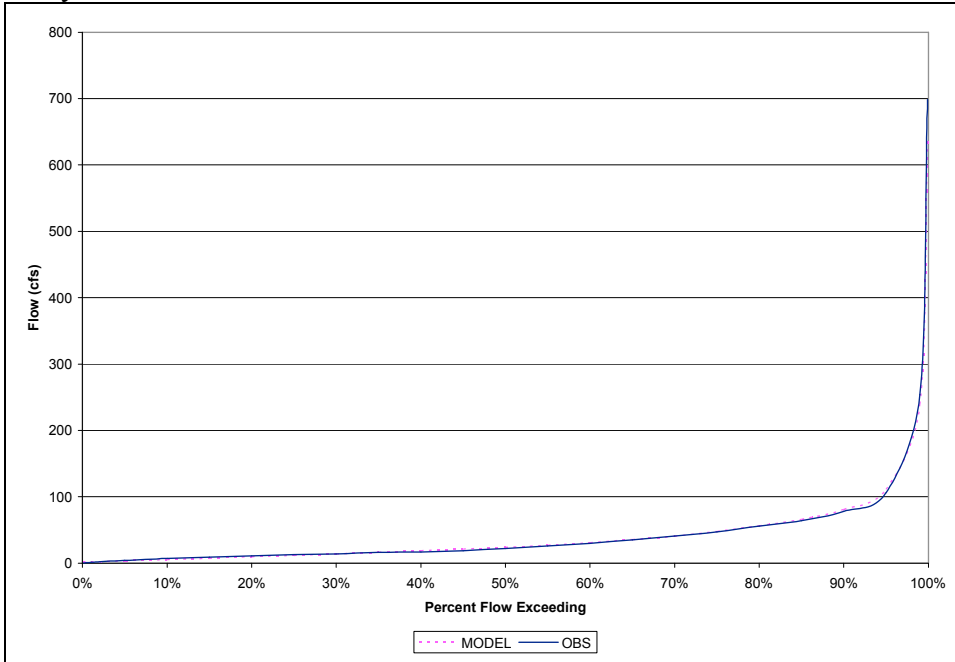
A.5 Daily Observed and Simulated Flows, Patuxent River near Unity



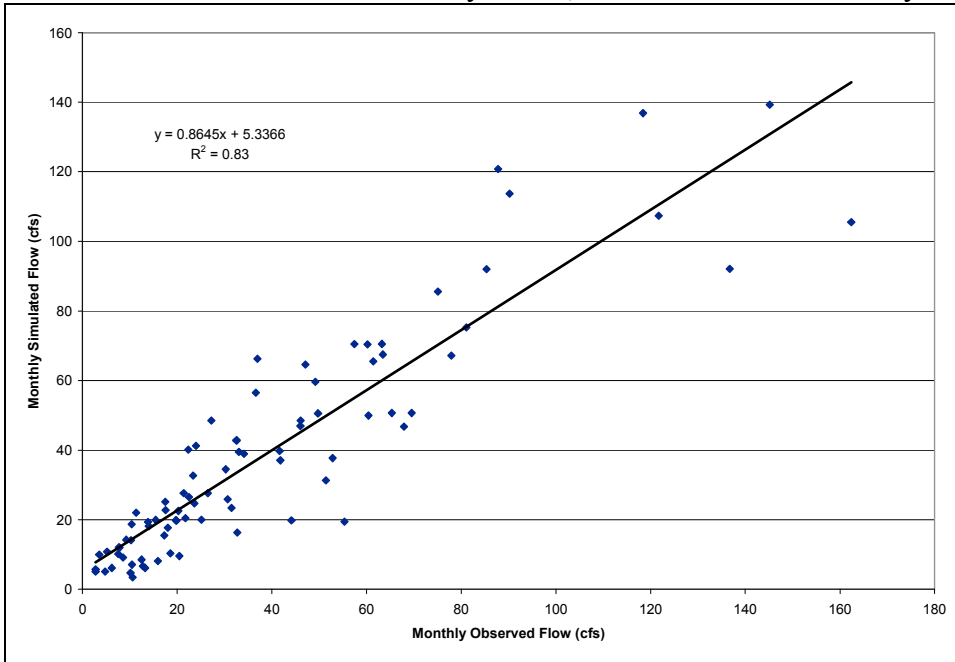
A.6 Observed vs. Simulated Daily Flows, Patuxent River near Unity



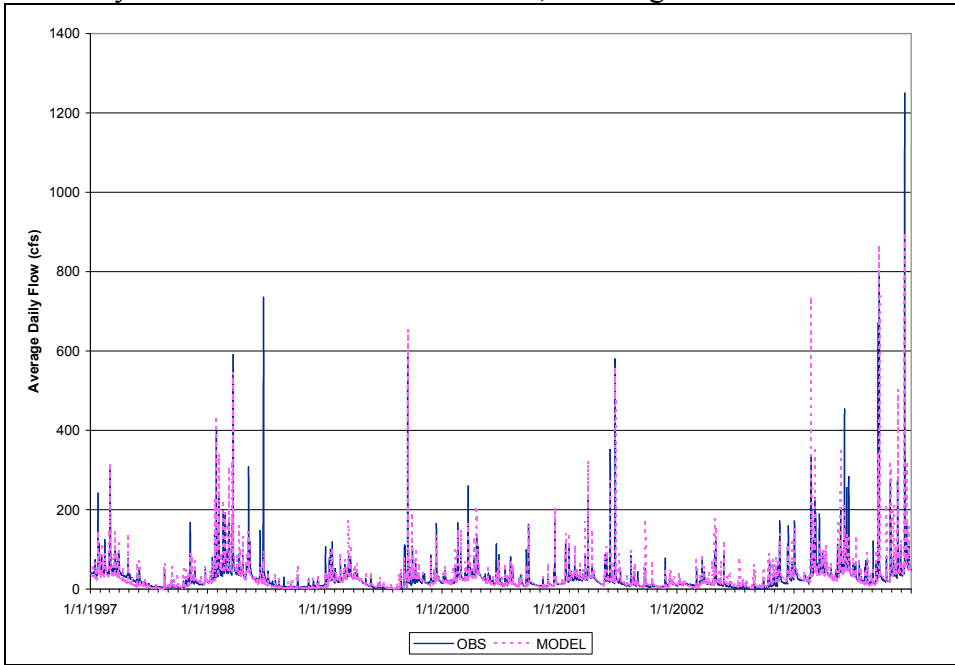
A.7 Cumulative Distribution of Observed and Simulated Flows, Patuxent River near Unity



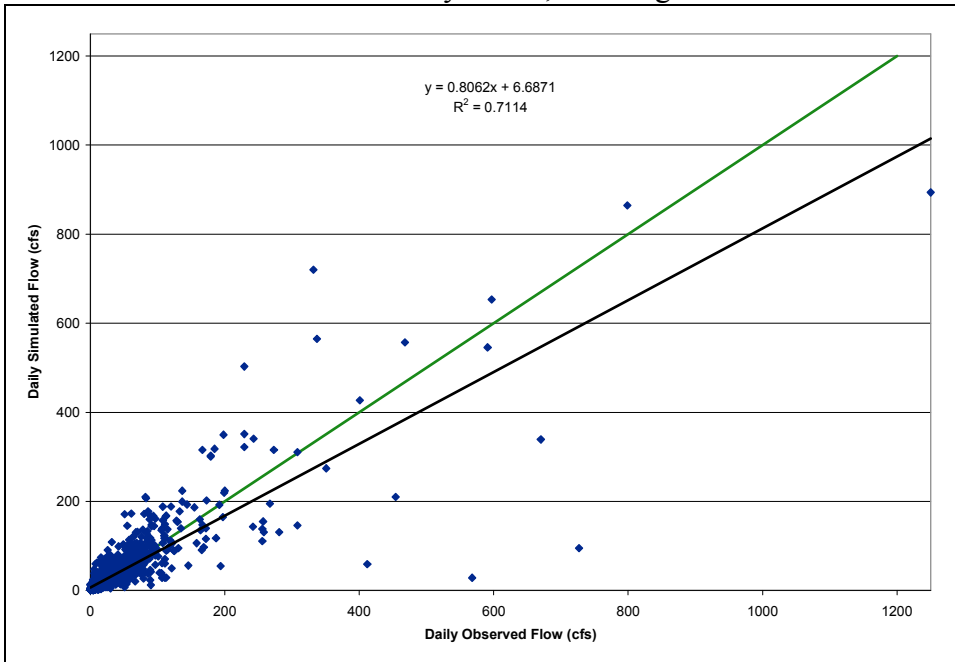
A.8 Observed vs. Simulated Monthly Flows, Patuxent River near Unity



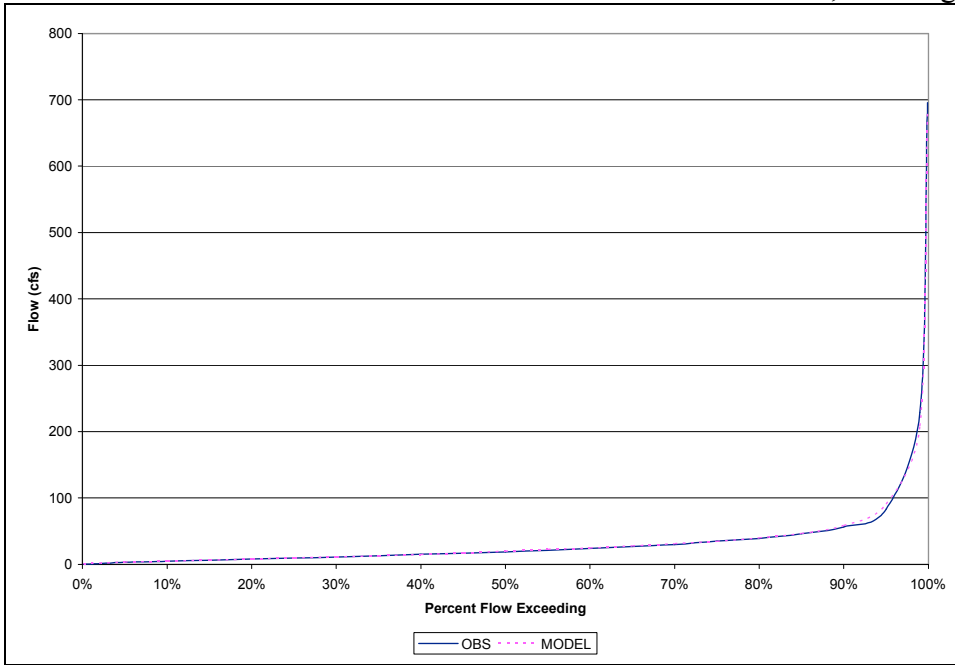
A.9 Daily Observed and Simulated Flows, Hawlings River



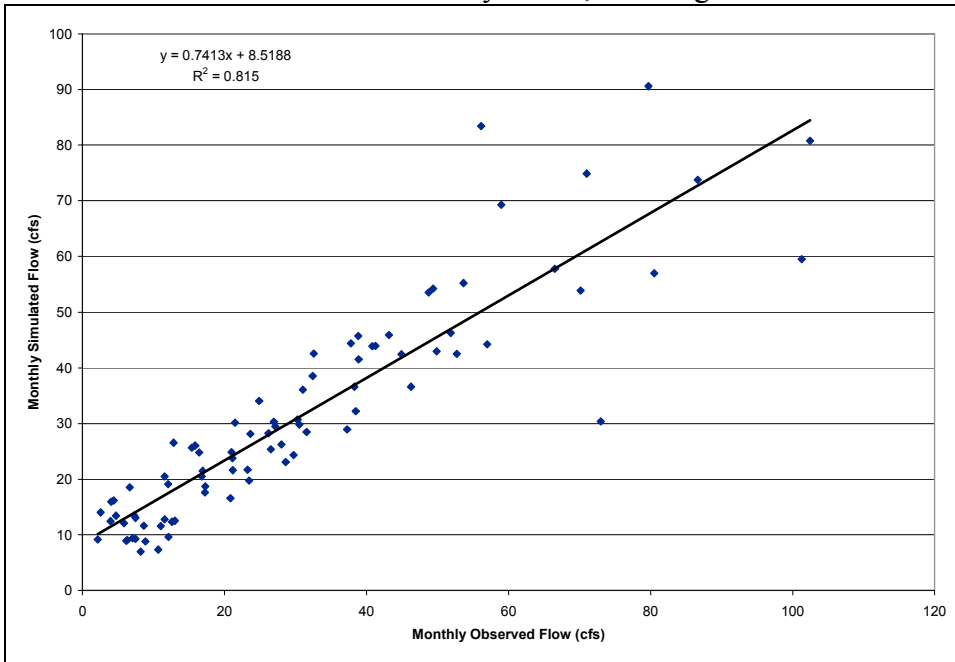
A.10 Observed vs. Simulated Daily Flows, Hawlings River



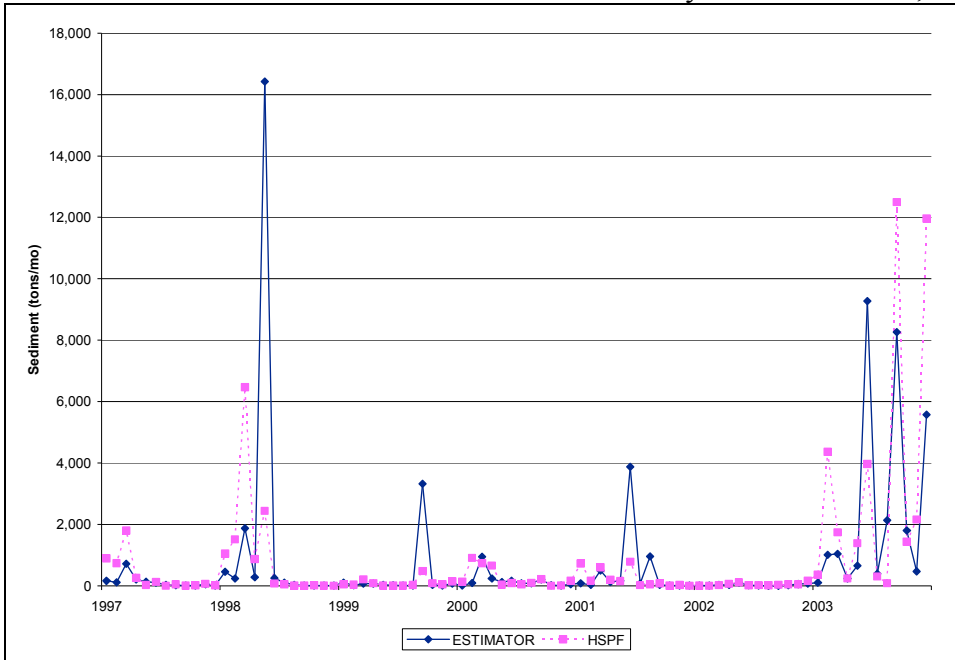
A.11 Cumulative Distribution of Observed and Simulated Flows, Hawlings River



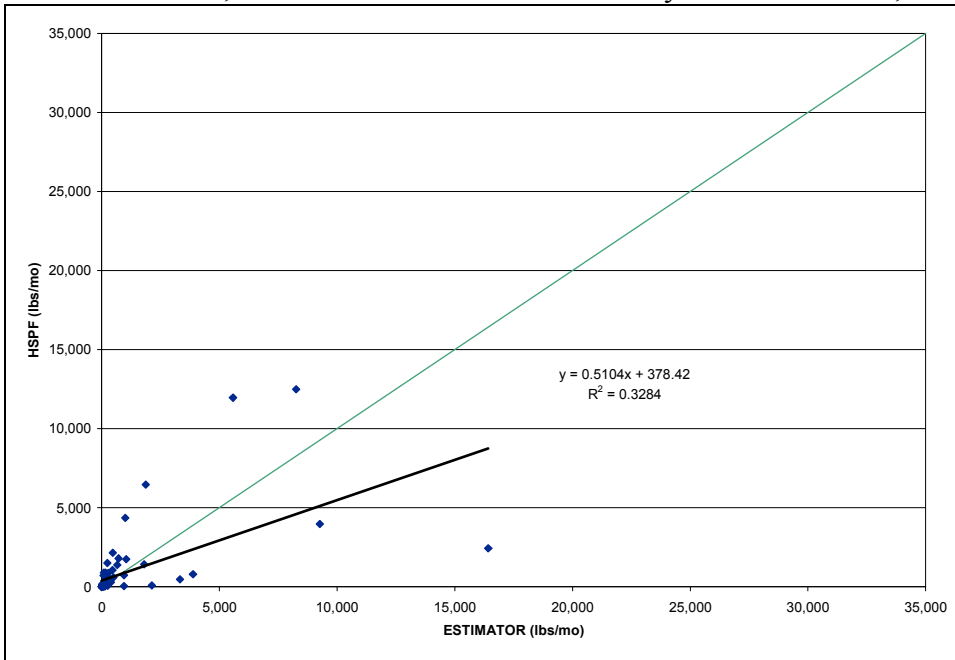
A.12 Observed vs. Simulated Monthly Flows, Hawlings River



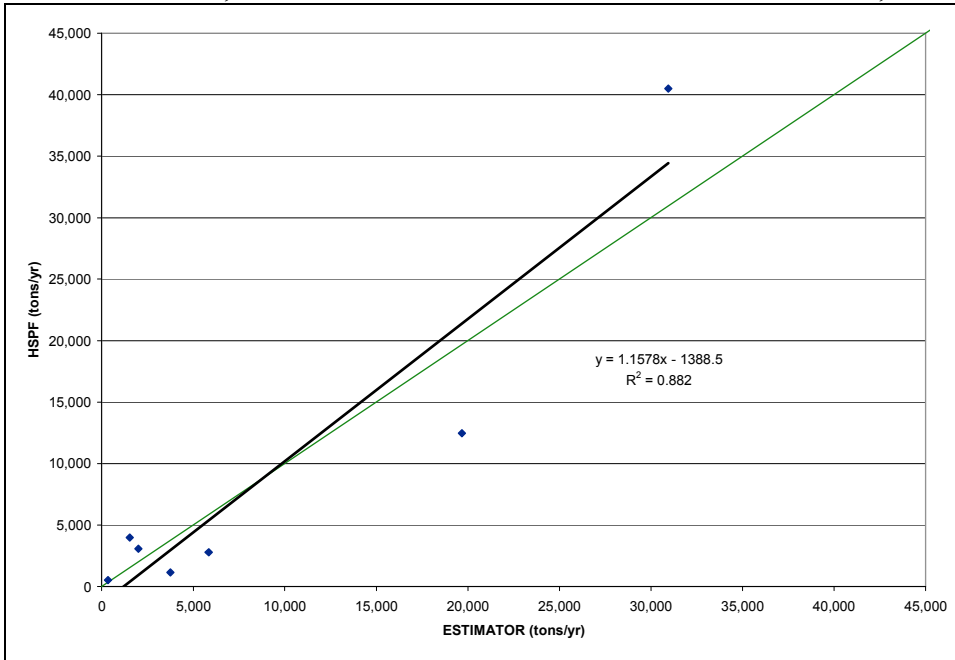
A.13 Time Series of ESTMATOR and HSPF Monthly Sediment Loads, Cattail Creek



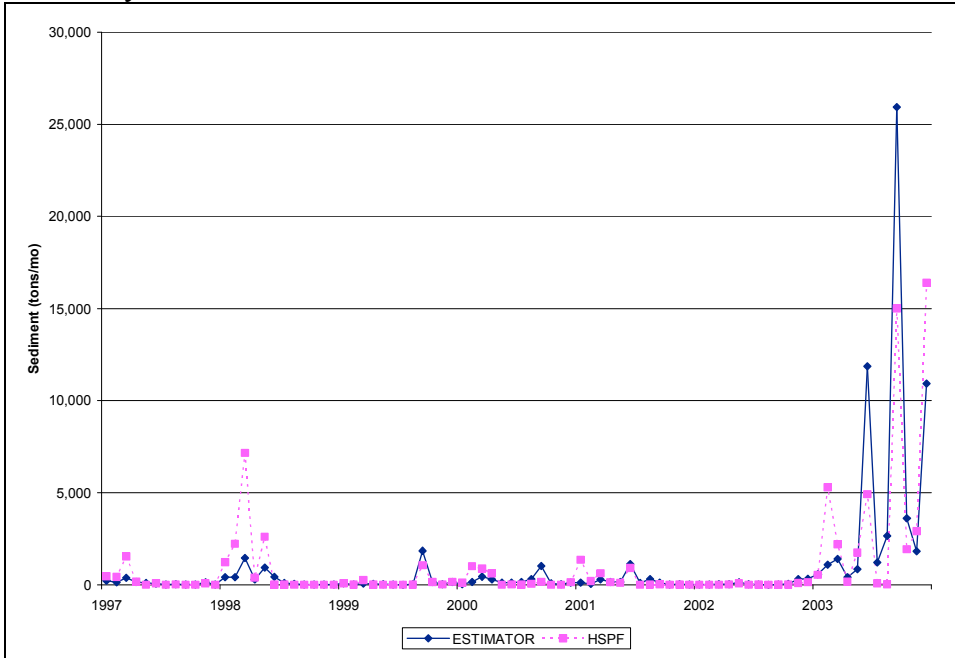
A.14 Scatter Plot, ESTMATOR and HSPF Monthly Sediment Loads, Cattail Creek



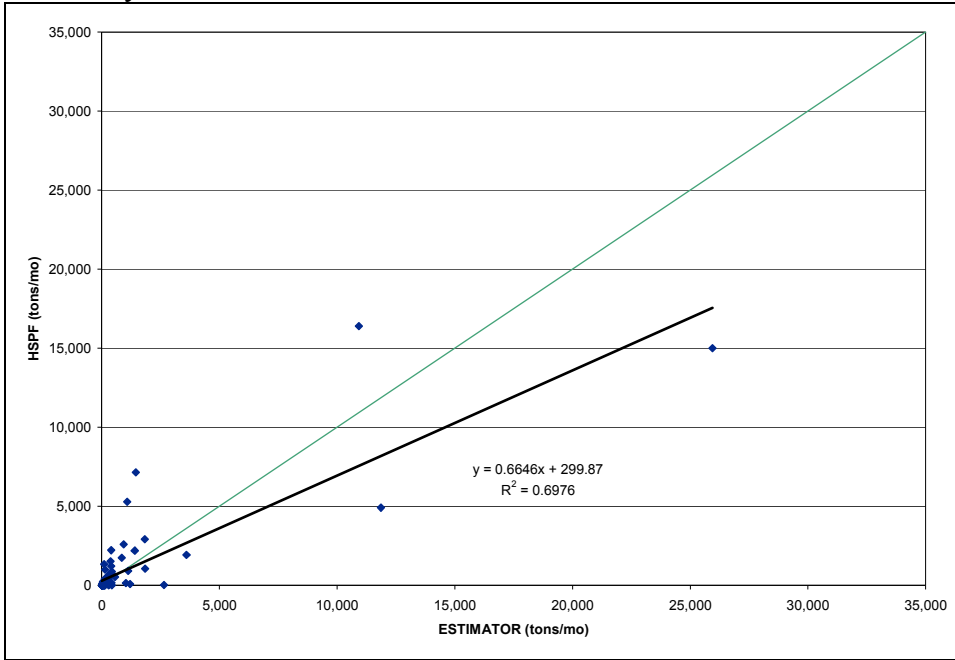
A.15 Scatter Plot, ESTIMATOR and HSPF Annual Sediment Loads, Cattail Creek



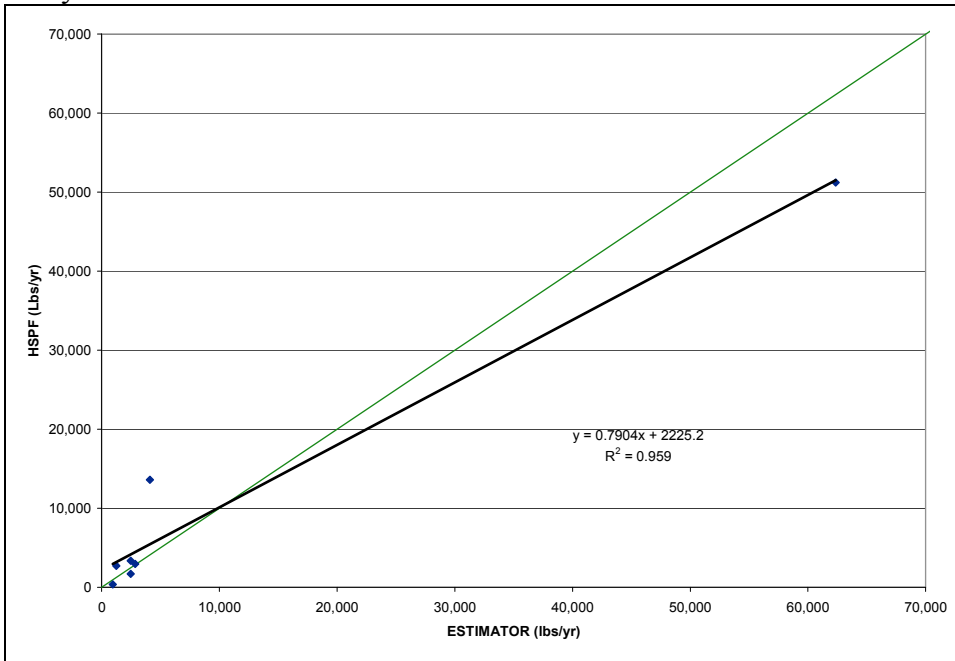
A.16 Time Series of ESTIMATOR and HSPF Monthly Sediment Loads, Patuxent River near Unity



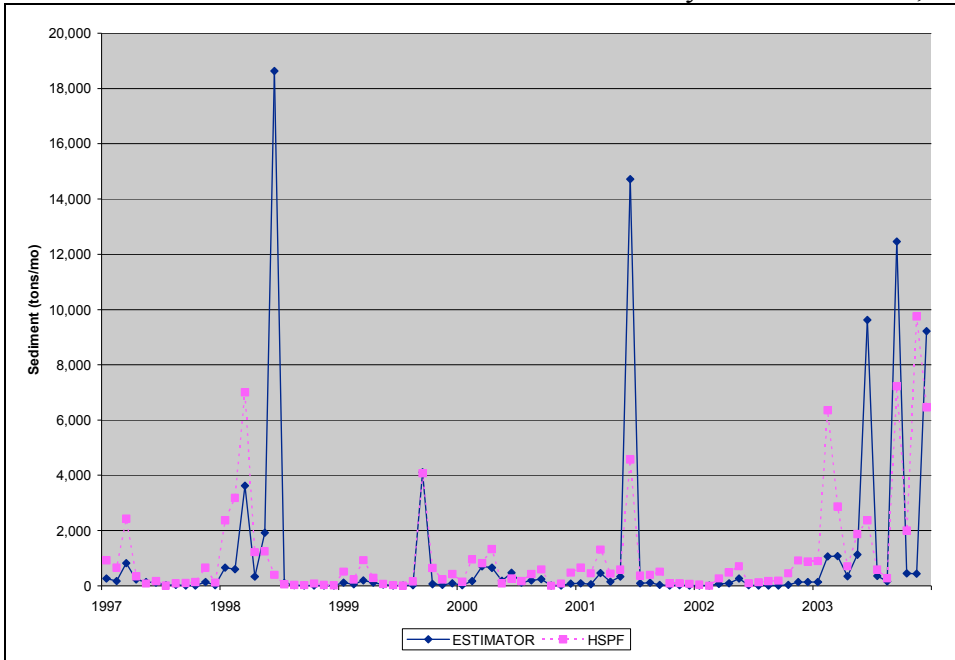
A.17 Scatter Plot, ESTIMATOR and HSPF Monthly Sediment Loads, Patuxent River near Unity



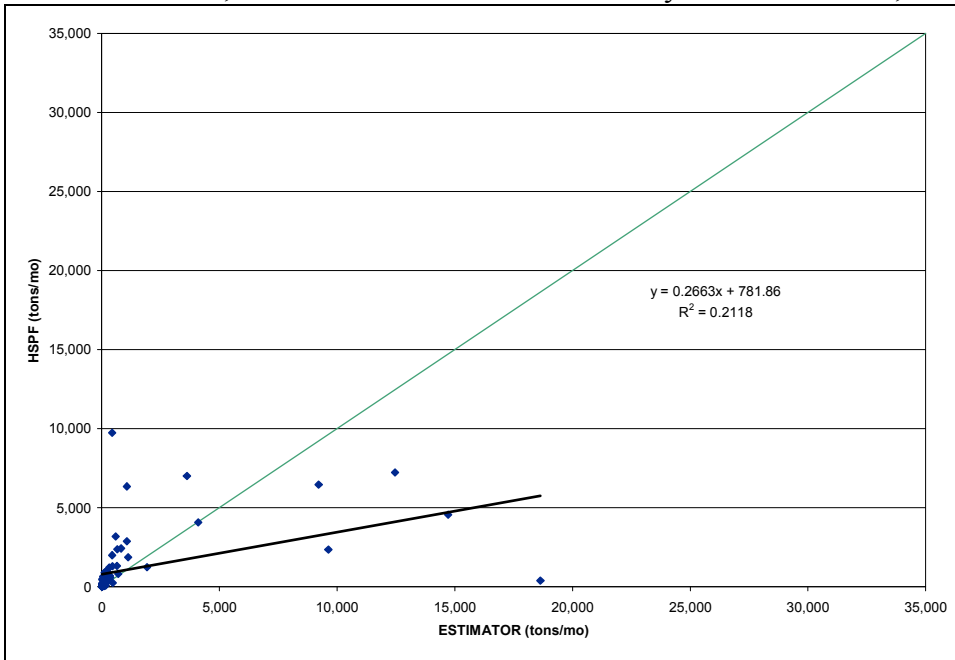
A.18 Scatter Plot, ESTIMATOR and HSPF Annual Sediment Loads, Patuxent River near Unity



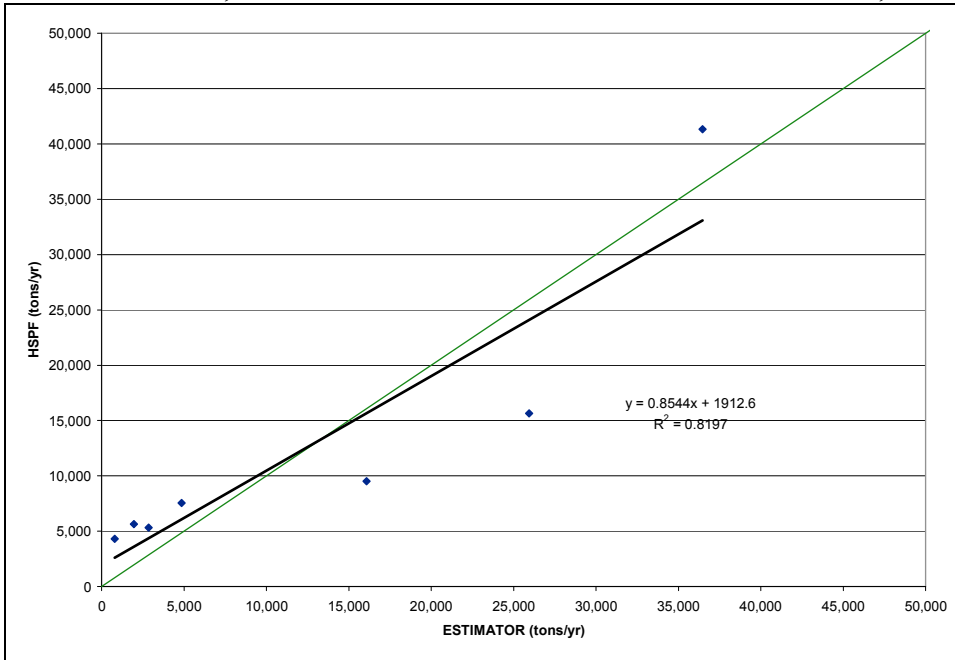
A.19 Time Series of ESTMATOR and HSPF Monthly Sediment Loads, Hawlings River



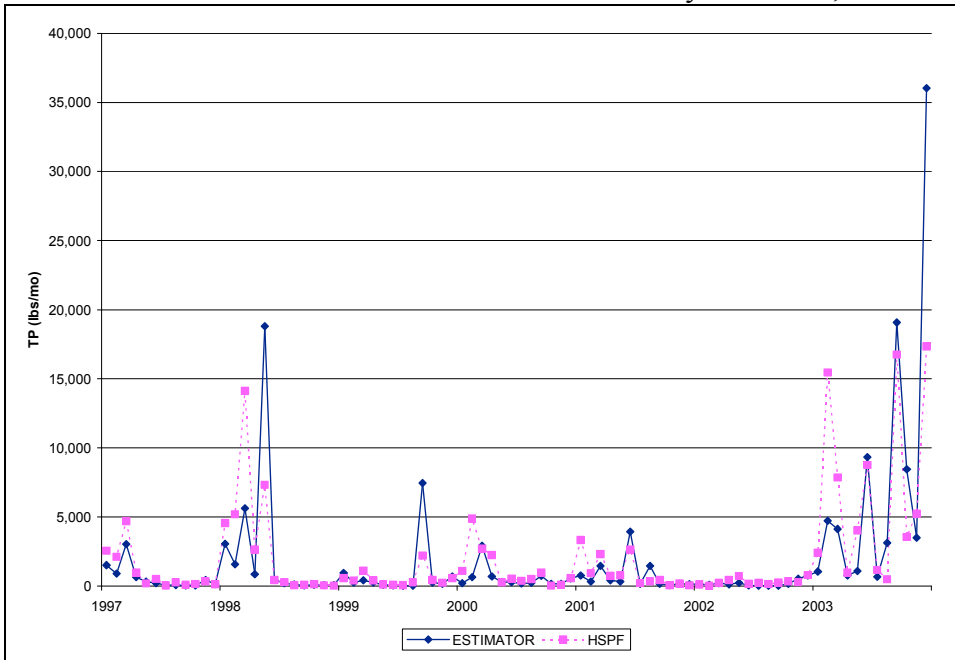
A.20 Scatter Plot, ESTMATOR and HSPF Monthly Sediment Loads, Hawlings River



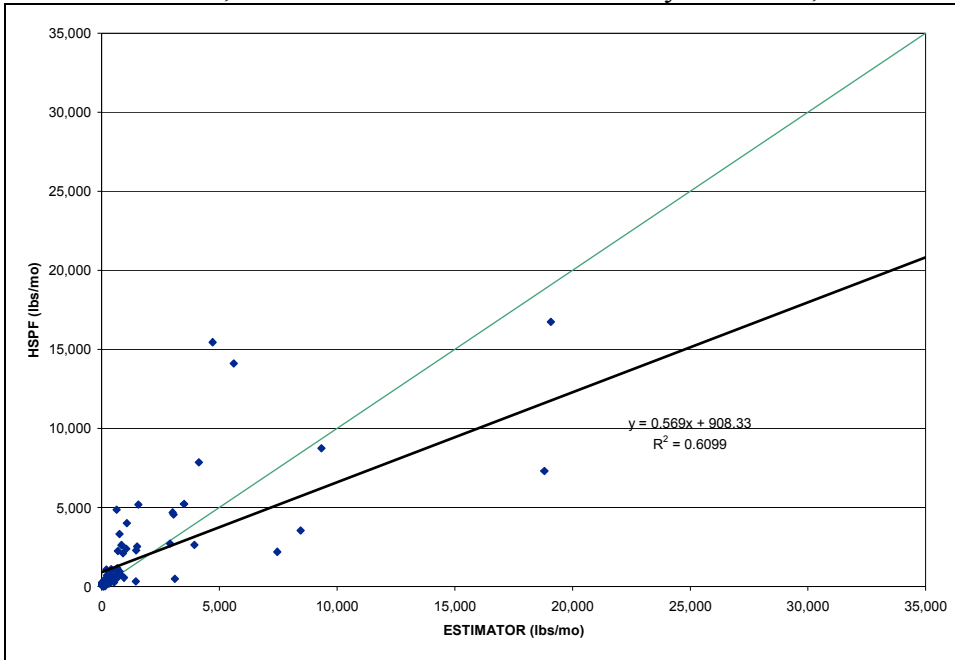
A.21 Scatter Plot, ESTIMATOR and HSPF Annual Sediment Loads, Hawlings River



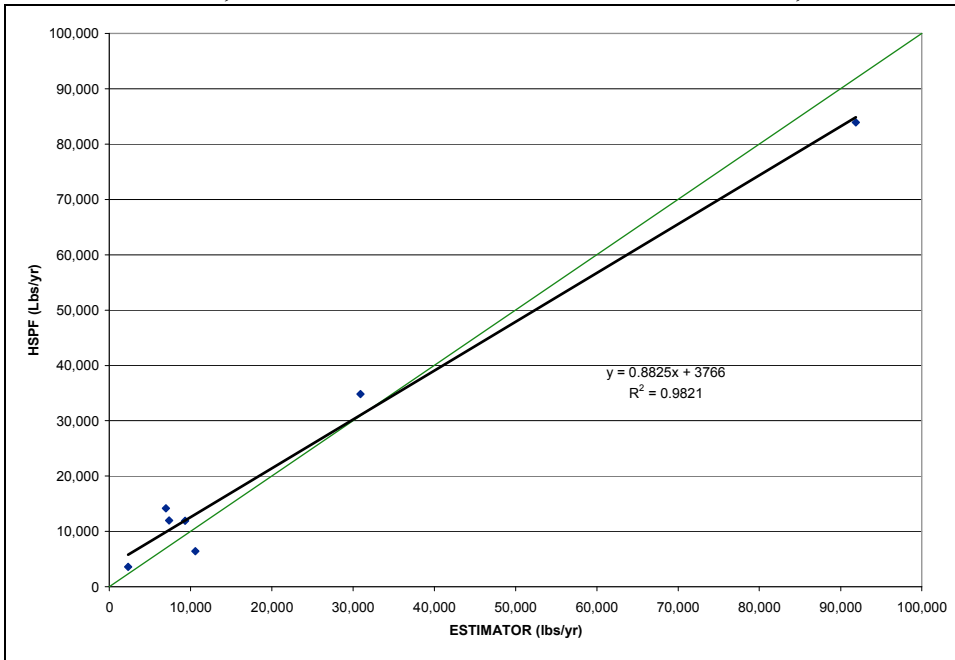
A.22 Time Series of ESTIMATOR and HSPF Monthly TP Loads, Cattail Creek



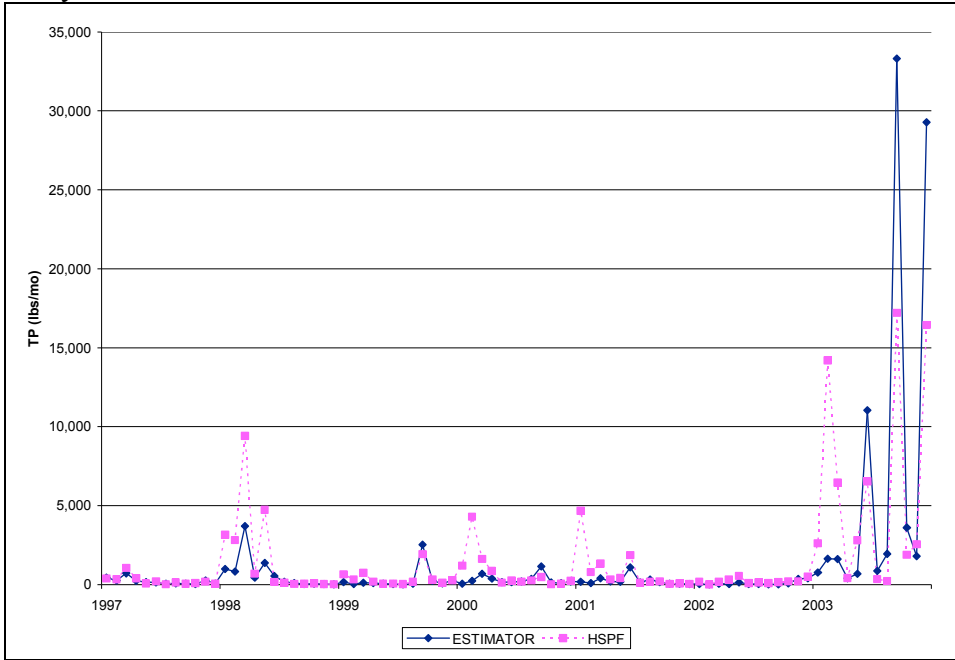
A.23 Scatter Plot, ESTIMATOR and HSPF Monthly TP Loads, Cattail Creek



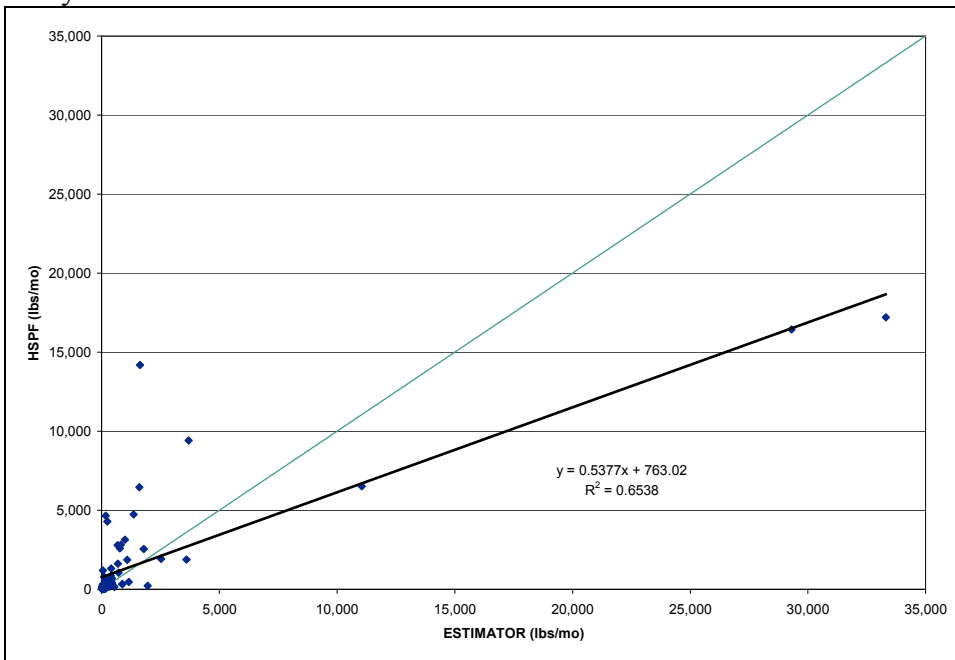
A.24 Scatter Plot, ESTIMATOR and HSPF Annual TP Loads, Cattail Creek



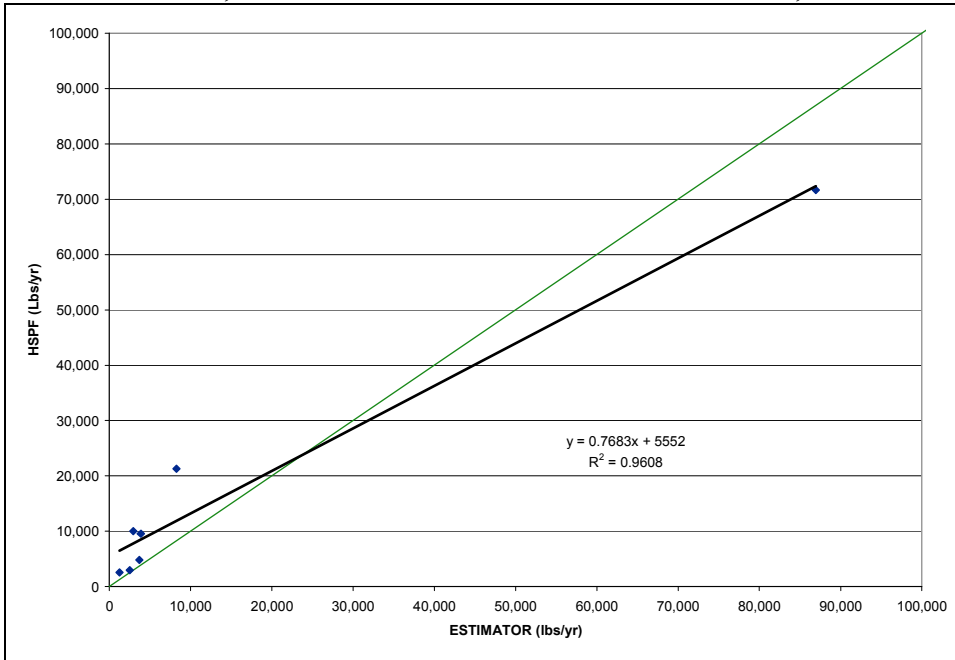
A.25 Time Series of ESTMATOR and HSPF Monthly TP Loads, Patuxent River near Unity



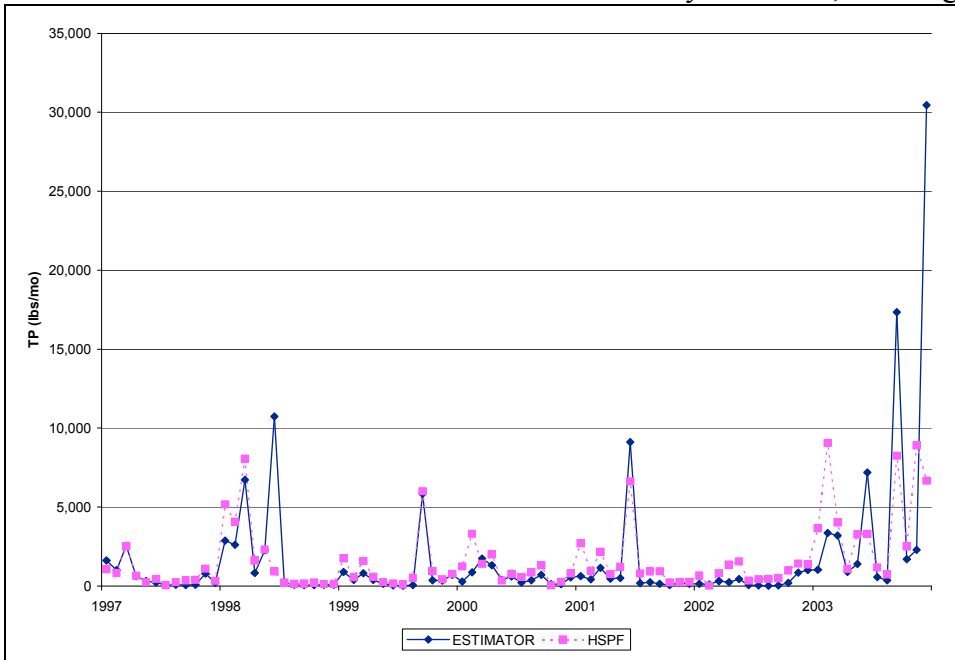
A.26 Scatter Plot, ESTMATOR and HSPF Monthly TP Loads, Patuxent River near Unity



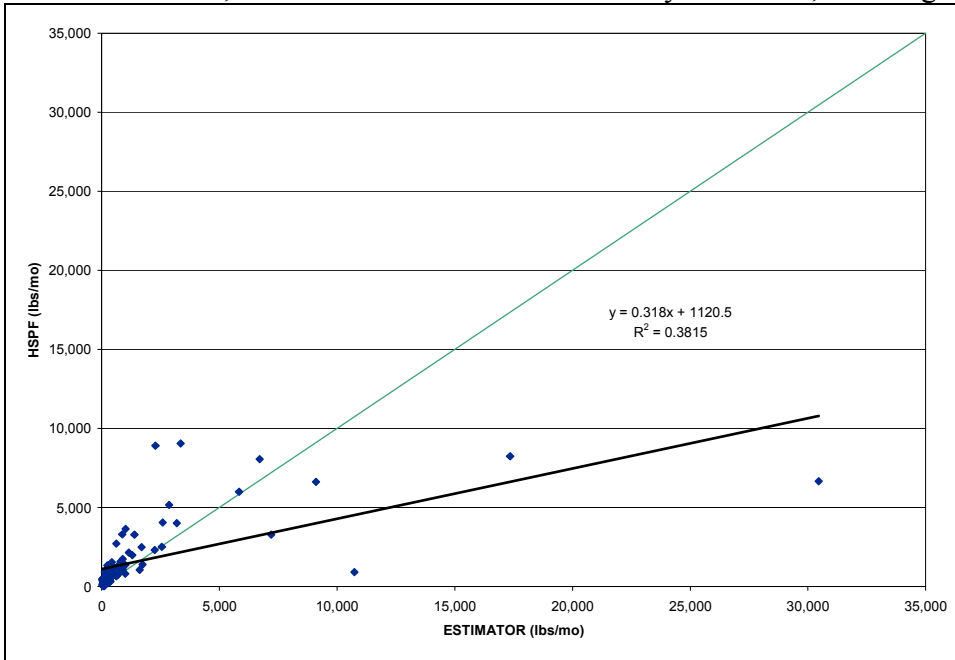
A.27 Scatter Plot, ESTIMATOR and HSPF Annual TP Loads, Patuxent River near Unity



A.28 Time Series of ESTIMATOR and HSPF Monthly TP Loads, Hawlings River



A.29 Scatter Plot, ESTIMATOR and HSPF Monthly TP Loads, Hawlings River



A.30 Scatter Plot, ESTIMATOR and HSPF Annual TP Loads, Hawlings River

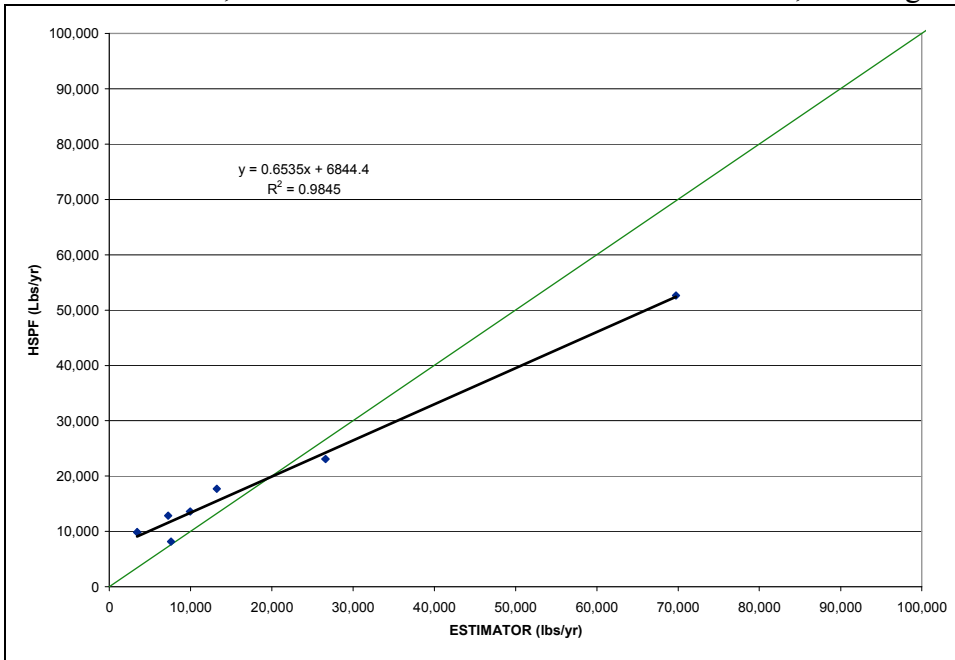


Table A.1 Average Annual Sediment Loads (tons/ac/yr) By Land Use, 1998-2003

Segment	Developed	Forest	Hay	HiTill	Impervious	LoTill	Pasture
10	0.01	0.06	0.23	1.09	0.27	0.66	0.18
20	0.00	0.06	0.30	1.17	0.26	0.70	0.18
30	0.00	0.08	0.32	1.51	0.26	0.89	0.25
40	0.01	0.06	0.22	1.08	0.28	0.63	0.17
50	0.00	0.12	0.46	2.12	0.26	1.27	0.35
60	0.01	0.11	0.42	1.92	0.27	1.18	0.32

Table A.2 Average Annual Total Phosphorus Loads (lbs/ac/yr) By Land Use, 1998-2003

Segment	Developed	Forest	Hay	HiTill	Impervious	LoTill	Pasture
10	0.41	0.12	0.71	2.13	2.74	1.36	0.68
20	0.34	0.12	0.86	2.06	2.61	1.36	0.62
30	0.34	0.18	0.90	2.18	2.61	1.43	0.79
40	0.39	0.11	0.69	2.06	2.77	1.31	0.67
50	0.33	0.24	0.87	2.07	2.61	1.30	1.07
60	0.49	0.23	0.75	2.25	2.74	1.42	1.23

Table A.3 Average Annual Ammonia-N Loads (lbs/ac/yr) By Land Use, 1998-2003

Segment	Developed	Forest	Hay	HiTill	Impervious	LoTill	Pasture
10	0.40	0.04	0.26	1.64	1.48	0.98	0.92
20	0.40	0.05	0.28	1.63	0.55	1.06	0.91
30	0.40	0.05	0.25	1.63	0.55	1.07	0.90
40	0.40	0.11	0.25	1.59	1.42	1.06	0.94
50	0.40	0.05	0.25	1.63	0.55	1.07	0.91
60	0.40	0.04	0.21	1.61	1.48	1.04	0.92

Table A.4 Average Annual Nitrate-N Loads (lbs/ac/yr) By Land Use, 1998-2003

Segment	Developed	Forest	Hay	HiTill	Impervious	LoTill	Pasture
10	6.53	0.40	5.08	14.94	7.38	16.87	4.98
20	6.51	0.32	5.01	14.80	2.73	16.89	5.02
30	6.55	0.38	5.03	14.80	2.73	16.87	5.04
40	6.56	0.77	5.05	14.46	7.09	16.59	5.00
50	6.51	0.38	5.03	14.80	2.73	16.87	5.06
60	6.49	0.29	5.05	14.57	7.38	16.50	5.00

Table A.5 Average Annual TP Loads (lbs/yr) By Segment and Land Use, Triadelphia Reservoir

Segment	Developed	Forest	Hay	HT Crop	Impervious	LT Crop	Pasture	Animal Waste	Scour	Total
10	1,176	584	1,679	4,002	1,669	7,668	1,338	1,033	15,543	34,690
40	510	1,061	1,895	4,505	684	8,574	1,269	968	1,761	21,227
60	284	476	94	223	198	422	510		169	2,377
61	67	28	103	245	71	463	10		144	1,131
62	45	56	125	295	31	559	76	45	181	1,413
63	329	59	49	117	288	221	253	91	89	1,497
64	223	88	56	132	245	249	258	91	103	1,444
65	218	162	151	358	184	678	131	45	244	2,172
Total	2,852	2,514	4,152	9,878	3,369	18,834	3,845	2,273	18,236	65,953

Table A.6 Average Annual TP Loads (lbs/yr) by Segment and Land Use, Rocky Gorge Reservoir

Segment	Developed	Forest	Hay	HT Crop	Impervious	LT Crop	Pasture	Animal Waste	Scour	Triadelphia	Point Source	Total
20	1,138	823	1,329	2,541	3,718	4,986	1,194	1,130	5,479		6	22,343
30	530	464	81	155	518	302	474	355	-2,706	15,627		15,800
50	431	761	172	324	791	603	481	253	238			4,055
51	62	103	21	40	185	74	129	51	120			783
52	87	122	53	99	209	185	89	51	186			1,080
53	37	86	27	51	126	95	107	51	111			693
54	38	71	0	0	44	0	138		73			365
55	97	86	49	93	110	172	36		171			813
56	77	35	0	0	75	0	45		79			311
57	114	93	4	8	140	15	165	101	53			693
Total	2,610	2,644	1,737	3,311	5,915	6,433	2,857	1,991	3,804	15,627	6	46,935

Table A.7 Average Annual Sediment Loads (tons/yr) By Segment and Land Use, Triadelphia Reservoir

Segment	Developed	Forest	Hay	HT Crop	Impervious	LT Crop	Pasture	Scour	Total
10	29	301	560	2,054	167	3,748	374	5,745	12,978
40	12	562	617	2,354	68	4,128	336	4,130	12,207
60	5	237	53	193	20	355	139	382	1,384
61	1	14	58	212	7	389	3	351	1,036
62	1	28	71	255	3	469	21	463	1,310
63	6	29	28	101	29	186	69	268	717
64	4	44	31	114	25	209	70	304	801
65	4	81	86	310	18	569	36	607	1,710
Total	63	1,296	1,505	5,593	337	10,051	1,047	12,249	32,143

APPENDIX B

Figure B.1. Isothermal Contours, at TR2, Triadelphia Reservoir, 1998-2003

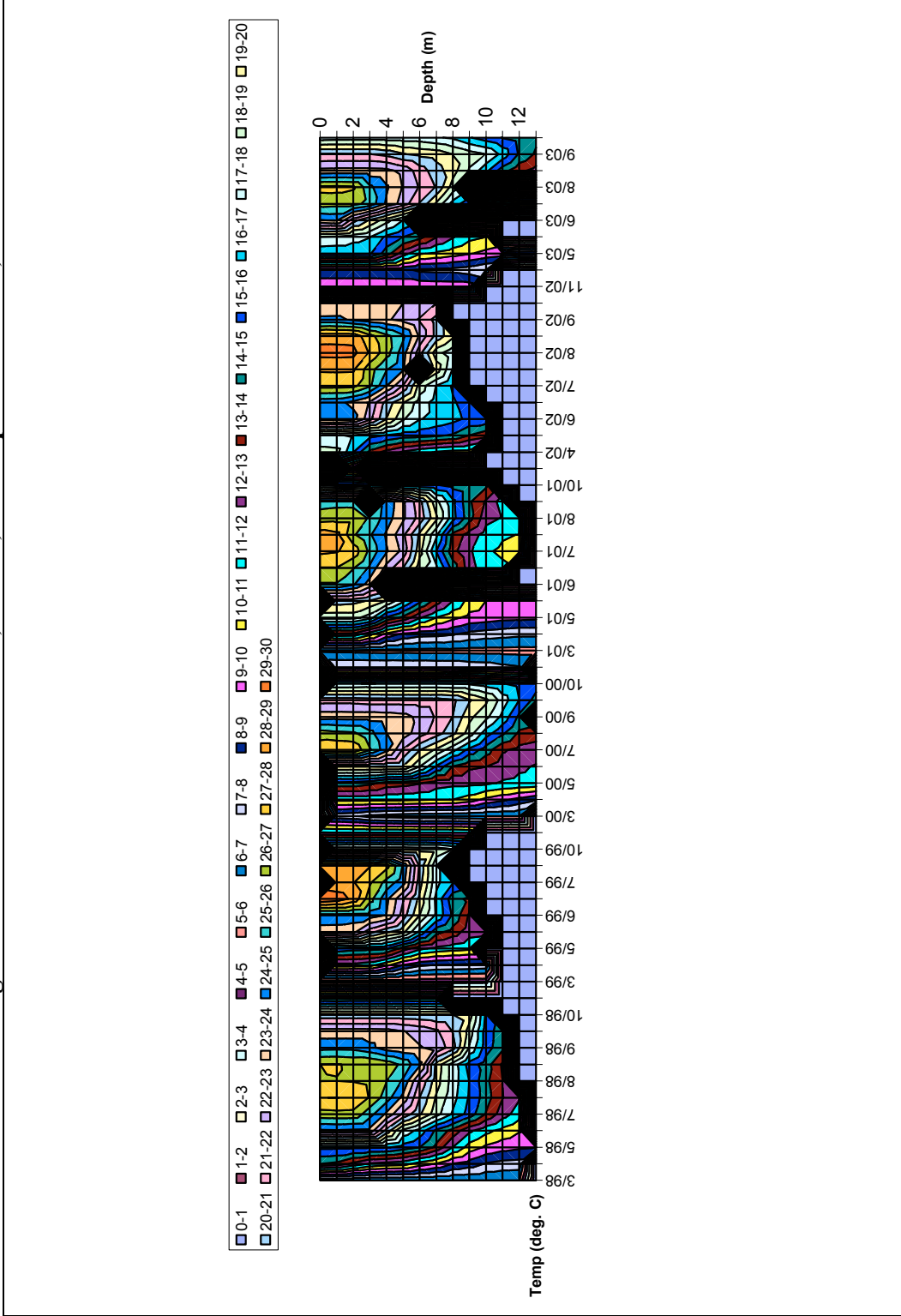


Figure B.2. Isothermal Contours, at TR3, Triadelphia Reservoir, 1998-2003

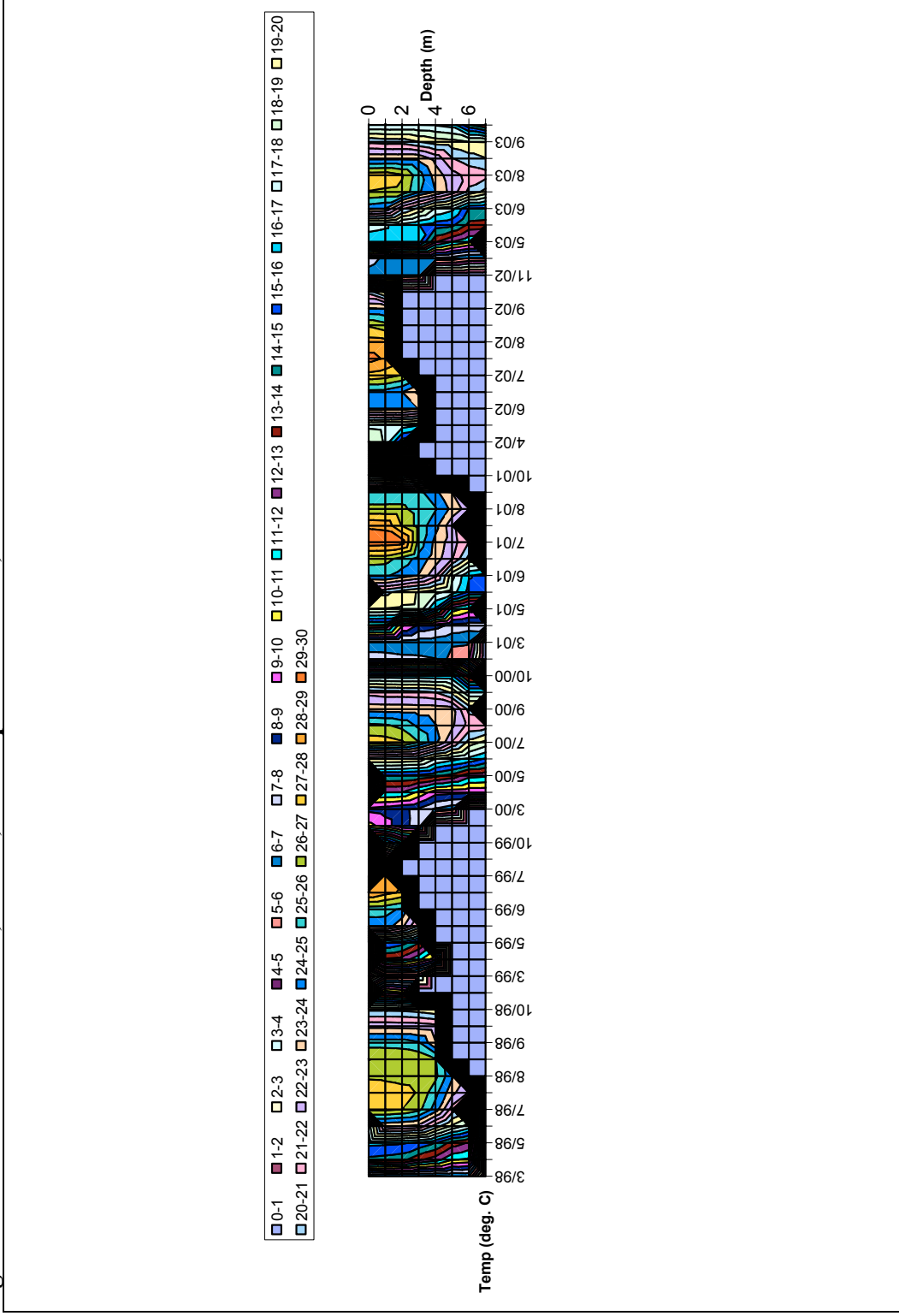


Figure B.3. Isothermal Contours, at RG1, Rocky Gorge Reservoir, 1998-2003

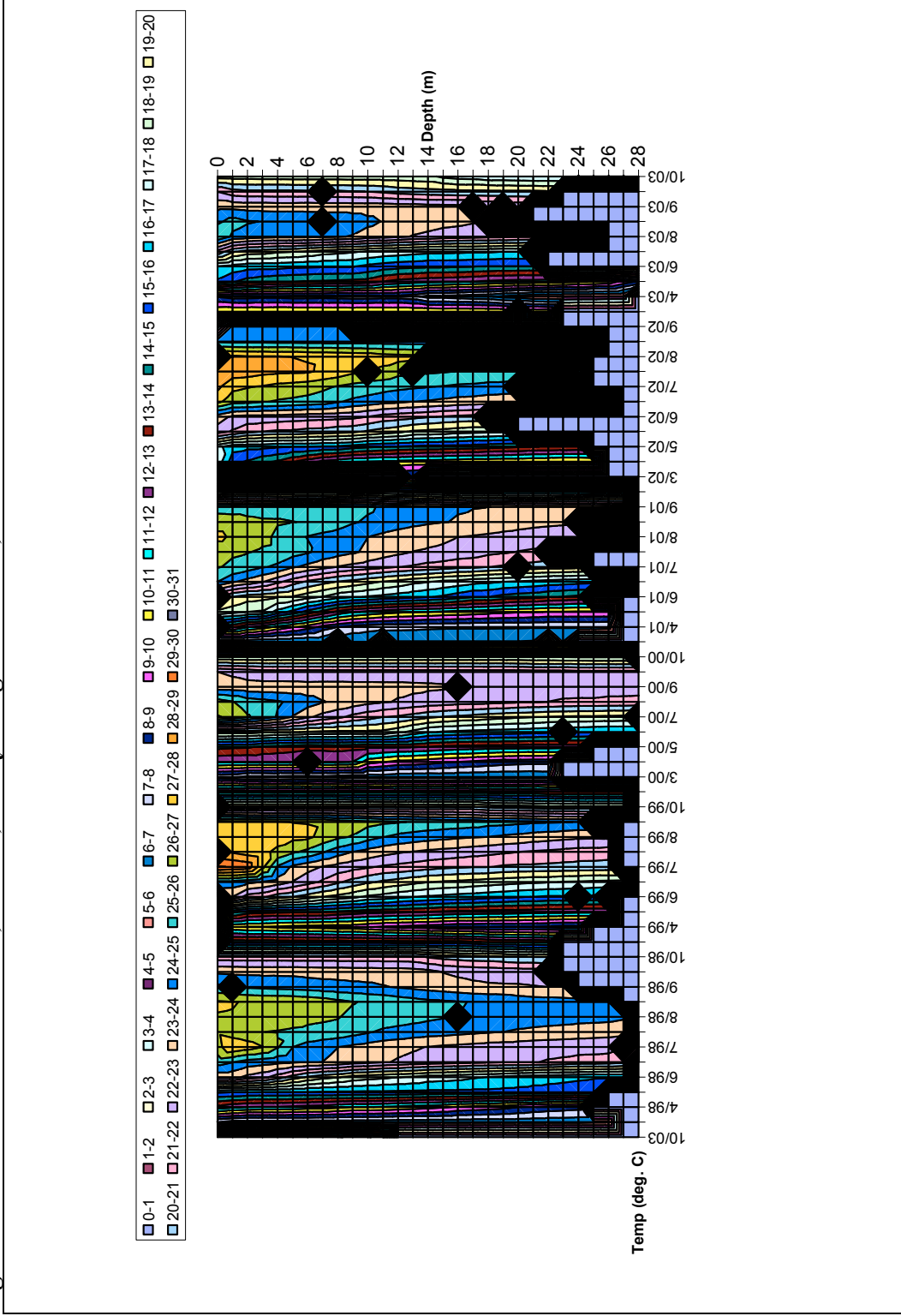


Figure B.4. Isothermal Contours, at RG2, Rocky Gorge Reservoir, 1998-2003

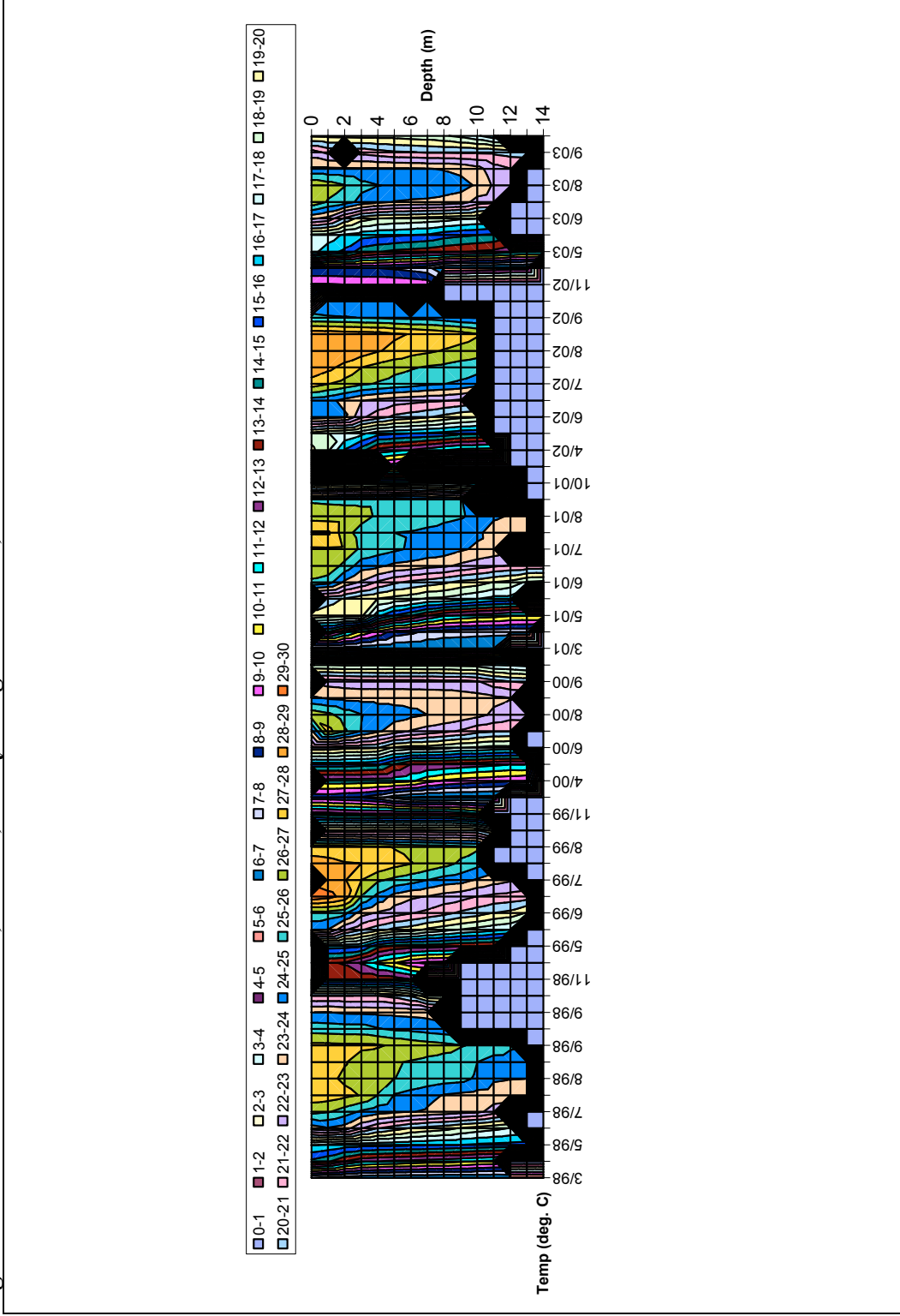


Figure B.5. Isothermal Contours, at RG3, Rocky Gorge Reservoir, 1998-2003

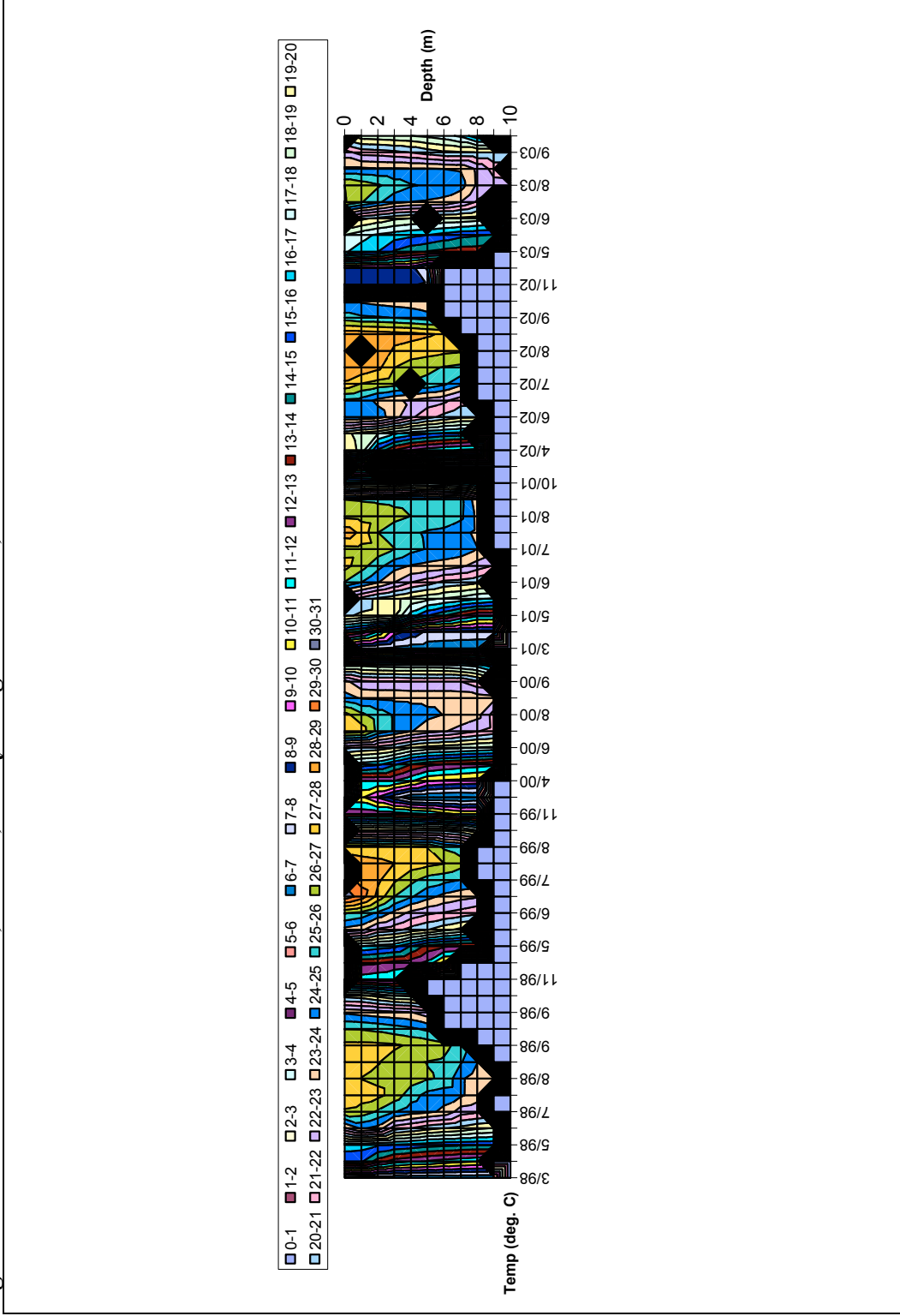


Figure B.6. DO Contours, at TR2, Triadelphia Reservoir, 1998-2003

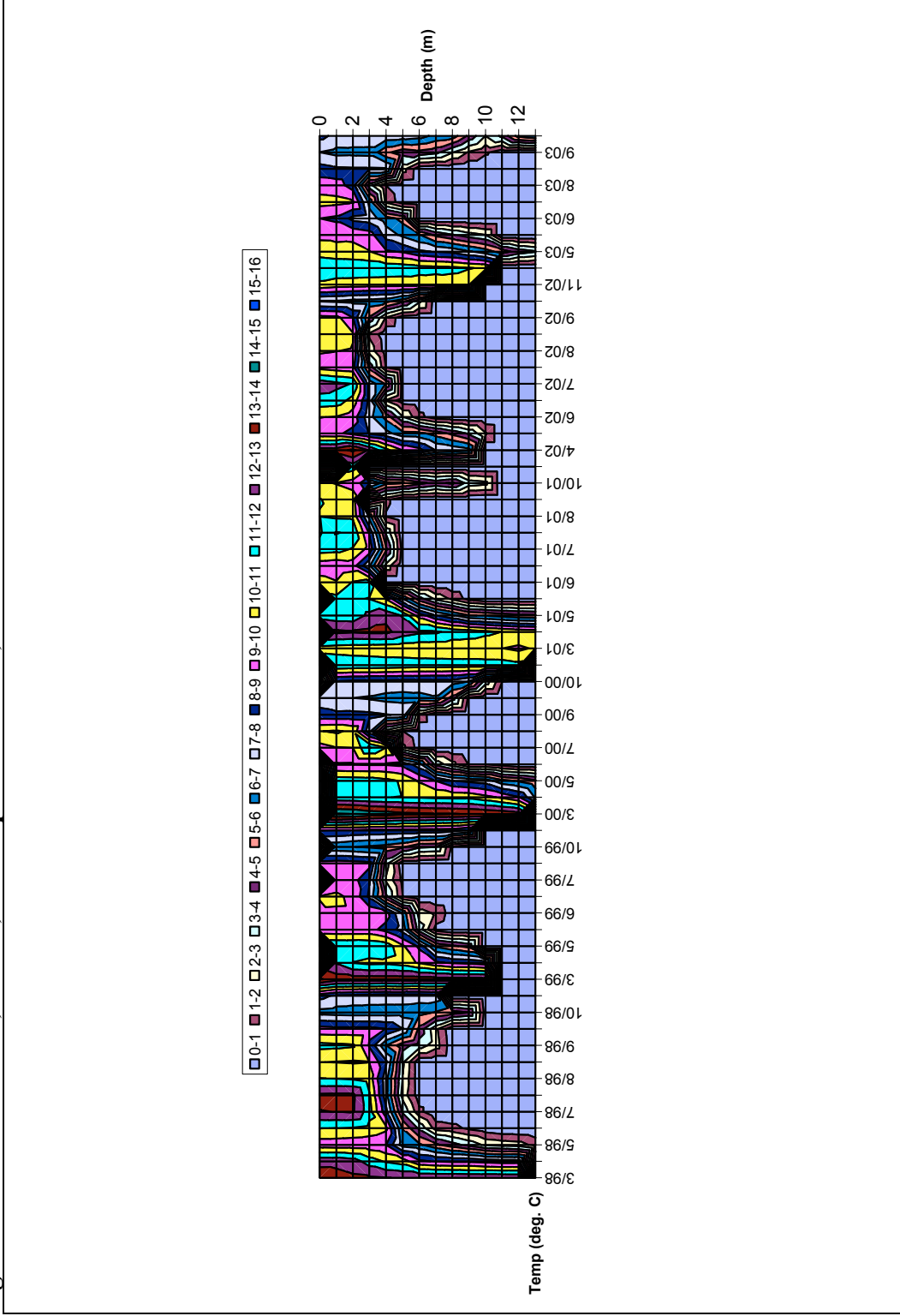


Figure B.7. DO Contours, at TR3, Triadelphia Reservoir, 1998-2003

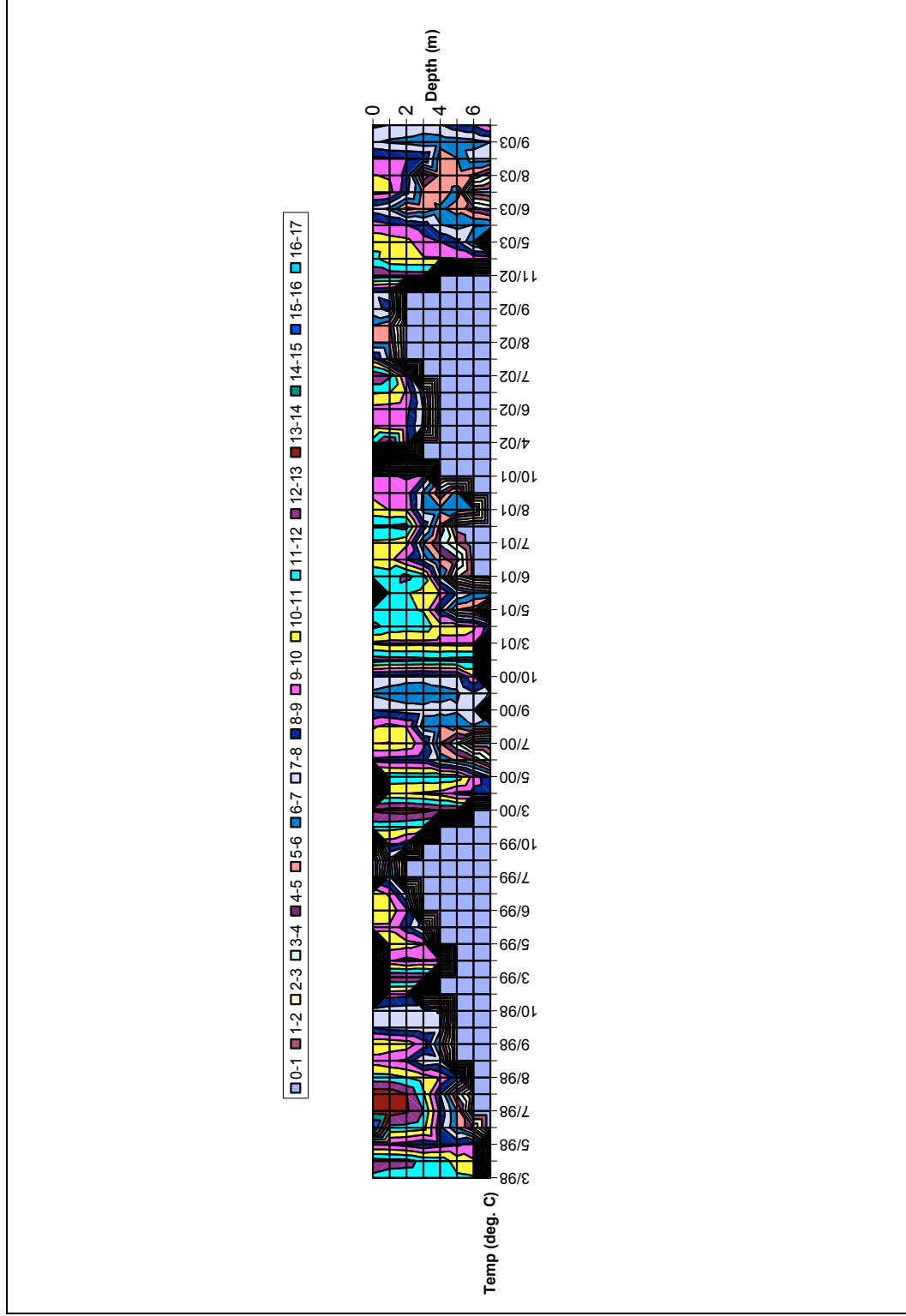


Figure B.8. DO Contours, at RG1, Rocky Gorge Reservoir, 1998-2003

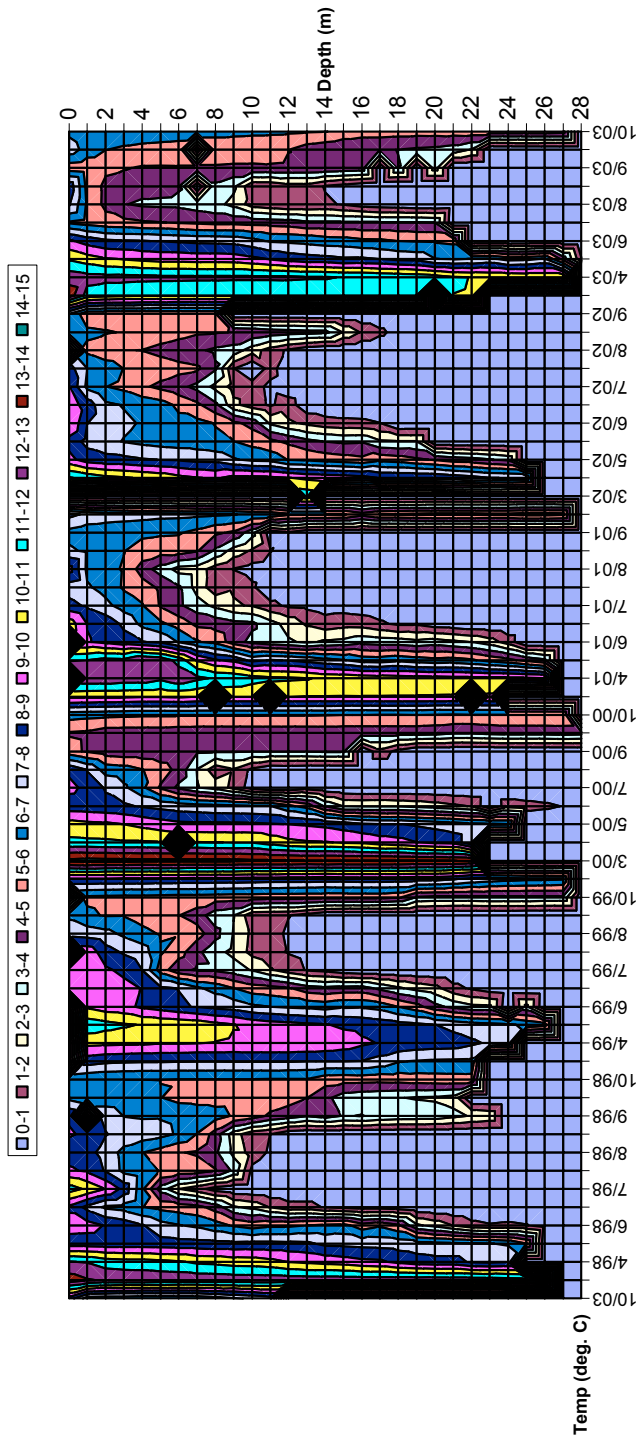


Figure B.9. DO Contours, at RG2, Rocky Gorge Reservoir, 1998-2003

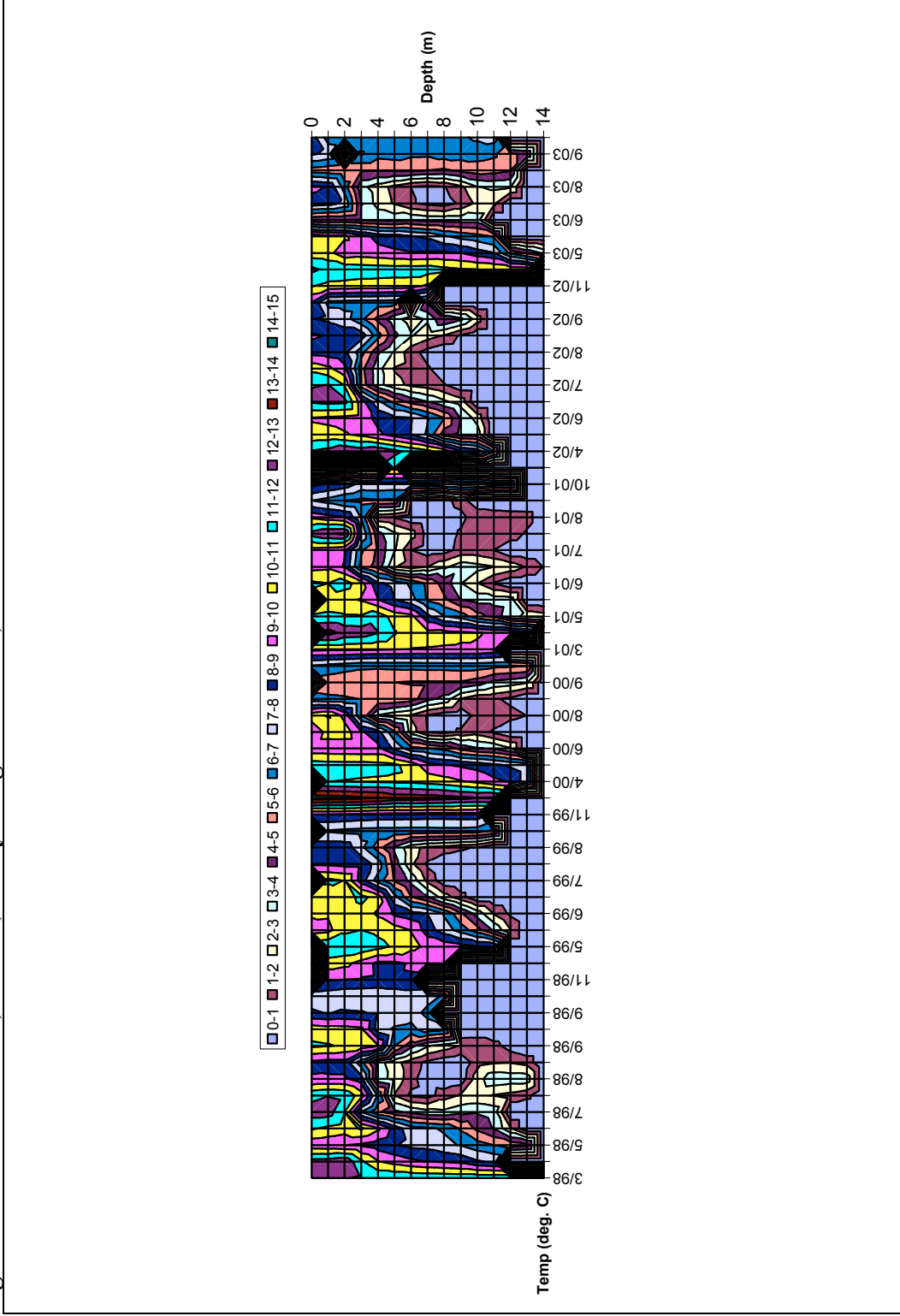


Figure B.10. DO Contours, at RG3, Rocky Gorge Reservoir, 1998-2003

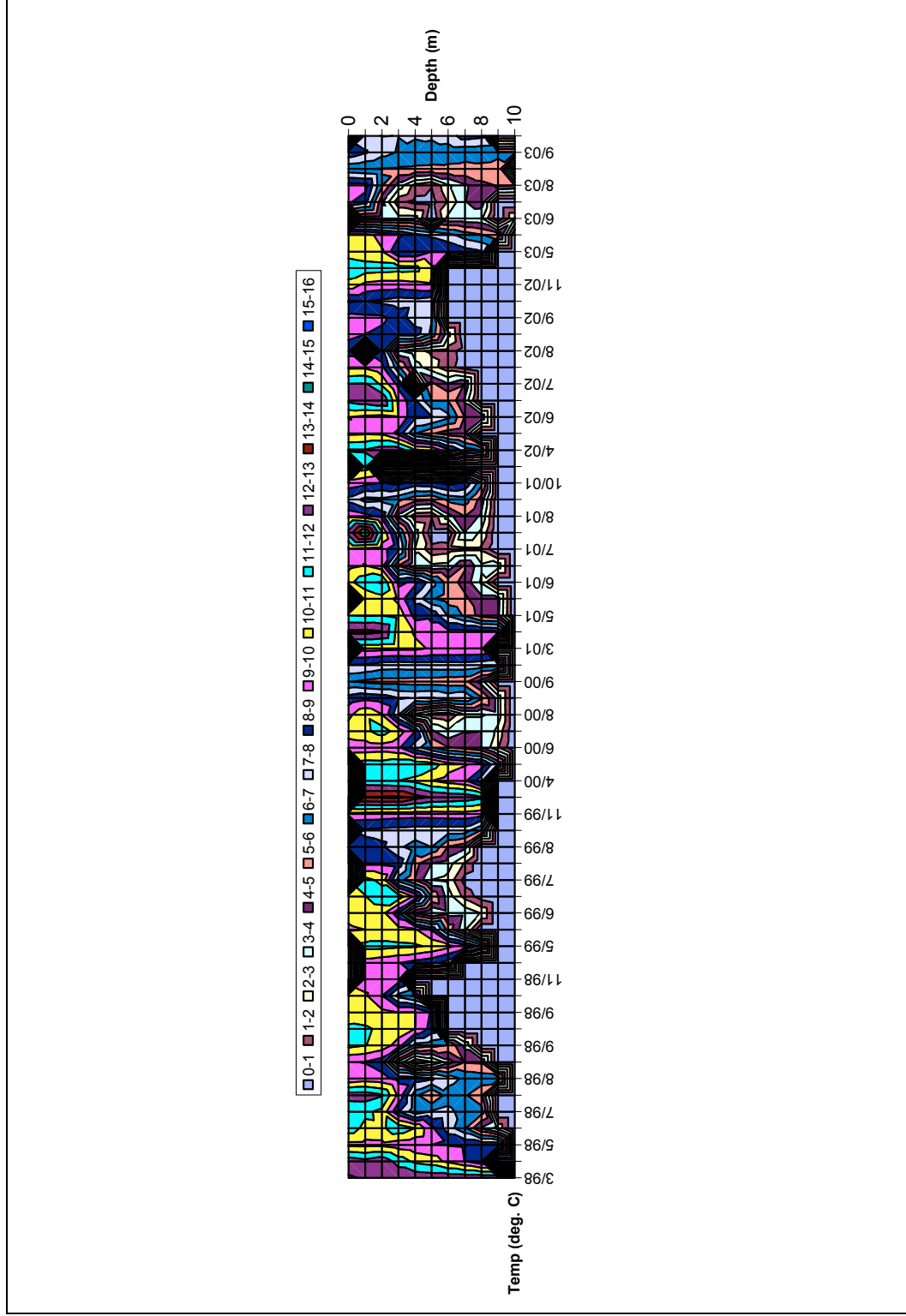


Figure B.13. Observed Total Phosphorus Concentrations at TR3, 1998-2003, Triadelphia Reservoir

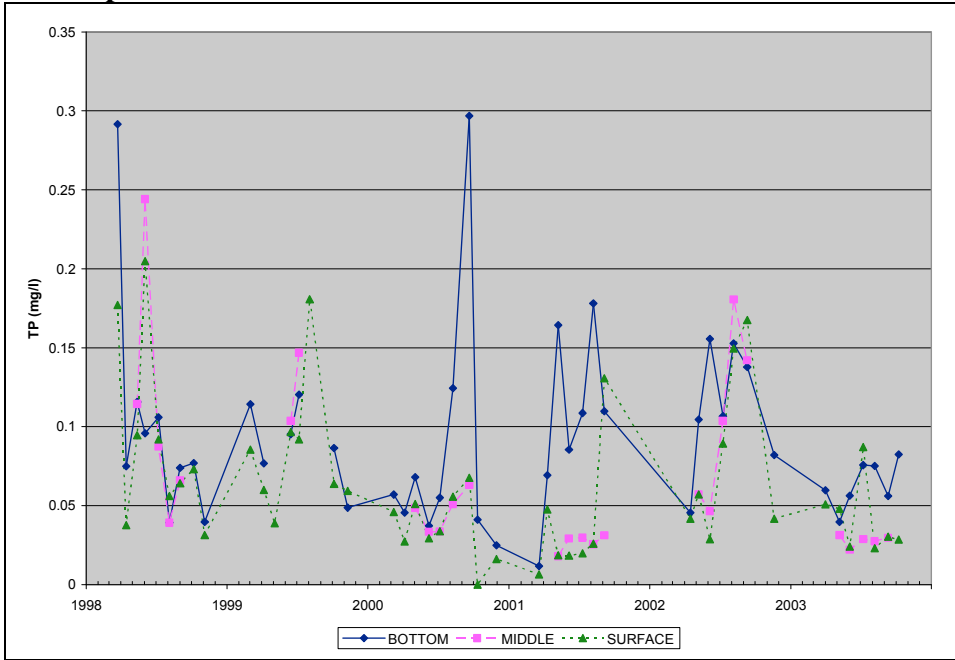


Figure B.14. Observed Total Phosphorus Concentrations at RG1, 1998-2003, Rocky Gorge Reservoir

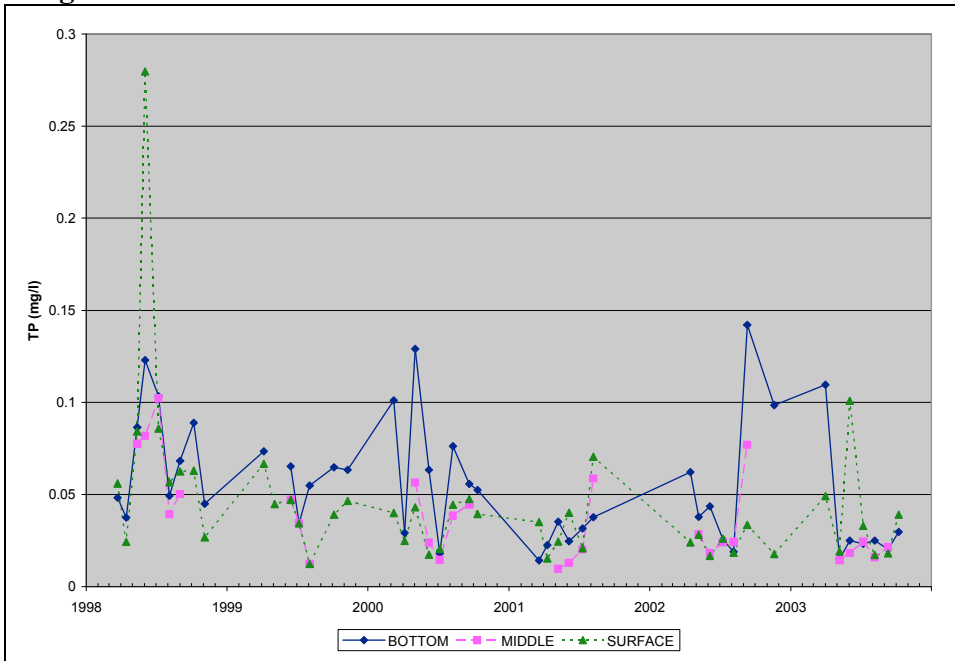


Figure B.15. Observed Total Phosphorus Concentrations at RG2, 1998-2003, Rocky Gorge Reservoir

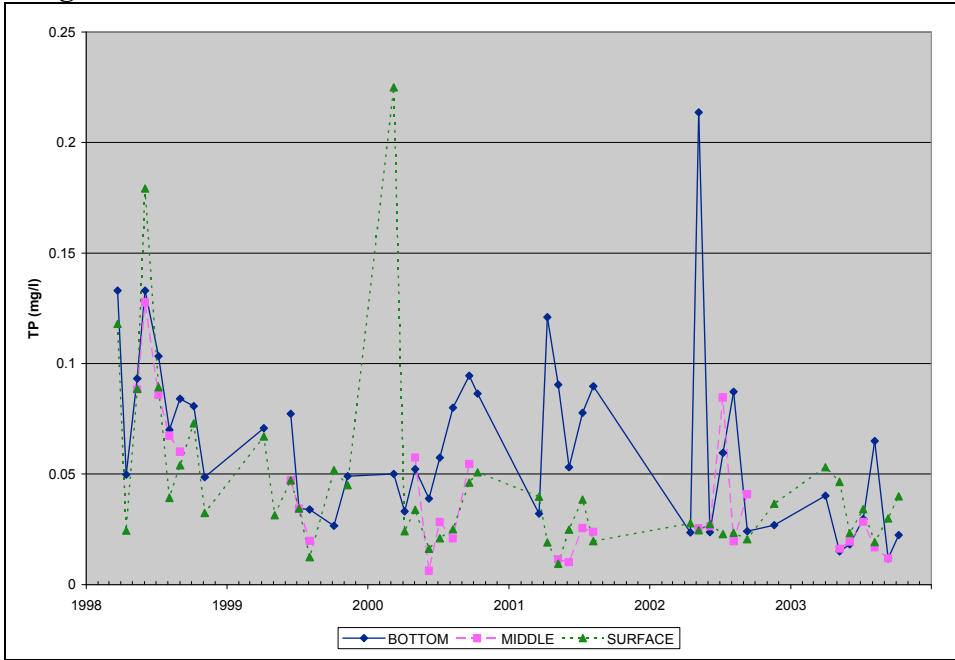


Figure B.16. Observed Total Phosphorus Concentrations at RG3, 1998-2003, Rocky Gorge Reservoir

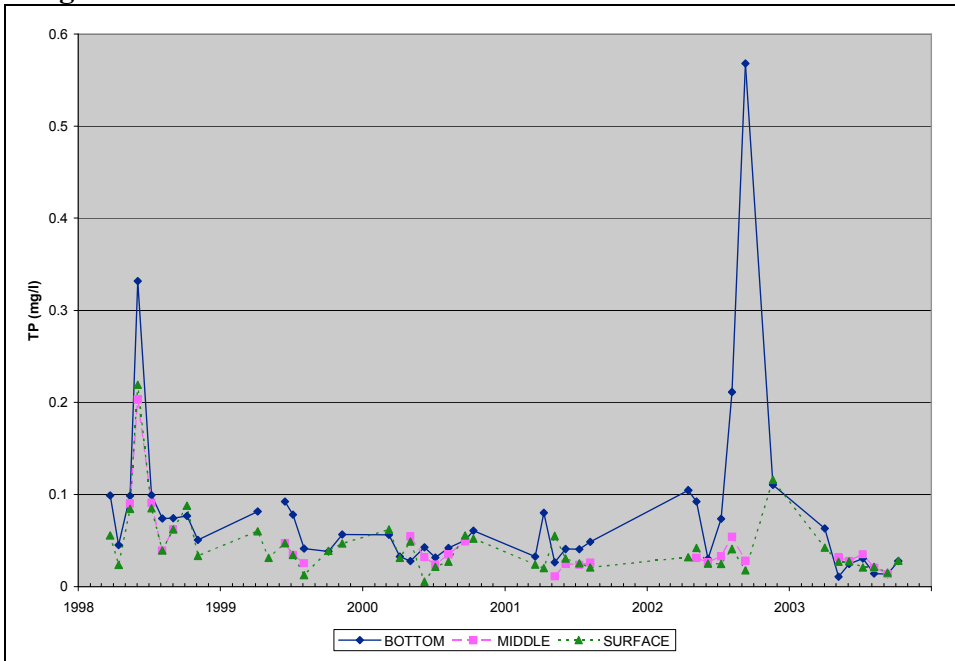


Figure B.17. Observed Total Phosphorus Concentrations at MDE Sampling Stations, 2000, Triadelphia Reservoir

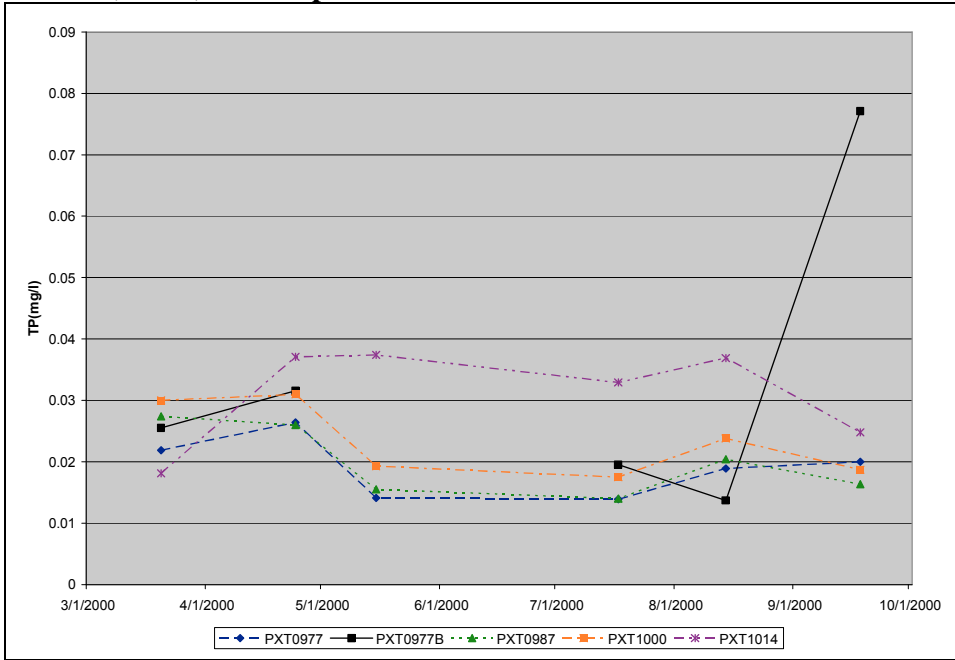


Figure B.18. Observed Total Phosphorus Concentrations at MDE Sampling Stations, 2000, Rocky Gorge Reservoir

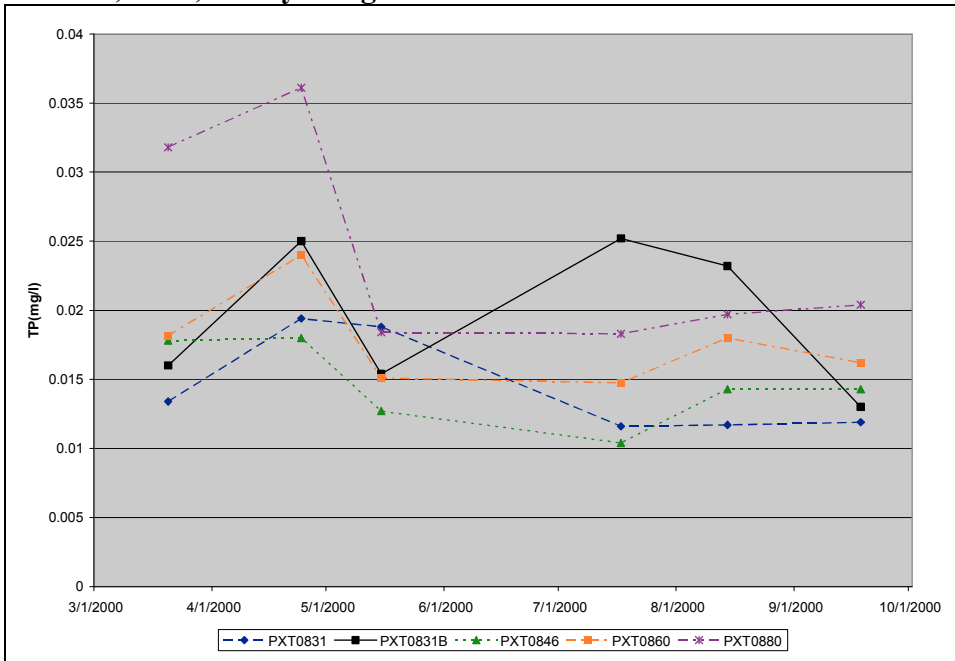


Figure B.19. Observed Phosphate-P Concentrations at TR1, 1998-2003, Triadelphia Reservoir

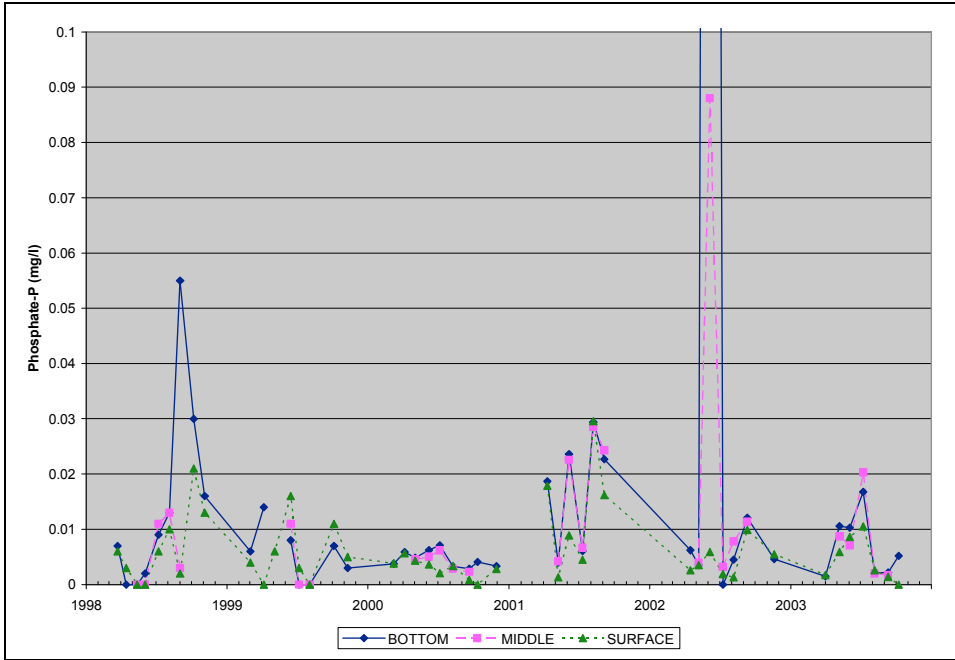


Figure B.20. Observed Phosphate-P Concentrations at TR2, 1998-2003, Triadelphia Reservoir

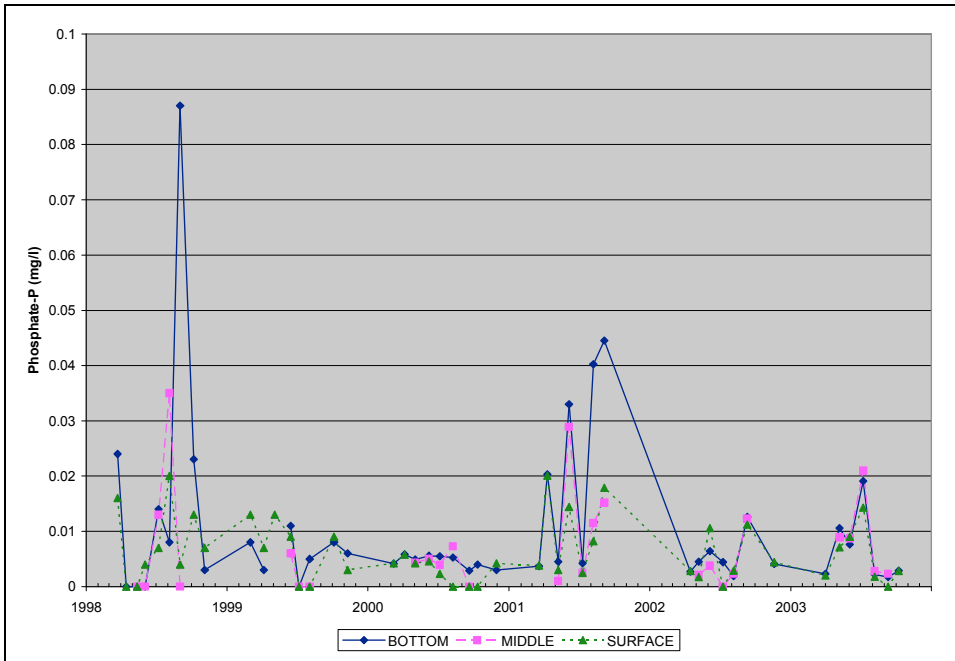


Figure B.21. Observed Phosphate-P Concentrations at TR3, 1998-2003, Triadelphia Reservoir

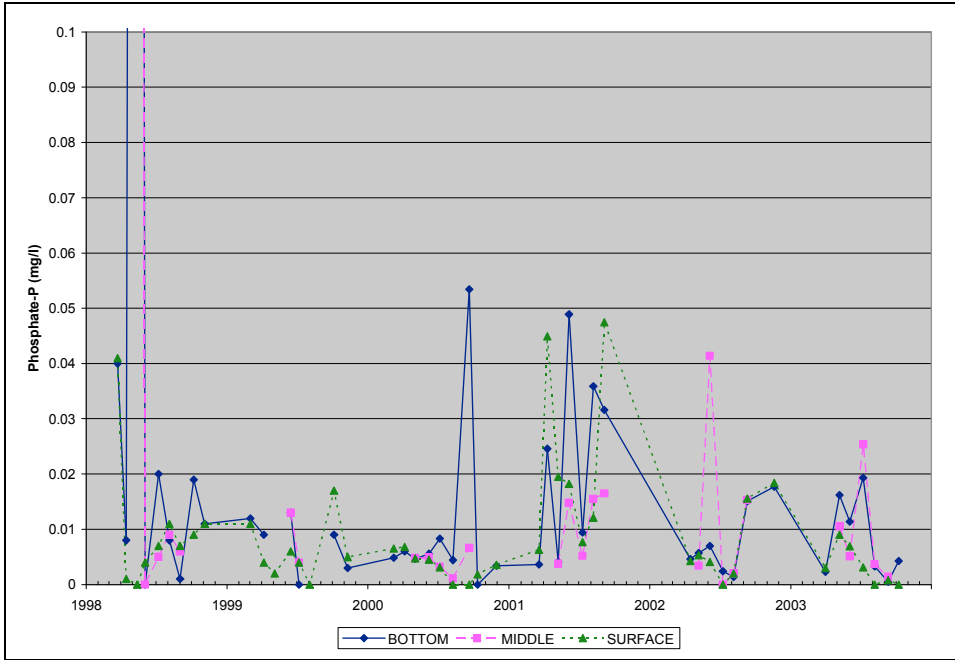


Figure B.22. Observed Phosphate-P Concentrations at RG1, 1998-2003, Rocky Gorge Reservoir

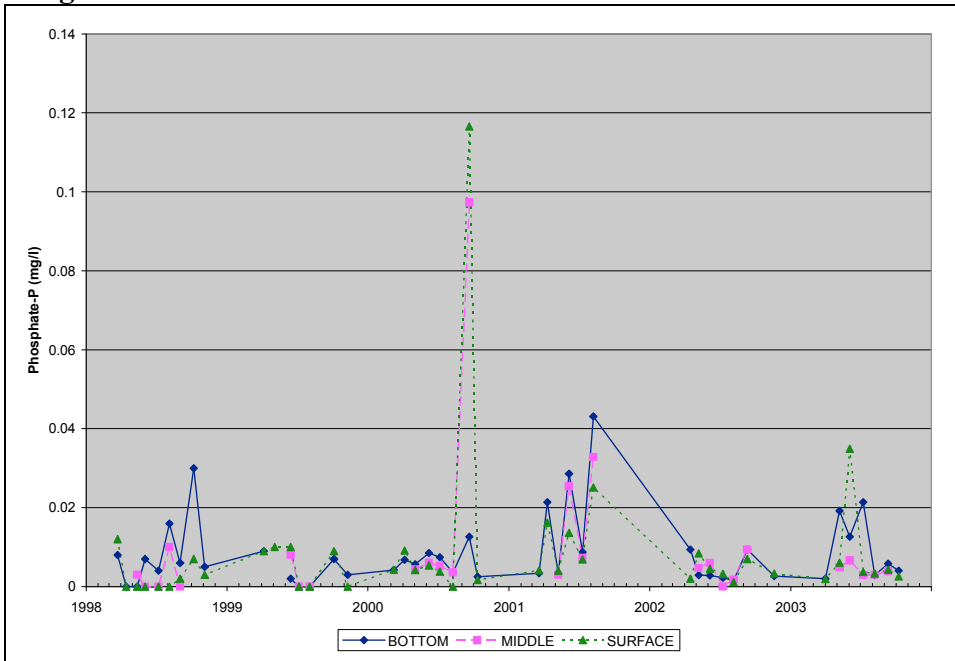


Figure B.23. Observed Phosphate-P Concentrations at RG2, 1998-2003, Rocky Gorge Reservoir

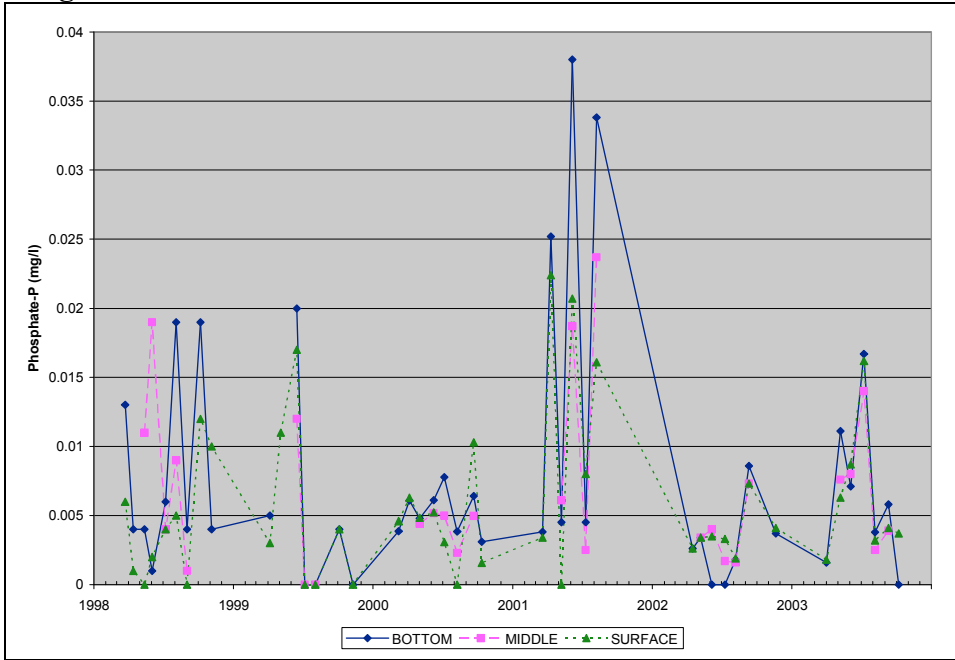


Figure B.24. Observed Phosphate-P Concentrations at RG3, 1998-2003, Rocky Gorge Reservoir

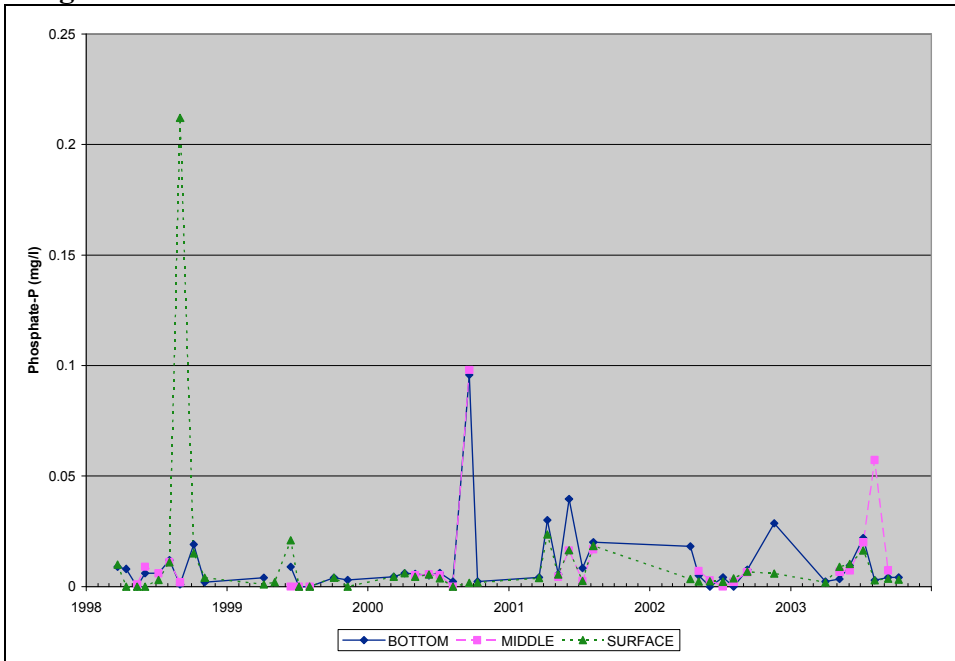


Figure B.25. Observed Phosphate-P Concentrations at MDE Sampling Stations, 2000, Triadelphia Reservoir

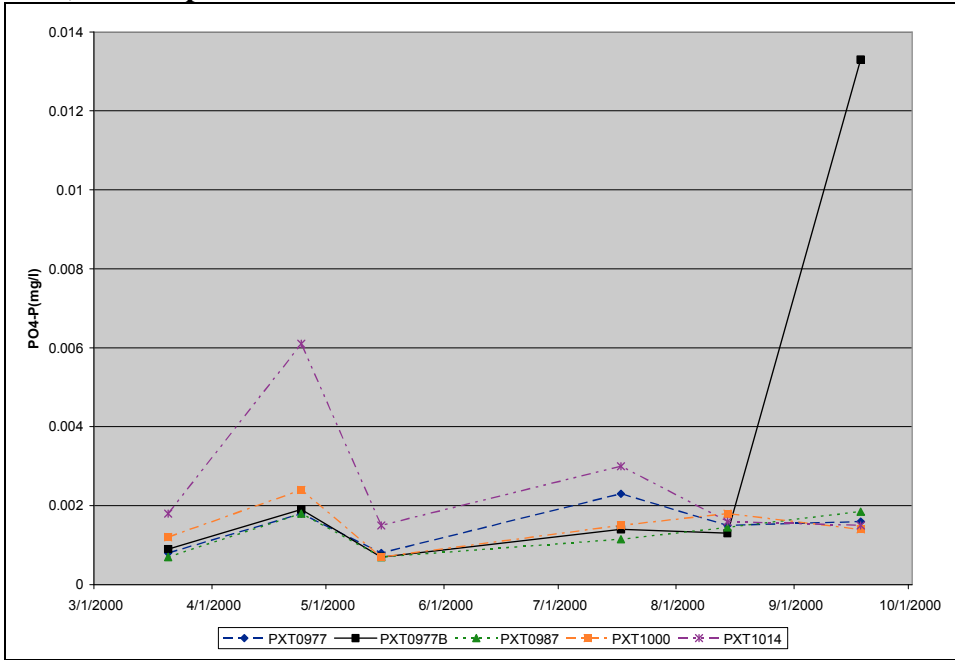


Figure B.26. Observed Phosphate-P Concentrations at MDE Sampling Stations, 2000, Rocky Gorge Reservoir

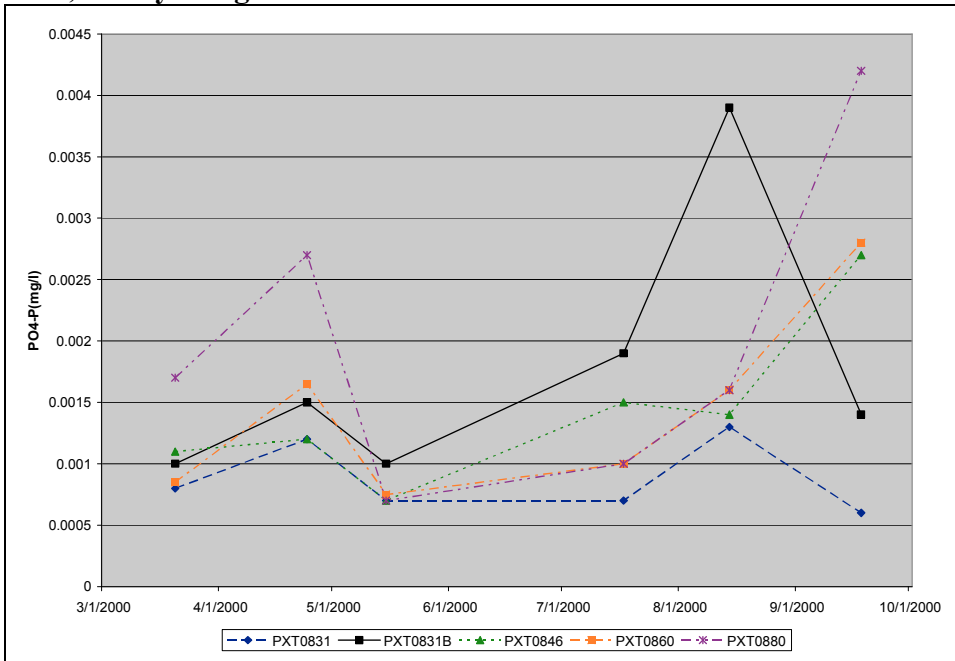


Figure B.27. Observed Ammonia-N Concentrations at TR1, 1998-2003, Triadelphia Reservoir

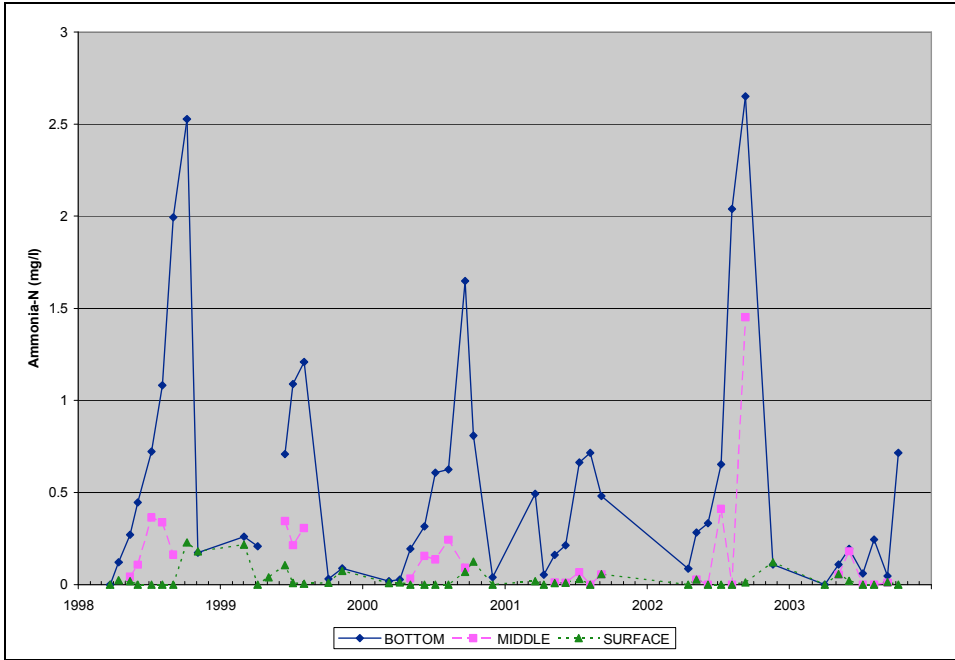


Figure B.28. Observed Ammonia-N Concentrations at TR2, 1998-2003, Triadelphia Reservoir

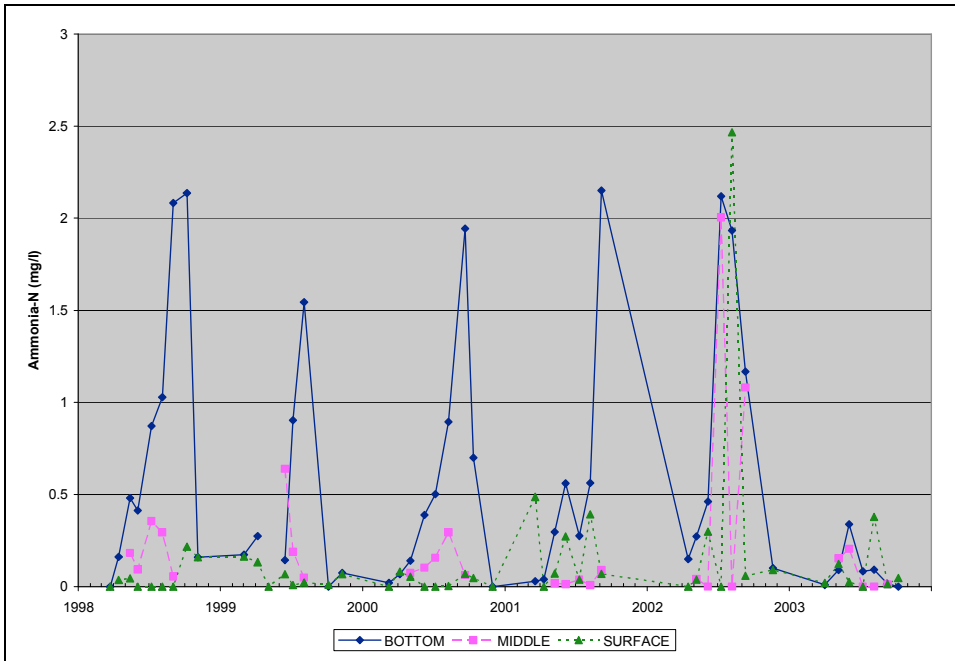


Figure B.29. Observed Ammonia-N Concentrations at TR3, 1998-2003, Triadelphia Reservoir

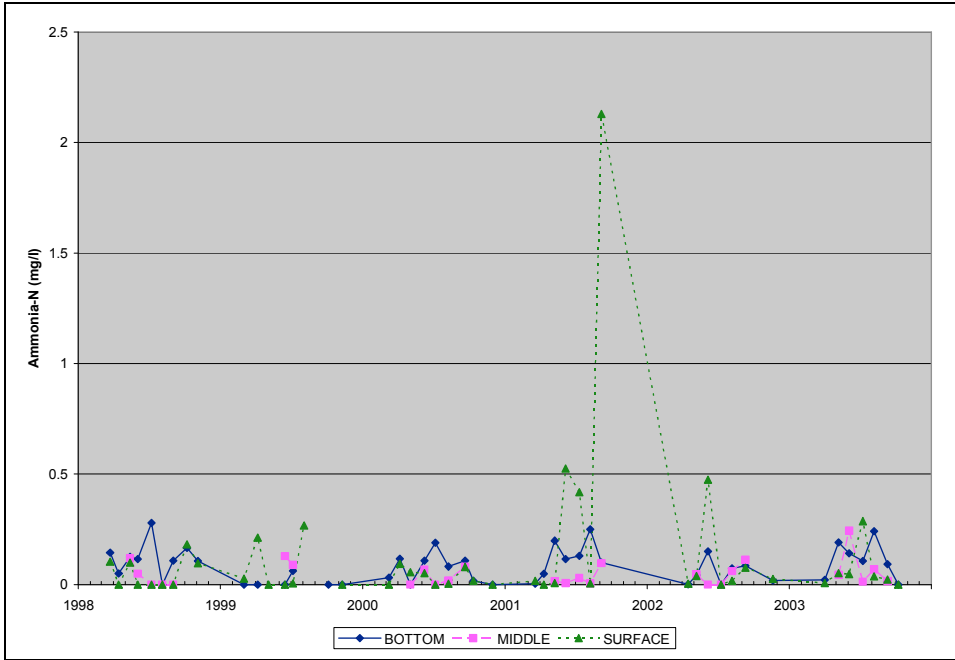


Figure B.30. Observed Ammonia-N Concentrations at RG1, 1998-2003, Rocky Gorge Reservoir

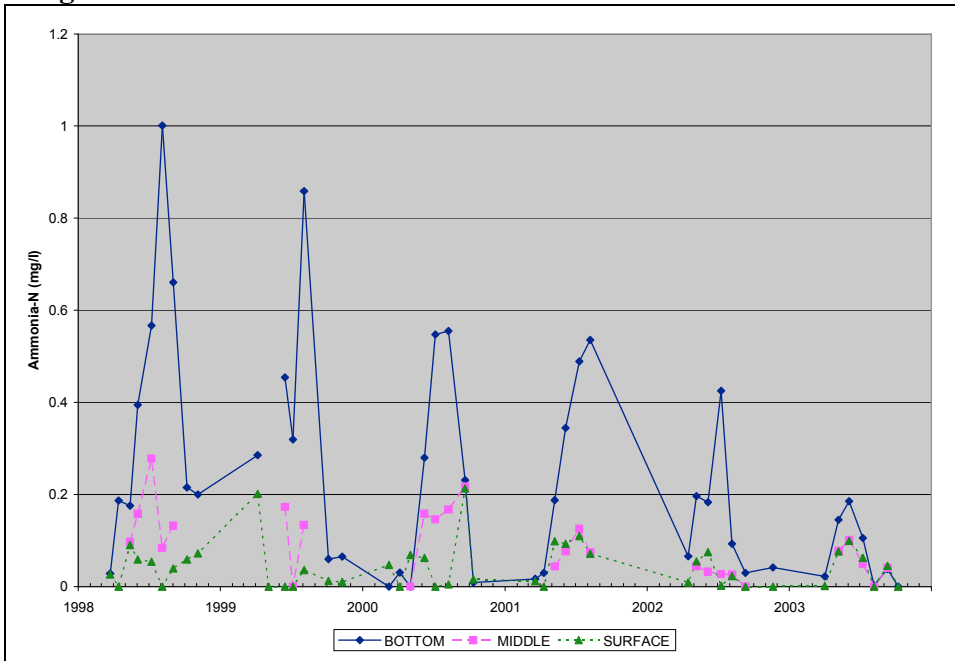


Figure B.33. Observed Ammonia-N Concentrations at MDE Sampling Stations, 2000, Triadelphia Reservoir

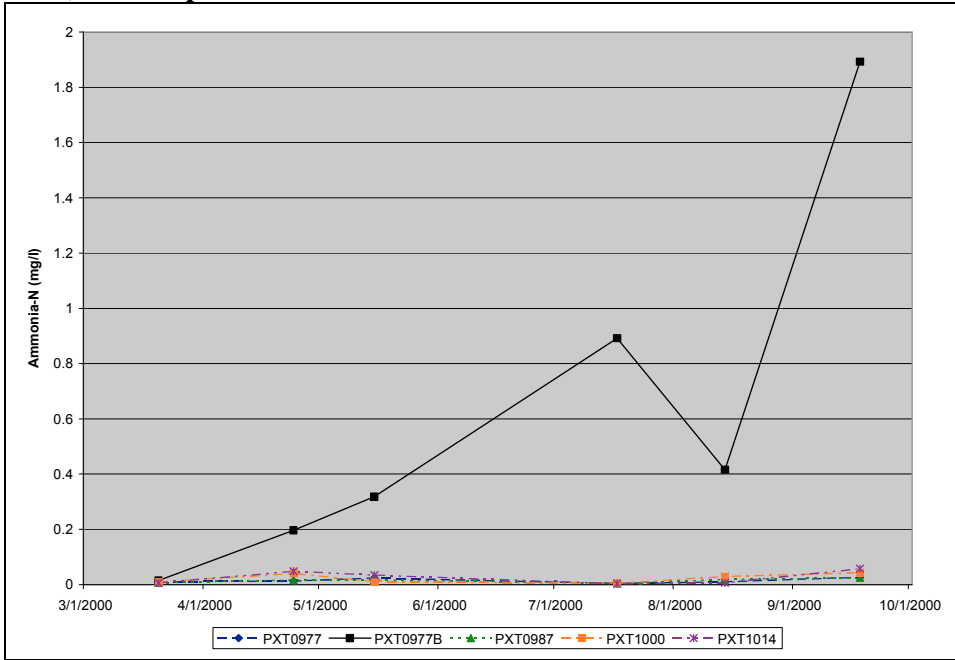


Figure B.34. Observed Ammonia-N Concentrations at MDE Sampling Stations, 2000, Rocky Gorge Reservoir

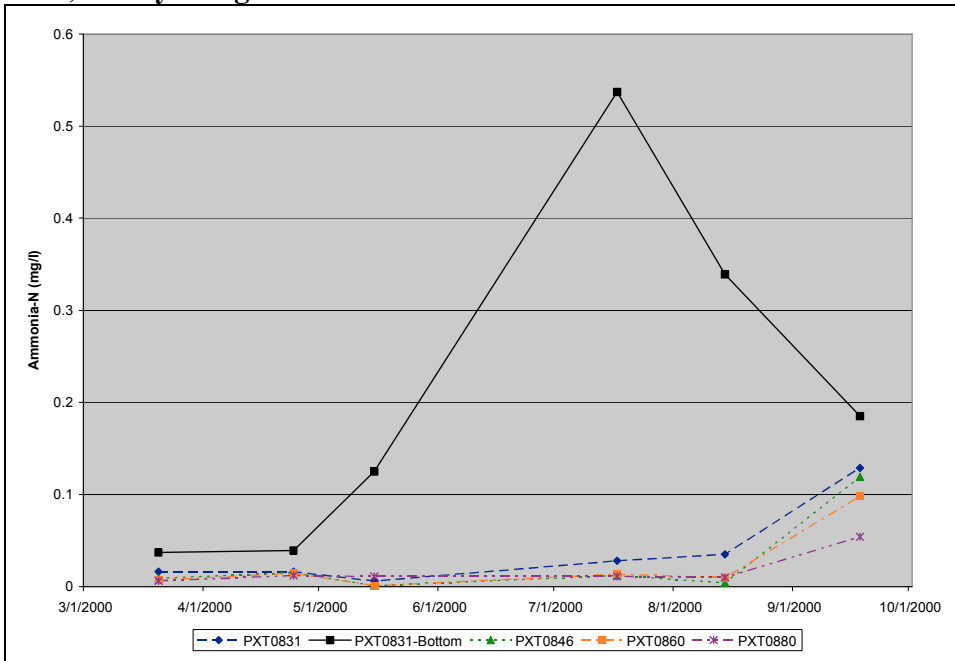


Figure B.35. Observed Nitrate-N Concentrations at TR1, 1998-2003, Triadelphia Reservoir

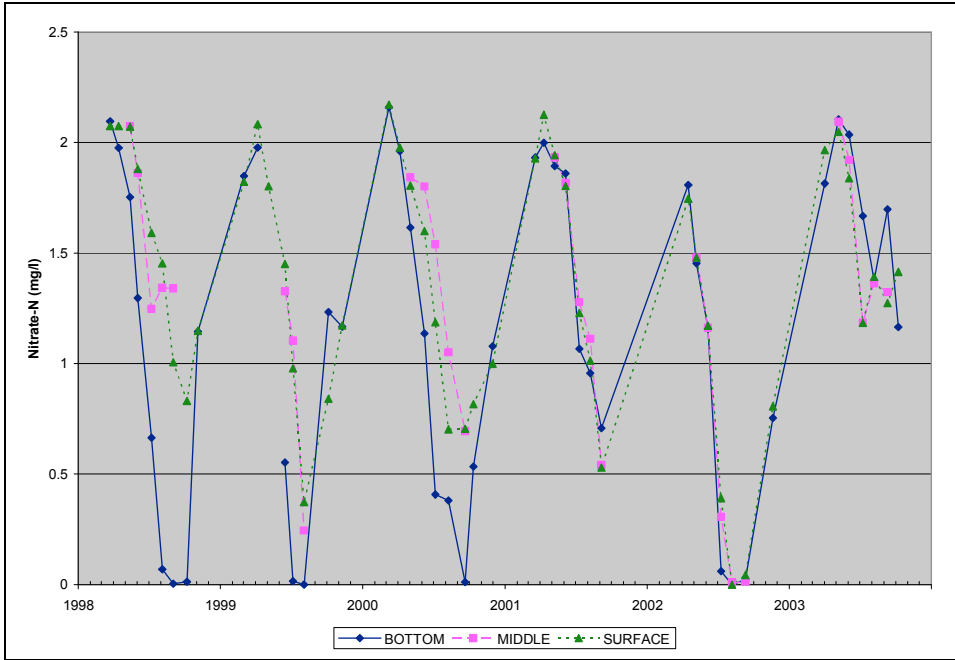


Figure B.36. Observed Nitrate-N Concentrations at TR2, 1998-2003, Triadelphia Reservoir

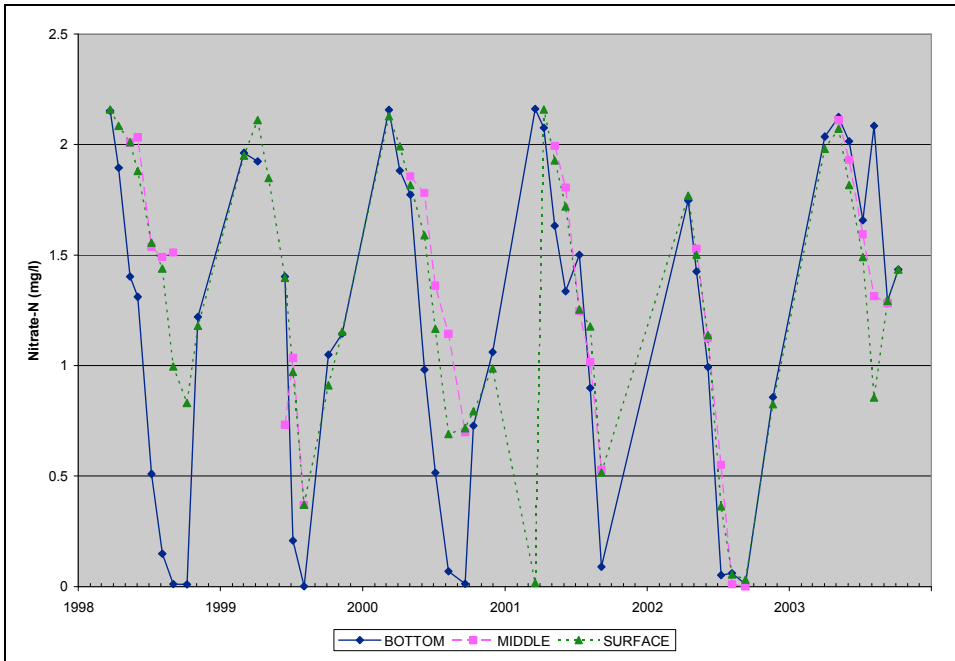


Figure B.37. Observed Nitrate-N Concentrations at TR3, 1998-2003, Triadelphia Reservoir

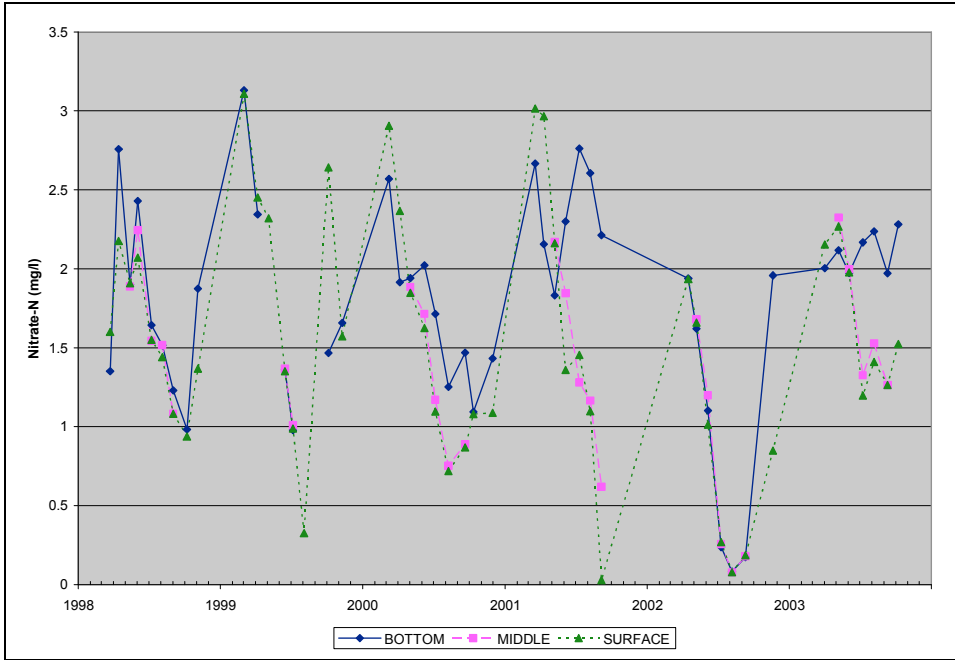


Figure B.38. Observed Nitrate-N Concentrations at RG1, 1998-2003, Rocky Gorge Reservoir

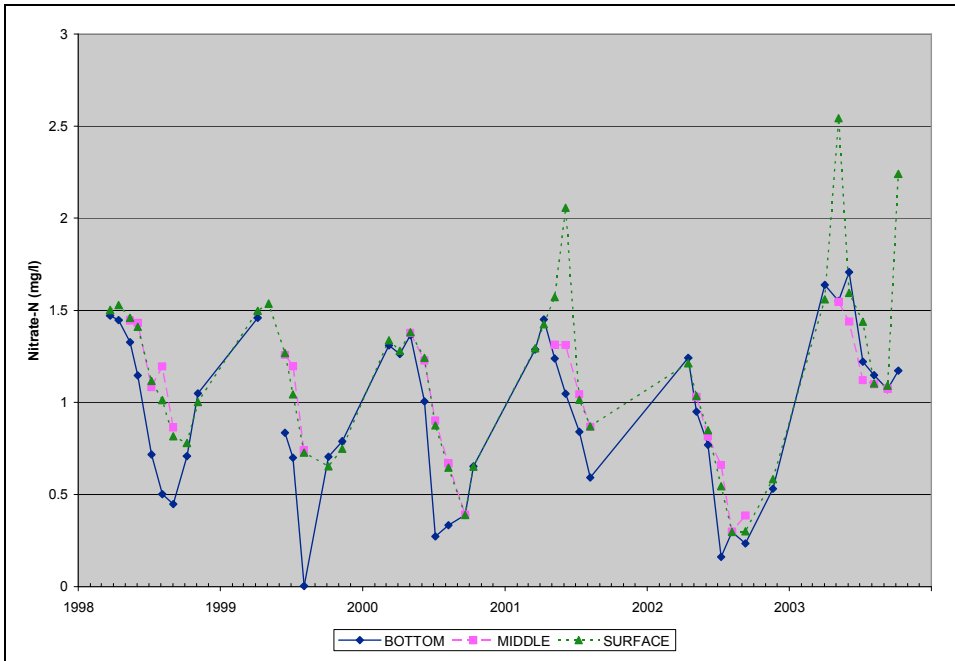


Figure B.39. Observed Nitrate-N Concentrations at RG2, 1998-2003, Rocky Gorge Reservoir

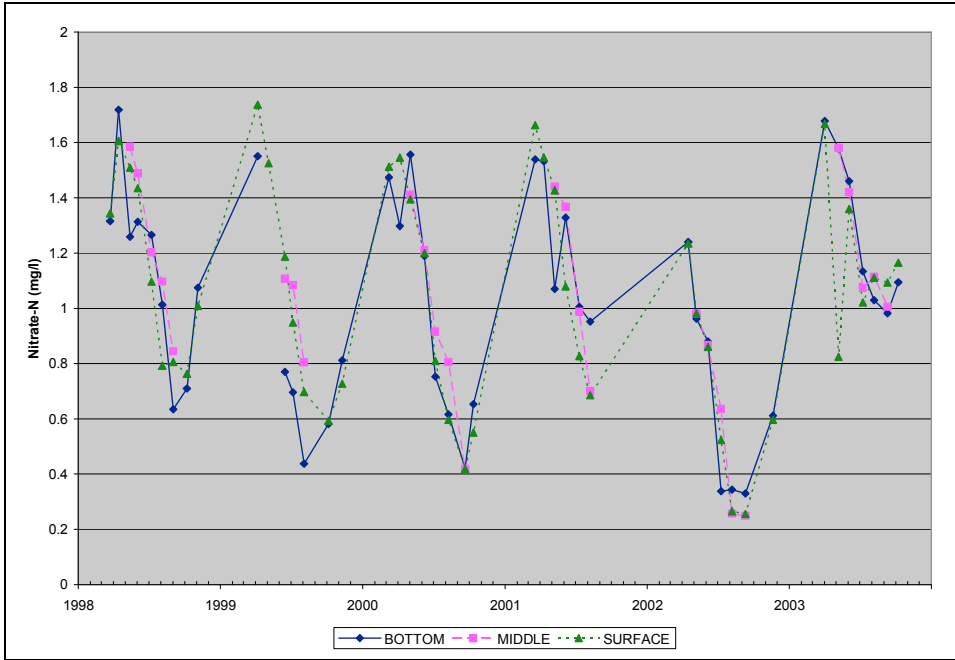


Figure B.40. Observed Nitrate-N Concentrations at RG3, 1998-2003, Rocky Gorge Reservoir

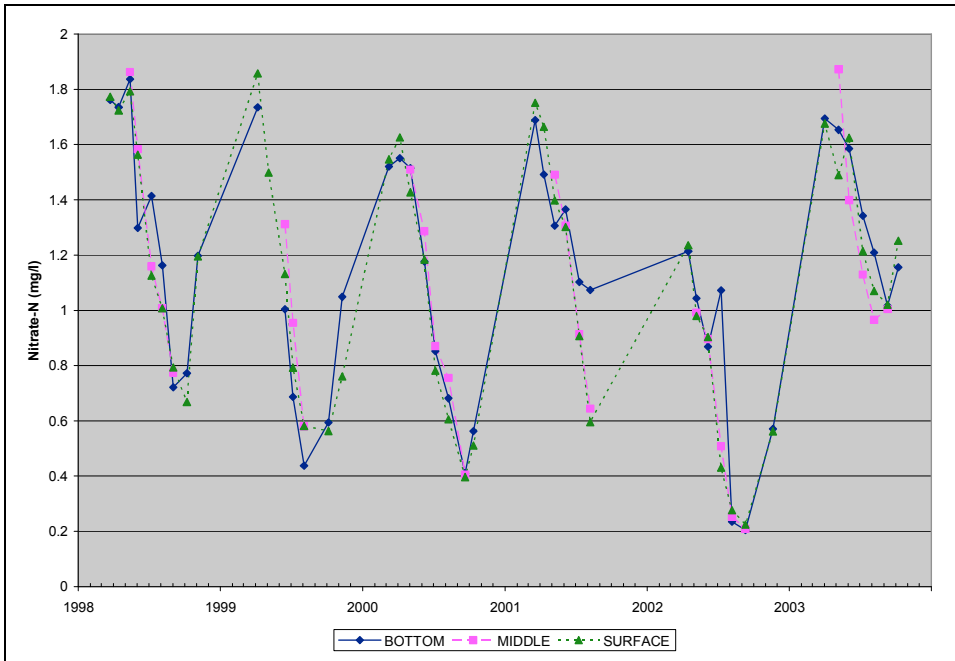


Figure B.41. Observed Nitrate-N Concentrations at MDE Sampling Stations, 2000, Triadelphia Reservoir

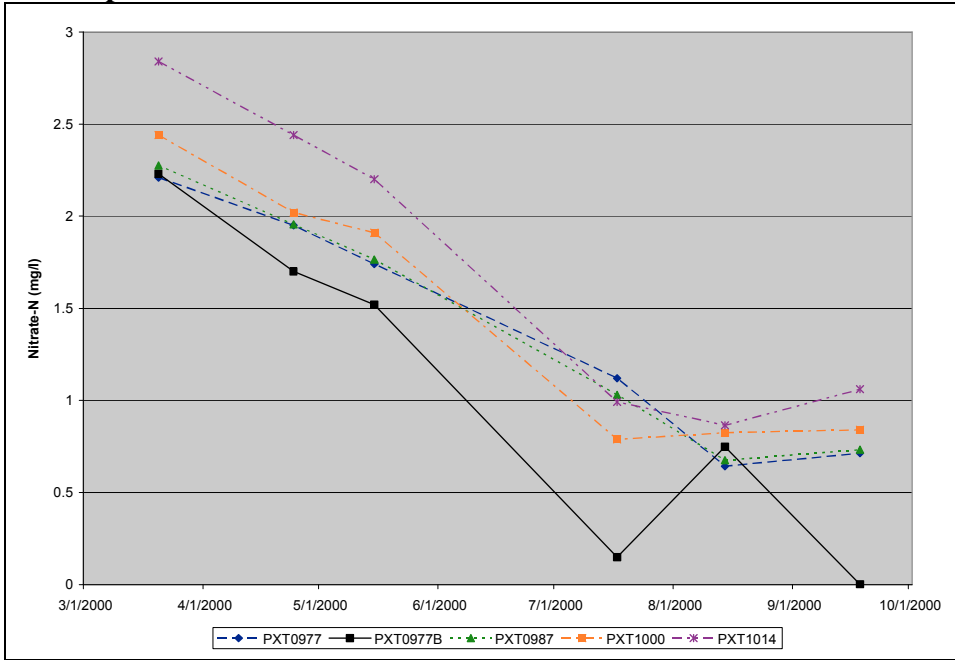


Figure B.42. Observed Nitrate-N Concentrations at MDE Sampling Stations, 2000, Rocky Gorge Reservoir

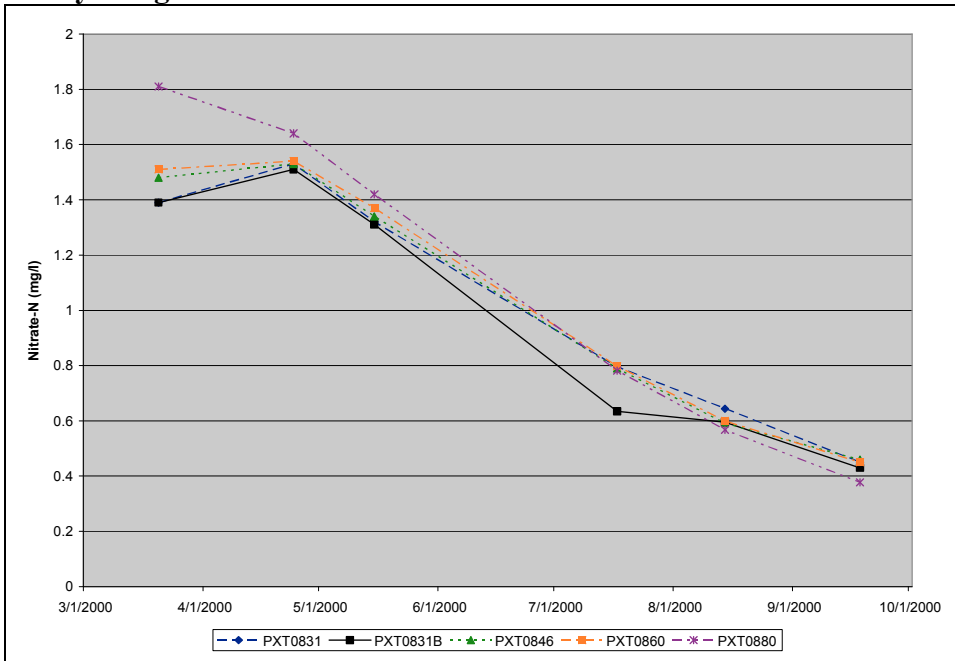


Figure B.43. Observed TN Concentrations at TR1, 1998-2003, Triadelphia Reservoir

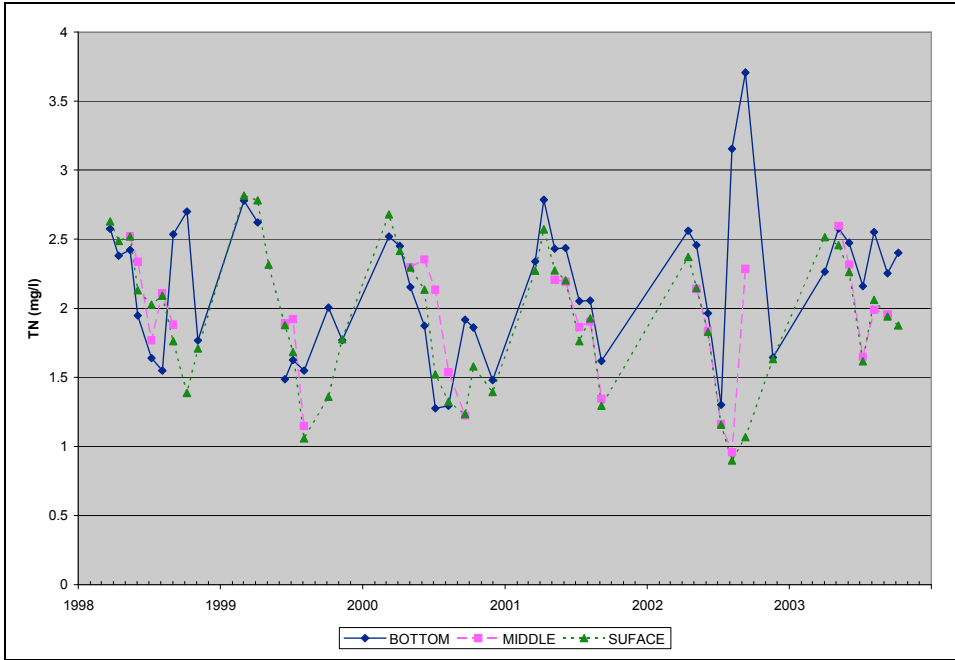


Figure B.44. Observed TN Concentrations at TR2, 1998-2003, Triadelphia Reservoir

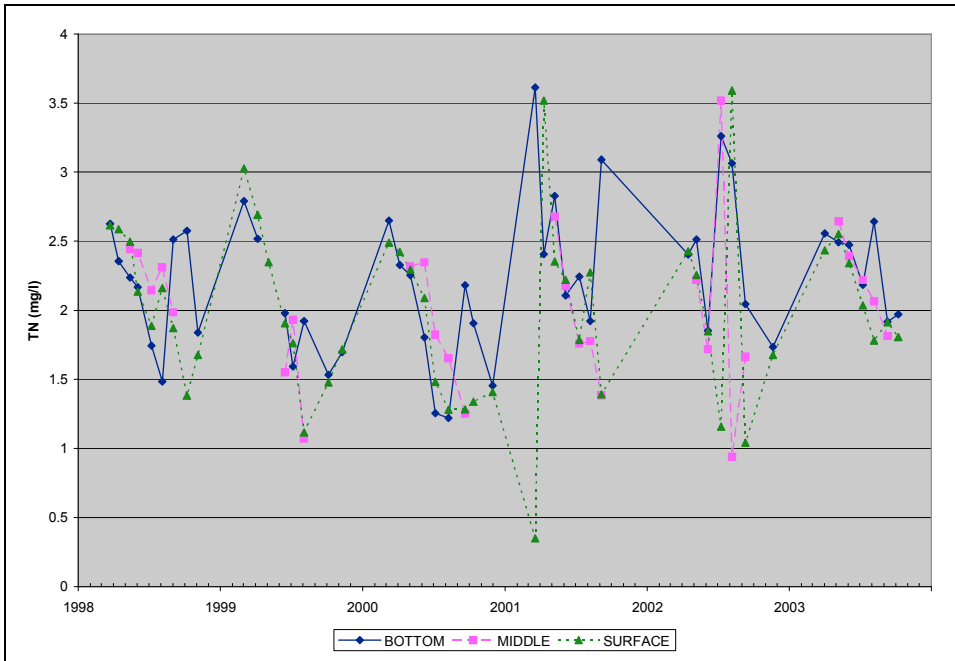


Figure B.47. Observed TN Concentrations at RG2, 1998-2003, Rocky Gorge Reservoir

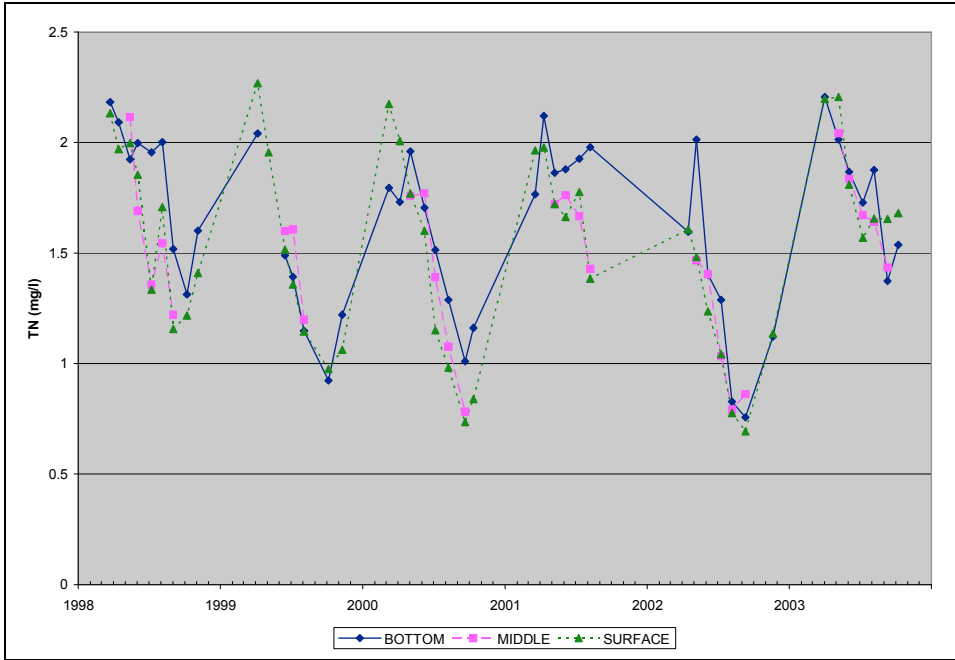


Figure B.48. Observed TN Concentrations at RG3, 1998-2003, Rocky Gorge Reservoir

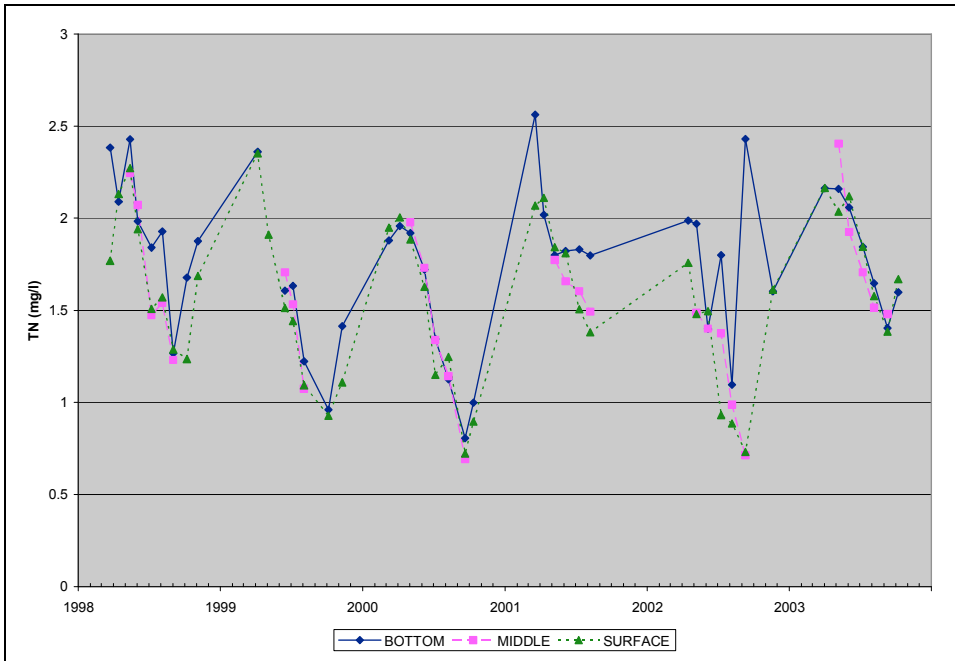


Figure B.49. Observed TN Concentrations at MDE Sampling Stations, 2000, Triadelphia Reservoir

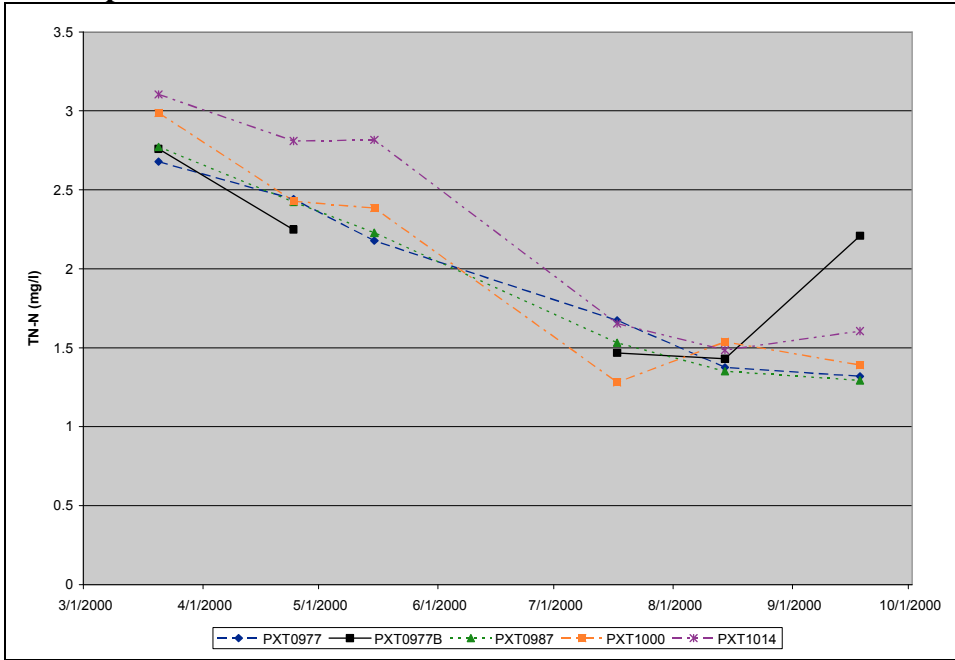


Figure B.50. Observed TN Concentrations at MDE Sampling Stations, 2000, Rocky Gorge Reservoir

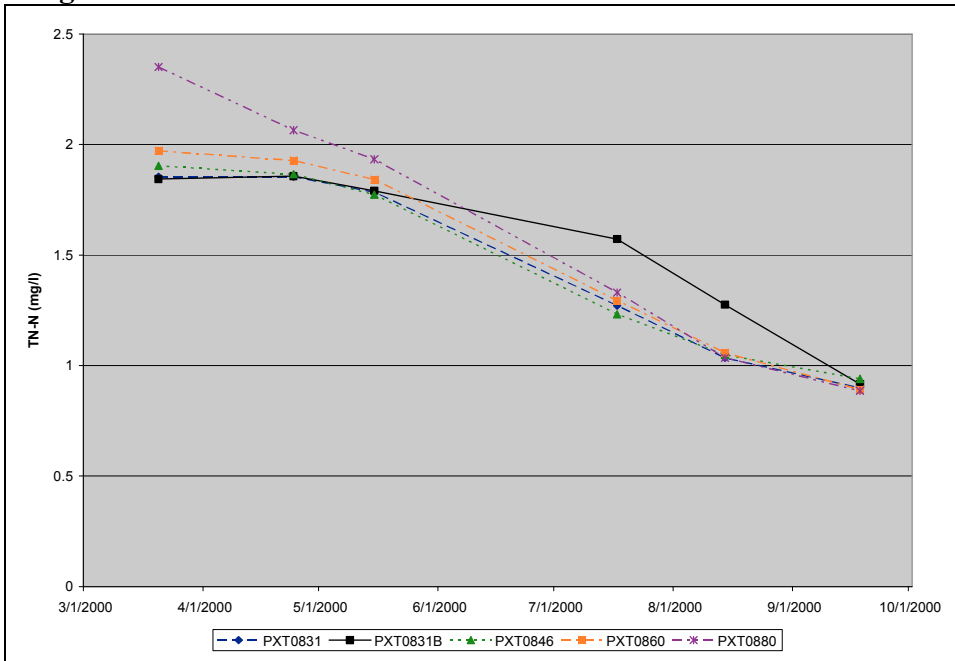


Figure B.51. Observed Chlorophyll *a* Concentrations at WSSC Sampling Stations, 1998-2003, Triadelphia Reservoir

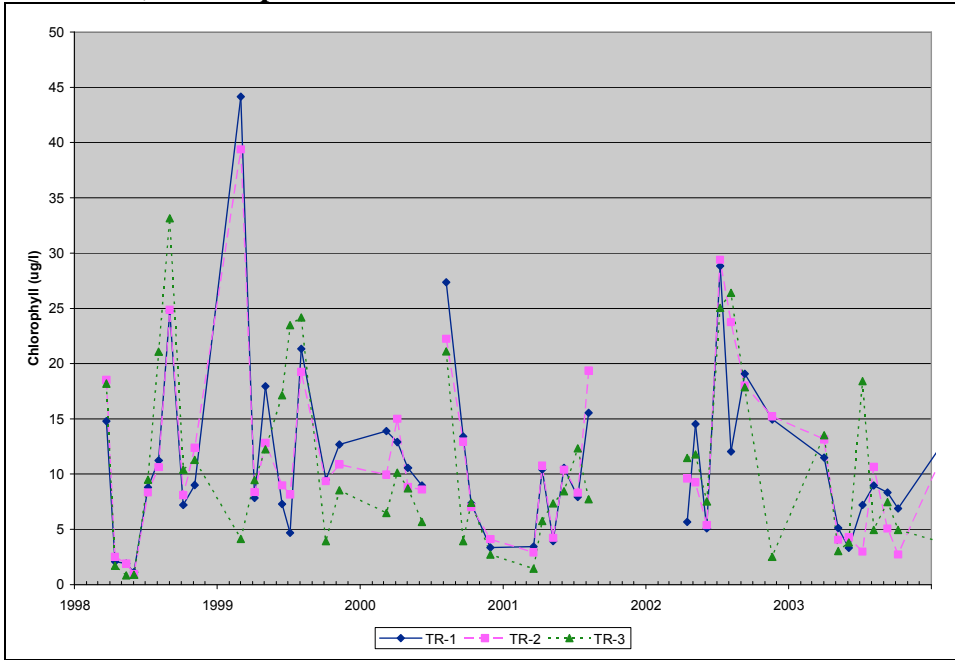


Figure B.52. Observed Chlorophyll *a* Concentrations at WSSC Sampling Stations, 1998-2003, Rocky Gorge Reservoir

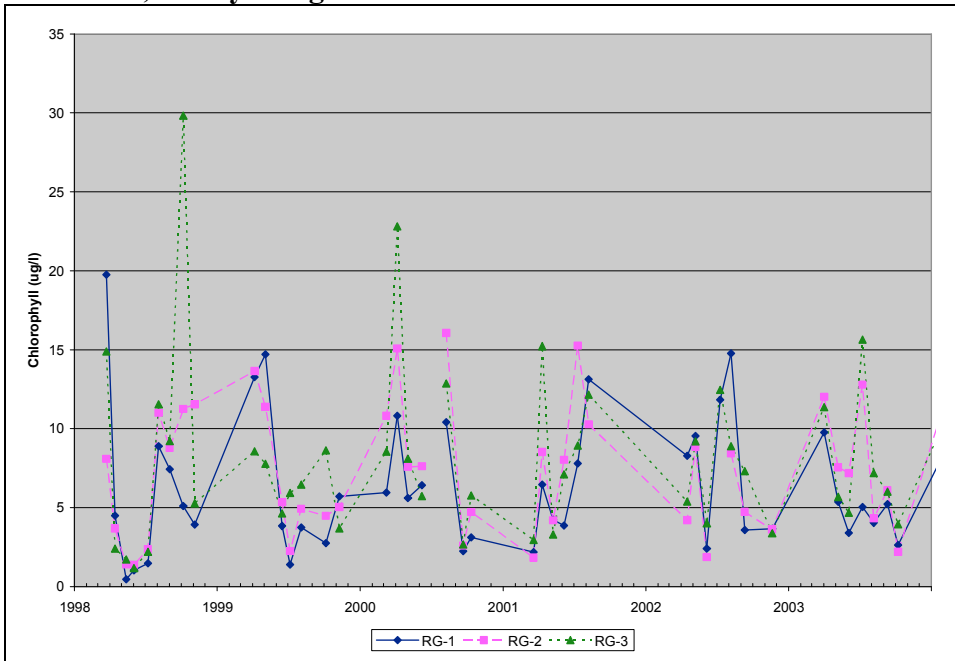


Figure B.53. Observed Chlorophyll *a* Concentrations at MDE Sampling Stations, 2000, Triadelphia Reservoir

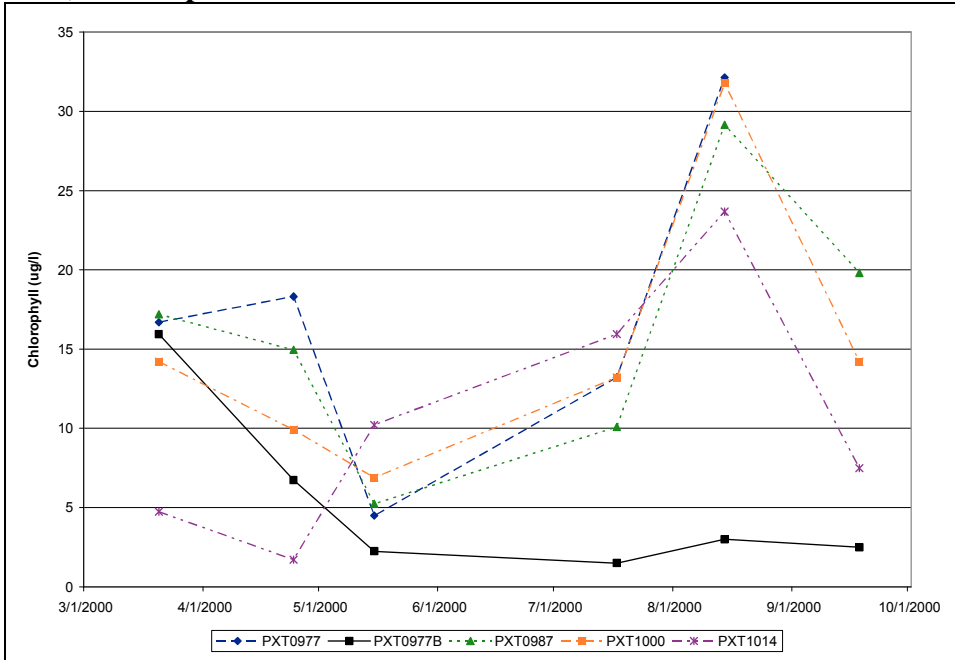
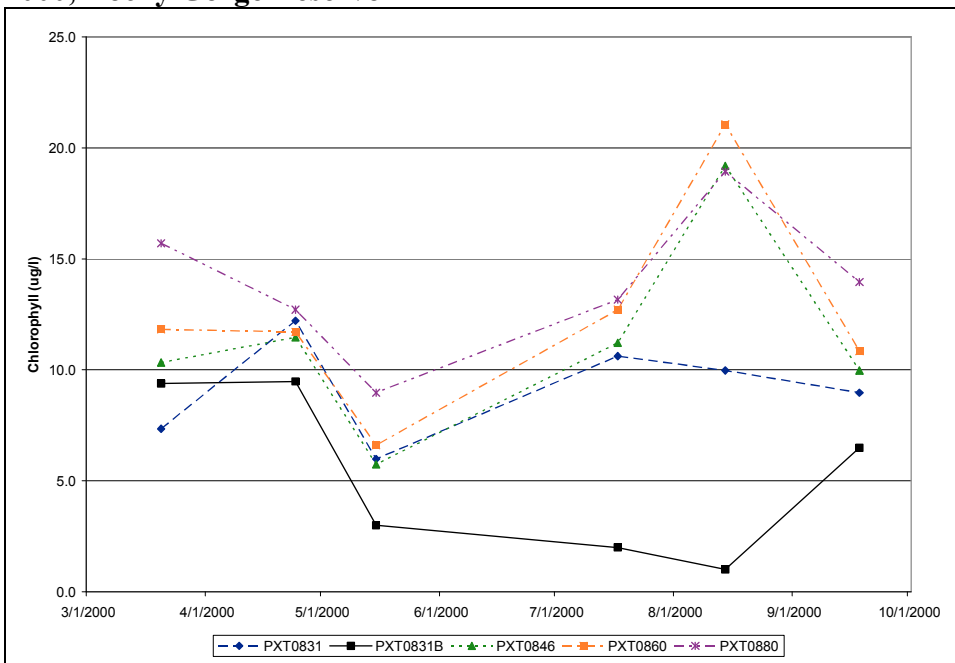


Figure B.54. Observed Chlorophyll *a* Concentrations at MDE Sampling Stations, 2000, Rocky Gorge Reservoir



APPENDIX C

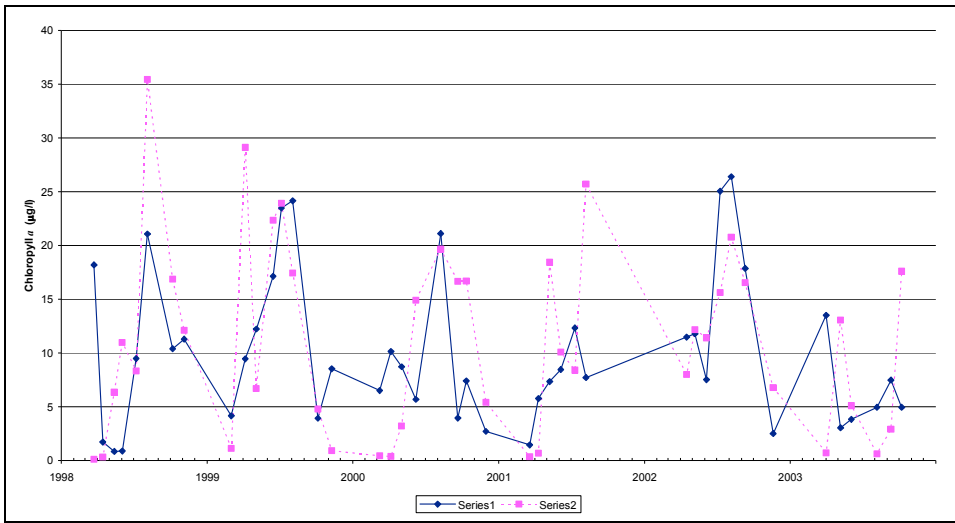


Figure C3. Observed and Simulated Max Chla Concentrations, TR3, Calibration Scenario, Triadelphia Reservoir

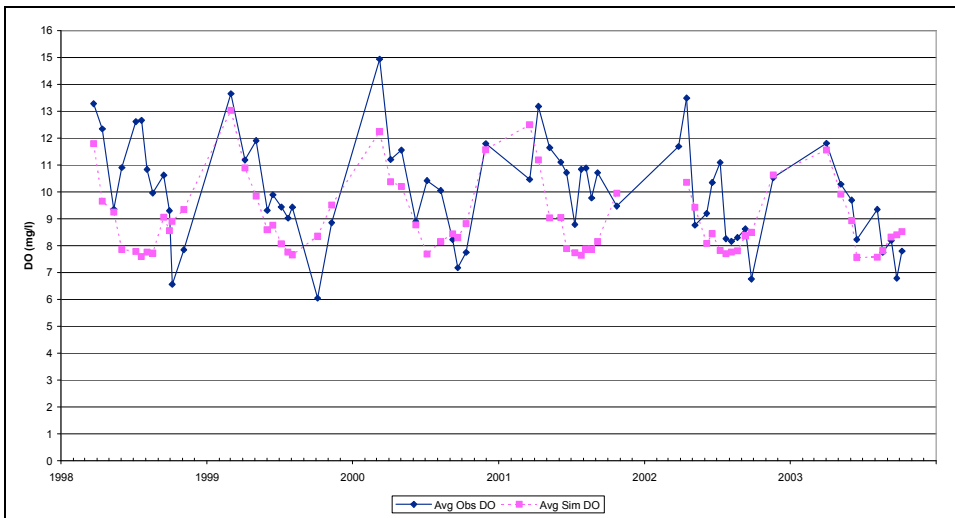


Figure C4. Observed and Simulated Average Surface DO Concentrations, TR2, Calibration Scenario, Triadelphia Reservoir.

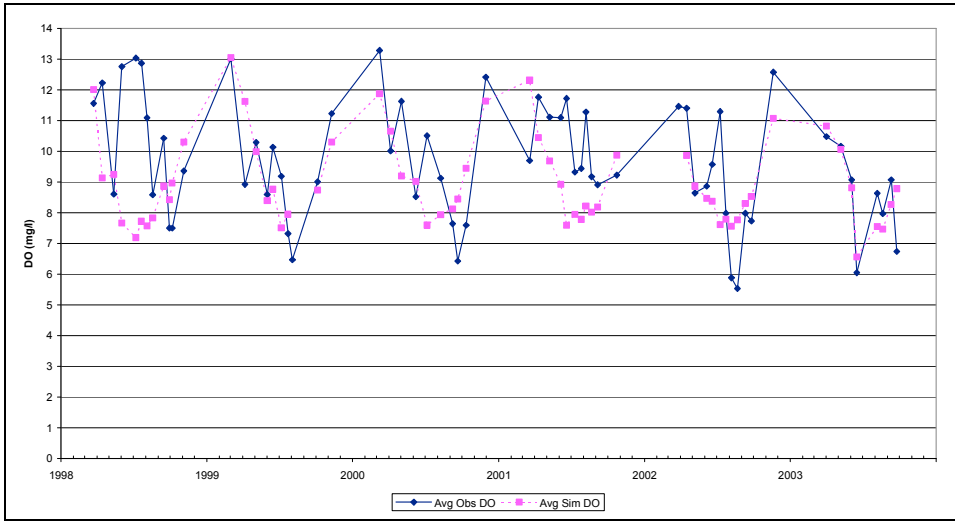


Figure C5. Observed and Simulated Average Surface DO Concentrations, TR3, Calibration Scenario, Triadelphia Reservoir

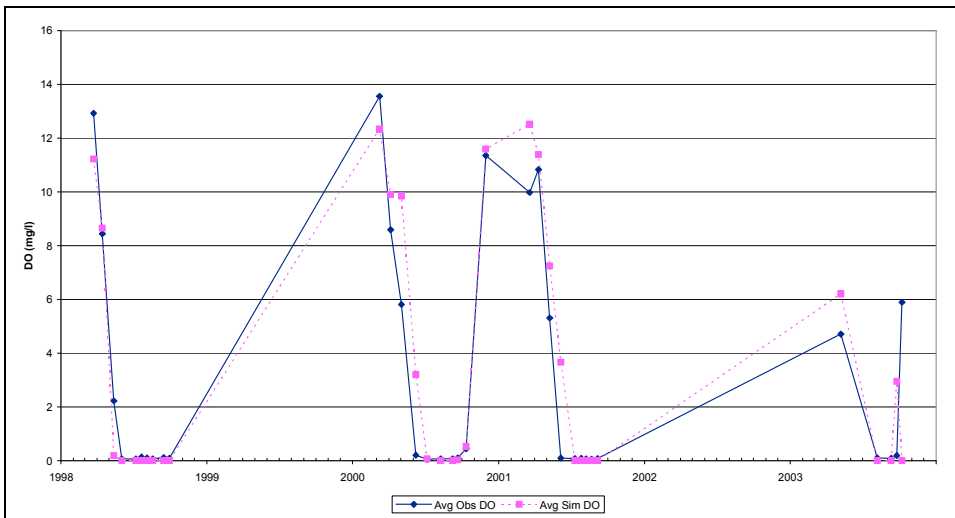


Figure C6. Observed and Simulated Average Bottom DO Concentrations, TR2, Calibration Scenario, Triadelphia Reservoir

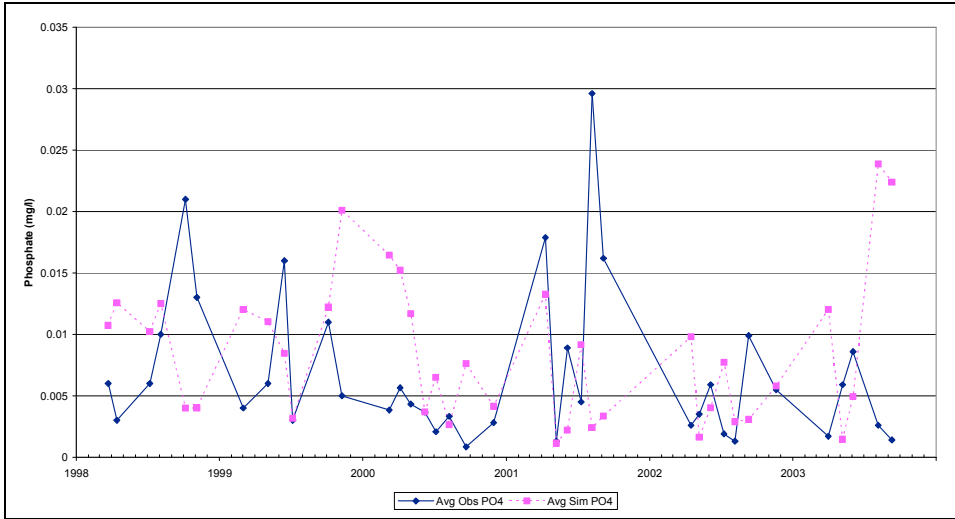


Figure C7. Observed and Simulated Average Surface Phosphate Concentrations, TR1, Calibration Scenario, Triadelphia Reservoir.

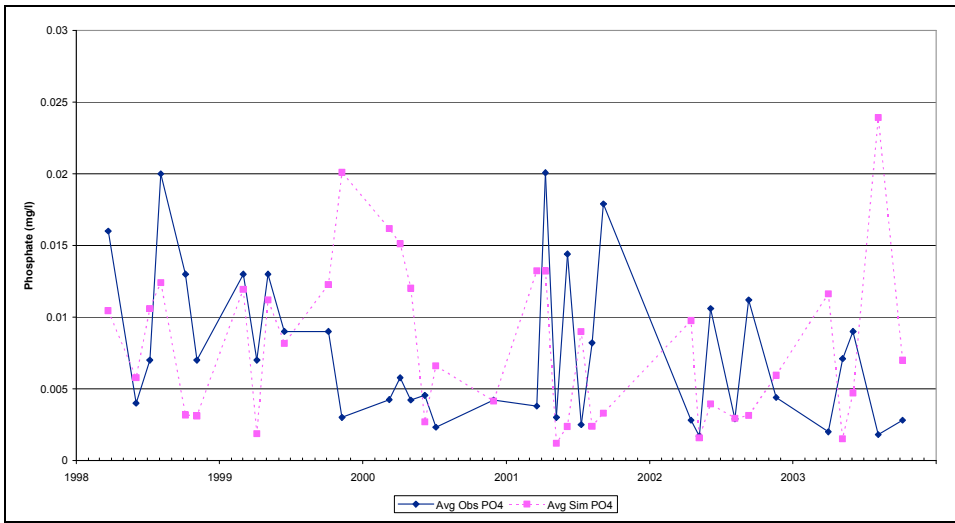


Figure C8. Observed and Simulated Average Surface Phosphate Concentrations, TR2, Calibration Scenario, Triadelphia Reservoir.

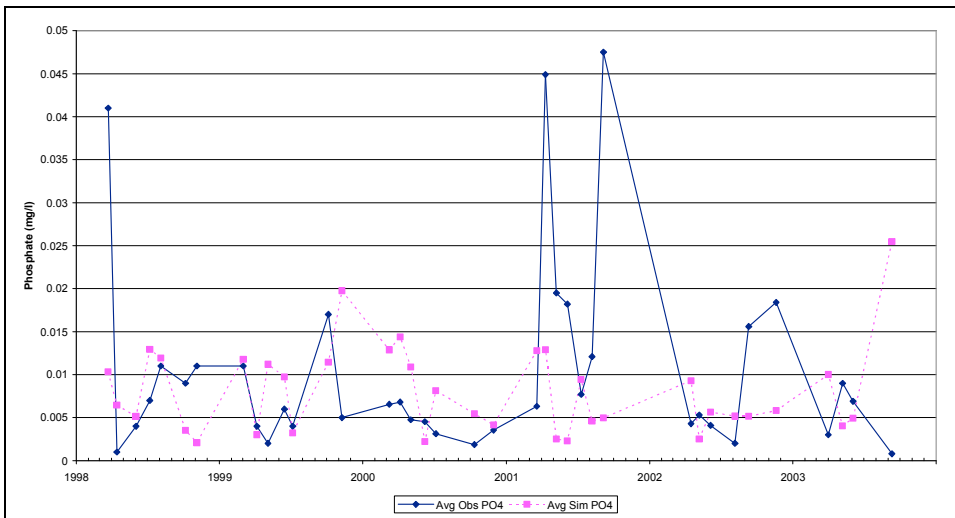


Figure C9. Observed and Simulated Average Surface Phosphate Concentrations, TR3, Calibration Scenario, Triadelphia Reservoir.

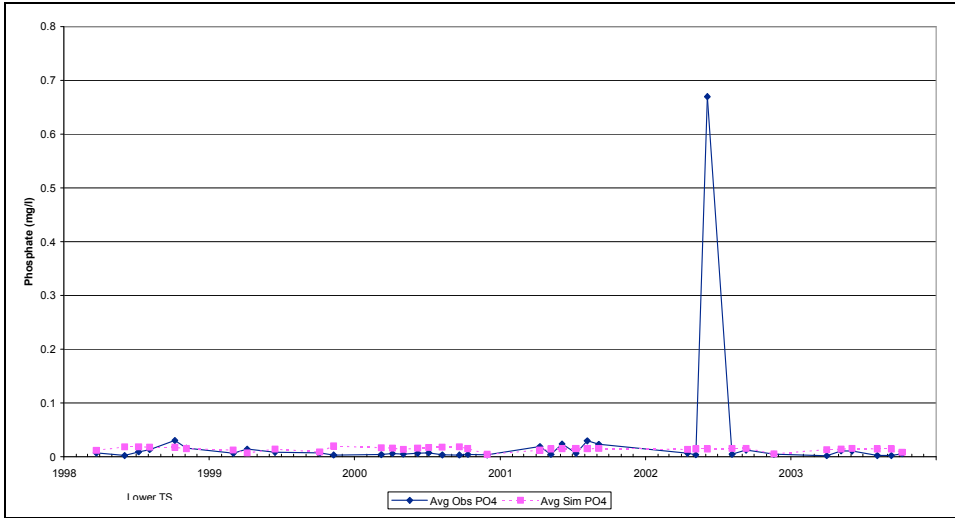


Figure C10. Observed and Simulated Average Bottom Phosphate Concentrations, TR1, Calibration Scenario, Triadelphia Reservoir

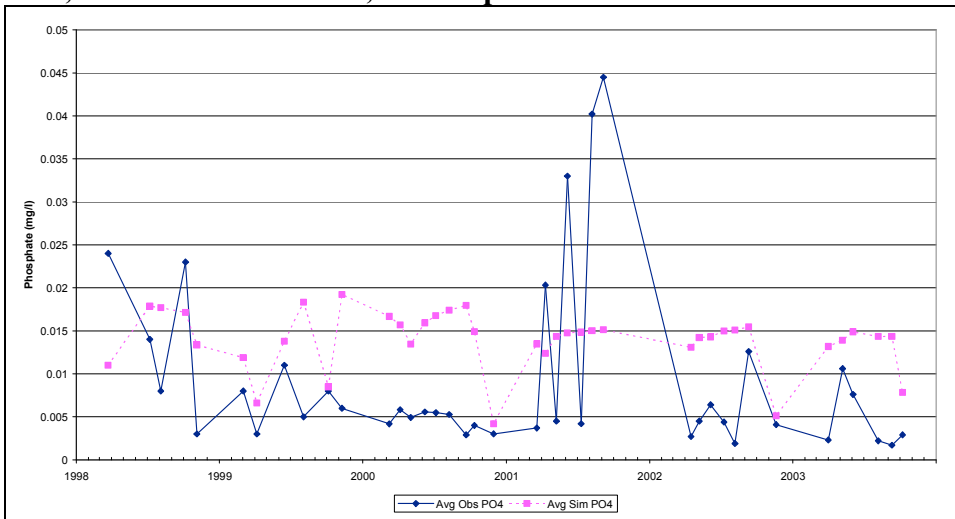


Figure C11. Observed and Simulated Average Bottom Phosphate Concentrations, TR2, Calibration Scenario, Triadelphia Reservoir

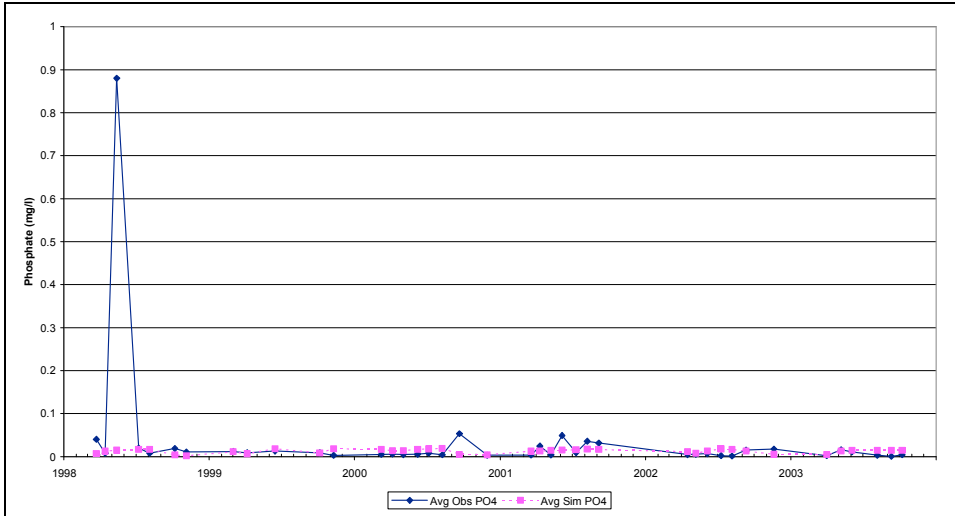


Figure C12. Observed and Simulated Average Bottom Phosphate Concentrations, TR3, Calibration Scenario, Triadelphia Reservoir

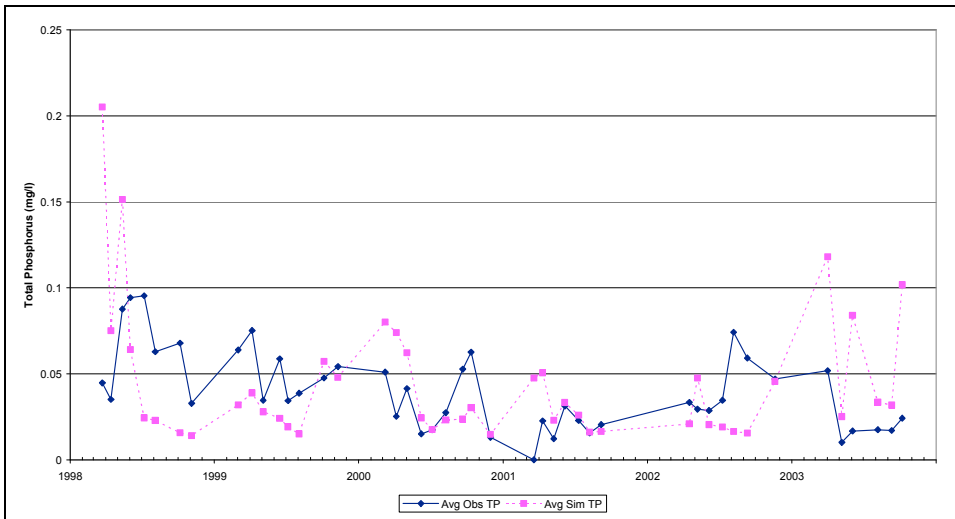


Figure C13. Observed and Simulated Average Surface Total Phosphorus Concentrations, TR1, Calibration Scenario, Triadelphia Reservoir.

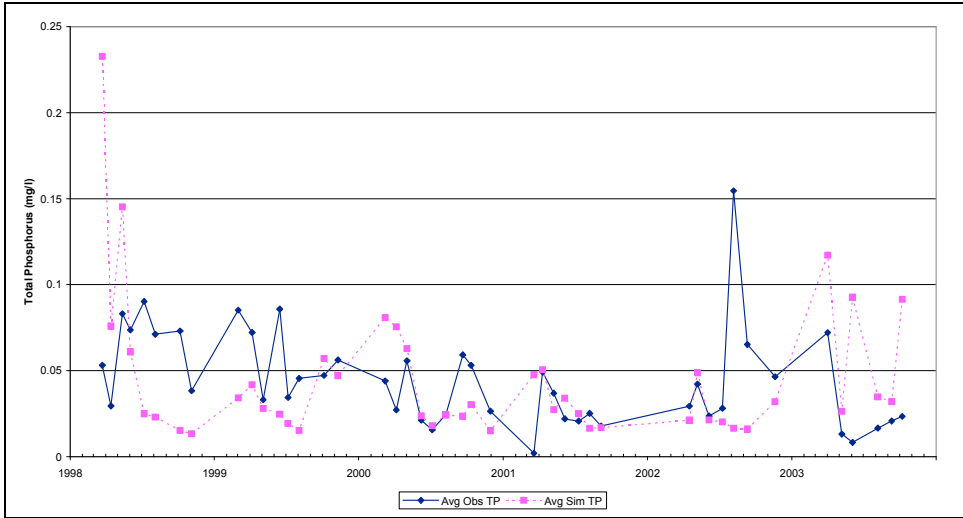


Figure C14. Observed and Simulated Average Surface Total Phosphorus Concentrations, TR2, Calibration Scenario, Triadelphia Reservoir.

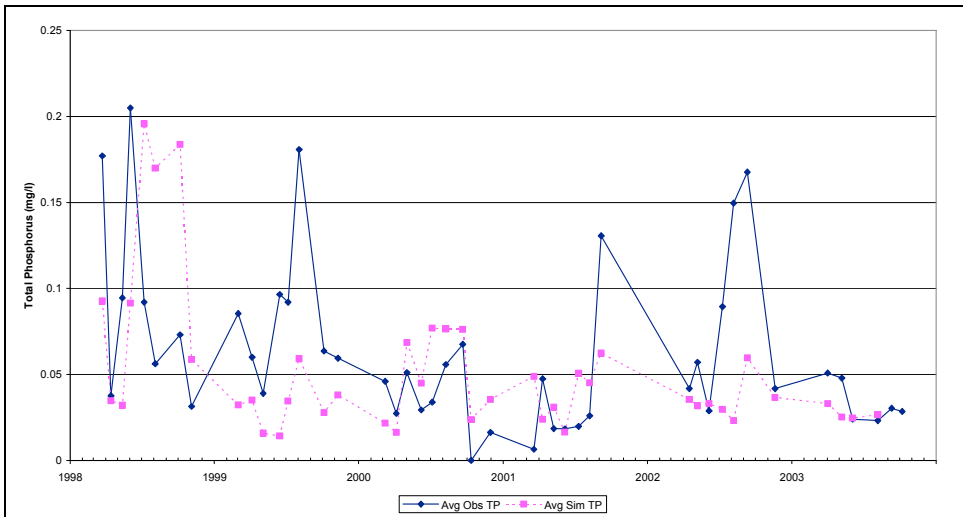


Figure C15. Observed and Simulated Average Surface Total Phosphorus Concentrations, TR3, Calibration Scenario, Triadelphia Reservoir.

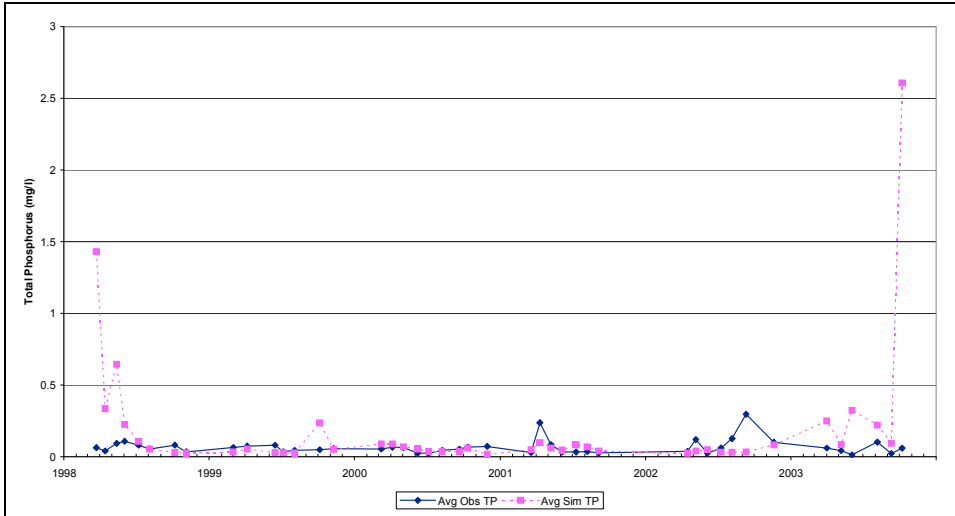


Figure C16. Observed and Simulated Average Bottom Total Phosphorus Concentrations, TR1, Calibration Scenario, Triadelphia Reservoir.

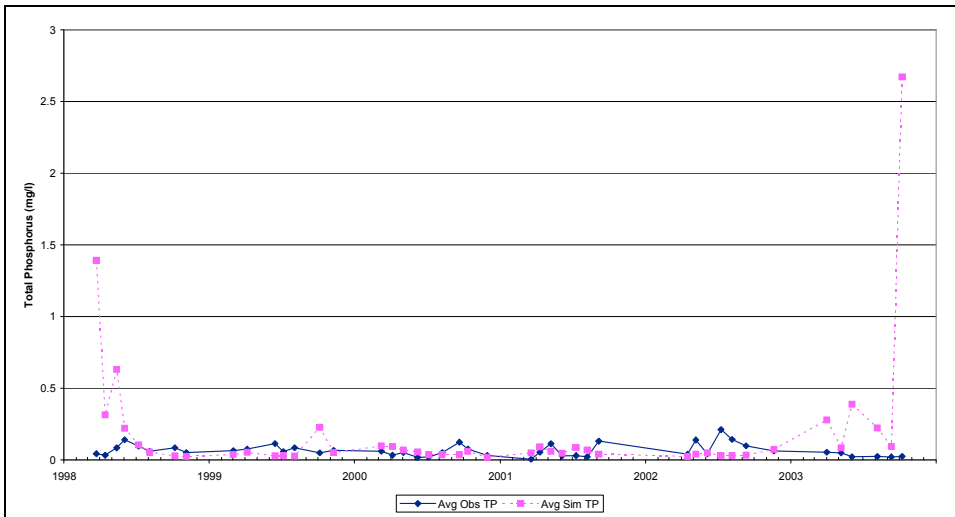


Figure C17. Observed and Simulated Average Bottom Total Phosphorus Concentrations, TR2, Calibration Scenario, Triadelphia Reservoir.

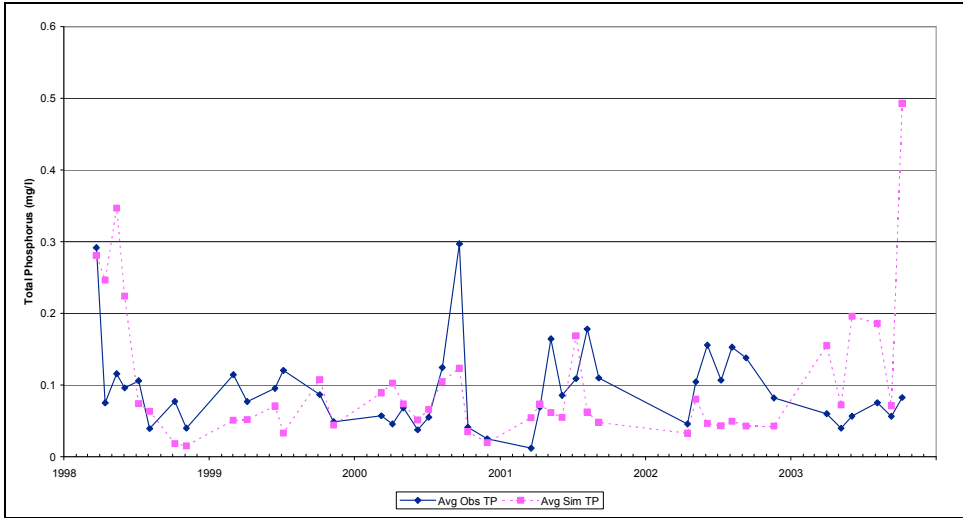


Figure C18. Observed and Simulated Average Bottom Total Phosphorus Concentrations, TR3, Calibration Scenario, Triadelphia Reservoir.

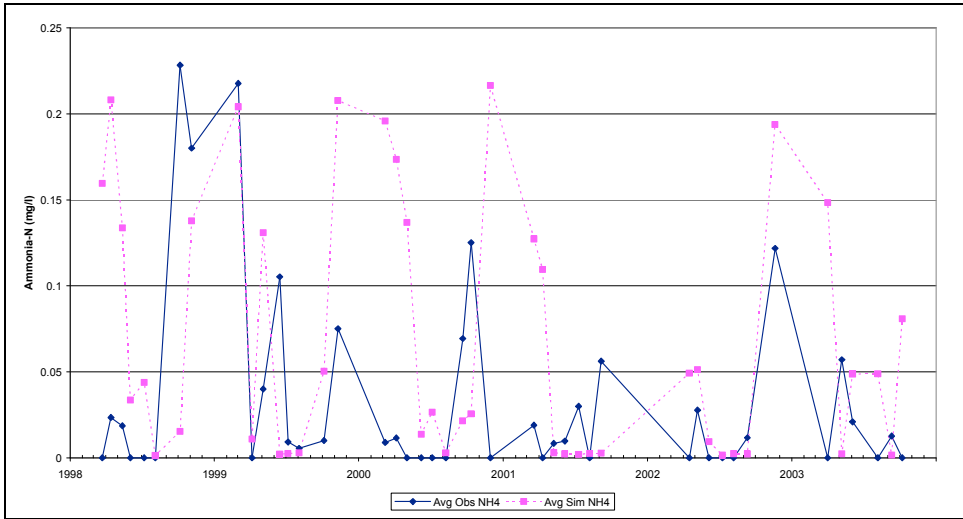


Figure C19. Observed and Simulated Average Surface Ammonia Concentrations, TR1, Calibration Scenario, Triadelphia Reservoir.

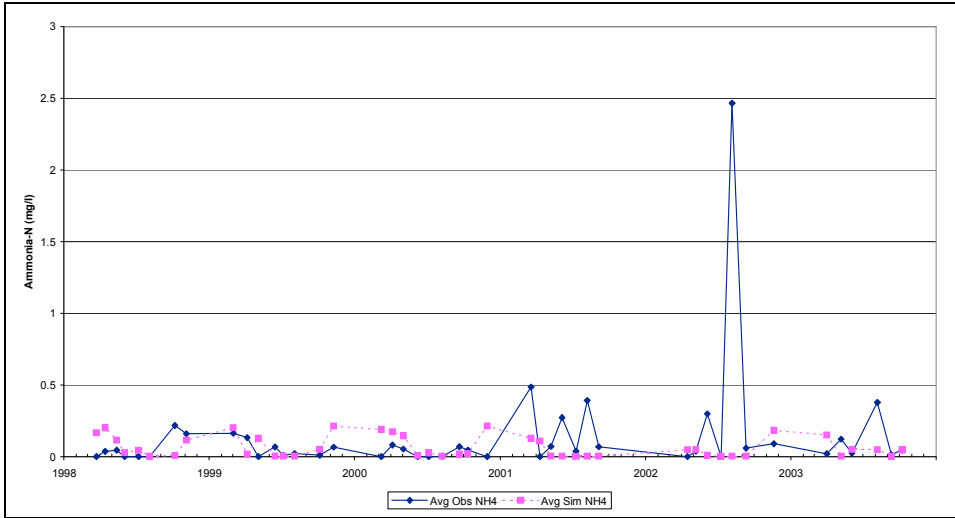


Figure C20. Observed and Simulated Average Surface Ammonia Concentrations, TR2, Calibration Scenario, Triadelphia Reservoir.

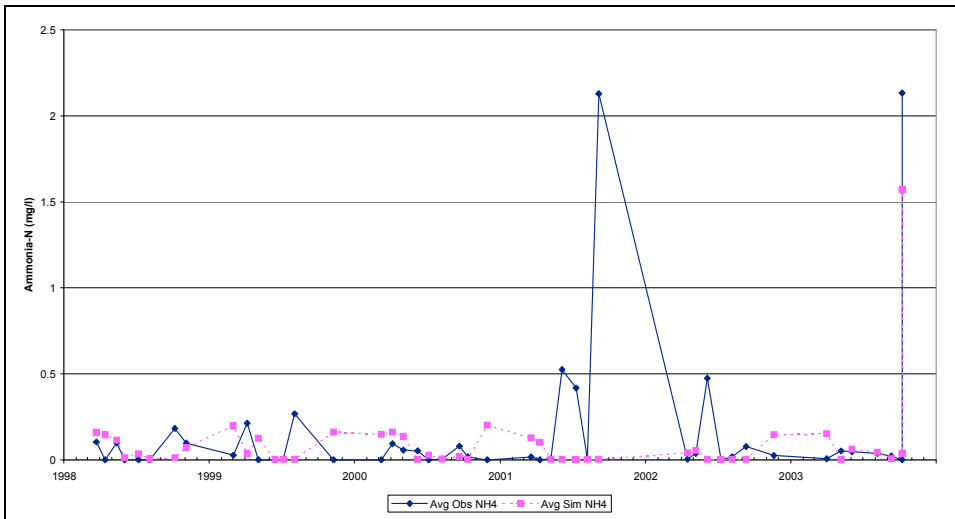


Figure C21. Observed and Simulated Average Surface Ammonia Concentrations, TR3, Calibration Scenario, Triadelphia Reservoir.

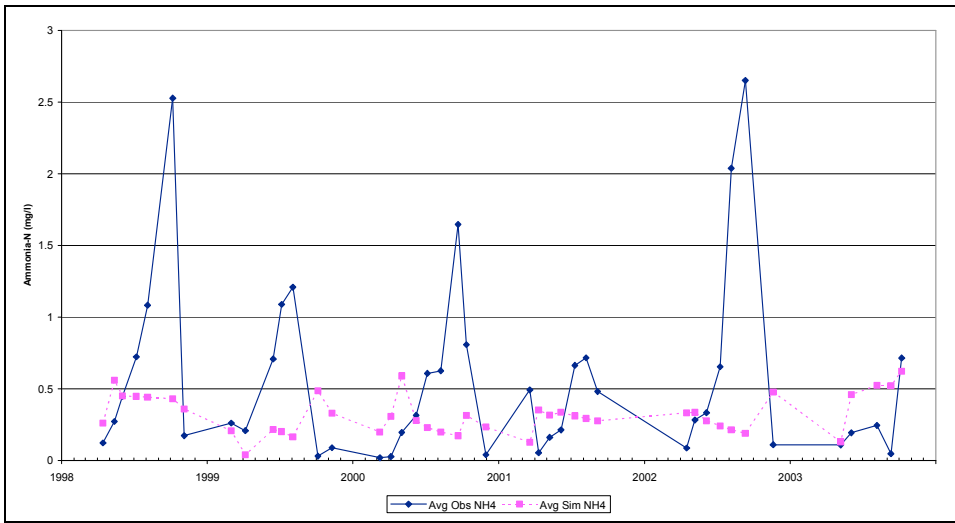


Figure C22. Observed and Simulated Average Bottom Ammonia Concentrations, TR1, Calibration Scenario, Triadelphia Reservoir.

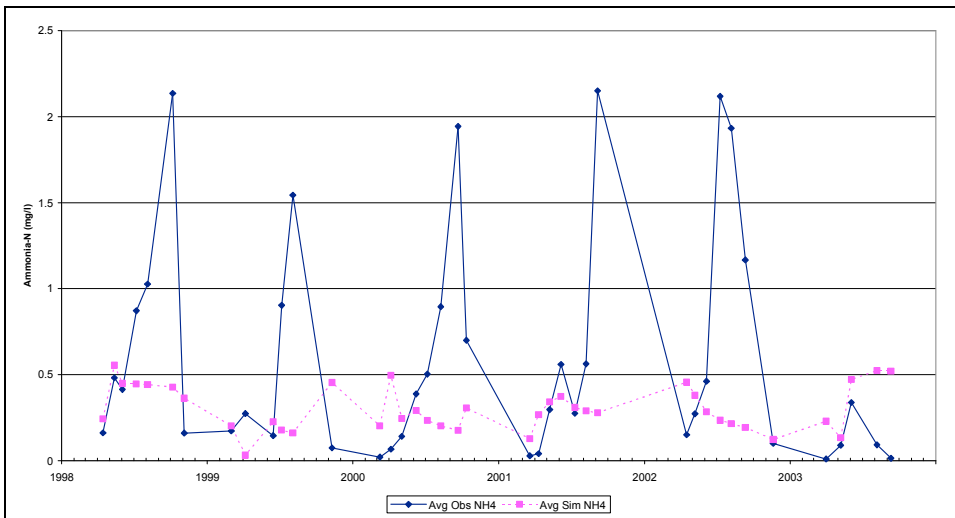


Figure C23. Observed and Simulated Average Bottom Ammonia Concentrations, TR2, Calibration Scenario, Triadelphia Reservoir.

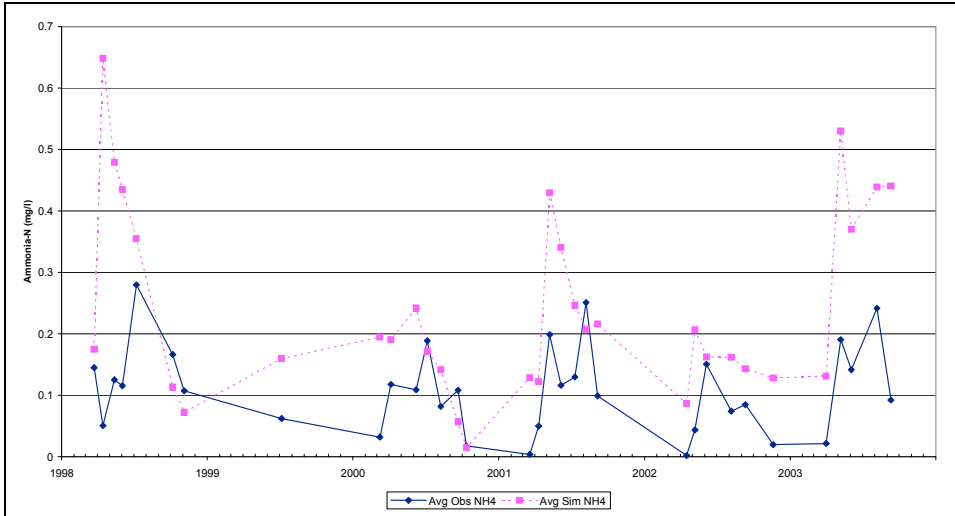


Figure C24. Observed and Simulated Average Bottom Ammonia Concentrations, TR3, Calibration Scenario, Triadelphia Reservoir.

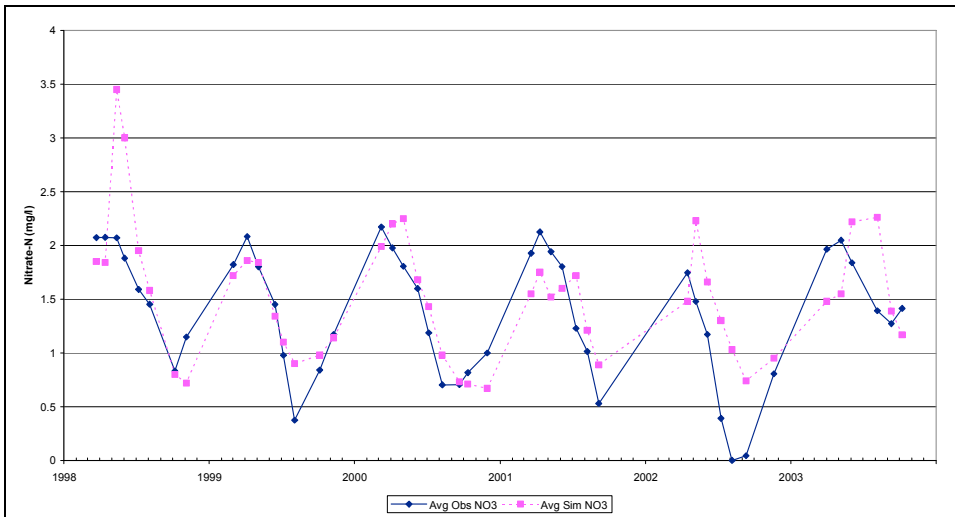


Figure C25. Observed and Simulated Average Surface Nitrate Concentrations, TR1, Calibration Scenario, Triadelphia Reservoir.

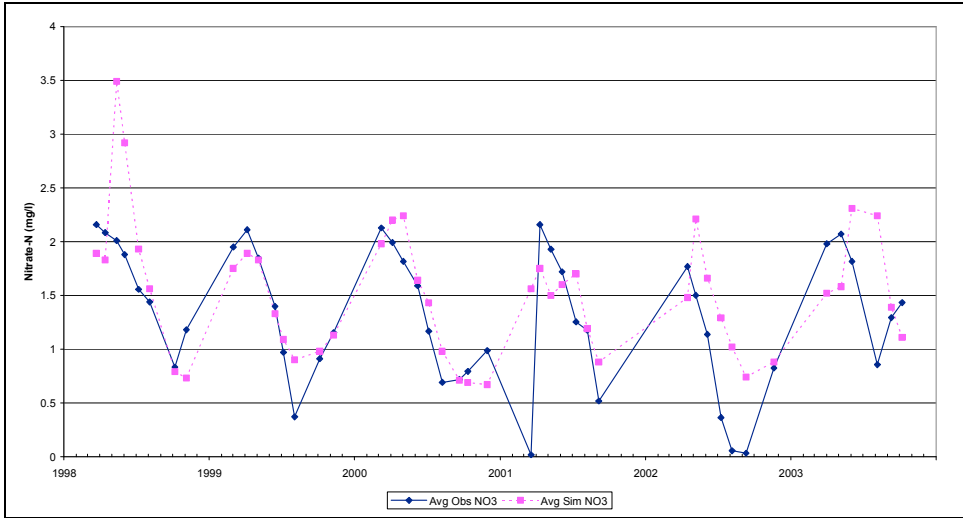


Figure C26. Observed and Simulated Average Surface Nitrate Concentrations, TR2, Calibration Scenario, Triadelphia Reservoir.

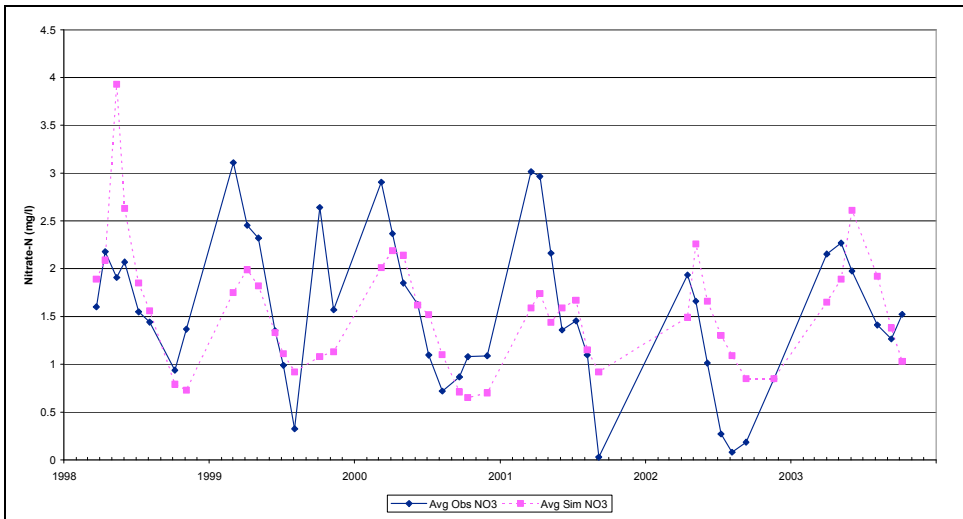


Figure C27. Observed and Simulated Average Surface Nitrate Concentrations, TR3, Calibration Scenario, Triadelphia Reservoir.

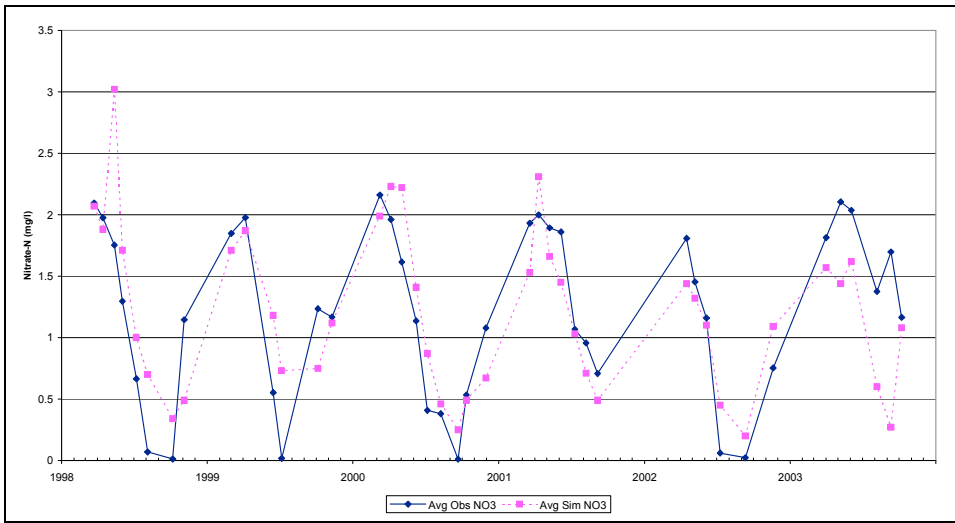


Figure C28. Observed and Simulated Average Bottom Nitrate Concentrations, TR1, Calibration Scenario, Triadelphia Reservoir.

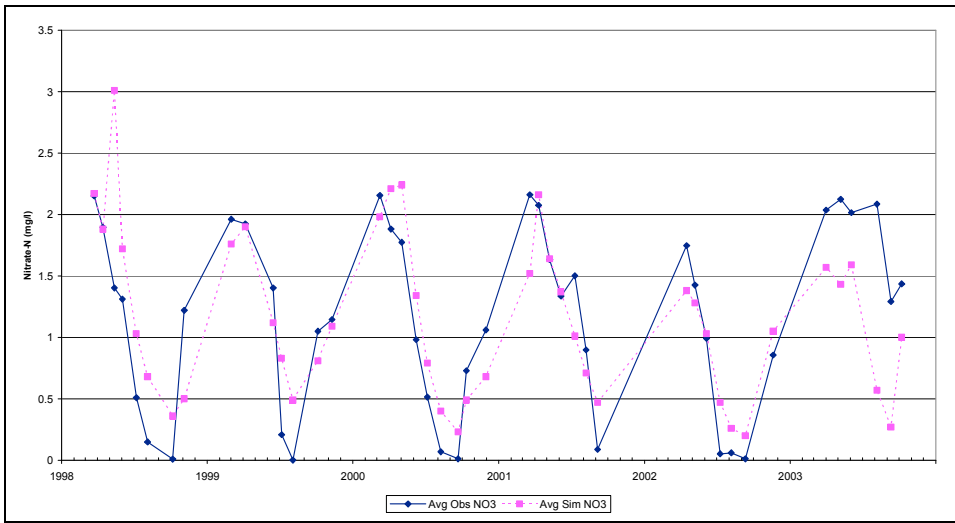


Figure C29. Observed and Simulated Average Bottom Nitrate Concentrations, TR2, Calibration Scenario, Triadelphia Reservoir.

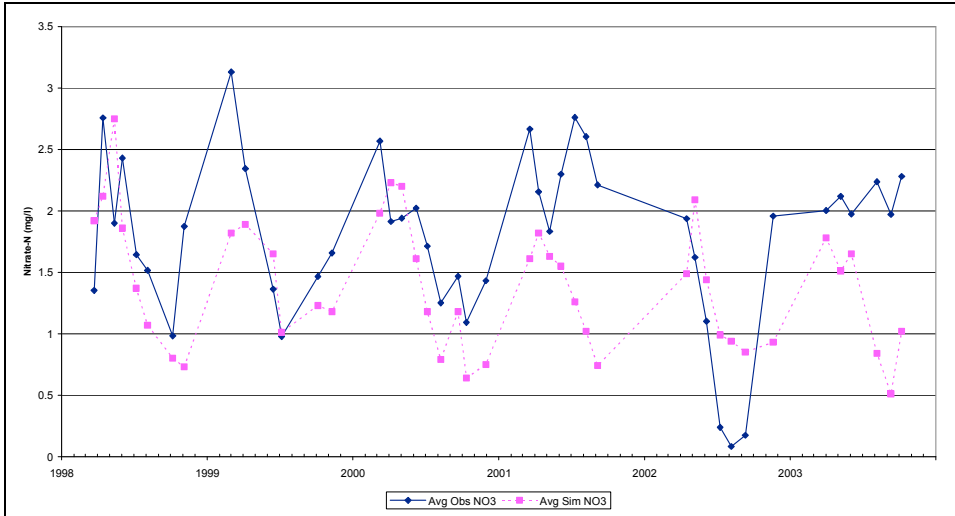


Figure C30. Observed and Simulated Average Bottom Nitrate Concentrations, TR3, Calibration Scenario, Triadelphia Reservoir.

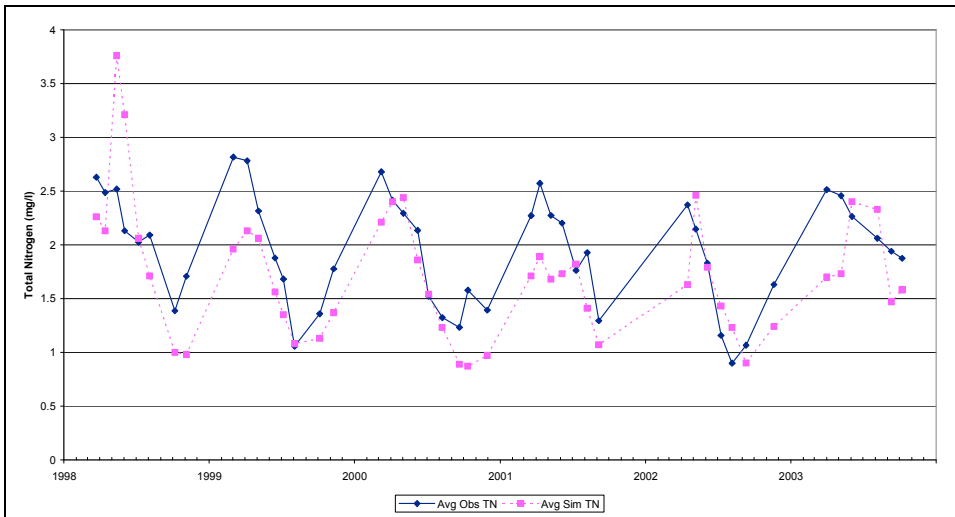


Figure C31. Observed and Simulated Average Surface Total Nitrogen Concentrations, TR1, Calibration Scenario, Triadelphia Reservoir

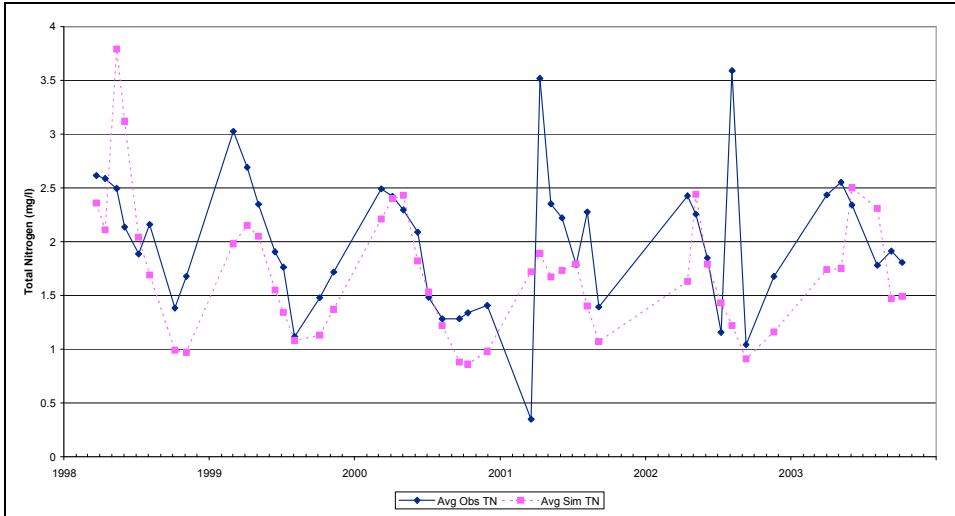


Figure C32. Observed and Simulated Average Surface Total Nitrogen Concentrations, TR2, Calibration Scenario, Triadelphia Reservoir

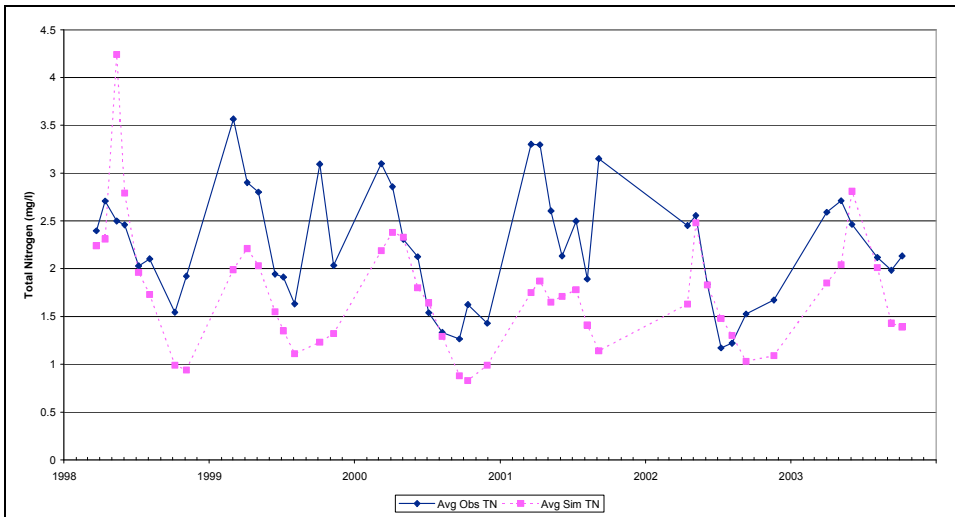


Figure C33. Observed and Simulated Average Surface Total Nitrogen Concentrations, TR3, Calibration Scenario, Triadelphia Reservoir

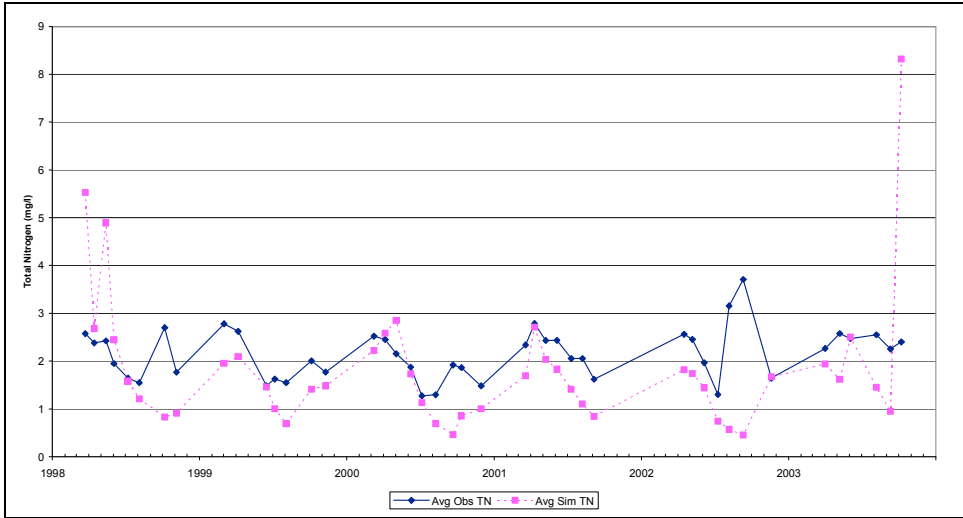


Figure C34. Observed and Simulated Average Bottom Total Nitrogen Concentrations, TR1, Calibration Scenario, Triadelphia Reservoir

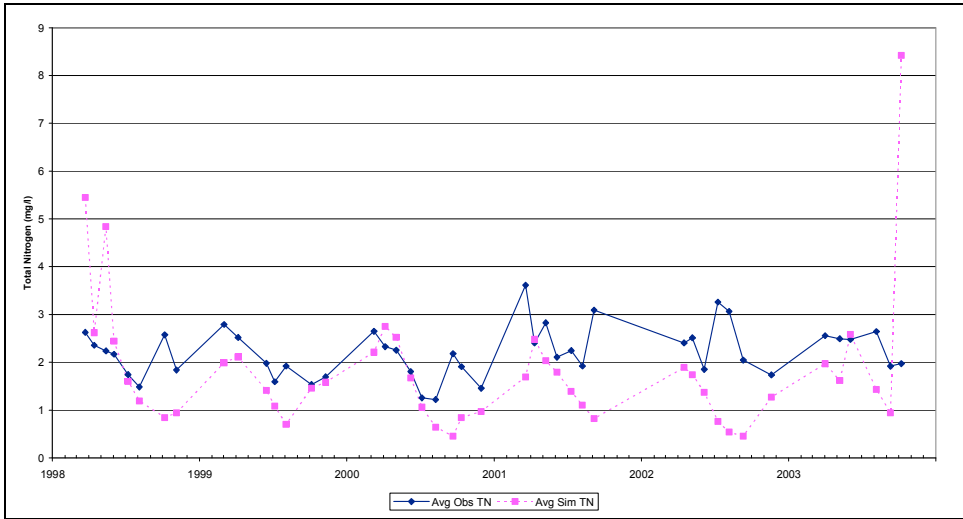


Figure C35. Observed and Simulated Average Bottom Total Nitrogen Concentrations, TR2, Calibration Scenario, Triadelphia Reservoir

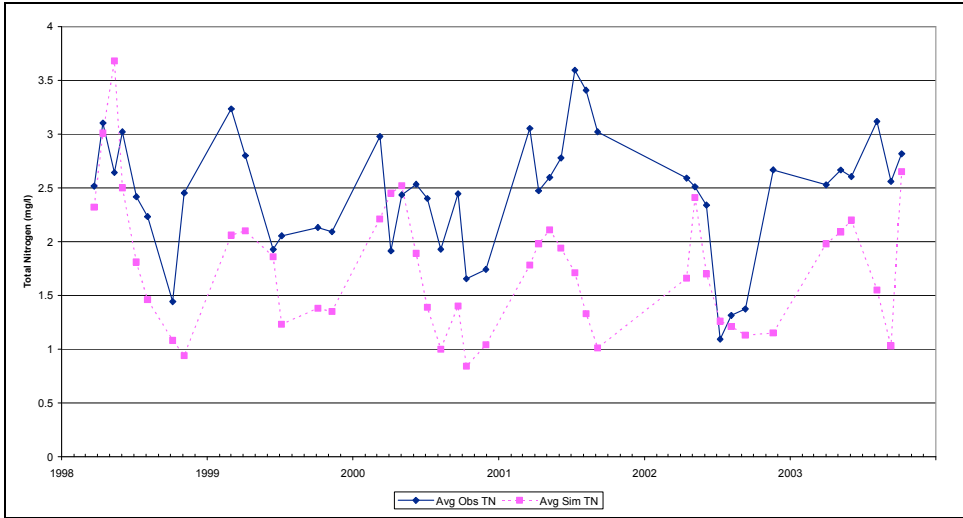


Figure C36. Observed and Simulated Average Bottom Total Nitrogen Concentrations, TR3, Calibration Scenario, Triadelphia Reservoir

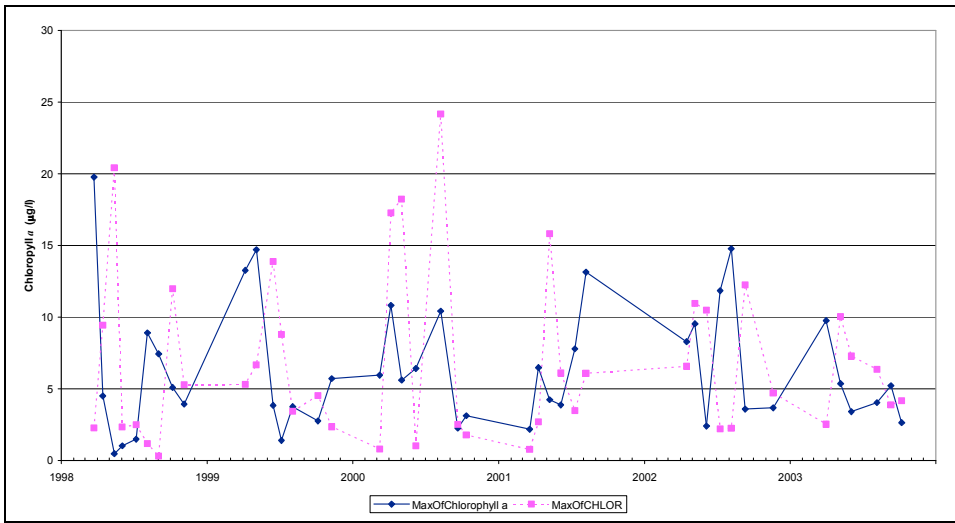


Figure C37. Observed and Simulated Max Chla Concentrations, RG1, Calibration Scenario, Rocky Gorge Reservoir

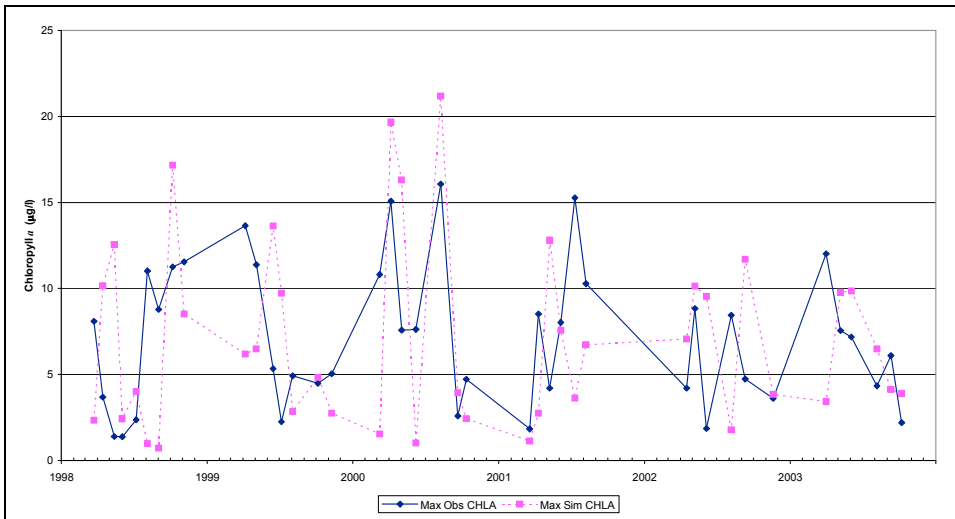


Figure C38. Observed and Simulated Max Chla Concentrations, RG2, Calibration Scenario, Rocky Gorge Reservoir

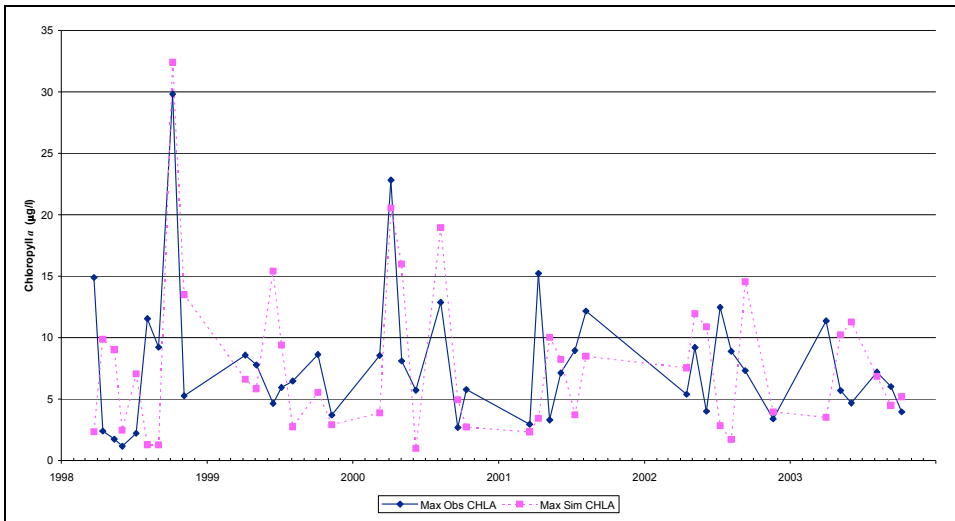


Figure C39. Observed and Simulated Max Chla Concentrations, RG3, Calibration Scenario, Rocky Gorge Reservoir

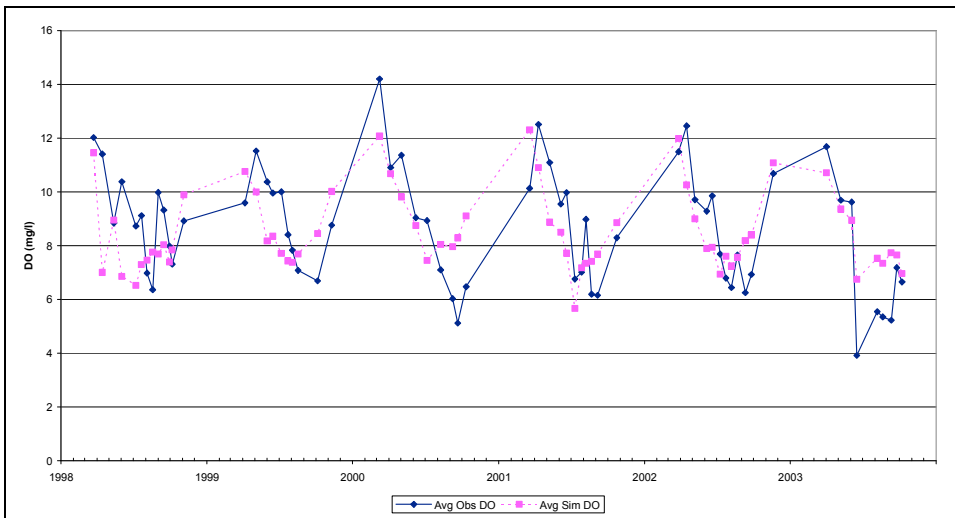


Figure C40. Observed and Simulated Average Surface DO Concentrations, RG2, Calibration Scenario, Rocky Gorge Reservoir.

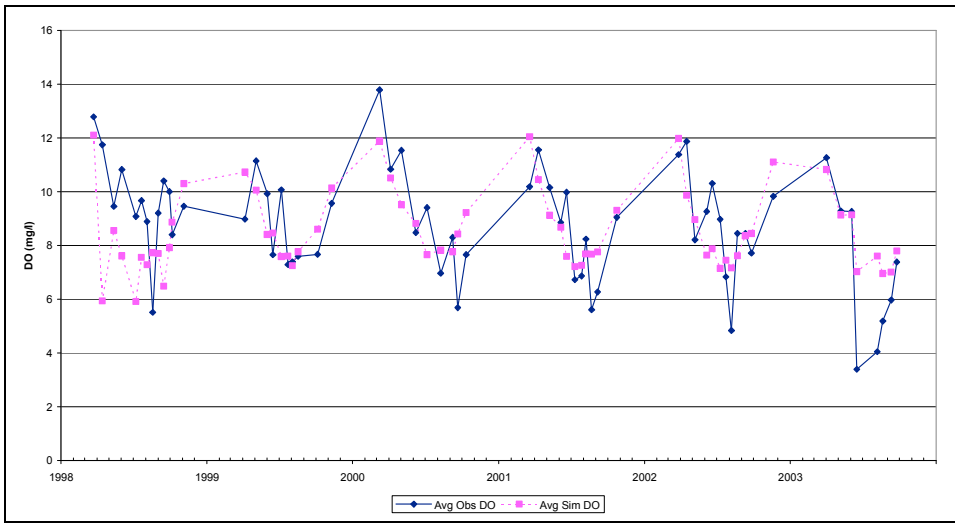


Figure C41. Observed and Simulated Average Surface DO Concentrations, RG3, Calibration Scenario, Rocky Gorge Reservoir

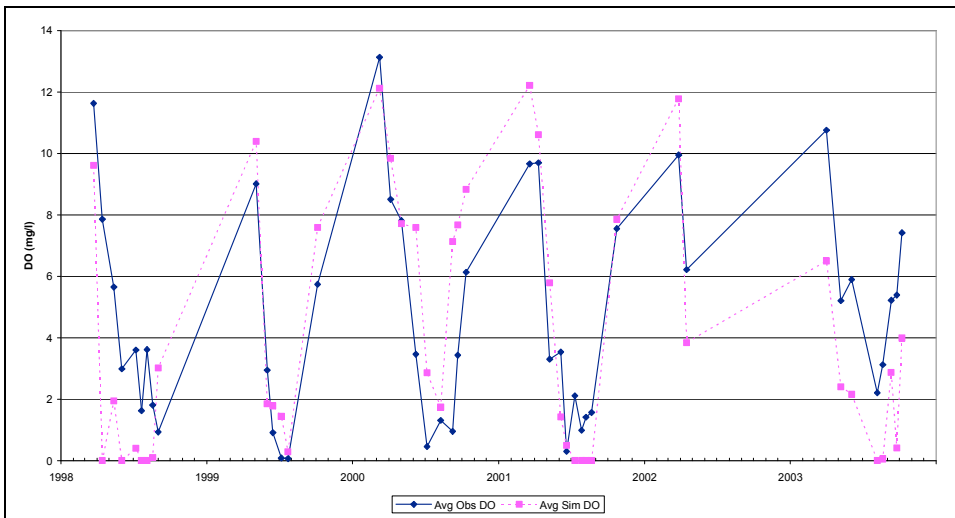


Figure C42. Observed and Simulated Average Bottom DO Concentrations, RG2, Calibration Scenario, Rocky Gorge Reservoir

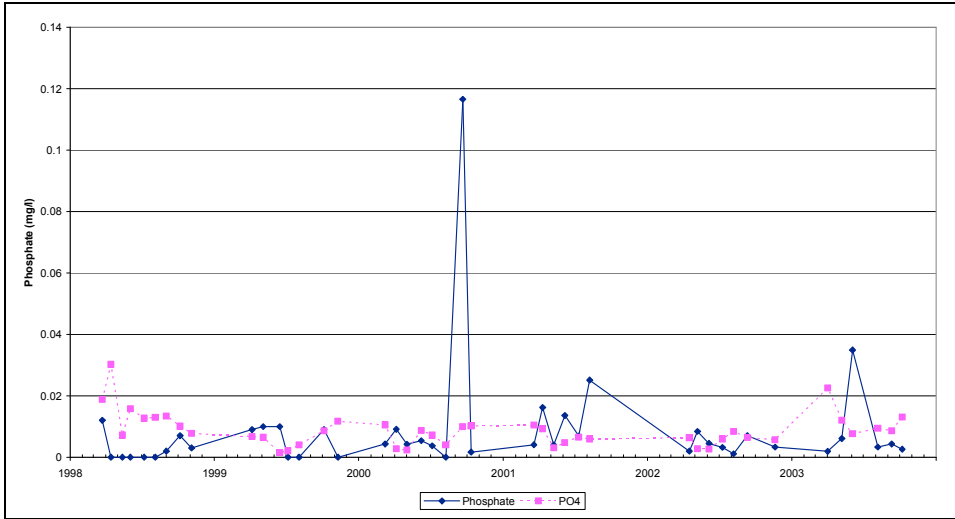


Figure C43. Observed and Simulated Average Surface Phosphate Concentrations, RG1, Calibration Scenario, Rocky Gorge Reservoir.

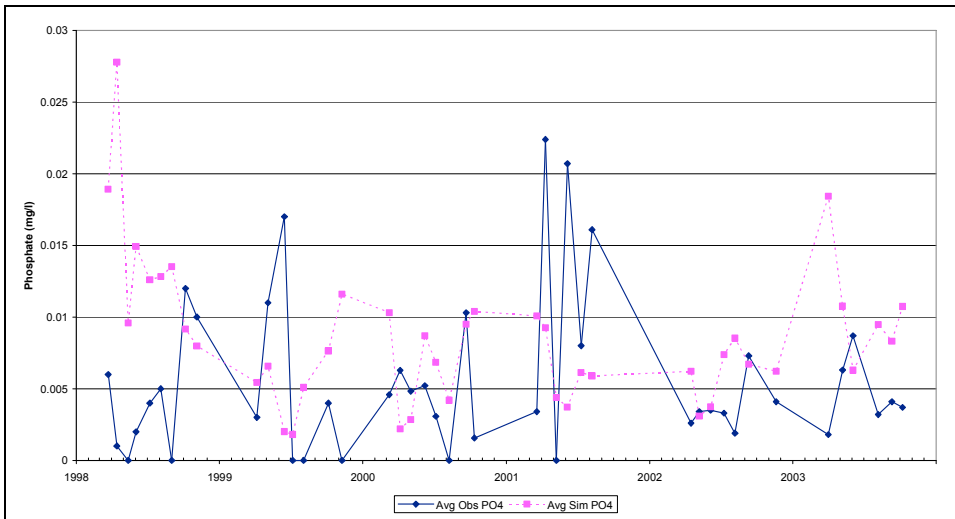


Figure C44. Observed and Simulated Average Surface Phosphate Concentrations, RG2, Calibration Scenario, Rocky Gorge Reservoir.

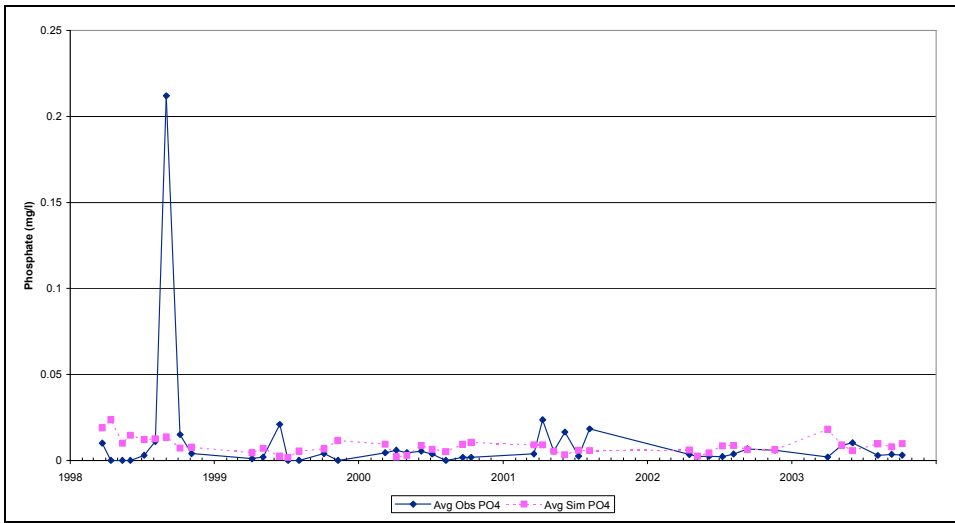


Figure C45. Observed and Simulated Average Surface Phosphate Concentrations, RG3, Calibration Scenario, Rocky Gorge Reservoir.

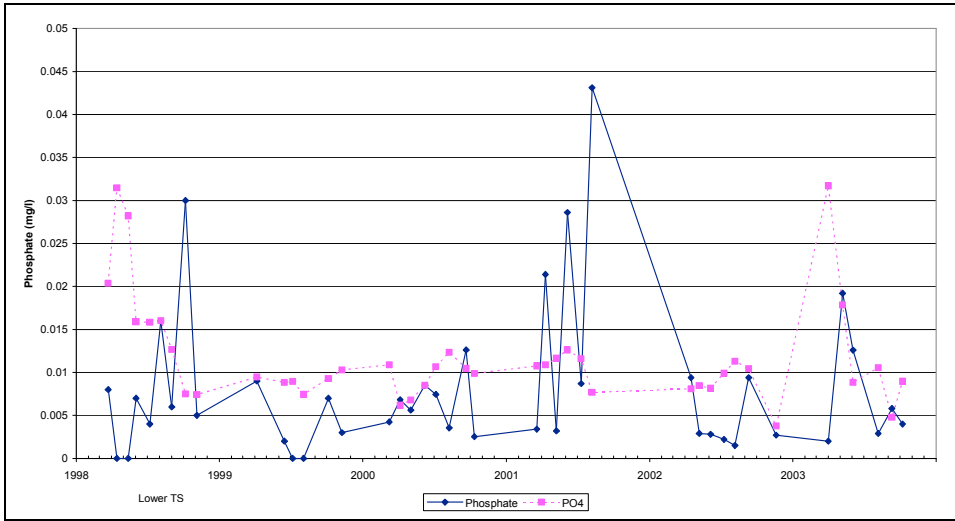


Figure C46. Observed and Simulated Average Bottom Phosphate Concentrations, RG1, Calibration Scenario, Rocky Gorge Reservoir

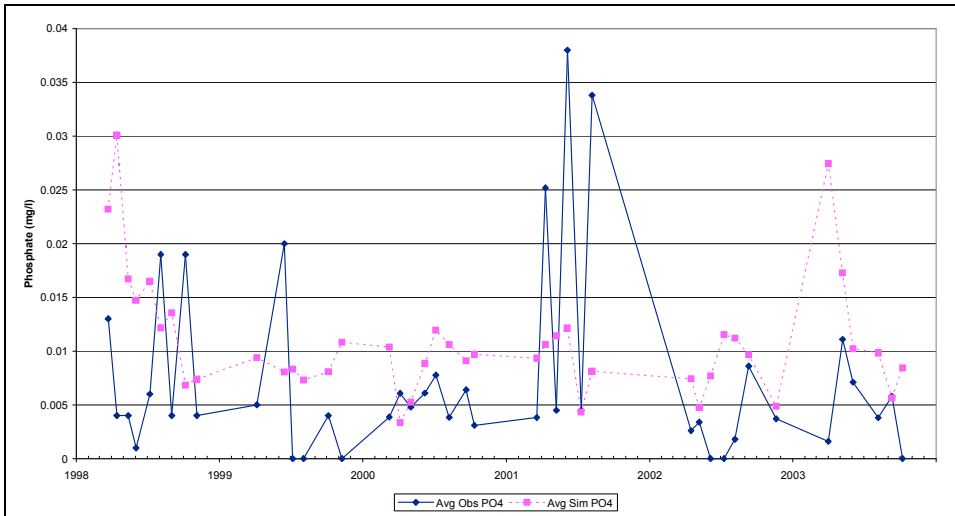


Figure C47. Observed and Simulated Average Bottom Phosphate Concentrations, RG2, Calibration Scenario, Rocky Gorge Reservoir

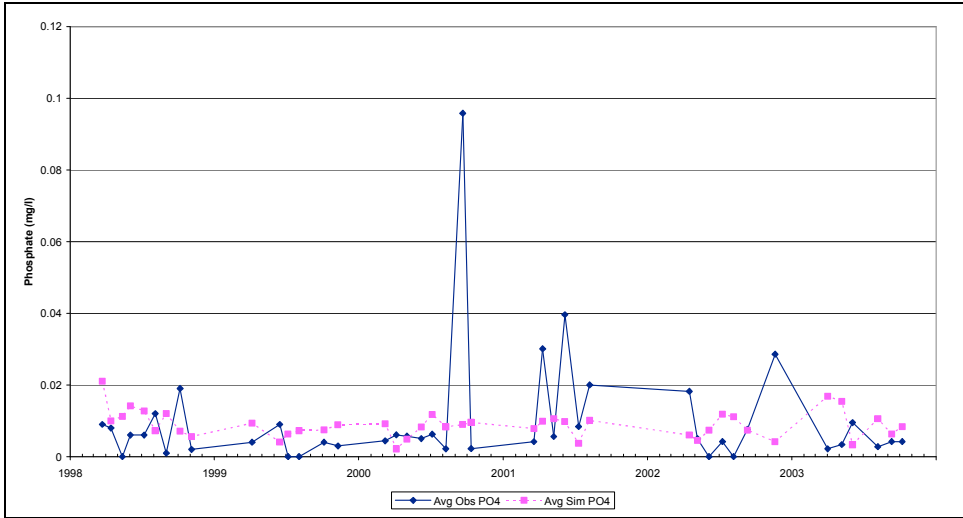


Figure C48. Observed and Simulated Average Bottom Phosphate Concentrations, RG3, Calibration Scenario, Rocky Gorge Reservoir

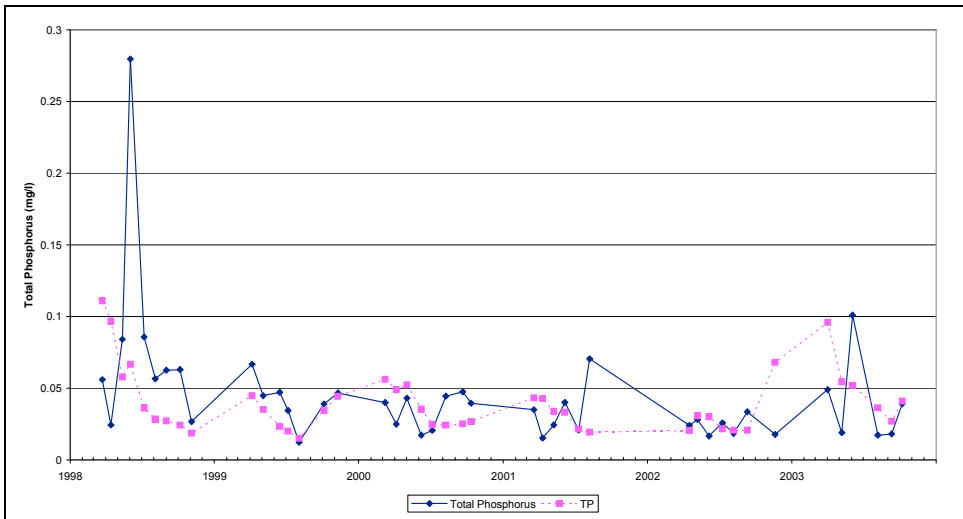


Figure C49. Observed and Simulated Average Surface Total Phosphorus Concentrations, RG1, Calibration Scenario, Rocky Gorge Reservoir.

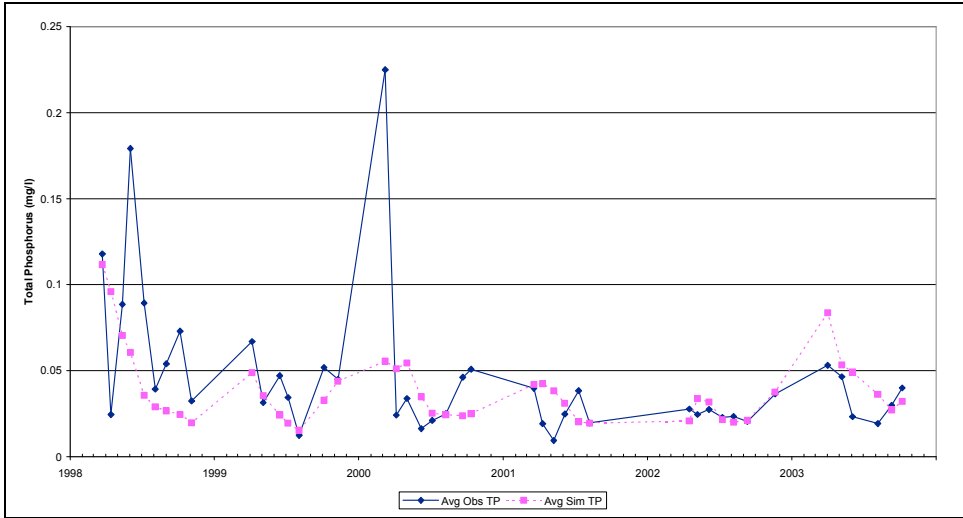


Figure C50. Observed and Simulated Average Surface Total Phosphorus Concentrations, RG2, Calibration Scenario, Rocky Gorge Reservoir.

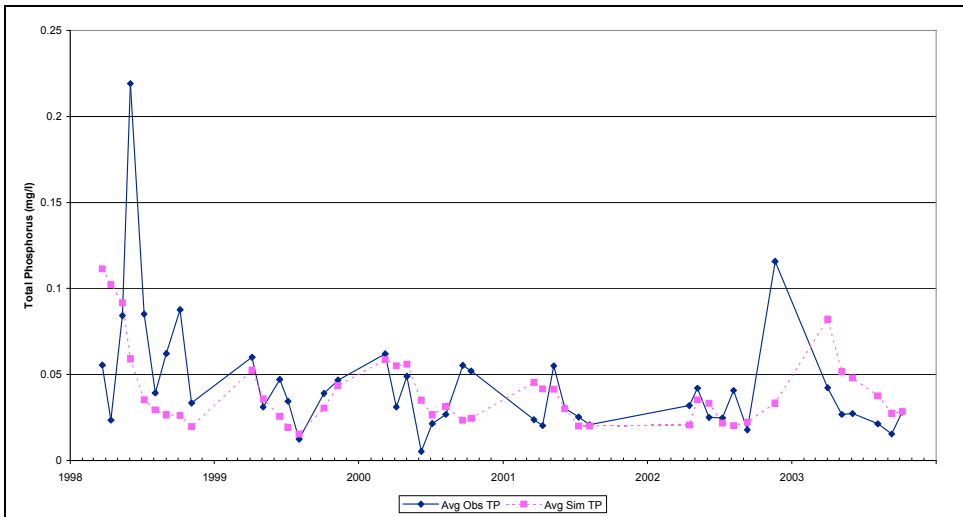


Figure C51. Observed and Simulated Average Surface Total Phosphorus Concentrations, RG3, Calibration Scenario, Rocky Gorge Reservoir.

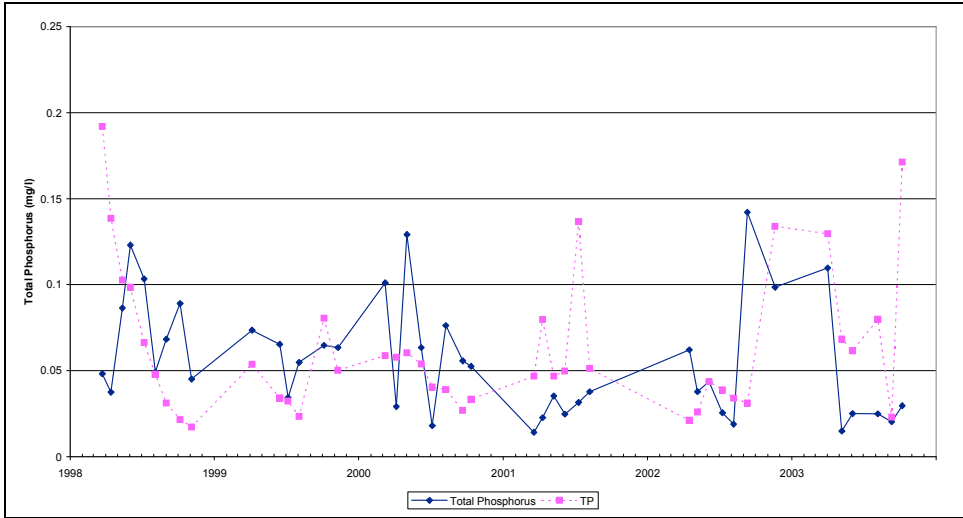


Figure C52. Observed and Simulated Average Bottom Total Phosphorus Concentrations, RG1, Calibration Scenario, Rocky Gorge Reservoir.

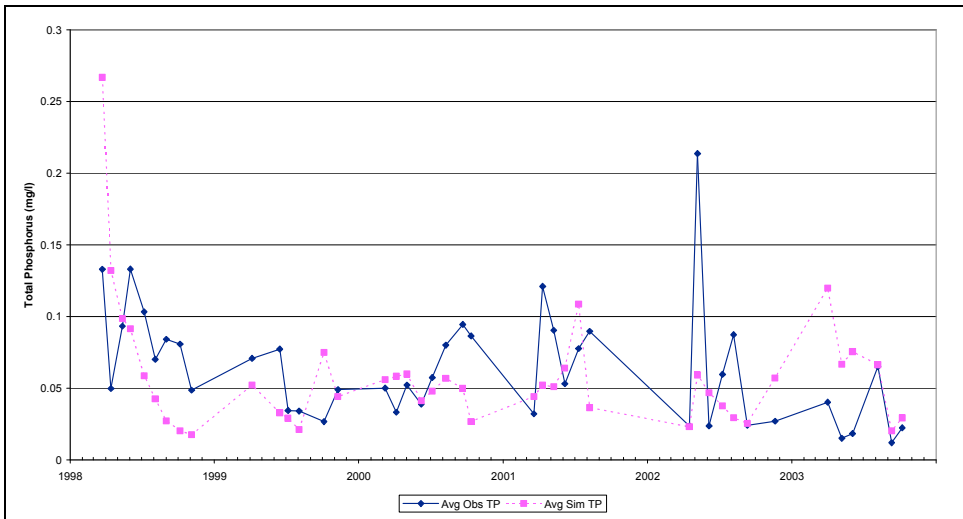


Figure C53. Observed and Simulated Average Bottom Total Phosphorus Concentrations, RG2, Calibration Scenario, Rocky Gorge Reservoir.

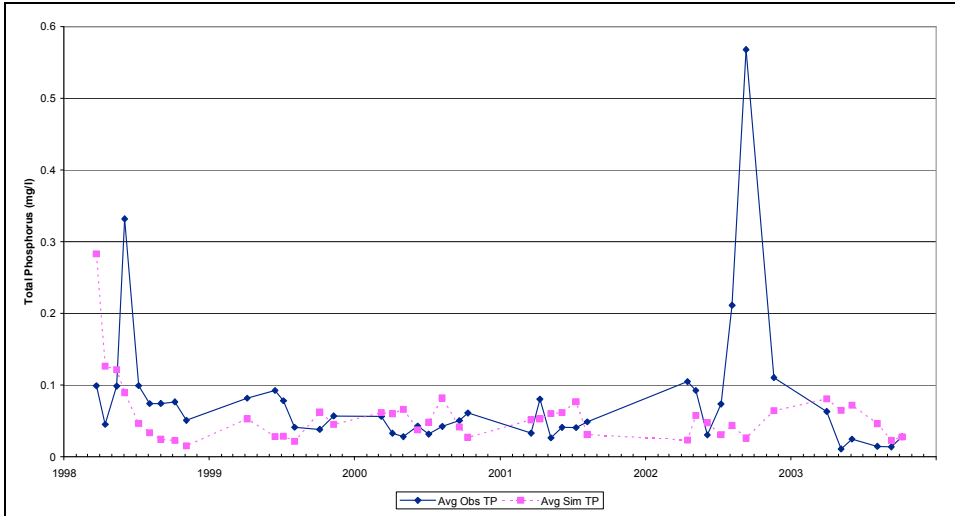


Figure C54. Observed and Simulated Average Bottom Total Phosphorus Concentrations, RG3, Calibration Scenario, Rocky Gorge Reservoir.

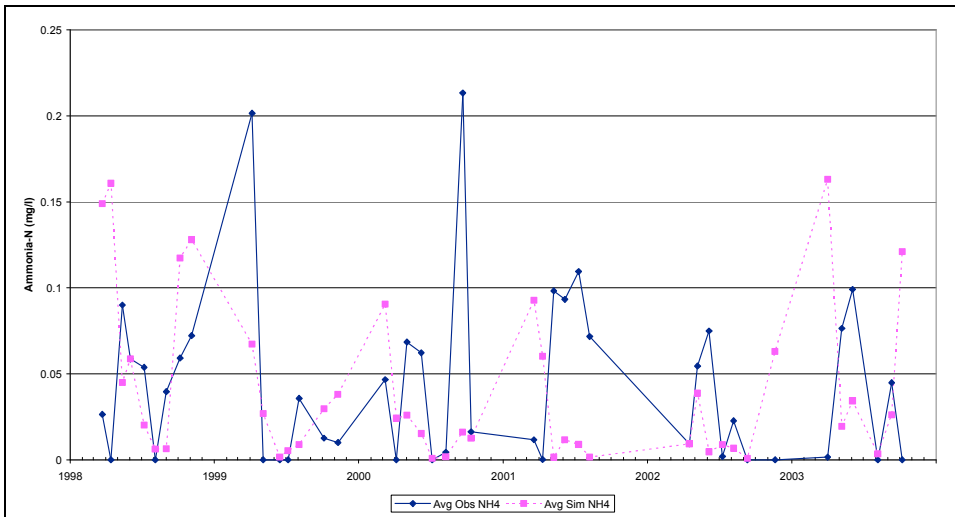


Figure C55. Observed and Simulated Average Surface Ammonia Concentrations, RG1, Calibration Scenario, Rocky Gorge Reservoir.

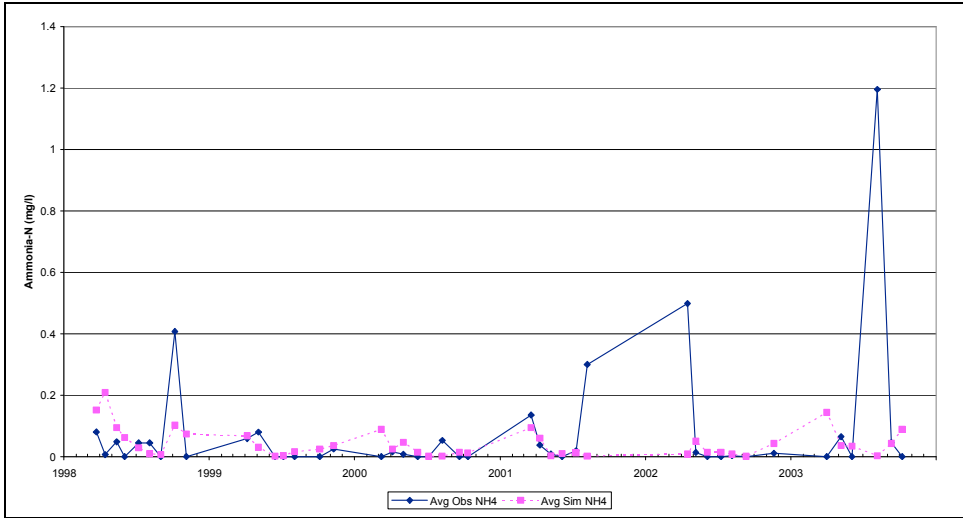


Figure C56. Observed and Simulated Average Surface Ammonia Concentrations, RG2, Calibration Scenario, Rocky Gorge Reservoir.

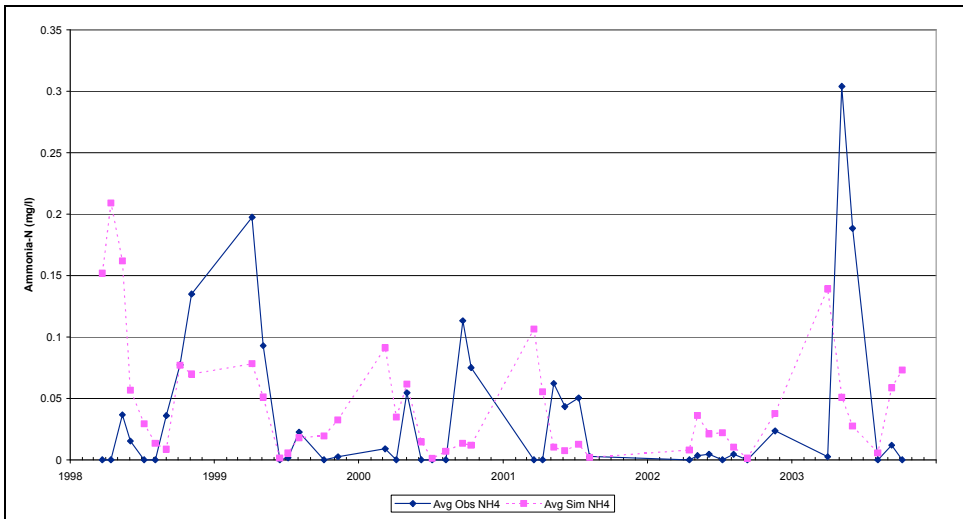


Figure C57. Observed and Simulated Average Surface Ammonia Concentrations, RG3, Calibration Scenario, Rocky Gorge Reservoir.

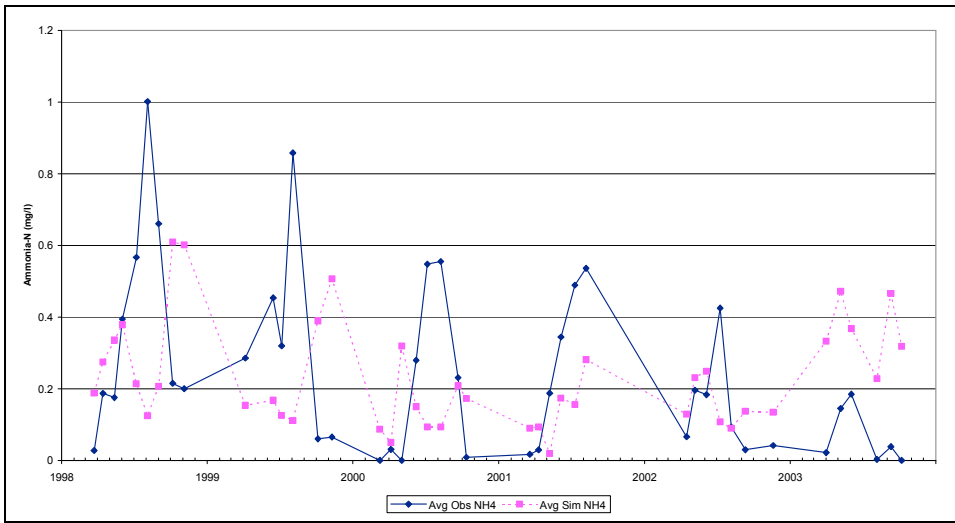


Figure C58. Observed and Simulated Average Bottom Ammonia Concentrations, RG1, Calibration Scenario, Rocky Gorge Reservoir.

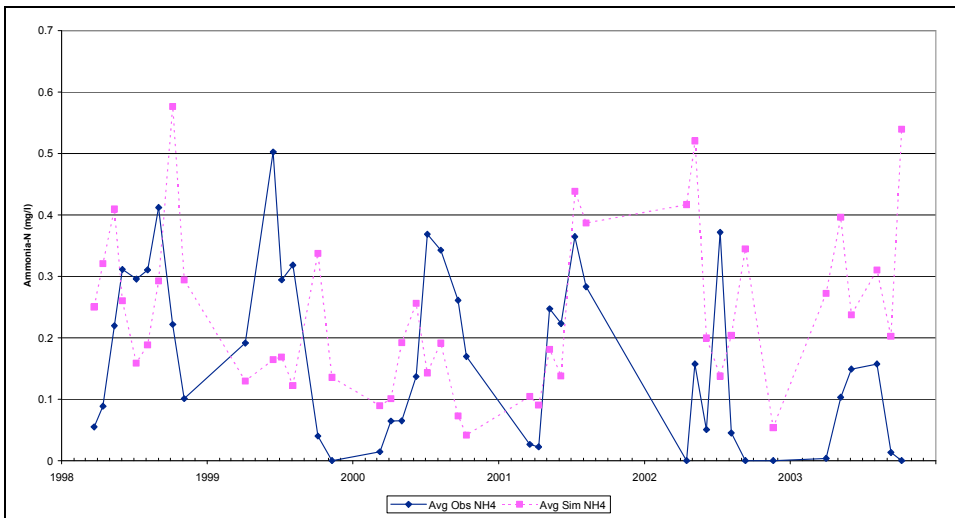


Figure C59. Observed and Simulated Average Bottom Ammonia Concentrations, RG2, Calibration Scenario, Rocky Gorge Reservoir.

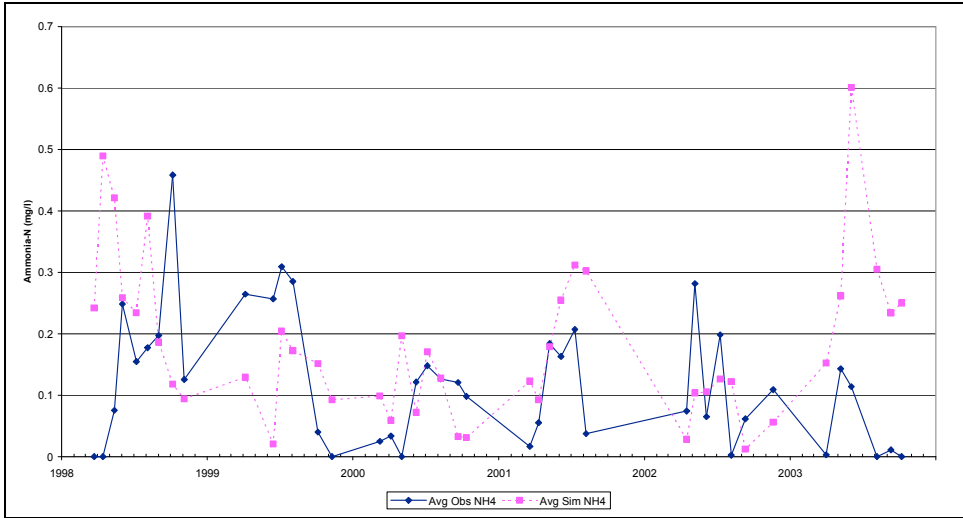


Figure C60. Observed and Simulated Average Bottom Ammonia Concentrations, RG3, Calibration Scenario, Rocky Gorge Reservoir.

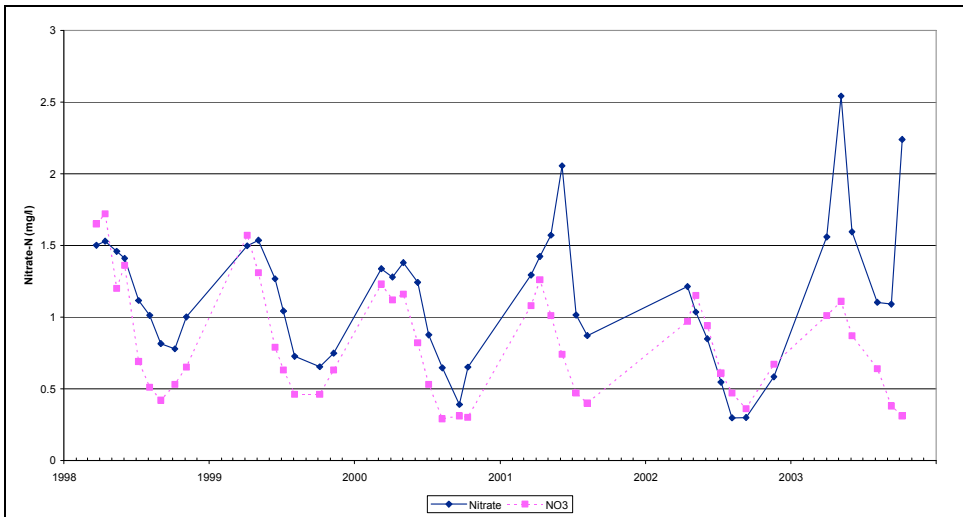


Figure C61. Observed and Simulated Average Surface Nitrate Concentrations, RG1, Calibration Scenario, Rocky Gorge Reservoir.

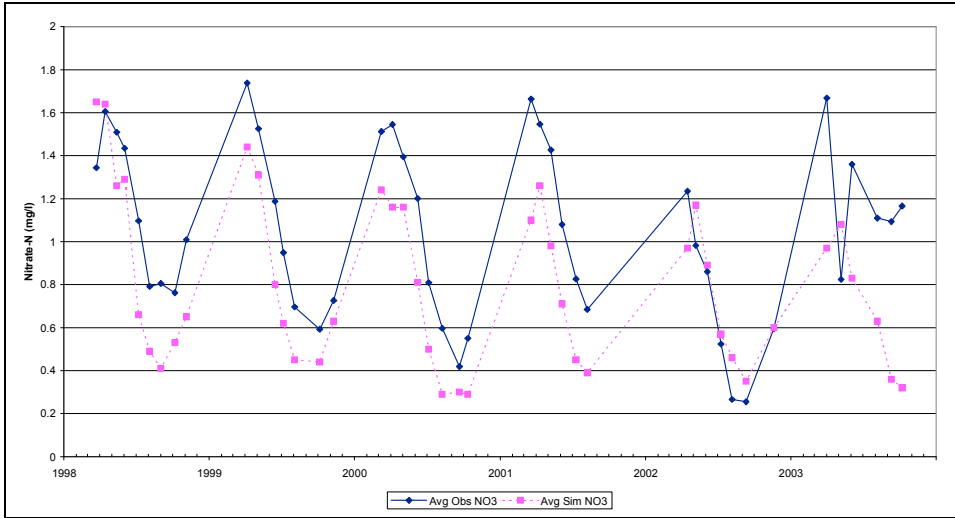


Figure C62. Observed and Simulated Average Surface Nitrate Concentrations, RG2, Calibration Scenario, Rocky Gorge Reservoir.

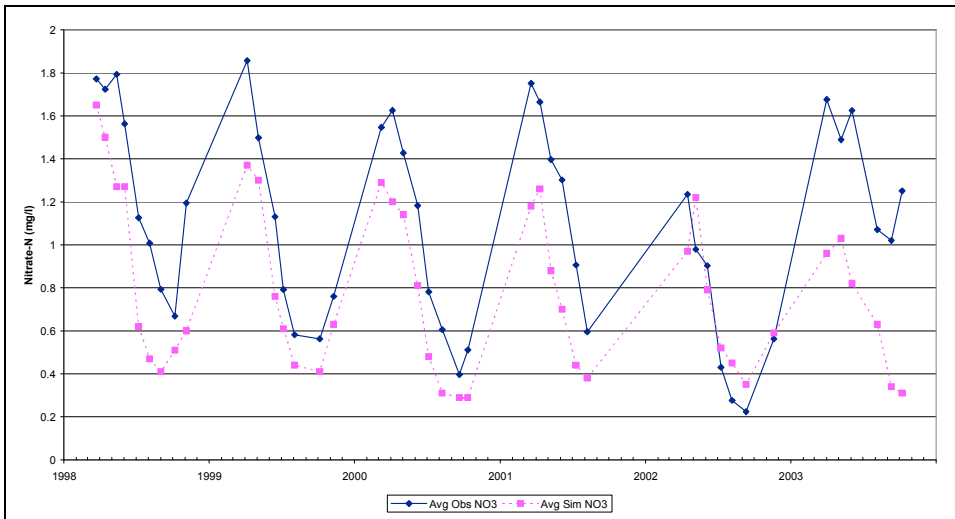


Figure C63. Observed and Simulated Average Surface Nitrate Concentrations, RG3, Calibration Scenario, Rocky Gorge Reservoir.

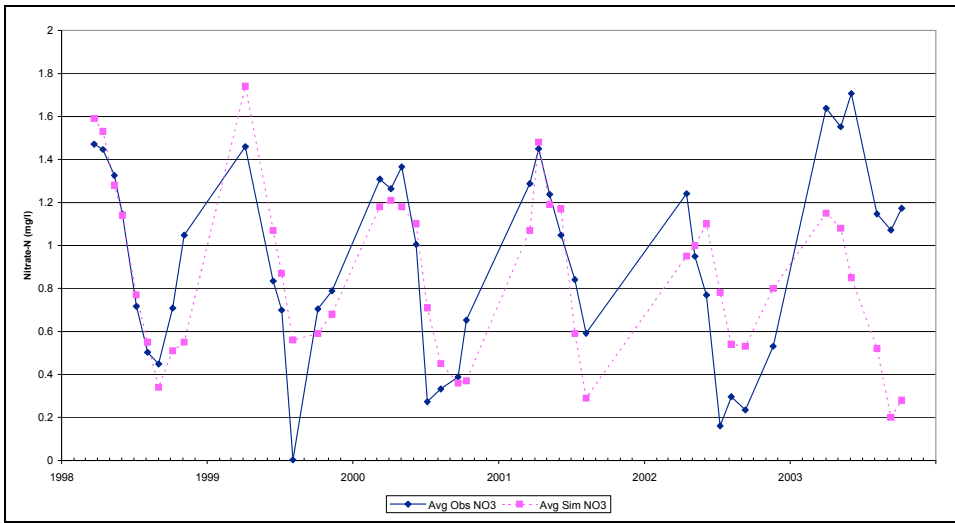


Figure C64. Observed and Simulated Average Bottom Nitrate Concentrations, RG1, Calibration Scenario, Rocky Gorge Reservoir.

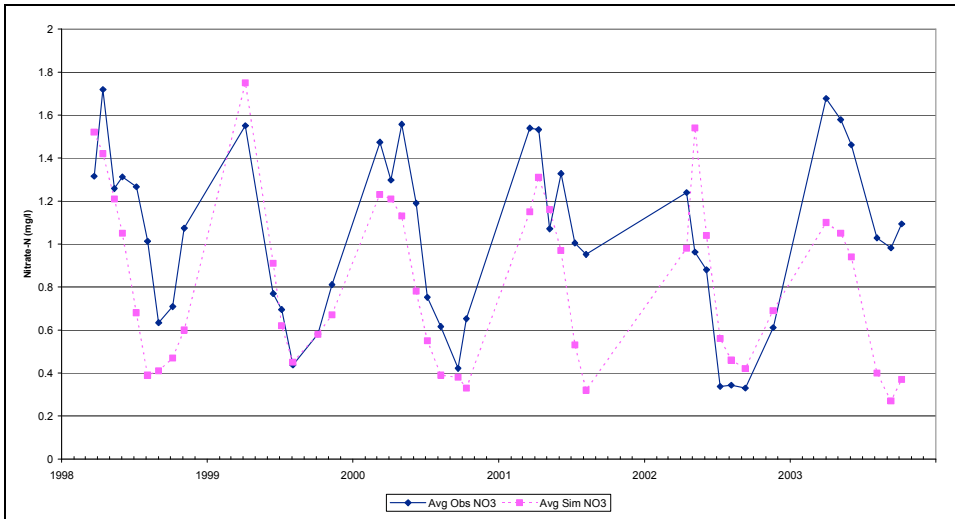


Figure C66. Observed and Simulated Average Bottom Nitrate Concentrations, RG2, Calibration Scenario, Rocky Gorge Reservoir.

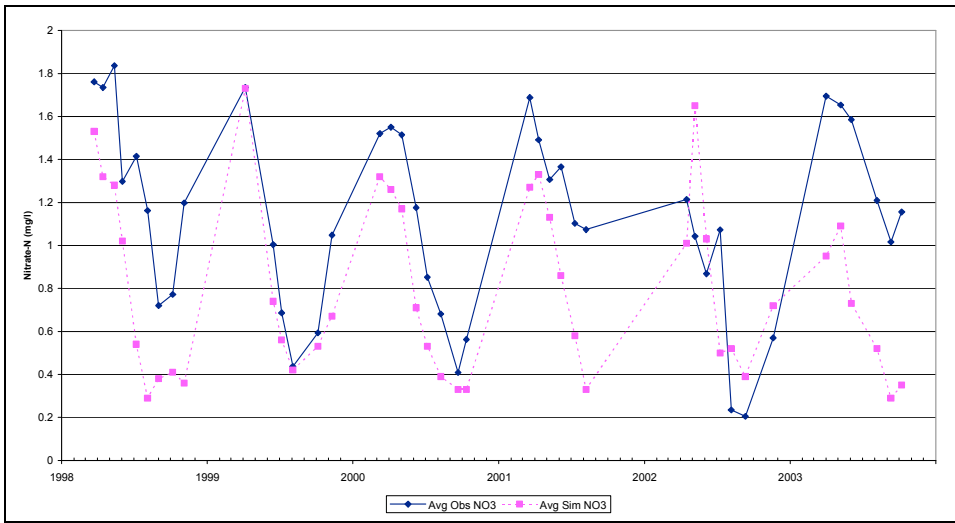


Figure C66. Observed and Simulated Average Bottom Nitrate Concentrations, RG3, Calibration Scenario, Rocky Gorge Reservoir.

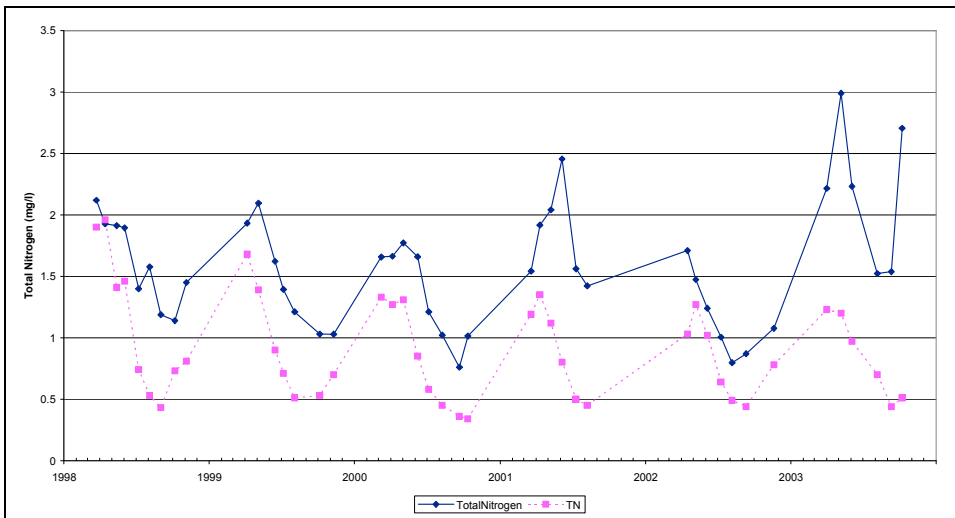


Figure C67. Observed and Simulated Average Surface Total Nitrogen Concentrations, RG1, Calibration Scenario, Rocky Gorge Reservoir

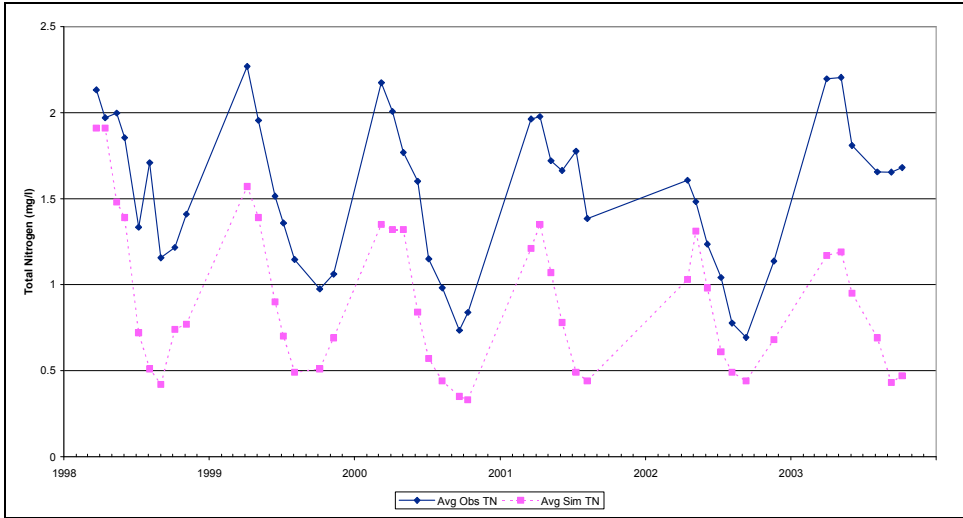


Figure C68. Observed and Simulated Average Surface Total Nitrogen Concentrations, RG2, Calibration Scenario, Rocky Gorge Reservoir

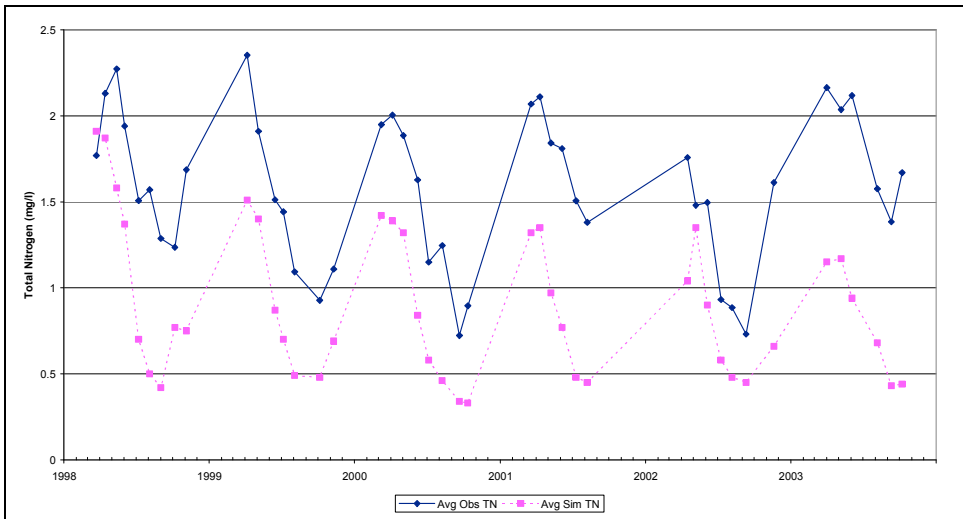


Figure C69. Observed and Simulated Average Surface Total Nitrogen Concentrations, RG3, Calibration Scenario, Rocky Gorge Reservoir

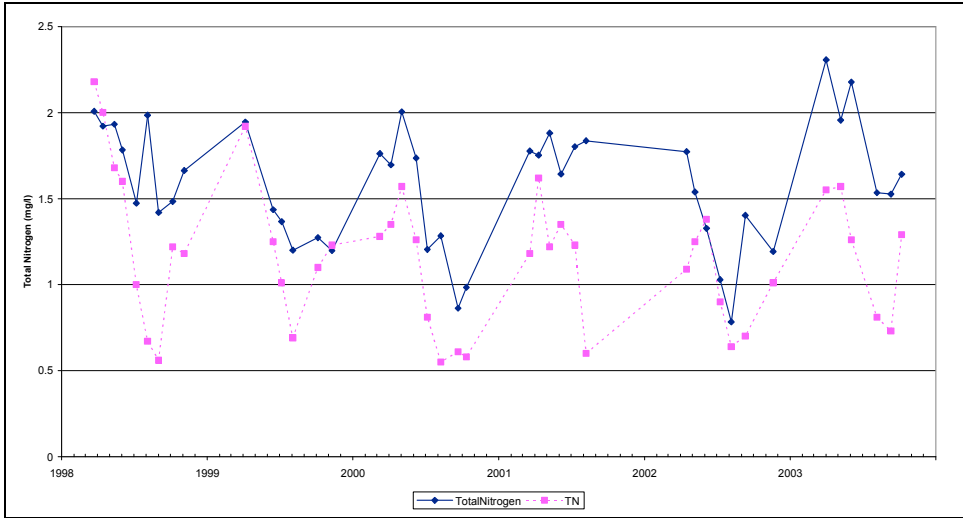


Figure C70. Observed and Simulated Average Bottom Total Nitrogen Concentrations, RG1, Calibration Scenario, Rocky Gorge Reservoir

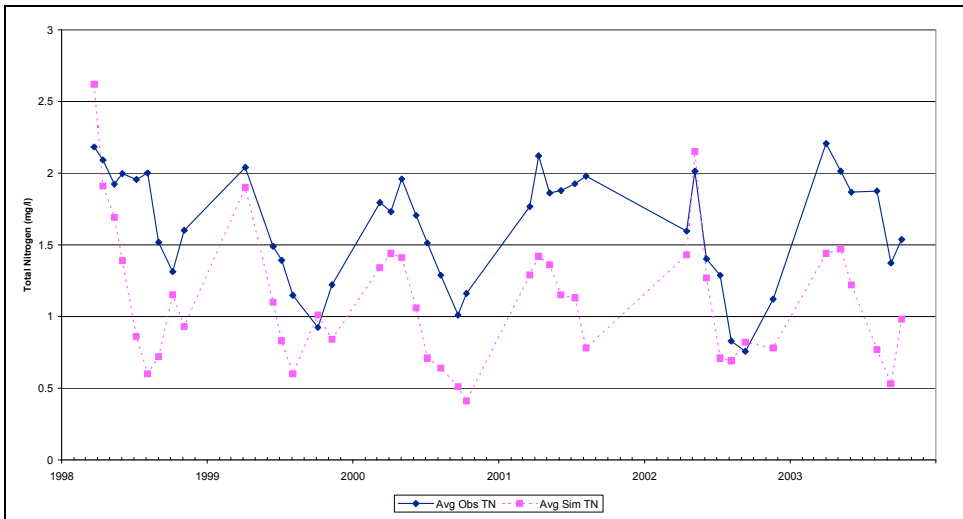


Figure C71. Observed and Simulated Average Bottom Total Nitrogen Concentrations, RG2, Calibration Scenario, Rocky Gorge Reservoir

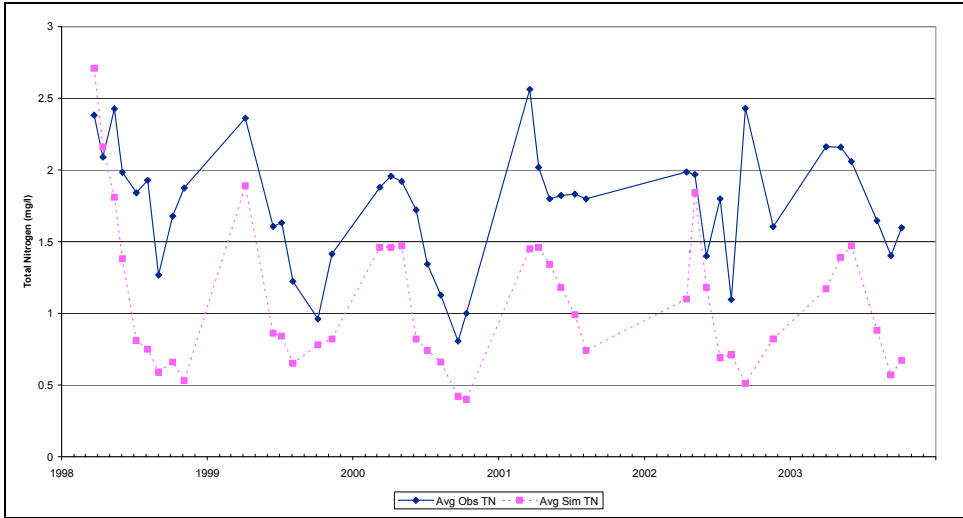


Figure C72. Observed and Simulated Average Bottom Total Nitrogen Concentrations, RG3, Calibration Scenario, Rocky Gorge Reservoir

Table C.1 Cell Width (m), CE-QUAL W2 Model of Triadelphia Reservoir

	1	2	3	4	5	6	7	8	9	10	11	12	13	14	15	16	17	18	19	20	21	22	23	24	25	
1																										
2		68	116	172	287	158	228	94	222	714	148	227	327	426	704	745	546	568	1852	671	1398	746	641	641	332	
3		39	99	150	278	146	207	87	211	622	139	205	290	397	671	714	518	531	1657	656	1259	707	614	614	312	
4			56	20	263	121	189	84	207	585	131	199	264	371	618	694	464	497	1455	640	1157	678	593	303		
5			27	118	224	98	169	77	195	515	124	191	245	345	567	676	424	471	1224	619	1025	641	574	293		
6				74	161	78	146	69	173	408	120	181	233	318	518	658	397	454	953	592	954	595	557	284		
7					78	56	135	67	162	355	113	168	202	288	448	618	384	427	853	531	876	529	531	278		
8						40	126	63	150	299	107	157	177	257	393	582	373	397	755	479	795	478	502	273		
9						33	118	57	133	228	101	148	162	227	363	557	363	365	669	447	712	450	470	271		
10						22	62	49	108	170	89	143	145	202	351	511	349	347	586	426	650	418	456	265		
11							25	37	75	84	69	134	128	175	324	460	337	334	521	404	577	387	440	257		
12							22	21	31	36	36	119	110	144	272	403	329	326	433	381	535	360	419	247		
13									22	25	30	61	64	84	185	324	303	297	343	370	461	343	398	237		
14													27	35	96	217	243	252	317	354	368	320	372	222		
15													26	26	23	55	114	181	267	318	319	281	333	198		
16																	47	82	130	164	262	241	294	190		
17																				33	184	180	240	179		
18																				28	65	74	150	153		
19																										

Table C.2 Segment Length and Cell Width, CE-QUAL W2 Model of Rocky Gorge Reservoir

	1	2	3	4	5	6	7	8	9	10	11	12	13	14	15	16	17	18	19	20	21	22	23	24	25	26	27	28
1																												
2	138	171	218	226	175	142	199	254	337	357	256	287	359	301	358	315	334	334	337	381	483	511	454	346	360	467		
3	138	132	171	178	146	122	171	223	301	308	231	256	324	274	322	295	306	307	311	361	445	470	419	326	342	439		
4	138	92	123	129	118	101	143	193	266	258	206	226	288	248	287	274	277	279	286	340	407	429	383	306	324	410		
5	56	52	76	81	89	81	81	115	162	230	209	181	196	252	221	254	249	252	260	320	370	389	348	286	307	382		
6	15	18	28	32	61	61	61	86	132	194	159	156	165	217	194	216	234	220	225	235	300	332	348	312	266	289	353	
7																												
8																												
9																												
10																												
11																												
12																												
13																												
14																												
15																												
16																												
17																												
18																												
19																												
20																												
21																												
22																												
23																												
24																												
25																												
26																												
27																												
28																												
29																												
30																												
31																												

APPENDIX D

Figure D.1 Maximum Chla, Observed Data and All Scenarios, TR1, Triadelphia Reservoir

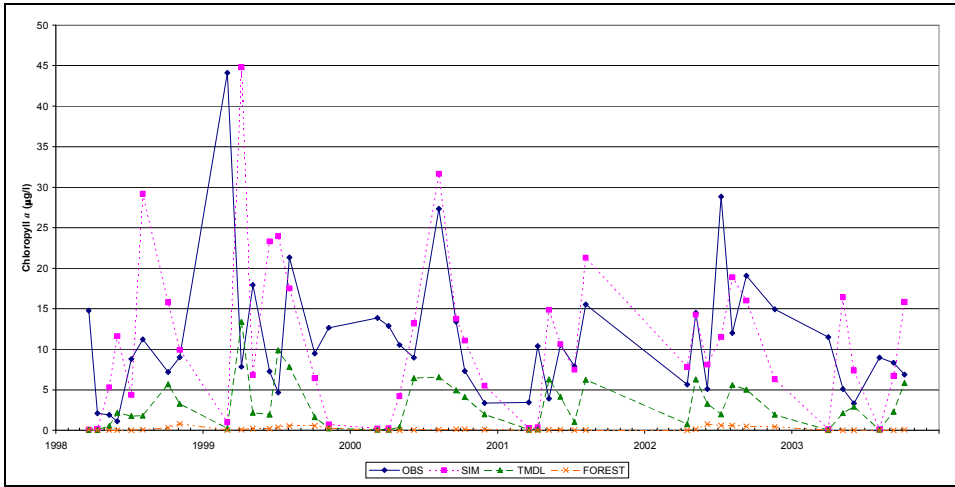


Figure D.2 Maximum Chla, Observed Data and All Scenarios, TR2, Triadelphia Reservoir

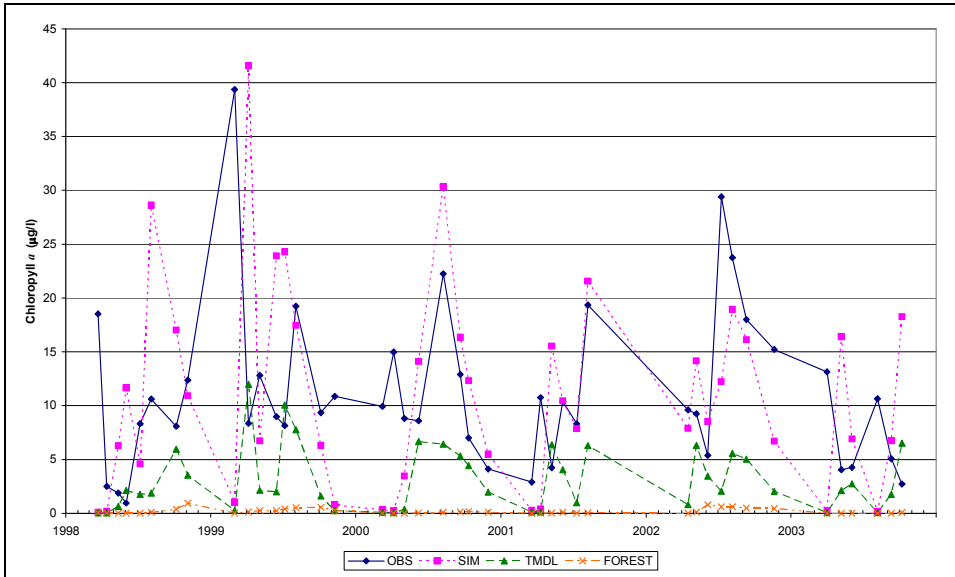


Figure D.3 Maximum Chla, Observed Data and All Scenarios, TR3, Triadelphia Reservoir

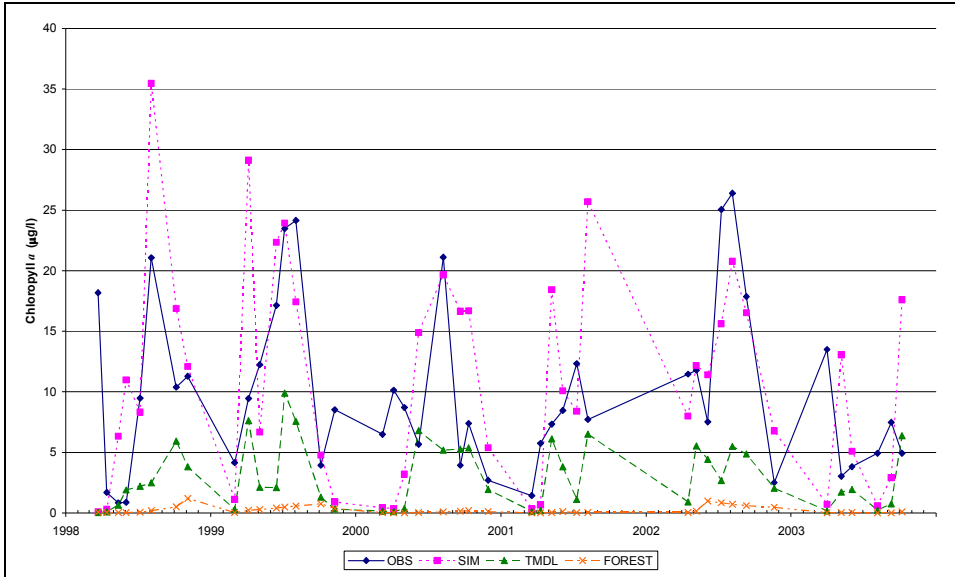


Figure D.4 Bottom DO, Observed Data and All Scenarios, TR2, Triadelphia Reservoir

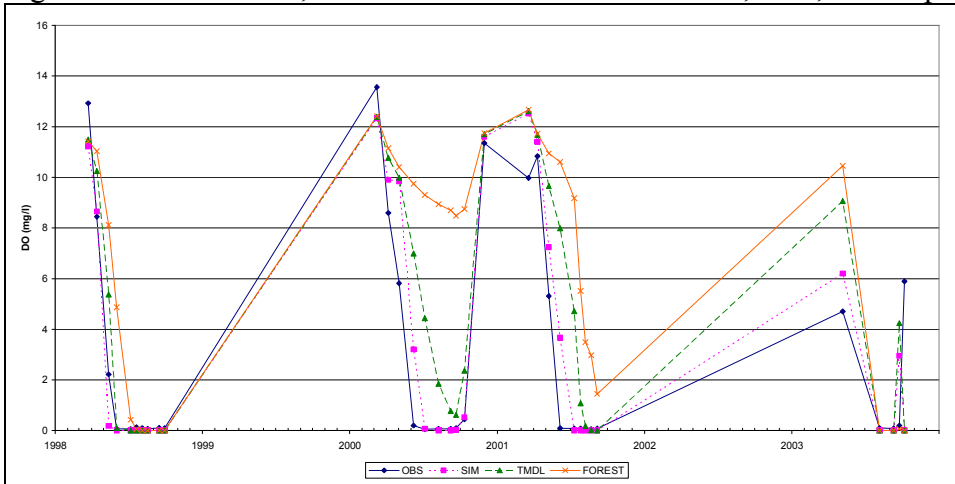


Figure D.5 Surface DO, Observed Data and All Scenarios, TR2, Triadelphia Reservoir

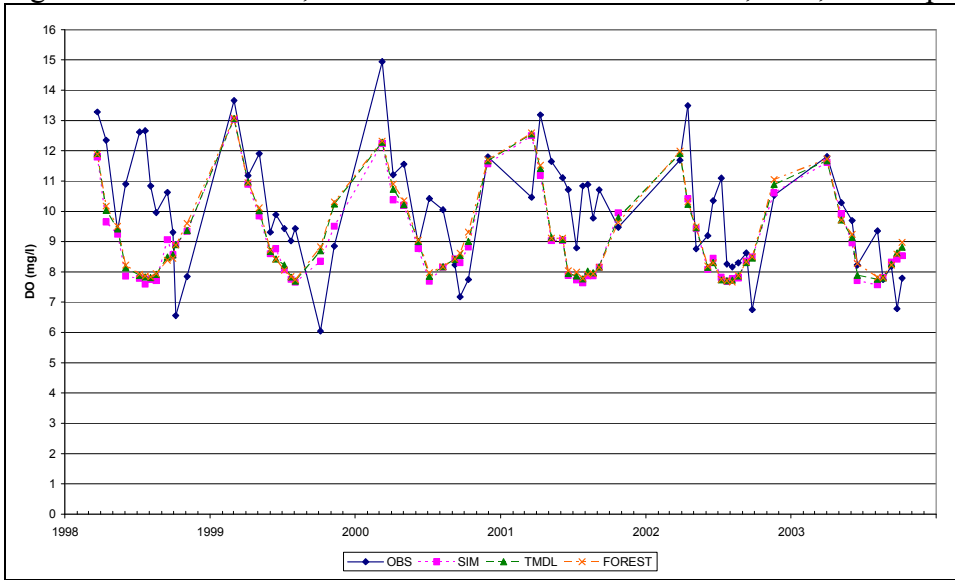


Figure D.6 Surface DO, Observed Data and All Scenarios, TR3, Triadelphia Reservoir

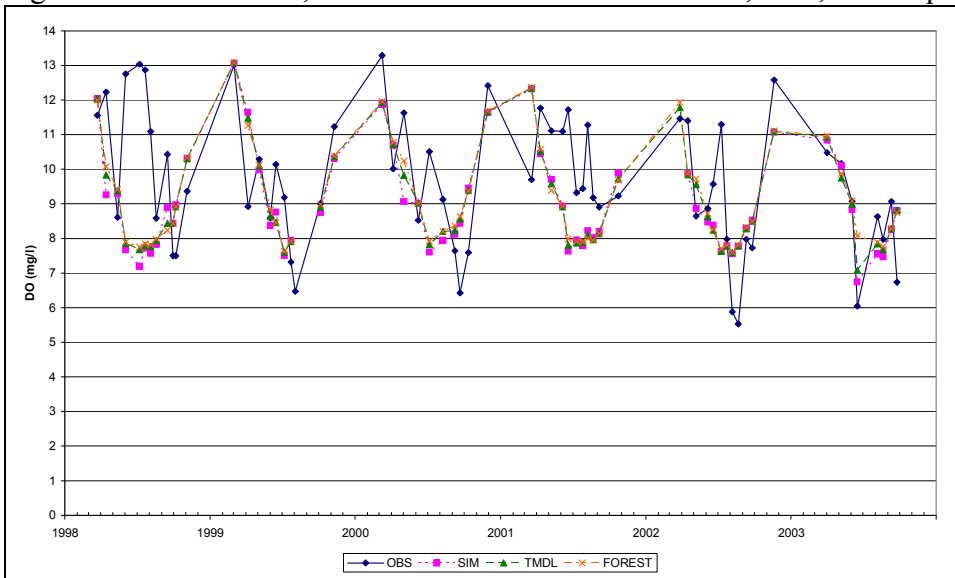


Figure D.7 Maximum Chla, Observed Data and All Scenarios, RG1, Rocky Gorge Reservoir

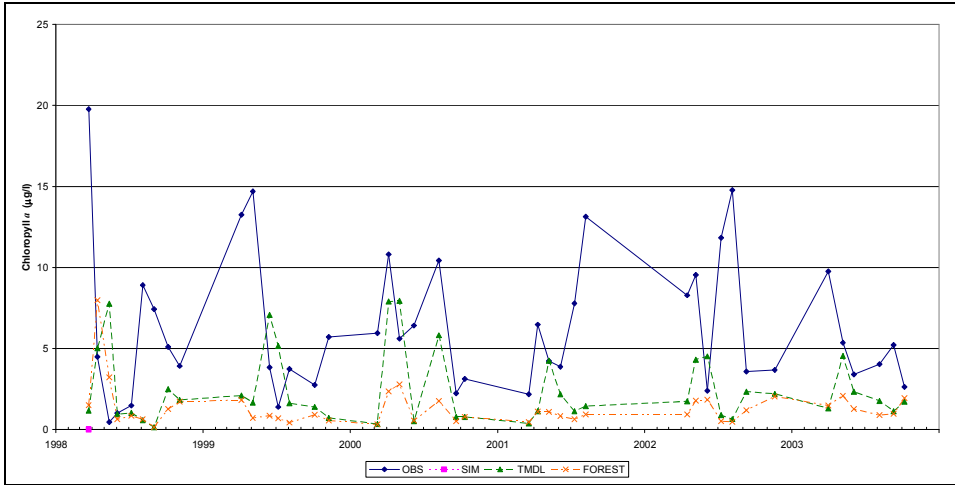


Figure D.8 Maximum Chla, Observed Data and All Scenarios, RG2, Rocky Gorge Reservoir

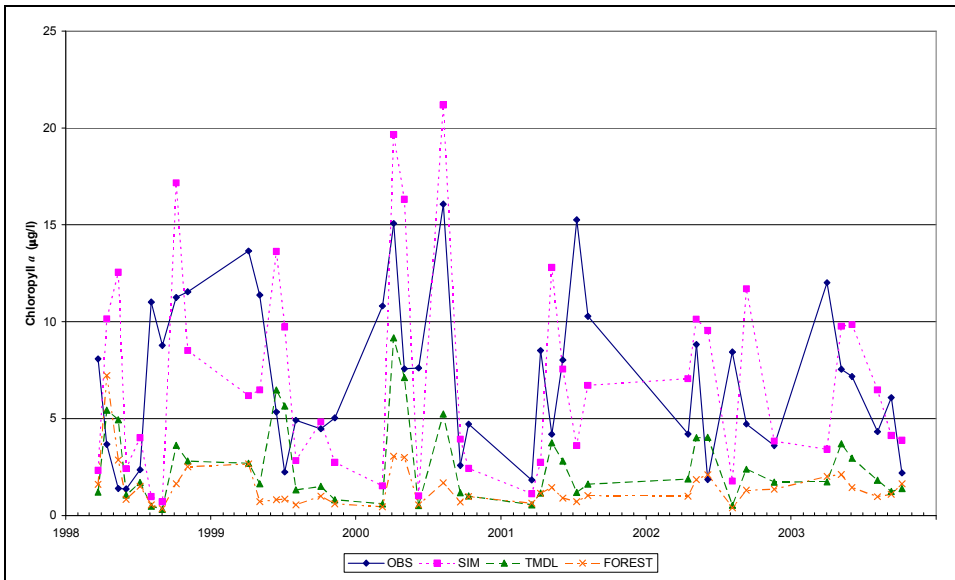


Figure D.9 Maximum Chla, Observed Data and All Scenarios, RG3, Rocky Gorge Reservoir

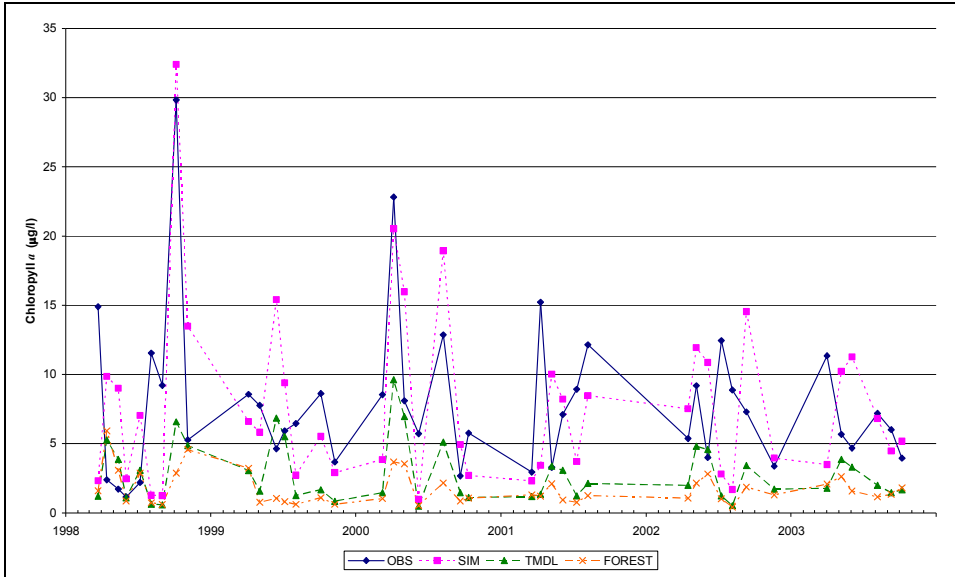


Figure D.10 Bottom DO, Observed Data and All Scenarios, RG2, Rocky Gorge Reservoir

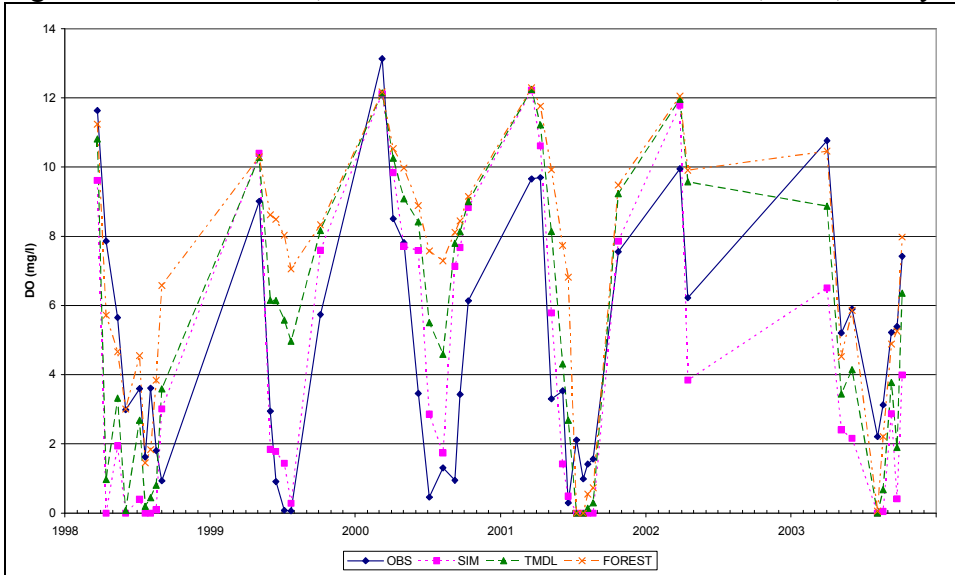


Figure D.11 Surface DO, Observed Data and All Scenarios, RG2, Rocky Gorge Reservoir

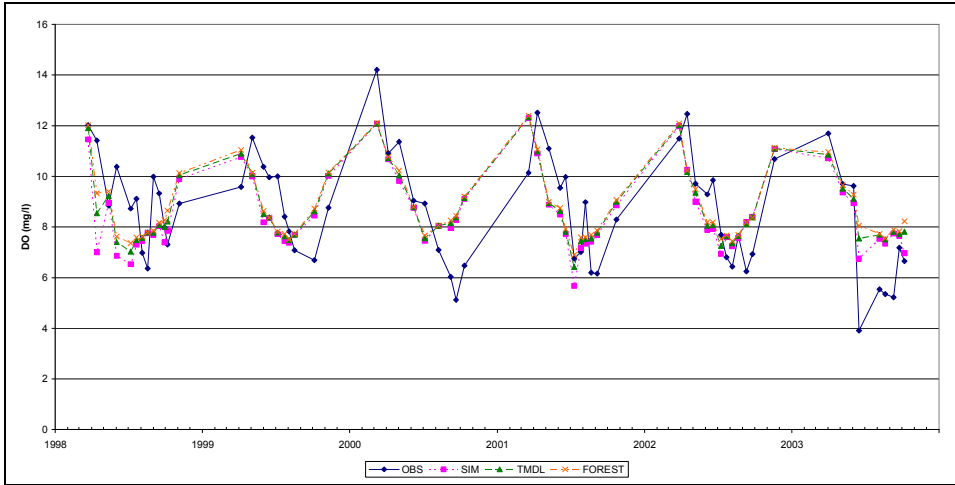


Figure D.12 Surface DO, Observed Data and All Scenarios, RG3, Rocky Gorge Reservoir

